MODIFICATION OF ZIRCONIUM AND HAFNIUM ALKOXIDES

THE EFFECT OF MOLECULAR STRUCTURE ON DERIVED MATERIALS

Gerald I. Spijksma

Leden van de promotie commissie:

Voorzitter/Secretaris:	prof. dr. ir. A. Bliek	University of Twente
Promotoren:	prof. dr. ing. D.H.A. Blank	University of Twente
	prof. dr. V.G. Kessler	SLU
Assistent promotor:	dr. H.J.M. Bouwmeester`	University of Twente
Leden:	prof. dr. J. Reedijk	Leiden University
	prof. dr. D.N. Reinhoudt	University of Twente
	prof. dr. M. Wessling	University of Twente
	dr. R.J. Errington	University of Newcastle
Referent:	dr. ir. N.E. Benes	Eindhoven University

ISBN: 90-365-2300-1

Printed by Febodruk bv, Enschede

MODIFICATION OF ZIRCONIUM AND HAFNIUM ALKOXIDES

THE EFFECT OF MOLECULAR STRUCTURE ON DERIVED MATERIALS

PROEFSCHRIFT

ter verkrijging van
de graad van doctor aan de Universiteit Twente,
op gezag van de rector magnificus,
prof. dr. W.H.M. Zijm,
volgens besluit van het College voor Promoties
in het openbaar te verdedigen
op vrijdag 20 januari 2006 om 15.00 uur

door

Gerald Iwan Spijksma
geboren op 27 maart 1976
te Leeuwarden

Dit proefschrift is goedgekeurd door de promotoren,
prof. dr. ing. D.H.A. Blank en *prof. dr. V.G. Kessler*
en de assistent promotor,
dr. H.J.M. Bouwmeester.

To my parents,
my brothers and
Katarina

Table of Contents

Chapter 1

General introduction

Abstract

A general introduction to the application of zirconia materials is provided in this chapter with a specific emphasis on the application in membrane and the use of zirconia as a high-k material. The main focus of this thesis is the preparation of suitable heteroleptic alkoxide precursors for the application in sol-gel and metal-organic chemical vapor deposition (MOCVD). Selecting suitable alkoxide precursors, precursor modification and sol preparation were the synthetic approaches in this study. The means by which these synthetic approaches have been used to date are discussed and the exciting research opportunities in this area are analyzed.

1.1 Applications of zirconia

The research within this thesis is focused on the synthesis and characterization of a new generation of thin oxide layers with nanostructured pore morphologies. In the present work it was chosen to work with zirconia and hafnia derived materials, including related heterometallic compounds with, for instance, titanium as an additional element.

Zirconia is a multifunctional ceramic material which is widely used in the field of sensors [1-3], structural ceramics [4-6], catalysts [7,8], optics [9,10], electronics [11,12] and ferroelectrics [13,14]. In recent years, the general focus of materials research has been on the preparation of nanostructured thin films [15], powders [16] and nanotubes, and rods and wires [17-19]. The main interest within this study is to explore materials suitable for the preparation of nanostructured thin films for membrane applications.

Due to the trend of further miniaturization there has been an increasing interest in zirconia and hafnia. These high-k materials are attractive candidates for very large scale integrated circuits and as gate dielectrics in metal oxide-semiconductor (MOS) devices [20,21]. The applicability of the studied precursors for dense dielectric thin films for electronic devices is also part of the scope of this study.

Ceramic membranes

Membranes are semi-permeable barriers that can specifically influence the movement of one or more particular species. By using membranes it is possible to inhibit the passage of a certain species, while other species are let through. A variety of membrane separation processes have been documented and literature on the subject is abundant [22,23].

With respect to membranes, the interest of this study is in the separation of components from liquids. The processes considered are nanofiltration (NF), reversed-osmosis (RO) and pervaporation (PV). What is characteristic for these processes is the fact that the solvent is the continuous phase and the concentration of the solute is relatively low. The particle or molecule size and the chemical

properties of the solute determine the properties of a suitable membrane, *i.e.*, surface charge, pore size and pore size distribution.

The membranes utilized in liquid separation systems should be resistant and stable towards the solvent. Ceramic membranes prepared from transition metal oxides (especially d^0 metal oxides) are attractive candidates, since these materials are resistant to many solvents, where as non-transition metal oxides (*e.g.*, Al_2O_3, SiO_2) do not have the required chemical stability [24,25].

Another membrane process of interest is gas separation. The major limitations of state of the art gas separation membranes, *i.e.*, microporous silica membranes, are their restricted thermal stability and poor resistance towards steam [26].

Asymmetric multiple layer membranes are used for all of the applications mentioned above. These membranes consist of several layers with the top-layer causing the separation. Ceramic membranes generally consist of two or three different layers depending on the type of application. The first layer is often an α-alumina support layer. This layer is macro-porous and provides the mechanical strength to the membrane. Other materials used in literature are ZrO_2 and TiO_2 [27]. The typical pore size of this layer is about 100 nm.

A mesoporous (intermediate) layer is deposited on top of this support layer. The materials available can be divided into three groups derived from transition metals (ZrO_2 [28-30], TiO_2 [31-34] and HfO_2 [35]), non-transition metals (*e.g.*, Al_2O_3 [28,36-39], SiO_2 [38,40]) and mixtures of these materials, *e.g.*, Si-Zr *etc.* [41-43].

If a microporous layer is deposited on top of the mesoporous layer, the membrane can become suitable for nanofiltration and pervaporation and, in some cases even for gas separation. This microporous layer can be fabricated from several materials *e.g.*, SiO_2 [44-46], TiO_2 [43,47-49], ZrO_2 [5] or HfO_2 [50,51]. It should be noted that no sharp distinction can be drawn between meso- and microporous layers, consequently both micro- and narrow mesoporous layers can be utilized for NF membranes.

Until now, it has only been possible to prepare silica membranes for gas separation [44-46]. For PV processes, titania membranes reported by Sekulic *et al.* [49], are probably state of the art, however, the chemical and thermal stability of these

membranes is not sufficient for most applications. Titania membranes for NF are commercially available, but their range of application can be improved. It should be noted that for all of these processes there is still a pressing need for improvement, either by optimizing the processing of the current materials or by replacing other materials with improved properties. The chemical and thermal properties of zirconia make it an attractive material for these applications.

Materials for dielectric applications

Dielectric ceramics are widely used as resonators in wireless communication apparatuses such as mobile phones, GPS systems and satellites. MOS (Metal Oxide Semiconductor) transistors are known as the building blocks of integrated circuits.

The number of transistors on an integrated circuit has doubled every two years, as Gordon E. Moore (CEO of Intel) predicted in 1965 in his famous article "Cramming more Components onto Integrated Circuits" [52], which is now known as Moore's Law in the semiconductor industry. Consequently, since the 1960's the device size has shrunken from the scale of micrometers to that of nanometers.

Traditionally, SiO_2, the native oxide of silicon with a dielectric constant (k) of ~3.9, has been used. However, the scaling down in dimension has resulted in reaching the physical minimal required thickness of the material. Further scaling down and/or improvement of the performance of the devices can only be achieved if materials with superior properties are utilized.

The need for new materials with a higher dielectric constant was described as the most challenging problem by International Roadmap of Semiconductor Industry (ITRS) [54]. In the current literature [20,53,54], numerous high-k candidates are proposed for replacing SiO_2, like HfO_2, ZrO_2, Ta_2O_5, CeO_2, Pr_2O_3 along with their complex derivatives like silicates and/or aluminates. One of the preparation methods of thin films for high-k materials, *i.e.*, ZrO_2 and HfO_2, is by chemical vapor deposition (CVD). State of the art precursors for the preparation of these materials by CVD have recently been reviewed by Jones [55] and Hubert-Pfalzgraf [56]. The main conclusion drawn in these reports is that up to now there has been no (alkoxide) precursor that allows reproducible preparation of dielectric materials by CVD.

1.2 Processing techniques

For the preparation of (thin) oxide layers, several physical and chemical techniques can be applied, including sol-gel and CVD. A great advantage of sol-gel and CVD methods, with respect to mixed metal oxide materials or dopants concentration, is their ability to easily change the chemical composition of the obtained materials.

Sol-gel chemistry

The history of sol-gel chemistry goes back several decades and Livage made an enormous contribution to establishing the research field as it is now. Major studies within the field especially in the early years were performed on the silica systems, mainly due to the moderate reactivity of the precursors. Studies on the synthesis and characterization of zirconium alkoxides were part of Don Bradley's early research [57,58]. The major sol-gel chemistry research on this and other transition metal alkoxide precursors was performed about two decades ago by Sanchez *in particular* [59-61].

Sol-gel synthesis can be subdivided into two methods [*e.g.*, 62,63]. The first one is based on the formation of colloids in aqueous media where the particles are prevented from agglomeration by mutual repulsion of similar charges at the particle surface. The second method uses metal-organic precursors in alcoholic media, where the polymeric particles remain as separated particles in solution because of their small size. Depending on the synthesis route and the reaction conditions, oligomers or particles, with a dimension ranging from 1 nm – 1 μm, are formed in the solution.

The transition from sol into gel in colloidal systems is a result of electrolytic effects that also determine the particle distance at the gelation point, thereby influencing the capability of a gel to remain monolithic during the drying process. On the other hand, gelation of sols that contain oligomers occurs as a result of a polymerization reaction. The nature and kinetics of these reactions determine the properties of the gel and the resulting inorganic polymer [64]. It should be noted that the concept presented above is deduced from the work on silica. In theory it should also apply to transition metals, however, this is not entirely supported by experimental

evidence. A more detailed overview on the sol formation and the reactions involved will be provided below.

Chemical vapor deposition

Chemical vapor deposition or CVD is a generic name for a group of processes which involve depositing a solid material from a gaseous phase and is similar in some respects to physical vapor deposition (PVD). PVD differs from CVD in that the precursors are solid, and the material to be deposited is vaporized from a solid target and then deposited onto the substrate.

In cases where metal alkoxide or β-diketonate precursors are used, the method is referred to as metal organic chemical vapor deposition (MOCVD). Materials are deposited from precursors or precursor solutions that are evaporated to a gaseous state during MOCVD. Therefore, precursors for CVD processes must be volatile, and be able to decompose thermally but at the same time stable enough to be able to be delivered to the reactor.

Precursor gasses (often diluted in carrier gases) are delivered into the reaction chamber at ambient or somewhat elevated temperatures. As they pass over or come into contact with a heated substrate, they react or decompose forming a solid phase and are deposited onto the substrate. The substrate temperature is critical and can influence which reactions will take place [65].

1.3 Processing strategy

The research presented here is dedicated to preparing materials via sol-gel and MOCVD. The starting point for both synthesis methods can be from the same type of precursors, *i.e.*, metal alkoxides in the present study. After several processing steps, films can be obtained; in sol-gel these films are either porous or dense where as in MOCVD the processing should result in dense films. The different steps for the preparation of these films are shown in Figure 1.1. The highlighted processing steps and their state of the art development are considered in this thesis and will be discussed in more detail below.

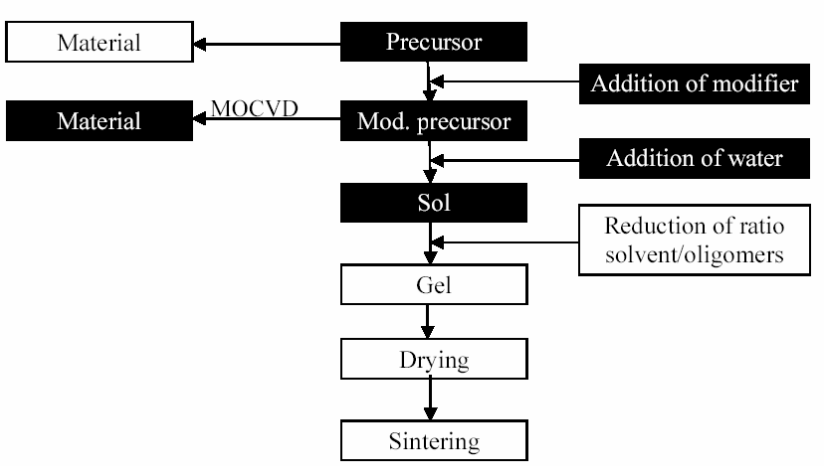

Figure 1.1: Processing scheme of metal alkoxide precursors by sol-gel and MOCVD.

Stateof the art zirconium and hafnium alkoxides

Despite being commonly used, the homometallic zirconium and hafnium alkoxide complexes have been insufficiently explored. None of the zirconium compounds commercially available can be considered an ideal precursor. The cheap *n*-propoxide, "$Zr(O^nPr)_4$" is delivered commercially in a 70 wt% solution in *n*-propanol, of which the molecular composition is unknown. In previously reported research by Day *et al.* [66], an attempt was made at purifying the precursor. Three different fractions were obtained upon vacuum distillation and $Zr_4(O^nPr)_{16}$ crystals could be isolated from one of these fractions. In the same way, zirconium *n*-butoxide is commercially available at an 80 wt% solution in *n*-butanol. According to data of mass spectrometry presented by Turevskaya *et al*. [67], the main compound found in their data is also $Zr_4(OR)_{16}$, *i.e.,* similar to that in commercial zirconium *n*-propoxide. Much more stable and structurally well-defined zirconium isopropoxide isopropanol solvate, $[Zr(O^iPr)_4(^iPrOH)]_2$ [68], is rather expensive and poorly soluble in its parent alcohol as well as in toluene at room temperature. A mixed-ligand alkoxide $[Zr(O^iPr)(O\text{-}neo\text{-}C_5H_{11})_3(HO\text{-}neoC_5H_{11})]_2$ has been reported by Boyle *et al.* [69]. It is claimed to be an attractive precursor for MOCVD, but not for sol-gel preparations due to its costs and the fact that it cannot be used in its parent alcohol. Recently, a very promising mixed ligand precursor, $[Zr(O^nPr)(O^iPr)_3(^iPrOH)]_2$ was

reported by Seisenbaeva *et al*. [70]. In addition to the above compounds, hafnium isopropoxide isopropanol solvate, and hafnium and zirconium *t*-butoxides are also commercially available.

Modification of precursors

A general method used to moderate the reactivity of precursors, is the exchange of the alkoxide ligands by chelating organic ligands [59,60,71]. In sol-gel studies, acetic acid and acetylacetone are most often applied for this purpose [72]. Acetic acid has the undesired ability to react with alcohol upon release of water. This will initiate the hydrolysis and subsequent condensation reactions and, hence, make reproducible and controlled modification impossible.

The modification of zirconium isopropoxide by acetylacetone has been a topic of various studies. Saxena *et al.* [73] and Puri [74] described the formation of mono-, di- and trisubstituted compounds upon modification with stoichiometric amounts of Hacac. However, no data on the structures was provided. The further modification of these disubstituted compounds for precursors in MOCVD has recently been reported [75,76].

A model describing the effect of the Hacac modification on sol preparation was proposed by Ribot *et al.* [77]. The model proposed by Ribot *et al.* was based on the existence of a dimer with one equivalent of Hacac, *e.g*., half a mol equivalent of Hacac per zirconium, and of mono- and disubstituted intermediates. It should be mentioned that, this model was proposed on the basis of a study on cerium isopropoxide. It was thought that the model developed for cerium also applies for zirconium.

Ribot *et al*. [77] also discussed the effect of varying amounts of acetylacetone on the products obtained as a result of hydrolysis and condensation, as is schematically depicted in Figure 1.2. The borderlines of the different regimes match with the ratios where they expected one type of modified precursor to be predominant. In the regimes between these borders, a mixture of compounds is present and the nature of the obtained hydrolysis and condensation product is provided. In order to obtain sols that lead to transparent gels at least 0.5 mol

equivalent of the modifier should be added and upon addition of more than 1 mol equivalent, molecular clusters are obtained.

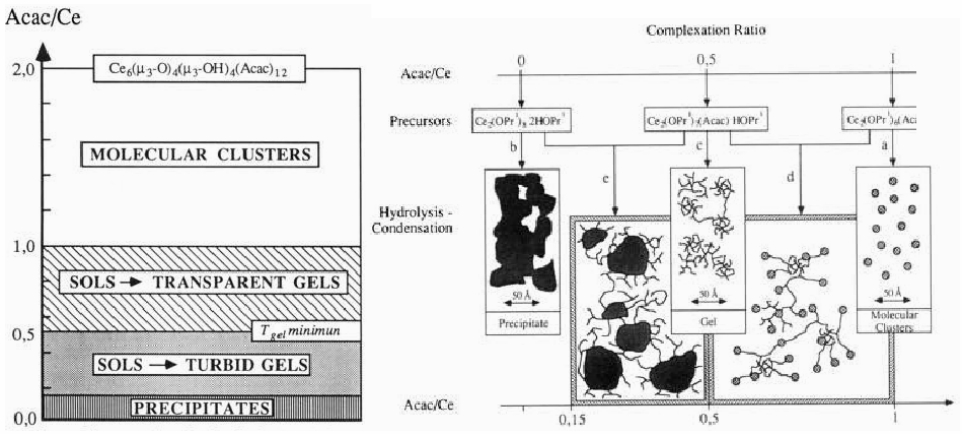

Figure 1.2: Proposed explanation of the nature of the products obtained on hydrolysis and condensation of Hacac modified cerium isopropoxide precursors. The borders of the different regimes match with the ratios where the authors expected one type of modified precursor to be predominant [77]. Reprinted with permission of Chem. Mater., 1991 3, 159-164. Copyright 1991 American Chemical Society.

The first generation CVD precursors of oxides were also zirconium and hafnium alkoxides modified by *β*-diketones. The modification was generally performed with 2,2,6,6,-tetramethyl-3,5-heptanedione (Hthd) in stead of Hacac, since Hthd provides a higher volatility *via* an improved shielding effect on the metal atom by the larger terminal organic groups.

The replacement of part of the alkoxide ligands of zirconium and hafnium isopropoxide precursors has been reported. Introduction of 1 thd ligand per zirconium or hafnium atom provided dimeric $[M(O^iPr)_3(thd)]_2$ (M = Zr or Hf) [78]. The behavior of these precursors in solution is not understood, and there is only a limited knowledge dealing with the preparation of films by MOCVD starting from this precursor [79-81].

An MOCVD-precursor which is applied more often is "$Zr(O^iPr)_2(thd)_2$" [82-85]. This currently, commercially available product was initially claimed to be a single compound [80]. However, in later publications it was said to be a stoichiometric mixture of mono- and dimeric structures and even suspected to be prone to some decomposition reactions [78,84]. Thus, despite being commercially available this

product had not been fully characterized and even its existence has not been unequivocally proved.

The complete replacement of alkoxide ligands by Hthd leads to the formation of the complex $M(thd)_4$ with M=Zr or Hf. Several studies have been devoted to the synthesis of these compounds [86], however, no determination of their structures have been published. The behavior of these compounds in solution and gas phase is remarkable. The compounds are, in spite of the very good shielding of the metal atom by the bulky organic ligands, very poorly soluble in hydrocarbon solvents and not nearly as volatile as one would expect. Nevertheless it is frequently applied as a precursor in MOCVD applications [82,85,87-89].

The modification of zirconium and hafnium isopropoxide precursors by Hthd is thus assumed to be more or less analogous with that of Hacac. The difference lies in the supposed existence of a compound modified with 0.5 mol equivalent of Hacac, while this is not assumed in the literature dealing with the modification with Hthd. In conclusion, the chemistry involved in the modification with β-diketones is not clear and not completely consistent.

The present generation of modified zirconium and hafnium propoxide precursors involves asymmetric chelating ligands. The commercially available *t*-butylacetoacetate is probably the most common modifying ligand of this kind. The monosubstituted compound obtained from zirconium isopropoxide is published by Patil *et al*. [90]. For MOCVD applications the general focus has been on the preparation of mononuclear compounds that can be obtained upon modification with 2 mol equivalents of *t*-butylacetoacetate [90,91]. The preparation and application of tetra substituted *t*-butylacetoacetate compounds has also been reported [90, 92]. Mononuclear compounds, similar to those obtained with 2 mol equivalents of *t*-butylacetoacetate, have been reported using 2 mol equivalents of N,N-diethylacetoacetamide [90] as the modifying ligand.

Zirconium and hafnium *t*-butoxide precursors are often considered for MOCVD applications. The alkoxide groups are bulkier than those in propoxide precursors, resulting in an improved shielding of the metal atom and subsequent higher volatility. The unmodified precursor is occasionally used as a source for MOCVD [93], however, the alkoxide is generally modified before application. It is proposed

that the modification with Hthd results in the formation of a disubstituted species [80]. Recently, the modification and application of zirconium and hafnium *t*-butoxide with 2 equivalents of 1-methoxy-2-methyl-2-propanolate [94] and 2-(4,4-dimethyloxazolinyl)-propanolate [95] have been reported.

There are reports where other modifying ligands *e.g.,* diethanolamine [96,97], diaminopentane [98], triethanolamine [4], are used in the sol-gel preparation of materials, however, the mechanism of modification is not considered. The compound formed upon the modification of zirconium *n*-propoxide with 0.5 mol equivalent of N-methyl-diethanolamine has been reported [99], however, its applicability for materials preparation was not investigated.

In this study, the modification of zirconium and hafnium propoxides with acetylacetone, 2,2,6,6,-tetramethyl-3,5-heptanedione, *t*-butylacetoacetate and diethanolamine will be explored.

Sol formation

The formation of a sol from a precursor solution is initiated upon the addition or release of water, this leads to the initiation of hydrolysis and subsequent condensation reactions [71].

The hydrolysis of an alkoxide leads to the formation of a reactive M-OH group. The following three step mechanism is generally proposed:

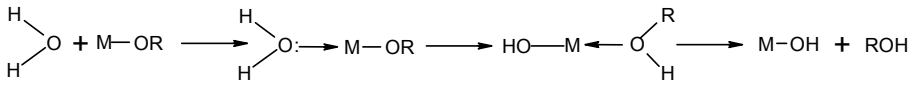

The first step is a nucleophilic addition of a water molecule to the positively charged metal atom M. This leads to a transition state where the coordination number of M has been increased by one. The second step involves a proton transfer within the intermediate leading to the next transition state. A proton from the entering water molecule is transferred to the negatively charged oxygen of an adjacent OR group. The third step is the departure of the better leaving group, which should be the most positively charged species within the second transition state.

The following parameters determine the kinetics of the reaction:

1. Electrophilic character of the metal atom: charge density increases from Si, Ti , Zr, in case of metal ethoxide respectively +0.32, +0.63 and +0.65
2. Nucleophilic character of the entering molecule
3. The nucleofugal character of the leaving group
4. The coordination state of the precursor: the more unsaturated the coordination, the lower the activation energy associated with the nucleophilic addition.
5. The ability to transfer a proton: the more acidic the proton, the lower the activation energy associated with the transfer will be.

If the synthesis is performed under acidic conditions, steps 3 and 5 are no longer rate determining.

After the initial hydrolysis, the product can react further, either *via* another hydrolysis reaction or a condensation reaction. In order to get non-branched or limitedly branched oligomers, the hydrolysis should be followed by a condensation reaction. Condensation is also a complex process, and depending on the experimental conditions, three competitive mechanisms have to be considered, *e.g.*, alcoxolation, oxolation and olation [60,62].

Alcoxolation is a reaction by which a bridging oxo group forms through the elimination of an alcohol molecule. The mechanism is basically the same as the hydrolysis with M replacing H in the entering group.

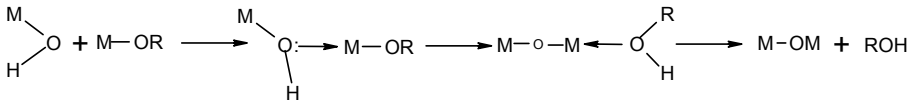

Oxolation follows the same mechanism as alcoxolation, but the R group of the leaving species is a proton:

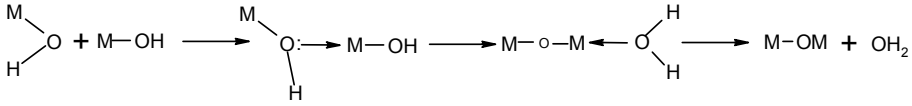

Olation can occur when the full coordination of a metal atom is not achieved (as is usually the case for titania, zirconia and hafnia). In this case bridging hydroxo groups can be formed through the elimination of a solvent molecule. The latter can be either H_2O or ROH depending on the water concentration in the medium:

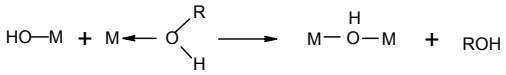

The kinetics of this nucleophilic substitution is governed by the charge distribution. The reaction is strongly favored when the nucleophilic character of the entering group and the electrophilic strength of the metal are high. Moreover, since no proton transfer is involved within the transition state (assuming the metal coordination is not saturated) the reaction rate is usually quite fast.

1.4 Problem definition

Up to date, the major difference between silica and transition metals has not been underlined. However, it is well known that TEOS, a typical precursor for the preparation of silica sols, and "$Zr(O^nPr)_4$", a commonly used precursor for zirconia sols, show very different reactivity when mixed with a water-alcohol solution. "$Zr(O^nPr)_4$" hydrolyzes several orders of magnitude faster than TEOS. This difference in reactivity is partly caused by the difference in charge density (δ(M) in $M(OET)_4$ 0.32 and 0.65 for Si and Zr, respectively) [71].

The coordination of silica and zirconium atoms in the precursors is also very different. The silica precursors have a saturated tetra-coordination, while zirconium precursors have at least a coordination number of 6, but the coordination is most stable with 8 donor atoms. These higher coordination numbers cause these compounds to become multi nuclei and in some cases they contain solvating alcohol. It is necessary to point out that the coordination number can change through the hydrolysis-polycondensation procedure.

The effect of modifiers on the structure, stability and reactivity of a precursor is rarely considered, despite their great impact on sols for the preparation of thin

films, membranes and nanoparticles. For silica, it is possible to influence the sol properties and thus also the properties of the eventual material simply by varying the pH and the concentration. The much higher reactivity and the influence of modification, *i.e.,* incorporation of non-hydrolysable ligands, for zirconium precursors make the concepts developed for silica inapplicable for these systems.

The starting point for this research was to evaluate the influence of parameters like choice of precursor, amount and type of additive, and the ratio of water and solvent. In order to achieve reproducible preparation of high-tech materials, the composition of the starting chemicals, *i.e.*, the modified precursors, should be the same every time.

Therefore the chemistry of the modifying effect of the additives should be understood since this reproducibility can only be achieved when intermediate thermodynamically stable compounds are used. If this stability is not present, rearrangement of ligands will occur, which will effect the eventual material properties.

It should be noted that precursors need to fulfill additional requirements in order to be suitable for MOCVD application. They should have, in addition to the solution stability, shelf stability (*e.g.,* modified precursors are generally not prepared *in situ* as in sol-gel) and should be volatile enough to allow deposition through the gas-phase.

Aim

The general aim of the present study is to investigate the influence of modifying ligands on precursors and sol particles. The structure and stability of the modified precursors is examined. The scope with respect to the modification of precursors is to find a modification that is thermodynamically stable and thus allows the reproducible preparation of materials. Regarding the influence of the modifying ligands on sol particles, the mechanisms of their transformation on hydrolysis and condensation is evaluated. Finally, the properties of derived materials are also studied.

1.5 Thesis outline

The second chapter of this thesis deals with the characterization of some of the precursors utilized in the present study. The preparation of a new hafnium propoxide precursor is also discussed.

The next section of this thesis covers the chemistry involved in the modification of zirconium and hafnium alkoxides by acetylacetone (Chapter 3) and 2,2,6,6,-tetramethyl-3,5-heptanedione (Chapter 4). The modification of zirconium and hafnium alkoxides by *t*-butylacetoacetate and zirconium and hafnium *t*-butoxides by 2,2,6,6,-tetramethyl-3,5-heptanedione are combined in Chapter 5. The modification of zirconium propoxides by diethanolamine is the topic of Chapter 6, while the heterometallic compounds obtained with diethanolamine as the modifier are presented in Chapter 7.

The next part of the thesis deals with the preparation of materials from the modified precursors. In Chapter 8 the effect of modifying ligands on sol particles is evaluated. Subsequently, the preparation and application of hollow spheres by sol-gel synthesis (Chapter 9) is discussed in more detail. The preparation and characterization of sol-gel derived materials using a zirconium-titanium heterometallic precursor completes this section of the thesis (Chapter 10).

In the last chapter the general trends are summarized and an outlook for further research is provided.

1.6 References

1 H. Kurosawa, Y.T. Yan, N. Miura and N. Yamazoe, *Solid State Ionics,* **79**, 338 (1995).

2 C.M.S. Rodrigues, J.A. Labrincha and F.M.B. Marques, *Solid State Ionics*, **136-137**, 671 (2000).

3 N. Miura, M. Nakatou and S. Zhuiykov, *Sensor Actuat. B-Chem.*, **93**, 221 (2003).

4 S. Benfer, U. Popp, H. Richter, C. Siewert and G. Tomandl, *Separ. Purif. Technol*., **22-23**, 231 (2001).

5 R.J. Vacassy, C. Guizard, J. Palmeri and L. Cot, *Nanostruct. Mater*., **10**, 77 (1998).

6 C.R. Xia, H.Q. Cao, H. Wang, P.H. Yang, G.Y. Meng and D.K. Peng, *J. Membr. Sci*., **162**, 181 (1999).

7 A. Knell, P. Barnickel, A. Baiker and A. Wokaun, *J. Catal*., **137**, 306 (1992).

8 Y. Li, D. He, Z. Cheng, C. Su, J. Li and Q. Zhu, *J. Mol. Catal. A: Chem*., 175, 267 (2001).

9 J. Gottmann and E.W. Kreutz, *Surf. Coat. Tech.,* **119**, 1189 (1999).

10 R. Reisfeld, *J. Alloy Compd*., **341**, 56 (2002).

11 X.Y. Zhao and D. Vanderbilt, *Phys. Rev. B,* **65**, Art. No. 075105 (2002).

12 V. Fiorentini and G. Gulleri, *Phys. Rev. Lett*., **89**, Art. No. 266101 (2002).

13 S. Hoffmann, M. Klee and R. Waser, *Integr. Ferroelectr.,* **10**, 155 (1995).

14 M. Klee, U. Mackens, W. Hermann and E. Bathelt, *Integr. Ferroelectr.,* **11**, 247 (1995).

15 B. Zhu, *Solid State Ionics*, **119**, 305 (1999).

16 X.M. Wang, G. Lorimer and P. Xiao, *J. Am. Ceram. Soc*., **88**, 809 (2005).

17 X. Hui, D.-H. Qin, Z. Yang and H.-L. Li, *Mater. Chem. Phys.*, **80**, 524 (2003).

18 H.Q. Cao, X.Q. Qiu, B. Luo, Y. Liang, Y.H. Zhang, R.Q. Tan, M.J. Zhao and Q.M. Zhu, *Adv. Funct. Mater.,* **14**, 243 (2004).

19 S.J. Limmer, S. Seraji, M.J. Forbess, Y. Wu, T.P. Chou, C. Nguyen and G.Z. Cao, *Adv. Mater.*, **13**, 1269 (2001).

20 G.D. Wilk, R.M. Wallace and J.M. Anthony, *J. Appl. Phys*., **89**, 5243 (2001).

21 A.C. Jones, H.C. Aspinall, P.R. Chalker, R.J. Potter, K. Kukli, A. Rahtu, M. Ritala and M. Leskelä, *J. Mater. Chem.*, **14**, 3101 (2004).

22 R.H. Perry and D.W. Green, "*Perry's Chemical Engineers' Handbook*," 7th edition, McGraw-Hill, New York, (1997).

23 M. lder, "*Basic principles of membrane technology*," second edition, Kluwer Academic Publisher, Dordrecht, (1996).

24 T. Van Gestel, C. Vandecasteele, A. Beukenhoudt, C. Dotremont, J. Luyten, R. Leysen, B. Van der Bruggen and G. Maes, *J. Membr. Sci.*, **207**, 73 (2002).

25 T. Van Gestel , C. Vandecasteele, A. Buekenhoudt, C. Dotremont, J. Luyten, B. Van der Bruggen and G. Maes, *J. Membr. Sci.*, **214**, 21 (2003).

26 J. Campaniello, C.W.R. Engelen, W.G. Haije, P.P.A.C Pex and J.F. Vente, *Chem. Commun*., 834 (2004).

27 T. Tsuru, *Separ. Purif. Method.*, **30**, 191 (2001).

28 X. Ju, P. Huang, N. Xu and J. Shi, *J. Membr. Sci.*, **166**, 41 (2000).

29 J. Etienne, A. Larbot, A. Julbe, C. Guizard and L. Cot, J. *Membr. Sci*., **86**, 95 (1994).

30 Xia C., Yang W., Peng R., Peng D., and G. Meng, *Solid State Ionics*, **133**, 278 (2000).

31 M.D. Moosemiller, C.G. Hill jr. and M.A. Anderson, *Separ. Sci. Technol*., **24**, 641 (1989)

32 K-N.P. Kumar, PhD thesis, University of Twente, The Netherlands, (1993).

33 G. Tomandl, M. Mangler, E. Pippel and J. Woltersdorf, *Mater. Chem. Physics*, **63**, (2000).

34 K.M.S. Khalil and M.I. Zaki, *Powder Technol*., **120**, 256 (2001).

35 P. Blanc, A. Larbot, M. Persin and L. Cot, *J. Membr. Sci.,* **134**, 109 (1997).

36 A.F.M. Leenaars, K. Keizer and A.J. Burggraaf, *J. Mater. Sci*., **19**, 1077 (1984).

37 K. Keizer and A.J. Burggraaf, "*Porous ceramic materials in membrane applications*," In Science of Ceramics, **14**, Eds. D. Taylor. The Institute of Ceramics, Sholton, Stoke-on-Trent, UK, 1988. Proc. 14th Int. Conf. on Science of Ceramics, Canterbury, pp 83 (1987).

38 A. Larbot, J.A. Alary, C. Guizard, L. Cot and J. Gillot, *Int. J. High Technol.*, **3**, 143 (1987).

39 A. Larbot, S. Alami-Younssi, M Persin., J. Sarrazin and L Cot, *J. Membr. Sci.*, **97**, 167 (1994).

40 Y.F. Lu, Y. Yang., A. Sellinger, M.C. Lu, J.M. Huang, H.Y. Fan, R. Haddad, G. Lopez, A.R. Burns, D.Y. Sasaki, J. Shelnutt and C.J. Brinker, *Nature*, **410**, 913 (2001).

41 M. Asaeda, Y. Sakou, J. Yang and K. Shimasaki, *J. Membr. Sci.*, **209**, 163 (2002).

42 T. Tsuru, T. Sudoh, T. Yoshioka and M. Asaeda, *J. Membr. Sci*., **185**, 253 (2001).

43 T. Tsuru, D. Hironaka, T. Yoshioka and M. Asaeda, *Sep. Purif. Technol.,* **21**, 307 (2001).

44 B.N. Nair, K. Keizer, W.J. Elferink, M.J. Gilde, H. verweij and A.J. Burggraaf, *J. Membr. Sci.*, **116**, 161 (1996).

45 S. Vercauteren, K. Keizer, E.F. Vansant, J. Luyten and R. Leysen, *J. Porous Mater.*, **5**, 241 (1998).

46 R.M. De Vos, W.F. Maier and H. Verweij, *J. membr. Sci.,* **158**, 277 (1999).

47 P. Puhlfürß, A. Voigt, R. Weber and M. Morbe, *J. Membr. Sci.,* **174**, 123 (2000).

48 T. Van Gestel, C. Vandecasteele, A. Beukenhoudt, C. Dotremont, J. Luyten, R. Leysen, B. Van der Bruggen and G. Maes, *J. Membr. Sci.,* **209,** 379 (2002).

49 J. Sekulic, J.E. ten Elshof and D.H.A. Blank, *Adv. Mater*., **16**, 1546 (2004).

50 P. Blanc, A. Larbot, J. Palmeri, M. Lopez and L. Cot, *J. Membr. Sci*., **149**, 151 (1998).

51 J. Palmeri, P. Blanc, A. Larbot and P. David, *J. Membr. Sci.,* **179**, 243 (2000).

52 G.E. Moore, *Electronics*, **38**, 114 (1965).

53 D.S. Yoon, J.S. Roh, H.K. Baik and S.M. Lee, *Critical Rev. Solid State Mat. Sci*., **27**, 143 (2002).

54 International Roadmap of Semiconductor Industry (ITRS), http://public.itrs.net/ (accessed 04-May-2005)

55 A.C. Jones, H.C. Aspinall, P.R. Chalker, R.J. Potter, K. Kukli, A. Rahtu, M. Ritala and M. Leskelä, *J. Mater. Chem*., **14**, 3101 (2004).

56 L.G. Hubert-Pfalzgraf, *J. Mater. Chem.*, **14**, 3113 (2004).

57 D.C. Bradley, R.C. Mehrotra and C.P. Gaur, "*Metal alkoxides*," Academic Press, Londen, (1978).

58 D.C. Bradley, F. M. Abd-El Halim, E.A. Sadek and W. Wardlaw, *J. Chem. Soc*., 2032 (1952).

59 C. Sanchez, J. Livage, M. Henry and F. Babonneau, *J. Non-Cryst. Solids*, **100**, 65 (1988).

60 J. Livage, M. Henry and C. Sanchez, *Prog. Solid St. Chem*., **18,** 259 (1988).

61 P. Judeinstein and C. Sanchez, *J. Mater. Chem*., **6**, 511 (1996).

62 J.C. Brinker and G.W. Scherer, "*Sol-Gel Science: The Physics and Chemistry of Sol-Gel Processing*," Elsevier, Florida, (1990).

63 C. Guizard, "*Sol-gel chemistry and its application to porous membrane processing*," In Fundermentals of Inorganic Membrane Science and Technology, Membrane Science and Technology Series, Eds. A.J. Burggraaf and L. Cot, pp. 227 (1996).

64 R. De vos, PhD thesis, University of Twente, The Netherlands, (1998).

65 H.O. Pierson, "Handbook of Chemical Vapor Deposition - Principles, Technology and Applications," (2nd Edition), William Andrew publishing, Noyes, (1999).

66 V.W. Day, W.G. Klemperer and M.M. Pafford, *Inorg. Chem.*, **40**, 5738 (2001).

67 E.P. Turevskaya, N.I. Kozlova, N.Y. Turova, A.I. Belokon, D.V Berdyev, V.G. Kessler and Y.K. Grishin, *Russ. Chem. Bull.*, **44**, 734 (1995).

68 B.A. Vaartstra, J.C. Huffman, P.S. Gradeff, L.G. Hubert-Pfalzgraf, J.-C. Daran, S. Parraud, K. Yunlu and K.G. Caulton, *Inorg. Chem*., **29**, 3126 (1990).

69 T.J. Boyle, J.J. Gallegos, D.M. Pedrotty, E.R. Mechenbier and B.L. Scott, *J. Coord. Chem*., **47**, 155 (1999).

70 G.A. Seisenbaeva, S. Gohil and V.G. Kessler, *J. Mater. Chem.*, **14**, 3177 (2004).

71 J. Livage and C. Sanchez, *J. Non-Cryst. Solids* **145**, 11 (1992).

72 U. Schubert, *J. Sol-Gel Sci. Techol.*, **26**, 47 **(**2003).

73 U.B. Saxena, A.K. Rai, V.K. Mathur, R.C. Mehrotra and D. Radford, *J. Chem. Soc*. (A), 904 (1970).

74 D.M. Puri, *J. Indian Chem. Soc,,* **47**, 535 (1970).

75 M. Morstein, *Inorg. Chem.*, **38**, 125 (1999).

76 M. Pathak, R. Bohra, R.C. Mehrotra, I.P. Lorenz and H. Piotrowski, *Z. Anorg. Allg. Chem.*, **629***,* 2493 (2003).

77 F. Ribot, P. Toledano and C. Sanchez, *Chem. Mater*., **3**, 159 (1991).

78 K.A. Fleeting, P. O'Brien, D.J. Otway, A.J.P. White, D.J. Williams and A.C. Jones, *Inorg. Chem.,* **38**, 1432 (1999).

79 A.C. Jones, T.J. Leedham, P.J. Wright, D.J. Williams, M.J .Crosbie, H.O. Davies, K.A. Fleeting and P. O'Brien, *J. Eur. Ceram. Soc*., **19**, 1431 (1999).

80 A.C. Jones, T.J. Leedham, P.J. Wright, M.J. Crosbie, P.A. Lane, D.J. Williams, K.A. Fleeting, D.J. Otway and P. O'Brien, *Chem. Vapor. Depos.*, **4,** 46 (1998).

81 D.H. Kim, J.S. Na and S.W. Rhee, *J. Electrochem. Soc.*, **148**, C668 (2001).

82 H. Ahn, H.W. Chen, D. Landheer, X. Wu, L.J. Chou and T.-S. Chao, *Thin Solid Films*, **318**, 455 (2004).

83 H.W. Chen, T.Y. Huang, D. Landheer, X. Wu, S. Moisa, G.I. Sproule, J.K. Kim, W.N. Lennard and T.S. Chao, *J. Electrochem. Soc.*, **150**, C465 (2003).

84 A.C. Jones, T.J. Leedham, P.J. Wright, M.J. Crosbie, D.J. Williams, K.A. Fleeting, H.O. Davies, D.J. Otway and P O'Brien, *Chem. Vapor. Depos.*, **4**, 197 (1998).

85 J.F. Roeder, T.H. Baum, S.M. Bilodeau, G.T. Stauf, C. Ragaglia, M.W. Russell and P.C. Van Buskirk, *Adv. Mater. Opt. Electr.*, **10**, 145 (2000).

86 J. Si, S.B. Desu and C.Y. Tsai, *J. Mater. Res.*, **9**, 1721 (1994).

87 C. Dubourdieu, S.B.Kang, Y.Q. Li, G. Kulesha and B. Gallois, *Thin Solid Films*, **339**, 165 (1999).

88 S. Chevalier, M. Kilo, G. Borchardt and J.P. Larpin, *Appl. Surf. Sci.*, **205**, 188 (2003).

89 M. Putkonen and L. Niinistö, *J. Mater. Chem*., **11**, 3141 (2001).

90 U. Patil, M. Winter, H.W. Becker and A. Devi, *J. Mater. Chem.,* **13**, 2177 (2003).

91 A. Baunemann, R. Thomas, R. Becker, M. Winter, R.A. Fischer, P. Ehrhart, R. Waser and A. Devi, *Chem. Commun*., 1610 (2004).

92 S. Pasko, L.G. Hubert-Pfalzgraf and A. Abrutis, *Mater. Lett*, **59**, 1836 (2005).

93 S. Mathur, J. Altmayer and H. Shen, *Z. Anorg. Allg. Chem.*. **630**, 2042 (2004).

94 P.A. Williams, J.L. Roberts, A.C. Jones, P.R. Chalker, J.F. Bickley, A. Steiner, H.O. Davies and T.J. Leedham, *J. Mater. Chem.*, **12**, 165 (2002).

95 Y.F. Loo, R. O'Kane, A.C. Jones, H.C. Aspinall, R.J. Potter, P.R. Chalker, J.F. Bickley, S. Taylor.and L.M. Smith, *J. Mater. Chem*., **35,** 1896 (2005).

96 T. Okubo, T. Takahashi, B.N. Nair, M. Sadakata and H. Nagamoto, *J. Membr. Sci*., **125**, 311 (1997).

97 T. Okubo, T. Takahashi, M. Sadakata and H. Nagamoto, *J. Membr. Sci.*, **118**, 151 (1996).

98 Y. Gu, K. Kusakabe and S. Morooka, *Sep. Sci. Technol*., **36**, 3689 (2001).

99 G.J. Gainsford, N. Al-Salim and T. Kemmitt, *Acta Crystallogr., Sect. E.: Struct. Rep. Online*, **58**, M636 **(**2002).

Chapter 2

NMR and mass spectrometric analysis of zirconium propoxide and butoxide and hafnium *n*-propoxide precursors

Abstract

The structural composition of two commercial precursors, *i.e.*, zirconium *n*-propoxide and zirconium *n*-butoxide, has been investigated. Upon evaporation of the parent solvent, a two-phase system comprising of a solid and a waxy liquid phase is obtained for both precursors. ^{13}C NMR study of these phases indicated the presence of 4 different compounds, including a trinuclear zirconium oxo-alkoxide ($Zr_3O(OR)_{10}$). The presence of $Zr_3O(OR)_{10}$ has been confirmed by mass spectrometric analysis. The remaining species are all tetranuclear and it is estimated that at least 65-70% of the commercial product is $Zr_4(O^nPr)_{16}$. The other two compounds are expected to oxo-rich. The main compound in the home made hafnium *n*-propoxide is tetranuclear and its structure is different from the observed zirconium compounds.

A new route has been presented for synthesis of the mixed ligand precursor $[Zr(O^nPr)(O^iPr)_3(^iPrOH)]_2$, from zirconium *n*-propoxide. A high yield has been observed (~90%), indicative of an almost complete precursor transformation and provides support for the estimated contains of 65-70% $Zr_4(O^nPr)_{16}$. Mass spectrometry has shown that the synthesized mixed ligand precursor is dimeric, which makes it an attractive alternative for zirconium *n*-propoxide.

2.1 Introduction

The alkoxides of zirconium are widely used as precursors in the preparation of oxide materials for various applications, ranging from porous membranes [1-3] and matrices in catalysis [4,5] to dense dielectric and ferroelectric films in electronics [6,7]. However, both the homometallic and heterometallic zirconium alkoxide complexes have been as yet insufficiently explored.

None of the commercially available homometallic compounds can be considered an ideal precursor. The cheap *n*-propoxide, "$Zr(O^nPr)_4$", is a moisture-sensitive waxy solid at room temperature [8]. It is delivered commercially in the form of 70 wt% solution in *n*-propanol, of which the structural composition is unknown. In an attempt to purify the precursor, Day *et al.* [8] obtained three different fractions upon vacuum distillation and could isolate $Zr_4(O^nPr)_{16}$ crystals from one of these fractions. Analogously, zirconium *n*-butoxide is commercially available in a 80 wt% solution in *n*-butanol. According to data of mass spectrometry presented by Turevskaya *et al.* [9], the main compound is also $Zr_4(OR)_{16}$, *i.e.* similar to that in commercial zirconium *n*-propoxide.

Much more stable and structurally well defined zirconium isopropoxide isopropanol solvate, $[Zr(O^iPr)_4(^iPrOH)]_2$ [10], is rather expensive and at room temperature it is poorly soluble in its parent alcohol and even in toluene.

A mixed-ligand alkoxide $[Zr(O^iPr)(O\text{-}neo\text{-}C_5H_{11})_3(HO\text{-}neoC_5H_{11})]_2$ has been reported by Boyle *et al.* [11]. It is claimed to be an attractive precursor for MOCVD, but not for sol-gel preparations due to its high cost and the fact that it cannot be used in its parent alcohol. Recently, a very promising mixed ligand precursor, $[Zr(O^nPr)(O^iPr)_3(^iPrOH)]_2$ has been reported by Seisenbaeva *et al*. [12].

The present study is focused towards evaluation of the structural composition of commercially available zirconium *n*-propoxide and zirconium *n*-butoxide precursors. The composition of the zirconium *n*-propoxide precursor will be compared with the prepared hafnium *n*-propoxide. In addition $[Zr(O^nPr)(O^iPr)_3(^iPrOH)]_2$ is prepared *via* an alternative synthesis. Its properties are compared with those of the homoleptic zirconium precursors.

2.2 Experimental

All manipulations were carried out in a dry nitrogen atmosphere using the Schlenk technique or a glove box. The 70 wt% solution of "$Zr(O^nPr)_4$" (Lot: S20269-054) and 80 wt% solution of "$Zr(O^nBu)_4$" (Lot: S16020-473) were purchased from Aldrich. Isopropanol (Merck, *p.a.*) and *n*-propanol (Merck, *p.a.*) were purified by distillation over the corresponding $Al(OPr)_3$, and toluene (Merck, *p.a.*) by distillation over $LiAlH_4$. ^1H NMR and 2-d NMR, using COSY and HSQC, spectra were recorded in $CDCl_3$ solutions on a Bruker 400 MHz spectrometer at 243 K. Mass-spectra were recorded using a JEOL JMS-SX/SX-102A spectrometer applying electron beam ionization (U = 70 eV) with direct probe introduction.

The solvent removal processes in vacuum were studied using a Schlenk line evacuated by a oil pump ($P = 10^{-2}$ mmHg). The precursor solutions being studied were in a glass vessel, and during the course of evaporation of the solvents, the gaseous products were collected in a trap cooled with liquid nitrogen. After the removal of the solvents was completed, the system was filled with dry nitrogen and, warmed up to room temperature. A sample of the condensated evaporated compounds was investigated by GC-MS using a Hewlett-Packard 5890 Series II gas chromatograph supplied with a capillary separative column with DBWax film phase (manufactured by J&W Scientific, CA). This was coupled to a JEOL JMS-SX/SX102A Tandem mass spectrometer (electron beam ionization, direct probe introduction). The results of microanalysis (C, H, N) were obtained by Mikrokemi AB, Uppsala, Sweden.

Synthesis: For NMR analysis zirconium *n*-propoxide (~2 ml) was dried under vacuum (0.1 mm Hg) at room temperature, which resulted in a yellow, waxy liquid. During the drying, which was performed at room temperature, a small amount of solid phase was formed (up to a few percent of the total volume). The transformation of the waxy liquid into a waxy solid as is described in ref. [8], occurred only when the sample was heated (T ~100 °C) during the drying process.

NMR samples were prepared from a fresh sample of the waxy liquid and the solid phase formed in it. Samples of both phases were dissolved in $CDCl_3$ (which was dried on molecular sieves in order to avoid hydrolysis of the samples). Amounts of

both the viscous liquid and the solid phases were used for element analysis and mass spectrometry experiments.

Samples of zirconium *n*-butoxide, both of the yellow, waxy liquid and solid phase, were obtained and prepared in a corresponding manner. Both samples were analysed by ^{1}H NMR. The solid phase was also examined by mass spectrometry.

$[Zr(O^{n}Pr)(O^{i}Pr)_3(^{i}PrOH)]_2$ was prepared both according to a recently developed technique [12] and following a new synthesis route, as described hereafter. The solvent from 10 ml of 70 wt% solution of "$Zr(O^{n}Pr)_4$" was removed under vacuum (0.1 mm Hg) and the residue was then re-dissolved in 40 ml mixture of toluene/isopropanol (1:1 volume ratio). The solvent was removed by drying under vacuum (0.1 mm Hg). The first crystals appeared during the removal of the solvent. Subsequently, 10 ml of isopropanol was added and the solution was refluxed for 15 minutes. The sequence of re-dissolving, refluxing and removal of the solvent was repeated once more. Then the dried product was dissolved in a 10 ml mixture of toluene and isopropanol (1:1 volume ratio) and upon slight heating, a clear solution was obtained. After allowing the solution to stand over night at –30 °C, a large number of crystals were obtained. The solvent was removed from the crystals and concentrated by partial evaporation under vacuum (0.1 mm Hg). After the addition of 3 ml of isopropanol the solution was placed for crystallization at -30 °C. The latter procedure was repeated up to a yield of over 90%.

Hafnium *n*-propoxide was prepared by prepared by anodic oxidation of hafnium metal in *n*-propanol analogous to the preparation of hafnium isopropoxide [9]. tetraalkylammonium bromide was used a electolyte. Toluene was added to the obtained mixture of precursor, electrolyte and metal particles and left for sedimentation for about a month. The liquid phase was separated from the solid fraction and subsequently dried under vacuum (0.1 mm Hg). After removal of most of the volatiles the sample was graduatly heated under vacuum to ~220 °C and after about the 5 minutes the sample was let to cool again. The white/grey waxy solid was characterized by ^{1}H NMR and mass spectrometry.

2.3 Results and discussion

Several phases can be obtained upon the distillation of zirconium *n*-propoxide. Day *et al.* [8] identified one of them as $Zr_4(O^nPr)_{16}$. Its structure is depicted in Figure 2.1a. Upon evaporation of the solvent under vacuum (0.1 mm Hg) at room temperature both a solid phase and a waxy liquid phase were obtained from commercial zirconium *n*-propoxide in this study. Upon heating the formed viscous liquid will solidify giving the waxy solid described by Day *et al.* [8].

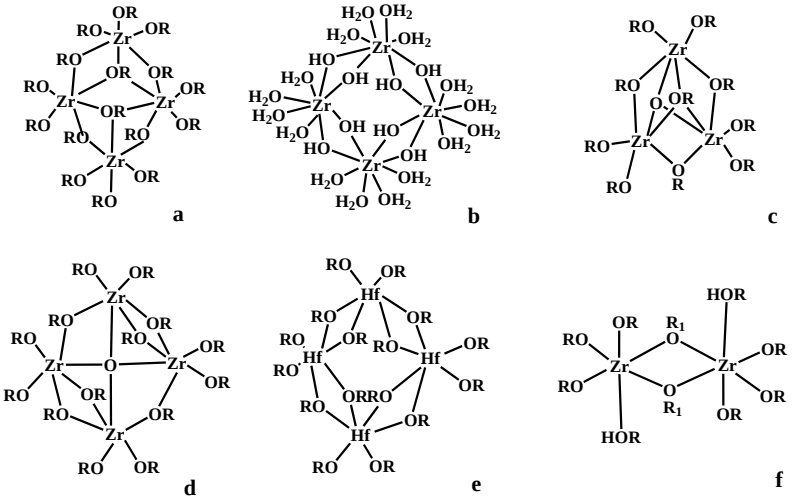

*Figure 2.1: Schematic representation of $Zr_4(OPr)_{16}$ (**a**), $Zr_4(OH)_8(H_2O)_{16}^{8+}$ (**b**), $Zr_3O(OR)_{10}$ (**c**), $Zr_4O(OPr)_{14}$ (**d**), $Hf_4(OPr)_{16}$ (**e**), and $[Zr(O^nPr)(O^iPr)_3(^iPrOH)]_2$ (**f**).*

Samples of the solid phase that was formed in the waxy liquid and the waxy-liquid itself were both analyzed by NMR. The analysis was performed on various samples which were obtained from different batches of zirconium *n*-propoxide. The observations for all samples were identical and thus regardless of the batch of commercial precursor used. Spectra of the waxy liquid phase were recorded at various temperatures. From Figure 2.2 it can be seen that the temperature has a tremendous influence on the quality of the spectrum. It can be seen that decreasing the temperature from 303 K, to 273 K and finally 243 K (Figure 2.2a, b and c, respectively) improves the resolving of the signals. The spectra recorded at 243 K clearly display a large number of unresolved signals due to the presence of several compounds.

A typical spectrum of the solid phase is depicted in Figure 2.2d. All samples of the solid phase showed the same signals. However, the intensity of signals marked with an asterisk differed per sample. The signals at 0.9, 1.6 and 3.6 ppm are expected for the propoxide sample, but the marked signal 1.49 and 1.7 ppm are unexpected and its origin is not yet clear.

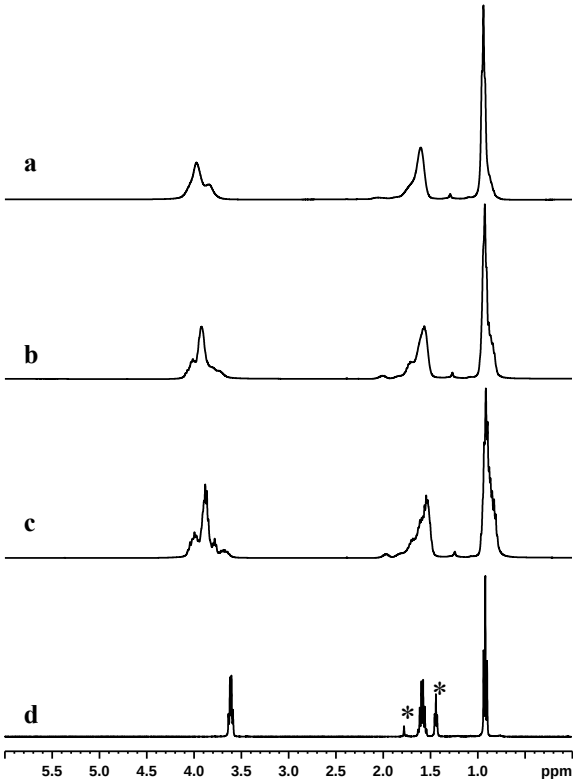

*Figure 2.2: NMR spectra obtained from the waxy liquid (bulk) phase recorded at: 303 K (**a**), 273 K (**b**) and 243 K (**c**), respectively. A typical spectrum of the solid phase formed upon drying of zirconium n-propoxide is displayed in **d**.*

From 2-d NMR COSY experiments it became clear that the signals around 1.45 ppm (marked with an asterisk) are three singlets and in HSQC mode it could clearly be seen that none of the protons of the signals at 1.49 ppm were coupled to a carbon atom. This indicates that they are most likely coupled to a nitrogen or an oxygen atom, which in the latter case could mean that hydrolyzed groups are present.

The presence of a residue of ammonium used in the preparation of zirconium *n*-propoxide may be considered. However, elementary analysis on the solid phase showed no indications for the presence of nitrogen. To evaluate wheater or not the unexpected signals found in the NMR spectrum are due to hydrolyzed species several experiments were preformed. The spectrum of $Hf_4(OH)_8(H_2O)_{16}Cl_8$ was recorded in order to identify the positions of the protons of the *OH* groups. The main signal is at 1.7 ppm and this position can also be expected for the analogous zirconium compound since the chemical shift is expected to be comparable. The presence of a small amount of hydrolyzed species, *e.g.*, the residual chloride with a $Zr_4(OH)_8(H_2O)_{16}^{8+}$ core as is depicted in Figure 2.1t might be an explanation for the small signal observed in the spectra obtained from the solid phase at this chemical shift. The origin of these species is not clear, since the solvents were subjected to appropriate drying, as will be discussed below, these species are thus already present in the commercial sample. The indication on what the nature of the signal at 1.7 ppm is leaves only the signals at 1.49 ppm unexplained.

The explanation for the nature of the signals at 1.49 ppm was, to our surprise, found when the experiment was repeated using d_8-toluene in stead of $CDCl_3$ as solvent. Several spectra were recorded while the sample was cooled from room temperature to 243 K. The specrum at room temperature was as displayed in Figure 2a and the first spectrum at low temperature showed still good resemblance with this spectrum. However, within the next few minutes the obtained spectra changed rapidly giving eventually a spectrum analogous to that depicted in Figure 2.2d. A closer look at the sample after it was removed from the NMR showed the formation of solids in the NMR tube. Apparently, a phase separation occurs, resulting from redistribution of oxo-ligands, *i.e.*, formation of poorly soluble poly-oxo-species and small amount of non-oxo-alkoxide. The three major signals in this spectrum are very close to those for *n*-propanol, and results from non-oxo-alkoxide in quick exchange with traces of residual alcohol. The signals at 1.49 ppm should thus be considered as corresponding to Zr-OH groups from highly condensed species resulting from this disproportionation. The formation of the solid as a result of hydrolysis due to traces of water in the solvent was excluded by preparing samples using the very moisture sensitive zirconium *t*-butoxide. These

samples did not show formation of any solids and the obtained spectra were as one would expect.

In addition we also evaluated if analogous observations would be obtained for zirconium *n*-butoxide in *n*-butanol. It turned out to be possible to obtain a solid and a waxy liquid phase. The obtained ^{1}H NMR spectra of these phases show great similarity to those obtained for zirconium *n*-propoxide. Again, the waxy liquid contains a number of unresolved peaks, while the spectra of the solid contain the expected four signals for butanol. This indicates that also a phase separation occurs in the NMR samples containing the solid phase and thus suggesting the presence of oxo-species.

Mass spectrometric experiments were conducted to get insight in the type of compounds. The mass spectrum (500-2000 m/z) of the waxy liquid phase displayed a major signal at 1148 m/z (100%) and a number of minor signals which are all summarized in Table 2.1 (TS1). From the assignment of the fragments in the gas phase can be seen that major part of the compounds are tetranuclear. A major difference is noticeable if the low mass spectrum of the solid phase is compared with that of the viscous liquid (Table 2.1, TS3 and TS2, respectively). It can be seen that a large part of the signals in the spectrum of the solid phase are due to fragments with a Zr_3 nature, indicating that the composition of the separated fraction is mainly $Zr_3O(OPr)_{10}$ (this type of molecular structure is depicted in Figure 2.1c). Unfortunately, the recorded spectra of the solid phase displayed only the masses up to 1000 m/z. The presence of signals at higher masses *e.g.*, due to tetranuclear compounds can not be excluded.

The presence of $Zr_3O(OR)_{10}$ in zirconium *n*-propoxide was already suggested by *e.g.*, Day *et al.* [8] and Turevskaya *et al.* [9]. However, up to now no evidence has been provided for the existence of $Zr_3O(O^nPr)_{10}$ in commercial zirconium *n*-propoxide. The amount of formed solid phase is in the order of a few percents and probably corresponds to the compound removed upon distillation at 185-220 °C [8]. This would imply the presence of 3-5 % of $Zr_3O(O^nPr)_{10}$ in separable form in commercial zirconium *n*-propoxide. We checked the possibility of the formation of $Zr_3O(O^nPr)_{10}$ during the removal of the solvents by collecting the volatiles removed from the commercial product. The GC-MS analysis of the

volatiles from the commercial 70 wt% solutions of "$Zr(O^nPr)_4$" and 80 wt% solutions of "$Zr(O^nBu)_4$" (which will be discussed below) displays only the parent alcohols and also traces of heptanes (used supposedly in the synthesis). It is thus possible to completely exclude the possibility of $Zr_3O(OR)_{10}$ formation in the course of the drying of the samples.

Table 2.1: Interpretation of M/z(I) spectrum of the liquid and solid phases of the zirconium n-propoxide. For reasons of clarity P = $Zr_3O(OR)_{10}$.

Gas phase fragments	Viscous liquid	Viscous liquid	Solid phase
$Zr_4O(OPr)_{13}^+$	1145 (100)		
$Zr_4O_2(OR)_{11}^+$	1045 (15)		
$Zr_4O_2(OR)_9^+$		923 (36)	923 (1.9)
$Zr_3O(OR)_9(OH)^+$, P – C_3H_6			834 (4.5)
$Zr_4O_3(OR)_7$	821 (26)	821 (100)	821 (9.0)
$Zr_3O(OR)_9^+$, P – OR	817 (21)	817 (71)	817 (8.1)
$Zr_3O(OR)_8(OH)_2^+$, P – $2C_3H_6$		792 (9)	792 (0.6)
$Zr(OPr)_8$ –CH_3	727 (15)		
$Zr_3O_2(OR)_7^+$, P – OR – R_2O	715 (5)	715 (22)	715 (18.5)
$Zr_3O_2(OR)_6(OH)_2^+$, P – $2C_3H_6$ – 2OR			690 (2.2)
$Zr_4O_2(OR)_5^+$			687 (1.8)
$Zr_3O_3(OR)_5^+$, P – OR – $2R_2O$	613 (19)	613 (15)	613 (10.1)
$Zr_2(OR)_7^+$		593 (16)	593 (3.5)
$Zr_3O_3(OR)_4(OH)_2^+$, P – $2C_3H_6$ – 2OR – R_2O			588 (3.0)
$Zr_4O_2(OR)_3(OH)^+$			586 (3.5)
$Zr_2O(OR)_6^+$			548 (17.8)
$Zr_4O_2(OR)_2(OH)_2^+$	544 (10)	544 (35)	544 (28.4)
$Zr_3O(OR)_4(OH)^+$, P – C_3H_6 – 5OR			539 (10.5)
$Zr_2(OR)_6^+$			534 (10.5)
$Zr_3O_4(OR)_3^+$, P – OR – $3R_2O$		511 (10)	511 (24.4)
$Zr_2O(OR)_5^+$, P – OR – $Zr(OR)_4$		491 (33)	491 (100)
$Zr_3O(OR)_3(OH)^+$, P – C_3H_6 – 6OR			480 (32.5)
$Zr_4O_3(OH)_2^+$			442 (13.8)
$Zr_2(OR)_3(OH)_2^+$			391 (12.6)
$Zr(OR)_3^+$			267 (20.5)
$Zr(OR)_2^+$			208 (2.4)

The ^{1}H NMR and mass spectrometry experiments were also performed on commercial zirconium n-butoxide. The removal of the volatiles provided again a solid phase and a viscous liquid and the ^{1}H NMR analysis displayed a behavior analogous to zirconium n-propoxide. Mass spectrometry experiments were performed to get confirmation for the presence of $Zr_3O(OBu)_{10}$. Data of mass spectrometry presented by Turevskaya *et al.* [9] indicate that the majority of zirconium *n*-butoxide consists of $Zr_4(OR)_{16}$. The major fragment found in that

study was $Zr_4O_3(OR)_9^+$ at 1065 *m/z* (100%). In the spectrum obtained for the solid phase the major fragment is found at 628 m/z (100%) and assigned to $Zr_3O(OR)_9$, the signal at 1065 m/z is <10%. The great difference between the spectra of the solid phase in this study and that of zirconium *n*-butoxide [9] indicates a high concentration of $Zr_3O(OBu)_{10}$ in the solid phase. This result is analogous with that obtained for zirconium *n*-propoxide.

With the identification of the rather small amounts (3-5%) of $Zr_3O(O^nPr)_{10}$ in the zirconium *n*-propoxide, the complex nature of the obtained ^1H NMR is still not explained. We attempted to get more insight in the present compounds by preparing samples with various amounts of solid phase and waxy liquid phase. The ^1H NMR spectra of these different samples displayed only marginal differences and did not provide any information on the composition. The ^{13}C NMR spectra of the various samples showed a clear difference. The spectra displayed in Figure 2.3 were taken from the waxy liquid (top spectrum) and waxy liquid with an amount of solid phase (largest amount for third spectrum from the top). A clear difference between the spectra is observed and the difference in intensities allows identification of sets four sets of signals, *i.e.*, marked with 1-4, respectively. This indicates that there are a corresponding amount of compounds present in zirconium n-propoxide. It should be noted that the signals of the α-carbon of the different compounds could be assigned. The β-carbons of some of the signals marked with 1 and 3 were already overlapping while the assignment of the signals around 10 ppm was no longer possible.

The main species in zirconium *n*-propoxide is $Zr_4(O^nPr)_{16}$ [8]. The most intense signals in the waxy liquid phase, indicated with 1, are in agreement with the spectrum of $Zr_4(O^nPr)_{16}$ [8]. It can also be seen that in the spectrum of the waxy liquid that there is also a significant amount of compound 2 (the unlabeled signals in the spectrum) and compound 3. Purification of 100 ml zirconium *n*-propoxide yields 40 g of $Zr_4(O^nPr)_{16}$, 10 g of an unknown compound and 20 g of unknown residual products [8]. The NMR data of the waxy liquid and the yields reported for the preparation of $Zr_4(O^nPr)_{16}$ suggest that the commercial product contains up to 65-70% $Zr_4(O^nPr)_{16}$.

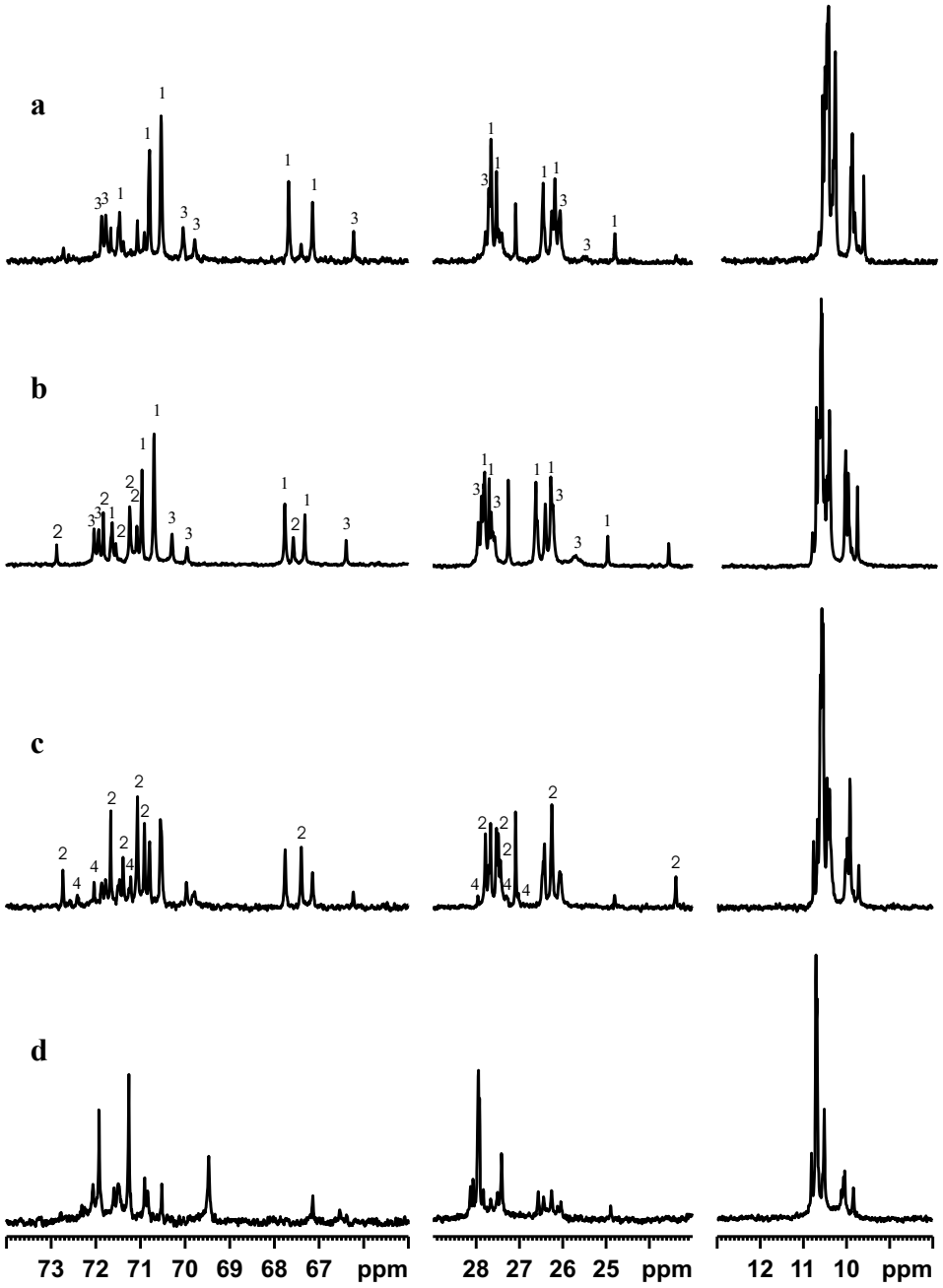

*Figure 2.2: NMR spectra (**a-c**) obtained from the waxy liquid (bulk) phase containing various amount of solid phase (concentration of solid phase is highest in c). The NMR spectrum of hafnium n-propoxide is depicted in **d**.*

On basis of the mass spectrometry data the unidentified compounds should include $Zr_3O(O^nPr)_{10}$ and tetranuclear compounds. The spectrum obtained from the sample containing the largest amount of solid phase displays three small signals (marked with 4) which are not observed in the other spectra. These signals could very well be due to $Zr_3O(O^nPr)_{10}$, since one would expect 3 signals for that compound. The spectrum with the largest amount of the solid phase is expected to rich of oxo-species, *i.e.*, phase separation occurs in non-polar solvents. This suggests that the signals marked with 2 are due to an oxo-compound and on the basis of the mass spectrometry data it should be a tetranuclear compound (*e.g.*, as depicted in Figure 2.1d). The exact nature of compounds 2 and 3 will remain unclear with only these data available.

The prepared hafnium *n*-propoxide was also characterized by mass spectrometry and also ^{13}C NMR spectra were recorded (depicted in bottom spectrum in Figure 2.3). The mass spectra displayed one major signal (1501 m/z(100%)) which is assigned to $Hf_4(OPr)_{13}(OH)^+$. The other intensities were observed at 1539 (13.8%) , 1485 (8.3), 1410 (21.0%), 1396 (12.3%), 1084 (16.7%) and assigned to $Hf_4(OPr)_{14}^+$, $Hf_4(OPr)_{12}(O)_4^+$, $Hf_4(OPr)(O)_3^+$, $Hf_4(OPr)(OH)_2^+$, $Hf_3(OPr)_9(OH)^+$, respectively.

From the mass spectrum it can be assumed that there are several tetranuclear compounds present in this sample and a minor amount of trinuclear. The appearance of the ^{13}C NMR spectrum of this sample differs strongly for the spectra obtained for zirconium *n*-propoxide. The NMR spectrum shows clearly that the structure of this compound is not analogous to that observed for zirconium (*i.e.*, the compound which the signals marked with 1 are attributed to). The solution structure of this hafnium compound could be as depicted in Figure 2.1e, which would be an explanation for the two most intense signals in the obtained NMR spectrum.

It has thus been demonstrated that in both zirconium *n*-propoxide and *n*-butoxide and hafnium n-propoxide industrial samples contain various compounds. Mass spectrometry clearly shows that there is 4-6% $Zr_3O(OR)_{10}$ present in commercial zirconium *n*-propoxide. The product contains further up to 65-70 % $Zr_4(O^nPr)_{16}$, indicating there is a serious amount of other compounds. The ^{13}C NMR studies

indicate that there are two other compounds present, which are tetranuclear according to the mass spectrometry data and at least one of these compound is expected to be an oxo-alkoxide species. The prepared hafnium *n*-propoxide turns out to be a mixture of various compounds. The main specie seems to be $Hf_4(O^nPr)_{16}$ but its solution structure seems to be different from that of zirconium *n*-propoxide

With the presence of several compounds *i.e.*, oxo-alkoxide species, there may be a need for alternative uniform structured zirconium precursors for reproducible preparation of materials. In this respect, the precursors with propoxide ligands are preferred above those with butoxide, since the propanol solvent can be removed more easily due to the lower boiling point.

Zirconium isopropoxide isopropanol solvate, $[Zr(O^iPr)_4(^iPrOH)]_2$ [10], is considered a poor alternative since it is rather expensive, and poorly soluble in parent alcohol and toluene. The mixed ligand precursor $[Zr(O^nPr)(O^iPr)_3(^iPrOH)]_2$ recently reported by Seisenbaeva *et al.* [12], is more interesting. Both precursors have the dinuclear structure as depicted in Figure 2.1e. As for the mixed ligand precursor, the *n*-propoxide ligands are in the position labeled with OR_1. The mixed ligand precursor has been prepared according to the synthesis described above and in ref. [12]. The yield, after the separation of three batches of crystals, of $[Zr(O^nPr)(O^iPr)_3(^iPrOH)]_2$ from 10 ml of zirconium *n*-propoxide was slightly higher compared to the route described in ref. [12] *e.g.*, 7.8 g and 7.4 g. The main advantage of the synthesis route presented here is the lower volume in the crystallization step.

The products of both routes were characterized by NMR and turned out to give spectra (Figure 2.3b) in accordance with the expected structure [12]. The triplets at 3.86 ppm and 0.87 ppm and the sextet at 1.65 ppm are due to the *n*-propoxide ligands in the bridging position ($\underline{OCH_2}$, $\underline{CH_3}$ and $\underline{CH_2}$, respectively). While the septet at 4.28 ppm and the doublet at 1.18 ppm can be assigned to the $\underline{CH}$ and $\underline{CH_3}$ of the isopropoxide groups in the terminal position.

It was judged to be of interest to see if the solution that was removed from the last batch of crystals contained the same complexity as that found for zirconium *n*-propoxide. The solution separated from the third batch of crystals of

$[Zr(O^nPr)(O^iPr)_3(^iPrOH)]_2$ was dried under vacuum. The spectrum of the obtained material is displayed in Figure 2.3b. The main difference in the present spectrum with that obtained for $[Zr(O^nPr)(O^iPr)_3(^iPrOH)]_2$ can be seen in the signals between 3.8 and 4.5 ppm and the disappearance of the signal at 3.65 ppm. The yield of $[Zr(O^nPr)(O^iPr)_3(^iPrOH)]_2$ was ~90% which means that the majority of oxo-species have been converted into an oxo-ligand free product. The residual of the synthesis contains ~10% of the zirconium precursor and from the NMR spectrum (Figure 2.3b) can be seen that there is still a small amount of $[Zr(O^nPr)(O^iPr)_3(^iPrOH)]_2$ present. This amount is estimated to be ~30% of the residual sample, hence 7% of the initial precursor is not converted. Above we postulated that up to 70% of the sample consisted of $Zr_4(OPr)_{16}$. If the remaining 30% would be oxo-species and the oxo-ligands (1:4 compared to the alkoxide ligands) concentrated into poly-oxoaggregates, $Zr_nO_{2n-x}(OPr)_{2x}$, as has been demonstrated for aluminium propoxide compounds [13], 7.5% of the original sample would be present in the residual. The composition of the residual seems to match our estimate considering the amount of $Zr_4(OPr)_{16}$ in the commercial sample.

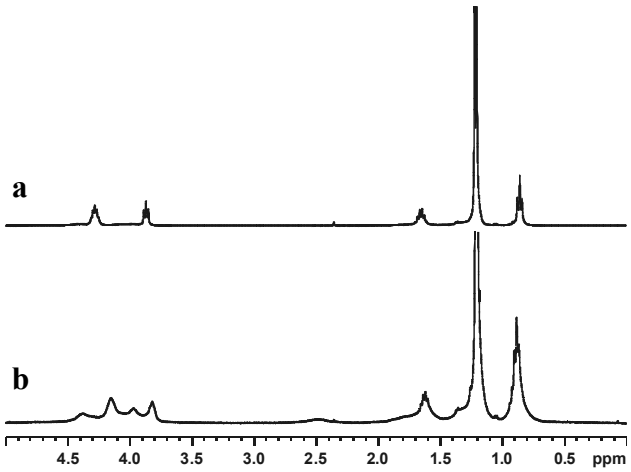

*Figure 2.3: NMR spectra of $[Zr(O^nPr)(O^iPr)_3(^iPrOH)]_2$ (**a**), and the residue of the synthesis (**b**).*

The mass spectrometric analysis of $[Zr(O^nPr)(O^iPr)_3(^iPrOH)]_2$ showed a great number of signals between 450 and 600 *m/z*. The most dominant peaks at 532 (100%), 564 (~97%) and 593 (~55%) *m/z* can be assigned to $Zr_2(OR)_6$,

$Zr_2(OR)_6(OCH_2)^+$ and $Zr_2(OR)_7$, respectively. Except for the signal at 817 *m/z* (<5%), there were no signals corresponding to a higher mass being present. The latter supposedly originates from partial decomposition on evaporation as indicated by its low intensity.

The mass spectrometry data clearly shows that $[Zr(O^nPr)(O^iPr)_3(^iPrOH)]_2$ is dimeric in the gas phase. This result is in contrast to the mass spectrometry data for zirconium isopropoxide [9], where a significant amount of Zr_4 compounds were present, *i.e.,* a lot of signals were obtained at higher masses. The fact that $[Zr(O^nPr)(O^iPr)_3(^iPrOH)]_2$ consists of dimeric species in the gas phase strengthens the assumption that the precursor consists of one compound.

2.4 Conclusions

The composition of zirconium *n*-propoxide and *n*-butoxide has been examined NMR and mass spectrometry. Upon evaporation of the parent solvent, a two-phase system comprising of a solid and a waxy liquid phase is obtained for both precursors. ^{13}C NMR study of these phases indicated the presence of 4 different compounds, including a trinuclear zirconium oxo-alkoxide ($Zr_3O(OR)_{10}$). The presence of $Zr_3O(OR)_{10}$ has been confirmed by mass spectrometric analysis. The remaining species are all tetranuclear and it is estimated that at least 65-70% of the commercial product is $Zr_4(OnPr)_{16}$. The other two compounds are expected to oxo-rich. The main compound in the home made hafnium *n*-propoxide is tetranuclear and its structure is different from the observed zirconium compounds.

A new route has been presented for synthesis of the mixed ligand precursor $[Zr(O^nPr)(O^iPr)_3(^iPrOH)]_2$, from zirconium *n*-propoxide. A high yield has been observed (~90%), indicative of an almost complete precursor transformation and provides support for the estimated contains of 65-70% $Zr_4(OnPr)_{16}$. Mass spectrometry has shown that the synthesized mixed ligand precursor is dimeric, which makes it an attractive alternative for zirconium *n*-propoxide.

2.5 References

1 S. Benfer, U. Popp, H. Richter, C. Siewert, G. Tomandl, *Sep. Purif. Technol*., **22-23**, 231 (2001).

2 R.J. Vacassy, C. Guizard, J. Palmeri and L. Cot, *Nanostruct. Mater*., **10**, 77 (1998).

3 C.R. Xia, H.Q. Cao, H. Wang, P.H. Yang, G.Y. Meng and D.K. Peng, *J. Membr. Sci*., **162**, 181 (1999).

4 M. Haruta, T. Kobayashi, H. Sano and N. Yamada, *Chem. Lett*., **829**, 405 (1987).

5 A. Knell, P. Barnickel, A. Baiker and A. Wokaun, *J. Catal*., **137**, 306 (1992).

6 S. Hoffman, M. Klee and R. Waser, *Integr. Ferroelectr*., **10**, 155 (1995).

7 M. Klee, U. Mackens, W. Hermann and E. Bathelt, *Integr. Ferrolectr*., **11**, 247 (1995).

8 V.W. Day, W.G. Klemperer and M.M. Pafford, *Inorg. Chem*., **40**, 5738 (2001).

9 E.P. Turevskaya, N.I. Kozlova, N.Y. Turova, A.I. Belokon, D.V. Berdyev, V.G. Kessler and Y.K. Grishin, *Russ Chem. Bull*., **44**, 734 (1995).

10 B.A. Vaartstra, J.C. Huffman, P.S. Gradeff, L.G. Hubert-Pfalzgraf, J.-C. Daran, S. Parraud, K. Yunlu and K.G. Caulton, *Inorg. Chem*., **29**, 3126 (1990).

11 T.J. Boyle, J.J. Gallegos, D.M. Pedrotty, E.R. Mechenbier and B.L. Scott, *J. Coord Chem*., **47,** 155 (1999).

12 G.A. Seisenbaeva, S. Gohil, V.G. Kessler, *J. Mater. Chem*., **14**, (21), 3177 (2004).

13 Z.A. Starikova, V.G. Kessler, N.Y. Turova, D.E. Tcheboukov, E.V. Suslova, G.A. Seisenbaeva and A.I. Yanovsky, *Polyhedron*, **23**, 109 (2004).

Chapter 3

Structure and stability of compounds formed upon the modification of zirconium and hafnium propoxide precursors by acetylacetone*

Abstract

The nature of the heteroleptic intermediates in the modification of different zirconium propoxides by acetylacetone characterized in this study is not in agreement with the structures and reaction mechanisms proposed in earlier literature. Upon addition of up to 1 mol equivalent of Hacac, the fairly stable $[Zr(O^iPr)_3(acac)]_2$ is formed. When additional Hacac is added, the structure of $[Zr(O^iPr)_3(acac)]_2$ is destabilized leading to the formation of the initial precursor and unstable $Zr(O^iPr)(acac)_3$. Spontaneous rearrangement of $Zr(O^iPr)(acac)_3$ to stable $Zr(acac)_4$ occurs rapidly at room temperature. This mechanism has also been proven for hafnium isopropoxide and zirconium *n*-butoxide. Both systems seem to involve analogous intermediates, of which $[Hf(O^iPr)_3(acac)]_2$ has been successfully isolated and characterized.

Quantum chemical calculations displayed that there is no inherent electronic difference in stability between zirconium and hafnium in the complex compounds studied here. ^1H NMR monitoring of the concentration of $[Zr(O^iPr)_3(acac)]_2$ and $[Hf(O^iPr)_3(acac)]_2$ suggests that these compounds transform relatively quickly in time. The driving force for this transformation is the formation and crystallization

* Part of this chapter has been published in: "Stabilization and destabilization of zirconium propoxide precursors by acetylacetone," Gerald I. Spijksma, Henny J.M. Bouwmeester, Dave H.A. Blank and Vadim G. Kessler, *Chem. Commun.*, **16**, 1874 (2004). Reproduced with the permission of The Royal Society of Chemistry.

of unreactive $M(acac)_4$. The effect of this rapid transformation on derived materials is evaluated by comparing the properties of sols derived from fresh and solid-state aged $[Zr(O^iPr)_3(acac)]_2$. SAXS data shows different scattering behavior for the sols obtained from fresh compared to those from aged samples. TEM images of the dried sols also show a clear difference in the size distributions of the initial sol particles. Light scattering experiments on the re-dispersed powder are in good agreement with TEM observations

.

3.1 Introduction

The application of unmodified zirconium and hafnium precursors in, for instance, MOCVD (molecular organic chemical vapor deposition) or sol-gel synthesis is a difficult task due to the extreme moisture sensitivity of these precursors. A method generally applied to moderate the reactivity is exchanging (part of) the alkoxide ligands with chelating organic ligands [1,2]. In sol-gel studies, acetic acid and acetylacetone are most often applied for this purpose [3]. Both of the complexing ligands mentioned are bidentate. The acetic acid can be bridging or chelating, while the acetylacetone is only chelating. The main drawback for the application of acetic acid is its ability to form an ester with alcohol, whereas water released in this reaction initiates hydrolysis and condensation of the precursor. Therefore acetylacetone can currently be considered the most commonly used modifier for zirconium and hafnium precursors in sol-gel applications.

There is a broad spectrum for the application of sol-gel derived materials, ranging from mesoporous materials for catalyst supports and for membranes [4,5], to high-tech applications like thin films, fibers [6,7], aerogels [8] and (nano-) particles [9-11]. Applications of thin films can be as microporous membrane layers [12-14], high-temperature thermal barrier coatings or as ferroelectrics [15]. In addition to all these applications, several theoretical studies have been performed using Hacac modified precursor systems [16-18].

Despite being frequently applied for various applications, there have been to the best of our knowledge, no reports published on zirconium and hafnium precursor structures formed upon modification with Hacac. In 1970, Saxena *et al.* and Puri [19,20] independently reported the formation of mono-, di- and trisubstituted derivatives upon the modification of zirconium isopropoxide with stoichiometric amounts of Hacac. The further modification of the disubstituted compounds, for precursors in MOCVD, has recently been reported [21]. However, no structural data was reported in these studies.

In 1991, a model describing the effect of the Hacac modification on sol preparation was proposed by Ribot *et al.* [22]. The authors proposed that the structure of the cerium isopropoxide precursor in propyl alcohol, $[Ce_2(O^iPr)_8(^iPrOH)_2]$, is altered

upon addition of 0.5, 1 or 2 mol equivalents of Hacac giving $[Ce_2(O^iPr)_7(acac)(^iPrOH)]$, $[Ce_2(O^iPr)_6(acac)_2(^iPrOH)_2]$ and $[Ce(O^iPr)_2(acac)_2]$, respectively. It is generally assumed that this model for cerium(IV) also applies for the modification of zirconium and hafnium by acetylacetone.

A di-acac-substituted zirconium *n*-butoxide compound, which is commercially available, has been used by Collins *et al.* [23] as a precursor. Collins *et al.* [23] claimed the existence of a relationship between the molecular configuration of the precursor and the resulting oxide after pyrolysis. For zirconium and hafnium isopropoxide modified with 2,2,6,6,-tetramethyl-3,5-heptanedionate (Hthd), a larger β-diketonate compared to Hacac, the monosubstituted structures, $[Zr(O^iPr)_3(thd)]_2$ and $[Hf(O^iPr)_3(thd)]_2$, have been reported [24]. Also, the existence of a disubstituted zirconium compound has been proposed [24-26] and this compound is commercially available and frequently used as a source for MOCVD. The modification of titanium precursors (*i.e.*, methoxide, ethoxide and isopropoxide) by Hacac involves the formation of $[Ti(OR)_3(acac)]_2$ and $Ti(OR)_2(acac)_2$ species [27]. One of the major differences between the Hacac modification of titanium and zirconium, hafnium and cerium is the ability of these last three systems to form completely substituted compounds, *i.e.*, $M(acac)_4$ [28]. These compounds do not have any alkoxide ligands and therefore are not suitable for sol-gel processing.

Currently, there is no consensus regarding the modification of zirconium and hafnium alkoxides by Hacac. The present work deals with the Hacac modification of zirconium and hafnium propoxide precursors. An attempt is made to isolate and characterize the heteroleptic intermediates formed in these systems. The modification of zirconium *n*-butoxide is also examined. The stability of the obtained intermediate compounds is evaluated and the effect of unstable compounds on the reproducible materials preparation is evaluated.

3.2 Experimental

All manipulations were carried out in a dry nitrogen atmosphere using the Schlenk technique or a glove box. Hexane and toluene (Merck, *p.a.*) were dried by distillation after refluxing with $LiAlH_4$, *n*-propanol (Merck, *p.a.*) was dried by

distillation after refluxing with $Al(O^nPr)_3$. Acetylacetone (Hacac) was purchased from Aldrich. Molecular sieves were added to the Hacac to assure that it remained water free. ^1H NMR spectra were recorded in $CDCl_3$ for all compounds on a Bruker 400 MHz spectrometer at 243 K.

Synthesis: The zirconium propoxide precursors used as starting materials in this work are zirconium isopropoxide, ($[Zr(O^iPr)_4(^iPrOH)]_2$ 99.9%), 70 wt% solution of "$Zr(O^nPr)_4$" in *n*-propanol, 80 wt% solution of "$Zr(O^nBu)_4$" in *n*-butanol (all purchased from Aldrich) and $[Zr(O^nPr)(O^iPr)_3(^iPrOH)]_2$ which was prepared according to a recently developed technique [29,30]. The zirconium isopropoxide was dissolved and recrystallized from toluene prior to use in order to remove impurities. The hafnium isopropoxide was prepared by anodic oxidation of hafnium metal in isopropanol [31] and recrystallized from toluene. All the different precursors were modified with various equivalent amounts of Hacac according to the techniques described below. The exact composition of the single crystals **1 - 3** was established with single crystal X-ray crystallography.

$[Zr(O^iPr)_3(acac)]_2$ (**1**): Zirconium isopropoxide solvate (weight: 3.78 g (9.8-mmol)) was dissolved in a 12 ml mixture of hexane and toluene (volume ratio 2:1). After adding an equivalent amount of acetylacetone (0.98 g, 9.8 mmol) the sample was dried under vacuum (0.1 mm Hg) and subsequently redissolved in 4 ml hexane. Crystallization occurred during cooling at -30 °C overnight. The solution was decanted from the obtained X-ray quality colorless crystals (4.02 g, yield 84%) that were identified as **1**.

$[Zr(O^iPr)(acac)_3]$ (**2**): Zirconium isopropoxide solvate (weight: 0.79 g (2.05 mmol)) was dissolved in a 3 ml mixture of hexane and toluene (volume ratio 2:1). After the addition of two mol equivalents of acetylacetone (0.41 g, 4.1 mmol) the sample was dried under vacuum (0.1 mm Hg) and subsequently redissolved in hexane. Crystallization occurred during cooling at -30 °C over night. The solution was decanted from the obtained X-ray quality crystals (0.45 g, yield 38%) that were identified as **2**.

$[Hf(O^iPr)_3(acac)]_2$ (**3**): Hafnium isopropoxide solvate (weight: 1.41 g (3.0 mmol)) was dissolved in a 6 ml mixture of hexane and toluene (volume ratio 1:1). After addition of 0.30 g (3.0 mmol) of Hacac, *i.e.*, 1 mol equivalent, the solution was

removed from the mixture under vacuum (0.1 mm Hg). The obtained yellow, viscous liquid product was subsequently redissolved in 1 ml hexane. The sample was stored overnight at -30 °C for crystallization. The solution was decanted from the obtained X-ray quality colorless crystals (1.15 g, yield 67%) that were identified as **3**.

Sol preparation: $[Zr(O^iPr)_3(acac)]_2$ was dissolved in a mixture of hexane and isopropanol (volume ratio 2:1) providing a concentration of zirconium of ~1 mol/l. The hydrolysis was performed by adding water that was diluted 20 times by a hexane and isopropanol (volume ratio 2:1) mixture. The ratio of water and zirconium was set at 1:1. Two different sols were prepared according to the described procedure using freshly prepared **1** or dried crystals of **1** that were aged for a week at room temperature, respectively. The obtained sols were sealed in capillaries (type Hilgenberg No. 14, 1.0 mm in diameter) and characterized by SAXS. The remaining sol was dried in air and the obtained slightly yellowish powder was characterized by transmission electron microscopy (TEM, PHILIPS CM30 Twin/STEM). The powder was redissolved in isopropanol (~1 g powder in 20 ml propanol) and deposited on a copper grid supported by an amorphous carbon film. The particle size of the redissolved powder was also measured by light scattering (Zetasizer 3000HS instrument).

Crystallography: Data collection for single crystals of all compounds was carried out at 22 °C on a SMART CCD 1k diffractometer with graphite monochromated MoKα radiation. All structures were solved by standard direct methods. The coordinates of the metal atoms as well as the majority of other non-hydrogen atoms were obtained from the initial solutions and for all other non-hydrogen atoms found in subsequent difference Fourier syntheses. The structural parameters were refined by least squares using first isotropic and then, also anisotropic approximations. The coordinates of the hydrogen atoms were calculated geometrically and were included in the final refinement in isotropic approximation for all the compounds. All calculations were performed using the SHELXTL-NT program package [32] on an IBM PC.

Calculations: All quantum chemical calculations were made using the program package *Gaussian 03* (Rev. C.02) [33], employing the hybrid density function

B3PW91. The basis sets used for H, C, N and O were of 6-311G quality including additional diffusion and polarization functions. The basis sets used for Zr and Hf employed quasi-relativistic (MWB) effective-core potentials, thus taking scalar relativistic effects into account, replacing 28 and 60 electrons, respectively, with adapted basis sets of (8s7p6d)/[6s5p3d] quality [34]. All metal complexes and ligands were geometrically optimized to a maximum of symmetry (Figure 3.1).

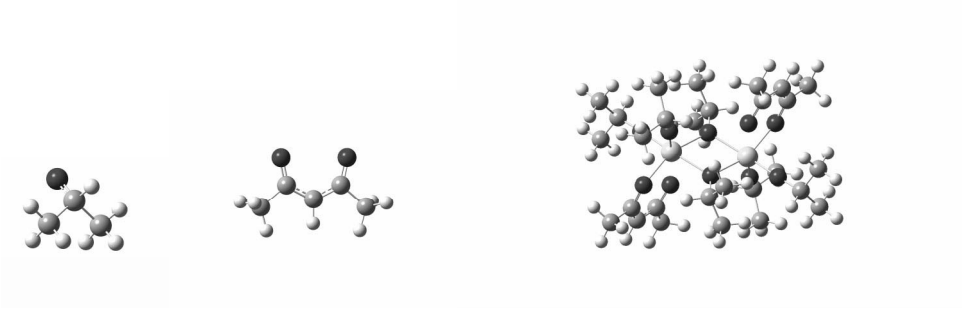

Figure 3.1: Optimized geometries for O^iPr^- (C_s), acac (C_3), $[M(O^iPr)_3(acac)]_2$ (with M = Zr or Hf) (C_i).

3.3 Results and discussion

The zirconium propoxide precursors utilized in this study, *i.e.*, zirconium *n*-propoxide, isopropoxide and mixed ligand compound, were modified with 1 mol equivalent of Hacac, in a manner analogous to one described in the experimental section for zirconium isopropoxide. Only from this latter system could X-ray quality single crystals be obtained and characterized as $[Zr(O^iPr)_3(acac)]_2$ (**1**)[1] as is depicted in Figure 3.2. A similar compound has recently been reported [29], but the unit cell parameters of the compound reported in [29] deviate significantly from the one presented in this study. The unit cell parameters of the one in the present study are larger, *i.e.*, 10.004(16), 10.686(14) and 12.27(2) for **1** compared to 9.818, 10.639 and 11.790 reported in [29]. The difference is probably due to traces of $Co_2(acac)_4(^iPrOH)_2$ – a molecule with the same topology and almost identical geometry – in the compound reported in [29] since zirconium isopropoxo-

[1] Crystal data: $C_{28}H_{56}O_{10}Zr_2$, M = 735.17, triclinic, a = 10.004(16), b = 10.696(14), c = 12.27(2) Å, α = 87.74(4)°, β = 67.16(3)°, γ = 64.75(5)°, V = 1081(3) Å^3, T = 295 K, space group P-1, Z = 1, μ = 0.520 mm^{-1}, 5582 reflections measured, 4123 unique (R_{int} = 0.0222 which were used in all calculations. The final discrepancy factors were R1 = 0.0469; wR2 = 0.1018 for 2261 observed reflections (I > 2sigma(I)).

acetylacetonate was a side product in the synthesis of a heterometallic compound of zirconium and cobalt.

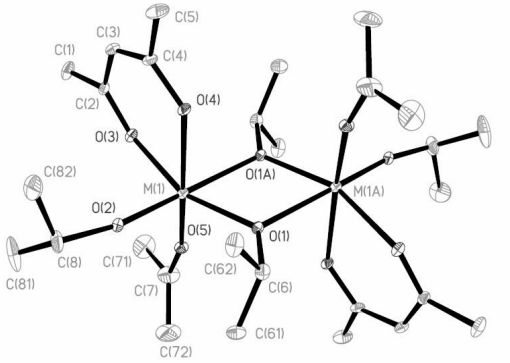

*Figure 3.2: Molecular structure of $[M(O^iPr)_3(acac)]_2$, with M = Zr (**1**) or Hf (**3**).*

Structural analogs of compounds **1** and its hafnium isomorph **3** have been reported earlier [35]. They were obtained upon the modification of zirconium and hafnium isopropoxide with 1 mol equivalent of 2,2,6,6,-tetramethylheptanedione (Hthd), the application of these compounds was proposed, however, for MOCVD (metal organic chemical vapor deposition). The utilization of the bulky Hthd as a modifier for sol-gel applications is not considered attractive due to the large amount of carbon in the (rather expensive) bulky ligand that has to be removed during thermal treatment of the derived material. The bulky ligands in Hthd make it a stronger chelating ligand compared to Hacac. This effect can also be seen when the bond lengths of $[Zr(O^iPr)_3(thd)]_2$ are compared with that of **1**. From Table 3.1 the expected elongation of all the metal-oxygen bonds can clearly be seen and also the angle O(1)-M-(O1A) is significantly larger.

*Table 3.1: Selected bond lengths and angles from the compounds **1**, **3**, $[Zr(thd)(O^iPr)_3]_2$ and $[Hf(thd)(O^iPr)_3]_2$. The data from the latter two compounds was taken from ref. [35].*

Bond / angle	**1**	**$[Zr(O^iPr)_3(thd)]_2$**	**3**	**$[Hf(O^iPr)_3(thd)]_2$**
M-O(1)	2.142(4)	2.119	2.058(9)	2.102
M-O(1A)	2.337(5)	2.219	2.147(9)	2.192
M-O(2)	2.022(4)	1.944	1.858(10)	1.953
M-O(3)	2.187(5)	2.153	2.096(10)	2.102
M-O(4)	2.264(4)	2.190	2.164(10)	2.169
M-O(5)	1.962(4)	1.931	1.906(10)	1.927
M(1)-M(1A)	3.598(6)	3.508	3.403(2)	3.476
O(1)-M-(O1A)	73.19(14)	72.07	71.9(4)	72.0

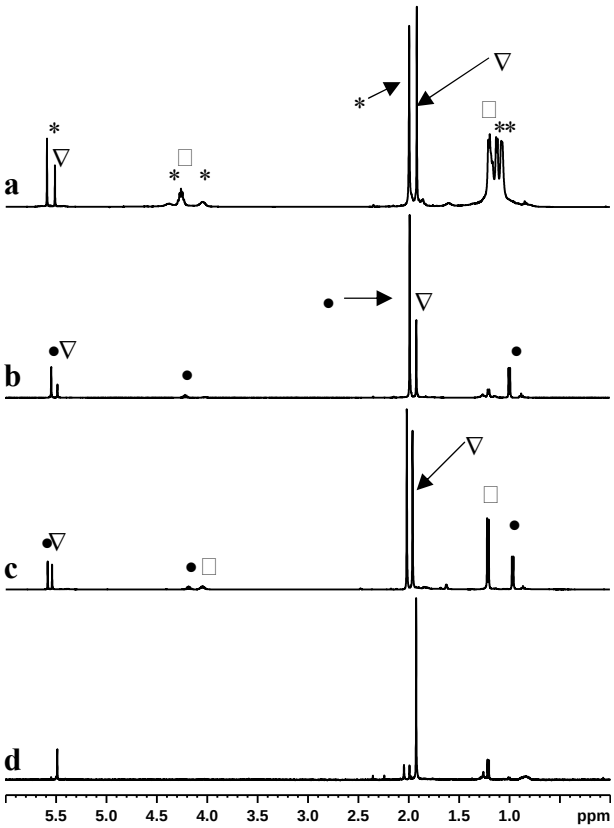

*Figure 3.3: Proton NMR spectra of (**a**) zirconium isopropoxide with 1 mol equivalent of acetylacetone. Spectrum (**b**) was obtained from Zr(O^{i}Pr)(acac)$_3$ (**3**)crystals. Spectrum (**c**) was recorded of the same compound about two hours later. Spectrum (**d**) is a reference spectrum of Zr(acac)$_4$. The signals corresponding to [Zr(O^{i}Pr)$_3$(acac)]$_2$ (**1**) are marked with (∗), to Zr(O^{i}Pr)(acac)$_3$ – with (•), to unmodified zirconium isopropoxide with (□) and Zr(acac)$_4$ – with (∇).*

^{1}H NMR spectra of **1** were recorded and a typical example of the obtained spectra is depicted in Figure 3.3a, the signals assigned to **1** are marked with (∗). The sharp singlet at 5.60 ppm and 1.97 ppm are the <u>*CH*</u> and <u>*CH$_3$*</u> of the acetylacetone, respectively. Their integrals are in the expected ratio of 1 to 6. The signals between 3.5 and 4.5 that are marked with (∗) were assigned to the <u>*CH*</u> of the alkoxide ligands and the signals in the region between 1.0 and 1.3 ppm are the <u>*CH$_3$*</u> signals of the compounds. The remaining signals, which are marked with (∇), were assigned to Zr(acac)$_4$, the reference spectrum of this compound is depicted in Figure 3.3d. The remaining signals are either due to the unmodified precursor

(marked with (□)) or some traces of the hydrocarbon solvents used in the synthesis, *i.e.*, toluene and hexane (not marked). Enhanced drying of the compound leads to a significant increase of the signals assigned to the unmodified precursor and $Zr(acac)_4$. This phenomenon will be discussed in detail below for **1**.

For the samples where zirconium *n*-propoxide or mixed ligand propoxide was modified with 1 mol equivalent with Hacac only spectra with multiple signals could be obtained, which indicates the formation of a mixture of compounds. The spectra contained the signals assigned to **1**, which is an indication for the formation of monosubstituted compounds. Recently, we reported the formation of analogous monosubstituted compounds from zirconium *n*-propoxide and mixed ligand precursors using Hthd as modifier [36]. The presence of the different compounds in the solution is probably one of the reasons why we did not succeed in the preparation of single-crystals from the Hacac modified systems. Another reason is the presence of *n*-propoxide ligands in these systems. These ligands make compounds very soluble in hydrocarbons and difficult to crystallize.

The existence of other compounds formed upon modification with Hacac was already seen in the NMR data. It was attempted to isolate the compound by modifying zirconium isopropoxide with 2 mol equivalents of Hacac. According to the literature this would yield a disubstituted compound [19-26]. To our surprise, the crystals prepared as described above could be identified as $Zr(O^iPr)(acac)_3$ (**2**)[2]. This mononuclear compound, depicted in Figure 3.4, has very poor stability. The decomposition of this compound was already observed during the single crystal diffraction experiments. A change in color and composition of the air tight sealed crystals was observed at the end of data collection (8-10 hours after mounting the crystals).

The structure of **2** is the first mononuclear alkoxide using a symmetric chelating ligand. Up to now only a limited number of structures using asymmetric chelating ligands like *t*-butylacetoacetate (tbaoac) [37,38], *N*,*N*-diethylacetoacetamide

[2] Crystal data: $C_{18}H_{28}O_7Zr$, M = 447.62, orthorhombic, a = 8.5444(17), b = 30.933(6), c = 8.2339(16) Å, V = 2176.3(7) Å^3, T = 295 K, space group Pna2(1), Z = 4, μ = 0.537 mm^{-1}, 8461 reflections measured, 3517 unique (R_{int} = 0.0792) which were used in all calculations. The final discrepancy factors were R1 = 0.0681; wR2 = 0.1609 for 2279 observed reflections (I > 2sigma(I)).

(deacam) [38], 1-methoxy-2-methyl-2-propyanolate (mmp) [39,40] and 2-(4,4-dimethyloxazolinyl)-propanolate (dmop) [41] have been reported. All of these compounds are disubstituted and have two alkoxide ligands. Table 3.2 lists the metal-oxide bond lengths of the alkoxide ligand and the chelating ligand in trans-position. The two metal-oxygen bond lengths of the acac ligand in **2** are almost identical while in all other complexes in Table 3.2 a clear difference in length is observed. This is due to the ability of asymmetric ligands to redistribute the multiplicity of bonds stabilizing complexes through trans-effect [37]. The absence of trans-stabilization in compound **2** probably explains the poor stability of the compound and the absence of trans-stabilization is probably the reason why mononuclear disubstituted derivatives with β-diketonate cannot be obtained.

*Table 3.2: Selected bond lengths of **2**, $Zr(O^iPr)_2(tbaoac)_2$ [37], $Zr(O^iPr)_2(deacam)_2$ [37] and $Zr(O^tBu)_2(mmp)_2$ [39].*

Bond lengths [Å]	**2**	**$Zr(O^iPr)_2(tbaoac)_2$ [37]**	**$Zr(O^iPr)_2(deacam)_2$ [37]**	**$Zr(O^tBu)_2(mmp)_2$ [39]**
M-OR	1.922(7)	1.908	1.942	1.942
M-O_1CL	2.150(7)	2.095	2.099	2.018
M-O_2CL	2.172(7)	2.233	2.205	2.405

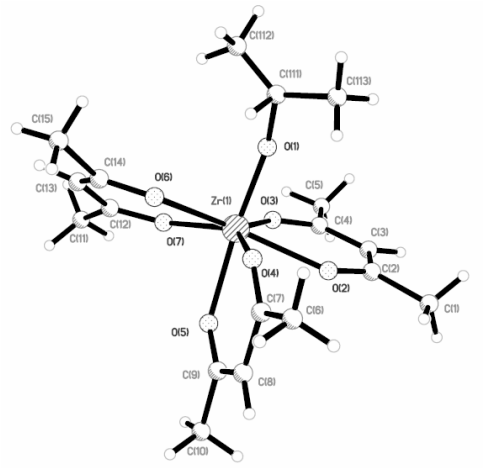

*Figure 3.4: Molecular structure of $Zr(O^iPr)(acac)_3$ (**2**).*

The ^{1}H NMR spectrum of this compound is depicted in Figure 3.3b. At first glance it looks like the signal of the <u>*CH*</u> proton of the central carbon in acetylacetone around 5.5 ppm is nicely split in a ratio of 2:1. However, after a comparison of the spectrum obtained for $Zr(acac)_4$ (see Figure 3.3d) and monitoring the evaluation of

the signals in time (as depicted in Figure 3.3c, recorded after aging the sample for two hours), it could be concluded that the signals marked with (∇) in the spectra of Figures 3.3b and 3.3c are due to the tetrasubstituted compound. The signals marked with (•) are that of **2**. The ratio of the integrals due to the protons of the *CH* and CH_3 of acetylacetone and the *CH* and CH_3 of the isopropoxide are perfectly in the expected ratio of 3 : 18 : 1 : 6. It should be noted that the chemical shift of the signal of the protons of *CH* and CH_3 of acetylacetone are very much alike for **1** and **2**, but a clear difference can be seen in the ratio of these signals compared to that of the alkoxides. The differences found between the spectra in Figures 3.2b and 3.2c suggest that upon aging of **2,** more $Zr(acac)_4$ and the unmodified precursor are formed, since the signals corresponding to these compounds increase compared to those assigned to compound **2**.

The existence of the trisubstituted compound was also evaluated for the zirconium mixed ligand precursor. After the addition of 2 mol equivalents of Hacac to the mixed-ligand precursor solution, the initial NMR spectra recorded 10 minutes after sample preparation showed multiple peaks around 5.5 ppm. The largest signal in the spectrum is assigned to $Zr(acac)_4$, since only this peak remained after 16 hours. The two minor peaks are attributed to the intermediate trisubstituted and the monosubstituted structure. The presence and disappearance after 16 hours of peaks assigned to *n*-propanol and isopropoxide CH_3 groups lend a support to the conclusion that the trisubstituted precursor is initially formed in this system. After 16 hours, the spectra changed with respect to the position of the peaks corresponding to the alkoxide groups in bridging positions. The presence of various species is also one of the reasons why the preparation of single crystals from these systems is hindered.

After isolation and characterization of the trisubstituted compound **2**, NMR experiments were conducted to look for the presence of compounds assumed to be formed upon modification with 0.5 and 2 mol equivalents of Hacac as proposed in literature. For samples of zirconium isopropoxide modified with 0.5 mol equivalent of Hacac, formation of only monosubstituted and unmodified precursors was observed. For zirconium isopropoxide with more than 1 mol equivalent the only signals present in the spectra were those assigned to **1**, **2** and $Zr(acac)_4$. Hence, we

believe that no compounds other than **2** are formed upon the modification of zirconium propoxides with Hacac.

It is thus clear that the nature of the heteroleptic intermediates of different zirconium propoxides characterized in this study is not in agreement with the mechanism and structures proposed in literature. Upon addition of up to 1 mol equivalent of Hacac, the most stable intermediate $[Zr(O^iPr)_3(acac)]_2$ is formed. When additional Hacac is added, the $[Zr(O^iPr)_3(acac)]_2$ structure is destabilized leading to the presence of the initial precursor and unstable $Zr(O^iPr)(acac)_3$. Spontaneous and rapid rearrangement of $Zr(O^iPr)(acac)_3$ to stable $Zr(acac)_4$ occurs at room temperature. The proposed stabilization and destabilization mechanism together with the accompanying structures of the intermediates are schematically depicted in Figure 3.5. It should be noted that the stability of the monosubstituted compound, **1**, will be discussed in more detail below.

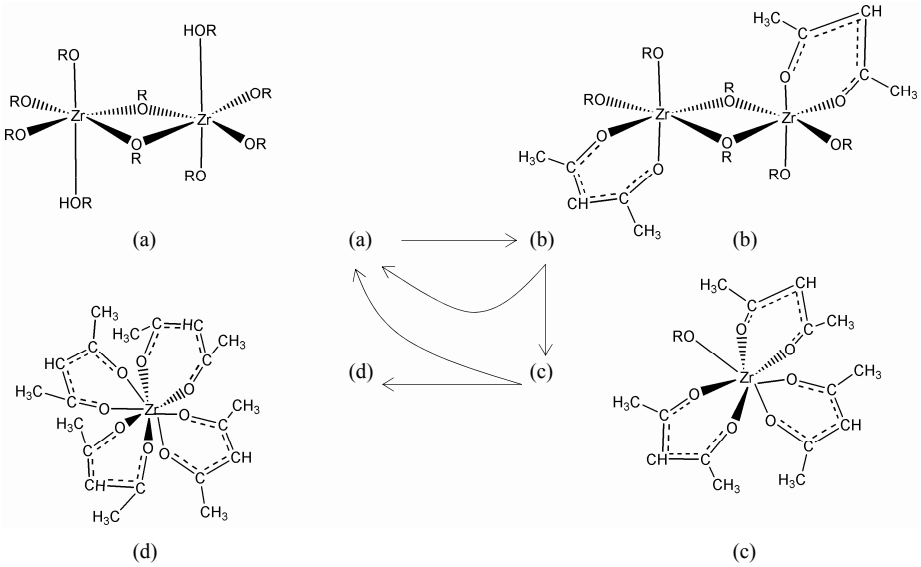

*Figure 3.5: The proposed mechanism and structures for the stabilization of zirconium propoxide in propanol. Addition of up to 1 mol equivalent Hacac to the initial precursor **(a)** leads to **(b)**. Addition of more than 1 mol equivalent leads to a reaction of **(b)** to **(a)** and **(c)**. Spontaneous and rapid rearrangement of **(c)** gives **(d)** and **(a)**. Different reactions are schematically depicted in the center of the figure.*

We have also attempted to get more insight into the intermediate structures formed upon the Hacac modification of zirconium *n*-butoxide. A sample with 1 mol

equivalent of Hacac was prepared and subsequently dried under vacuum. The ^{1}H NMR spectrum of this compound showed great similarities with that obtained for zirconium *n*-propoxide with 1 mol equivalent of Hacac, *i.e.*, the same signals were observed between 5 and 6 ppm. The attempts to isolate single crystals were, as could be expected, not successful. The removal of the parent solvents is even more complicated for *n*-butanol compared to that of *n*-propanol due to the higher boiling point of *n*-butanol. Despite the limited data, we do not expect that the heteroleptic intermediates differ from those that were obtained for the zirconium isopropoxide systems. It is then very unlikely that the commercially available di-acac-substituted zirconium *n*-butoxide precursor exists; it is probably a complex mixture of unmodified, mono-, tri- and tetrasubstituted compounds.

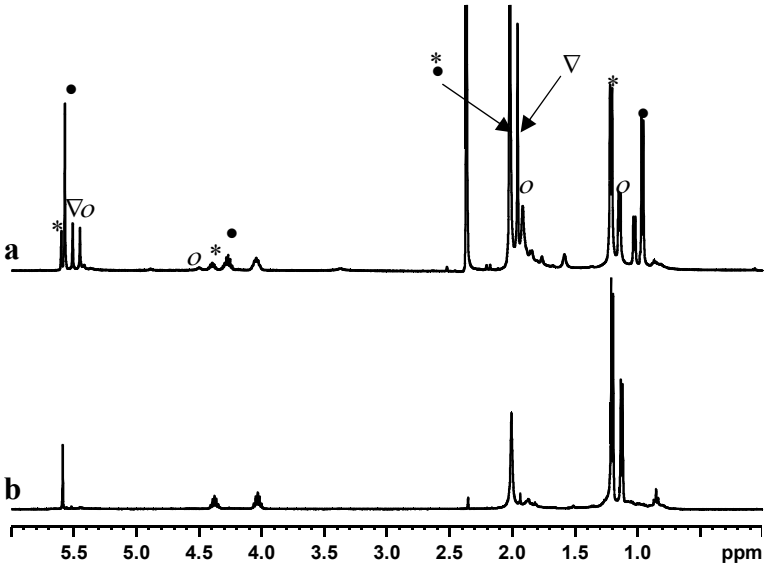

*Figure 3.6: The proton NMR spectrum (**a**) of hafnium isopropoxide with 2 mol equivalent of acetylacetone. Spectrum (**b**) was obtained from [Hf(O^{i}Pr)(acac)$_3$]$_2$ crystals. The signals corresponding to [Hf(O^{i}Pr)$_3$(acac)]$_2$ are marked with (∗), to Hf(O^{i}Pr)(acac)$_3$ – with (•),to Hf(acac)$_4$ with (∇) and the signals marked with (o) are probably due to the Hacac analogue of [Hf(OH)(O^{i}Pr)(thd)$_2$]$_2$.*

With the understanding of how the modification of zirconium isopropoxide with acetylacetone proceeds it was interesting to try and isolate the Hacac modified compounds for hafnium isopropoxide. Since the coordination chemistry of zirconium and hafnium is almost identical, the analogs of **1** and **2** were expected to be formed. A sample with 2 mol equivalents of Hacac was prepared and

subsequently dried under vacuum. The ^{1}H NMR spectra obtained from the dried product are displayed in Figure 3.6a. The signals marked with (∗), (•) and (∇) are assigned to $[Hf(O^iPr)_3(acac)]_2$, $Hf(O^iPr)(acac)_3$ and $Hf(acac)_4$ on the basis of the chemical shifts with respect to their zirconium analogs. This provides the first indication that the modification of hafnium isopropoxide also involves the formation of a mono- and trisubstituted compound. We subsequently attempted to isolate these heteroleptic intermediates.

A sample of hafnium isopropoxide was modified with 1 mol equivalent of Hacac and single crystals were obtained after performing the manipulation described in the experimental section. The isolated crystals were characterized as $[Hf(O^iPr)_3(acac)]_2$ (**3**)[3]. The unit cell parameters for **3** are smaller than those determined in both this report and in ref. [29] for **1**. The metal-oxide bonds are shorter for **3** compared to **1** as can be seen from Table 3.1, which reflects the smaller atomic radius for hafnium compared to zirconium, resulting from lanthanide contraction. The bond lengths of **3** are also shorter than those of $[Hf(O^iPr)_3(thd)]_2$ and $[Hf(O^nPr)_3(thd)]_2$ [36]. This is in contrast to the behavior observed for the zirconium compounds modified with Hacac or Hthd, where the shorter bond lengths were observed in the Hthd modified complex. The smaller atomic radius of hafnium causes some steric hindrance for the larger thd ligands, which results in somewhat elongated bond lengths.

The ^{1}H NMR spectrum of **3** was similar to that obtained for **1**. The ^{1}H NMR spectrum of this compound is depicted in Figure 3.6b. The spectrum beautifully displays the expected signals in the proper ratio.

There was also an attempt to isolate the trisubstituted compound. Various samples were prepared with the amount of the modifier varying between 2 and 2.5 mol equivalents. Despite several attempts to crystallize at low temperature as well by diffusion of the solvent at room temperature, it was not possible to obtain X-ray quality single crystals of the aimed compound. Every time the obtained crystals

[3] Crystal data: $C_{28}H_{56}O_{10}Hf_2$, M = 909.71, triclinic, a = 9.497(5), b = 10.257(5), c = 11.388(6) Å, α = 88.118(10)°, β = 68.849(10)°, γ = 64.744(9)°, V = 926.0(8) Å^3, T = 295 K, space group P-1, Z = 1, μ = 5.646 mm^{-1}, 3123 reflections measured, 1963 unique (R_{int} = 0.0429 which were used in all calculations. The final discrepancy factors were R1 = 0.0502; wR2 = 0.1205 for 1467 observed reflections (I > 2sigma(I)).

were either **3** or $Hf(acac)_4$. Despite the fact that the analogous hafnium compound of **2** has not been isolated; the NMR spectra of samples from these synthesis are in agreement with that displayed in Figure 3.6a. From the spectrum in Figure 3.6a it can be seen that the modification of hafnium involves a mono-and trisubstituted intermediate analogous to zirconium. In the spectrum (Figure 3.6a) some unassigned signals can be seen (marked with (o)), which were not observed in any of the spectra obtained for acetylacetone modified zirconium compounds. The ratio between acetylacetate and alkoxides ligands is 2:1 on the basis of the ratio between the signals at 5.45 and 4.5 ppm (*CH* of acetylacetate and alkoxides, respectively) and 1.90 and 1.04 ppm (*CH* of acetylacetate and alkoxides, respectively). In the work on the modification of hafnium propoxide with Hthd the formation of $[Hf(OH)(O^iPr)(thd)_2]_2$ was observed. Its formation occurred when mixtures of mono- and trisubstituted hafnium species were exposed to moisture from the air. No indication was found for the formation of an analogous zirconium compound. The observed signals in Figure 3.6a, marked with (o) could very well be due to an analogue of Hacac of $[Hf(OH)(O^iPr)(thd)_2]_2$, since the observed ratio of alkoxide and acetylacetate is in agreement and such a compound has not been observed in zirconium systems. Except for this partially hydrolyzed compound, the Hacac modification of hafnium propoxide analogues is thus analogue to that of zirconium propoxide

An interesting issue is the stability of the obtained compounds. It has already been mentioned that the stability of **2** is very low. With quantum chemical calculations it was evaluated if there exists any electronic reason for a difference in stability of **1** and **3**. The difference in total energy of the geometrically optimized structures was taken as an estimate of the binding energy. Any difference in electronic stability would become apparent from the calculations on the different systems. However, considering that the Group 4 cations formally have a +4 charge and that the ligands are multidentate and negatively charged, one should expect a dominance of electronic interaction and minimal effects of electronic factors.

For the reaction of interest in the parent study, we observed

$$2\ M^{4+} + 6\ O_iPr^- + 2\ acac^- \rightarrow M_2(\mu\text{-}O_iPr)_2(O_iPr)_4(acac)_2 \qquad (3.1)$$

that reaction (3.1) is associated with a binding energy of as much as 17200 kJ/mol. The difference in binding energy between the zirconium and hafnium compounds (M = Zr or Hf) is less than 0.5 % (91 kJ/mol).

It is clear that these compounds are very strongly electrostatically bonded. A survey of distances from the metal coordination centers essentially displays the same trend, as can be seen from Table 3.2: The Zr-O distances of the groups in bridging position are 2.146 and 2.249 Å, whereas the corresponding Hf-O distances of the groups in bridging position are 2.141 and 2.234 Å. Terminal Zr-O_t distances fall in two group, with two at about 1.96 Å and two at about 2.21 Å, whereas the corresponding groups of Hf-O_t distances end up at 1.96 and 2.21 Å. The Zr-Zr and Hf-Hf distances are 3.554 and 3.538 Å, respectively. Notably, the Hf-Hf distance is somewhat shorter in spite of hafnium being twice as heavy as zirconium (atom number 72 *vs.* 40). It seems clear that the presumptions are confirmed, thus highlighting the interesting effects of lanthanide contraction giving almost the same metal centre to ligand distances in all cases.

In conclusion it must be noted that a survey like this based on quantum chemical calculations will be very limited. It will only address the states more or less arbitrarily chosen from a very complex potential energy surface. With this limited view, it is clear that there is no inherent electronic difference in stability between zirconium and hafnium in the complex compounds studied here.

This does not mean that they will have to exhibit the same kinetic nor thermodynamic stability. In an experimental system, several competing reaction products and reaction paths may co-exist, which were not included in this computational study, and manifest themselves in a dramatic difference in the real stability of one class of compounds with respect to the other. The solution stability of **1** and **2** was experimentally evaluated. Batches of crystals of these compounds were synthesized. During drying, a color change was occasionally observed, *i.e.*, the initially white crystals turned yellow. This suggests a change in composition; the batches in which this occurred were not used for further experiments. NMR samples with various concentrations of **1** or **3** were prepared. After the addition of the solvent, $CDCl_3$, the NMR tubes were rapidly placed in the NMR spectrometer. A spectrum was recorded as soon as the sample had reached the measuring

temperature of 243 K. After the measurements, the samples were taken out of the spectrometer and stored on the lab bench (temperature 296.3 K) till the next measurement. The region between 5 and 6 ppm, corresponding to the signal of the *CH* of the acetylacetone ligand, was used for determining the concentration. The surface area of the signal assigned to **1** or **3** was normalized by the total area between 5 and 6 ppm. The change in composition was monitored by repeating the described procedure various times. For the interpretation of the data we assumed that the initially dissolved product was purely **1** or **3**. The results of experiments are depicted in Figure 3.7. It turned out that the signals in the spectra were only resolved in such a way that interpretation was possible when low concentrations of **1** and **3** were used; at higher concentrations interpretation was no longer possible.

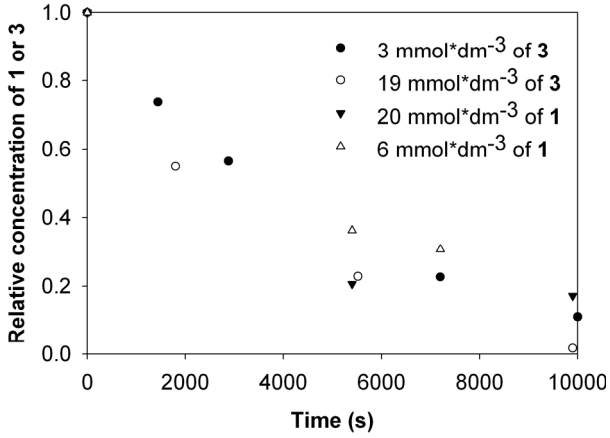

*Figure 3.7: The decrease of the concentration in time of **1** and **3** determined by ^1H NMR.*

The general trend for all experiments depicted in Figure 3.7 is a strong decrease in the concentration of the initial species in time. This is also what one would expect on the basis of the proposed mechanism for stabilization and destabilization. Compounds **1** and **3** rearrange through the formation of a trisubstituted and finally the formation of an unreactive tetrasubstituted compound. The driving force for the decreased concentration observed for **1** or **3** is thus the formation of tetrasubstituted compounds. An important factor that might influence the transformation towards $M(acac)_4$ is the facilitating effect of the residual alcohol [42]. The presence of traces of alcohol cannot be excluded and the possible effect should be taken into

consideration. This latter effect makes the quantitative interpretation of the data not completely reliable. However, further analysis of the data is possible and indicates that the reaction order of the rearrangement of compounds **1** and **3** is between 1 and 2, which is logical in the view of the need for intermolecular ligand transfer for this transformation.

From the data one can see that the composition of a precursor solution changes quite dramatically in time. It is obvious that the rearrangement of ligands is enhanced upon the heating of the system. This indicates that refluxing should be avoided in the modification of zirconium alkoxides, in contradiction to earlier recommendations by Mehrotra [21].

An interesting issue which still remains is to what extent materials derived from these precursor systems are influenced by the observed composition change. We estimate that the high-tech applications like thin films, *i.e.*, separative membrane layers, and nanoparticles would suffer most. Most of these materials are made from sols that have small particles in the range between 3-10 nm. The disadvantage of this is that a limited numbers of techniques are available for characterization. Quantitative information can be obtained from scattering techniques (light scattering or SAXS). The characterization of the deposited material by electron microscopy does not provide any information about the sol particles, as dense films are obtained [11,43]. Alternatively, the preparation of hollow spheres, as described in ref. [43,44], allows the use of electron microscopy, since (part of) the morphology in the sol is conserved upon film formation.

The effect of changes in the precursor composition on derived materials was evaluated by comparing the products obtained from a freshly prepared and aged precursor. In both cases, compound **1** was used as the precursor. The precursors were crystallized and after removal of the solvents, dried under vacuum. In one case the dried precursor was aged for about a week by storing it at room temperature in the lab, in the other case the sample was used directly after drying. The sols were prepared according to the procedure described above and it was noted that a slight color change occurred in the aged sample, *i.e.*, the initially white powder showed some yellowish traces. Capillaries were filled with the formed sols and the remaining sols were dried in air.

SAXS experiments were performed using the capillaries filled with sols and the obtained curve is depicted in Figure 3.8. A clear difference can be seen between the two curves. This difference is attributed to the aging of the precursor. Quantitative interpretation of the curves is not possible. The experimental SAXS data is normally fitted with a specific function that describes the scattering curve of a certain morphology, *e.g.*, the Teixeira function describes the scattering curve of a fractal object [45]. The particles in the sol phase are expected to be hollow spheres, as we will discuss in detail in chapter 9, and to the best of our knowledge, there are no functions describing the morphology of the used systems.

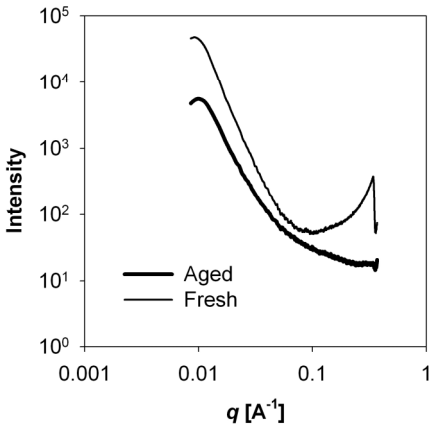

Figure 3.8: SAXS spectra for sols prepared from an aged and fresh precursor.

The advantage of using hollow spheres compared to dense sol particles lies in the fact that in this case TEM can be used for characterization. In Figure 3.9, the TEM images of the material derived from a fresh (Figure 3.9a) and an aged (Figure 3.9b) precursor are depicted. The striking difference between the two images is the apparent particle size distribution. The TEM image of the fresh precursor shows spheres with a size of about 250 nm, while the size found for the aged precursor varies between 50 and 500 nm. Light scattering experiments on the re-dispersed powder are in agreement with the observations made by TEM.

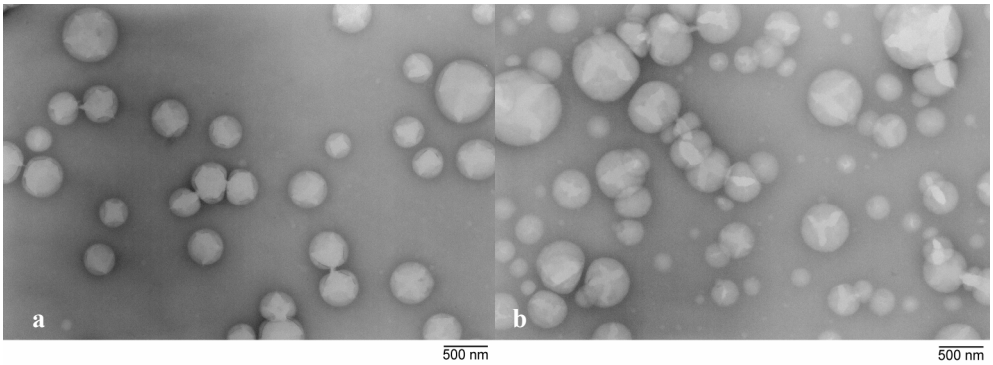

*Figure 3.9: TEM images of material derived from a fresh (**a**) and aged (**b**) precursor.*

We concluded above that compound **1** will transform in time, giving a mixture of unmodified, mono-, tri- and tetrasubstituted compounds. During the aging of the dried monosubstituted precursor this transformation will take place. While a fresh precursor, which is used as soon as possible after drying, will mainly consist of monosubstituted species. The effect of the aging of the precursor is clearly demonstrated in the SAXS, TEM and light scattering data. The observations are attributed to the presence of different species. During the formation of the hollow spheres, the outer surface is covered by acac ligands (as is discussed in ref. [43,44]). The presence of different species with different amounts of acac ligands determines the size of the obtained spheres, since the particle growth is terminated by saturation of the surface. The growth termination by saturation of the surface is also observed in Hacac modified systems for the preparation of dense films [46] and sol particles [17] (the interested reader is referred to ref. [43] for a detailed description of this mechanism). It can be concluded that the relatively poor stability of the compounds formed upon the modification of zirconium propoxide and hafnium propoxide precursors does have an influence on the derived materials. Therefore the system is not optimal for application in sol-gel. From the point of view of reproducibility it would be interesting to utilize modifiers that provide thermodynamically stable modified precursors.

3.4 Conclusions

It appears that the nature of the heteroleptic intermediates in the modification of different zirconium propoxides characterized in this study is not in agreement with

the mechanism and structures of intermediates proposed earlier in the literature. Upon addition of up to 1 mol equivalent of Hacac, the fairly stable $[Zr(O^iPr)_3(acac)]_2$ is formed. When additional Hacac is added, the $[Zr(O^iPr)_3(acac)]_2$ structure is apparently destabilized leading to the formation of the initial precursor and unstable $Zr(O^iPr)(acac)_3$. Spontaneous rearrangement of $Zr(O^iPr)(acac)_3$ to stable $Zr(acac)_4$ occurs at room temperature. The proposed stabilization and destabilization mechanism together with the accompanying structures of the intermediates are schematically depicted in Figure 3.5. The proposed mechanism has also been evaluated for hafnium isopropoxide and zirconium *n*-butoxide. Both systems seem to involve analogues intermediates, of which $[Hf(O^iPr)_3(acac)]_2$ was successfully isolated and characterized.

Quantum chemical calculations displayed that there is no inherent electronic difference in stability between zirconium and hafnium in the complex compounds studied here. NMR monitoring of the concentration of $[Zr(O^iPr)_3(acac)]_2$ and $[Hf(O^iPr)_3(acac)]_2$ suggests a relatively quick transformation of these compounds in time. The driving force for this transformation is the formation and crystallization of $M(acac)_4$. The effect of this rapid transformation on derived materials is evaluated by comparing the properties of materials derived from fresh and on solid state aged $[Zr(O^iPr)_3(acac)]_2$. The obtained SAXS data show a clear difference in scattering behavior for the fresh and aged samples and also TEM images of the dried sol show a clear difference in the size distribution of the initial sol particles. Light scattering experiments on the re-dispersed powder is in good agreement with the TEM observations.

3.5 References

1 J. Livage, M. Henry and C. Sanchez, *Prog. Solid St. Chem*.**, 18,** 259 (1988).

2 C. Sanchez and J. Livage, *New. J. Chem*., **14**, 513 (1990).

3 U. Schubert, *J. Sol-Gel Sci. Technol*., **26**, 47 (2003).

4 V.I. Parvulescu, H. Bonnemann, V. Parvulescu, U. Endruschat, A. Rufinska, Ch.W. Lehmann, B. Tesche and G. Poncelet, *Appl. Catal. A*, **214**, 273 (2001).

5 H.C. Zeng, J. Lin, W.K. Teo, F.C. Loh and J.L. Tan, *J. Non-Cryst. Solids*, **181**, 49 (1995).

6 G. De, A. Chatterjee, D. Ganguli, *J. Mater. Sci. Lett*., **9**, 845 (1990).

7 G. Emig, E. Fitzer and R. Zimmermann-Chopin, *Mat. Sci. Eng. A*, **189**, 311 (1994).

8 A. Lecomte, F. Blanchard, A. Dauger, M.C. Silva and R. Guinebretiere, *J. Non-Cryst. Solids*, **225**, 120 (1998).

9 P. Lobmann, U. Lange, W. Glaubitt, F. Hutter and D. Sporn, *High Preformance Ceramics 2001, Proceedings Key Engineering Materials*, **224**, 613 (2002).

10 J. Livage, F. Babonneau, M. Chatry and L. Coury, *Ceram. Int.*, **23**, 13 (1997).

11 M. Chatry, M. Henry, C. Sanchez and J. Livage, *J. Sol-gel Sci Technol.,* **1**, 233 (1994).

12 R.J. Vacassy, C. Guizard, J. Palmeri and L. Cot, *Nanostruct. Mater*., **10**, 77 (1998).

13 C.R. Xia, H.Q. Cao, H. Wang, P.H. Yang, G.Y. Meng and D.K. Peng, *J. Membr. Sci*., **162**, 181 (1999).

14 S. Benfer, U. Popp, H. Richter, C. Siewert and G. Tomandl, *Separ. Purif. Technol.*, **22-23**, 231 (2001).

15 I. Arcon, B. Malic, M. Kosec and A. Kodre, *Mater. Res. Bull*., **38** 1901 (2003).

16 M.J. Percy, J.R. Bartlett, J.L. Woolfrey, L. Spiccia and B.O. West, *J. Mater. Chem*., **9**, 499 (1999).

17 M.J. Percy, J.R. Bartlett, L. Spiccia, B.O. West and J.L. Woolfrey, *J. Sol-gel Sci. Technol.,* **19**, 315 (2000).

18 T. Lover, W. Henderson, G.A. Bowmaker, J.M. Seakins and R.P. Cooney, *J. Mater. Chem*., **7**, 1553 (1997).

19 U.B. Saxena, A.K. Rai, V.K. Mathur, R.C. Mehrotra and D. *Radford, J. Chem. Soc. (A)*, 904 (1970).

20 D.M. Puri, *J. Indian Chem. Soc.,* **47**, 535 (1970).

21 M. Pathak, R. Bohra, R.C. Mehrotra, I.P. Lorenz and H. Piotrowski, *Z. Anorg. Allg. Chem.*, **629***,* 2493 (2003).

22 F. Ribot, P. Toledano and C. Sanchez, *Chem. Mater*., **3**, 159 (1991).

23 D.E. Collins, K.A. Rogers and K.J. Bowman, *J. Eur. Ceram. Soc*., **18**, 1119 (1995).

24 K.A. Fleeting, P. O'Brien, D.J. Otway, A.J.P. White, D.J. Williams and A.C. Jones, *Inorg. Chem.,* **38**, 1432 (1999).

25 A.C. Jones, T.J. Leedham, P.J. Wright, M.J. Crosbie, P.A. Lane, D.J. Williams, K.A. Fleeting, D.J. Otway, and P. O'Brien, *Chem. Vapor. Depos.*, **4**, 46 (1998).

26 A.C. Jones, T.J. Leedham, P.J. Wright, M.J. Crosbie, D.J. Williams, K.A. Fleeting, H.O. Davies, D.J. Otway and P. O'Brien, *Chem. Vapor. Depos.*, **4**, 197 (1998).

27 R.J. Errington, J. Ridland, W. Clegg, R.A. Coxall and J.M. Sherwood, *Polyhedron*, **17**, 659 (1998).

28 W. Clegg, *Acta Cryst*., **C43**, 789 (1987).

29 G.A. Seisenbaeva, S. Gohil and V.G. Kessler, *J. Mater. Chem.*, **14**, 3177 (2004).

30 Chapter 2 of this thesis.

31 E.P. Turevskaya, N.I. Kozlova, N.Y. Turova, A.I. Belokon, D.V Berdyev, V.G. Kessler and Y.K. Grishin, *Russ. Chem. Bull*., **44**, 734 (1995).

32 SHELXTL-NT program manual, Bruker AXS, (1998).

33 M.J. Frisch, G.W. Trucks, H.B. Schlegel, G.E. Scuseria, M.A. Robb, J.R. Cheeseman, J.A. Montgomery, Jr., T. Vreven, K.N. Kudin, J.C. Burant, J.M. Millam, S.S. Iyengar, J. Tomasi, V. Barone, B. Mennucci, M. Cossi, G. Scalmani, N. Rega, G.A. Petersson, H. Nakatsuji, M. Hada, M. Ehara, K. Toyota, R. Fukuda, J. Hasegawa, M. Ishida, T. Nakajima, Y. Honda, O. Kitao, H. Nakai, M. Klene, X. Li, J.E. Knox, H.P. Hratchian, J.B. Cross, C. Adamo, J. Jaramillo, R. Gomperts, R.E. Stratman, O. Yazyev, A.J. Austin, R. Cammi, C. Pomelli, J.W. Ochterski, P.Y. Ayala, K. Morokuma, G.A. Voth, P. Salvador, J.J. Dannenberg, V.G. Zakrzewski, S. Dapprich, A.D. Daniels, M.C. Strain, O. Farkas, D.K. Malick, A.D. Rabuck, K. Raghavachari, J.B. Foresman, J.V. Ortiz, Q. Cui, A.G. Baboul, S. Clifford, J. Cioslowski, B.B. Stefanov, G. Liu, A. Liashenko, P. Piskorz, I. Komaromi, R.L. Martin, D.J. Fox, T. Keith, M.A. Al-Laham, C.Y. Peng, A. Nanayakkara, M. Challacombe, P.M.W. Gill, B. Johnson, W. Chen, M.W. Wong, C. Gonzalez, J. A. Pople, *Gaussian 03, Revision C.02* Gaussian, Inc., Wallingford CT, (2004).

34 D. Andrae, U. Häussermann, M. Dolg, H. Stoll and H. Preuss, *Theor. Chim. Acta*, **77**, 123 (1990).

35 K.A. Fleeting, P. O'Brien, D.J. Otway, A.J.P. White, D.J. Williams and A.C. Jones, *Inorg. Chem.,* **38**, 1432 (1999).

36 Chapter 4 of this thesis.

37 U. Patil, M. Winter, H.W. Becker and A. Devi, *J. Mater. Chem.,* **13,** 2177 (2003).

38 A. Baunemann, R. Thomas, R. Becker, M. Winter, R.A. Fischer, P. Ehrhart, R. Waser and A. Devi, *Chem. Commun*., 1610 (2004).

39 P.A. Williams, R.L. Roberts, A.C. Jones, P.R. Chalker, N.L. Tobin, J.F. Brickley, H.O. Davies, L.M. Smith and T.J. Leedham, *Chem. Vapor. Depos*., **8**, 163 (2002).

40 K.A. Fleeting, P. O'Brien, A.C. Jones, D.J. Otway, A.J.P. white and D.J. Williams, *J. Chem. Soc., Dalton Trans.*, 2853 (1999).

41 Y.F. Loo, R. O'Kane, A.C. Jones, H.C. Aspinall, R.J. Potter, P.R. Chalker, J.F. Bickley, S. Taylor and L.M. Smith, *J. Mater. Chem*., **35,** 1896 (2005).

42 V.G. Kessler, "*Chemistry and solution stability of alkoxide precursors*," in Handbook of Sol–Gel Science and Technology, ed. H. Kozuka, Kluwer Academic Publishers, Boston, Chap. 1 (2004)..

43 Chapter 8 of this thesis.

44 Chapter 9 of this thesis.

45 J. Teixeira, *J. Appl. Cryst*., **21**, 781 (1988).

46 P. Werndrup, M. Verdenelli, F. Chassagneux, S. Parola and V.G. Kessler, *J. Mater. Chem*., **14**, 344 (2004).

Chapter 4

The chemistry of 2,2,6,6,-tetramethyl-3,5-heptanedione (Hthd) modification of zirconium and hafnium propoxide precursors*

Abstract

The modification of different zirconium propoxide and hafnium isopropoxide precursors with 2,2,6,6,-tetramethyl-3,5-heptanedione (Hthd) was investigated by characterization of the isolated modified species. The complexes $[Zr(O^nPr)_3(thd)]_2$, $[Zr(O^nPr)(O^iPr)_2(thd)]_2$, $Zr(O^iPr)(thd)_3$ and $Hf(O^iPr)(thd)_3$ were isolated and characterized. Additionally, the structure of the *n*-propoxide analogous of $Zr(O^iPr)(thd)_3$ could not be refined, but its existence was clearly demonstrated by XRD and ^1H NMR. The modification involves mono- and trisubstituted intermediate compounds, but it does not involve a disubstituted compound, and thus, the commercial product claimed to be "$Zr(O^iPr)_2(thd)_2$" most commonly "used" for the MOCVD preparation of ZrO_2 does not exist. No evidence was found for the presence of such a compound in either zirconium- or hafnium-based systems. Formation of the dimeric hydroxo-di-thd-substituted complex, $[Hf(OH)(O^iPr)(thd)_2]_2$, could be observed only for the hafnium-based system and occurs on micro-hydrolysis. All heteroleptic intermediates are eventually transformed to the thermodynamically stable $Zr(thd)_4$ or $Hf(thd)_4$. The compounds obtained from isopropoxide precursors showed a higher stability than those with *n*-propoxide ligands or a combination of both types. In addition, it is important to

* Part of this chapter has been submitted for publication to *Inorg. Chem.*: "The chemistry of 2,2,6,6,-tetramethyl-3,5-heptanedione (Hthd) modification of zirconium and hafnium propoxide precursors," Gerald I. Spijksma, Henny J.M. Bouwmeester, Dave H.A. Blank, Andreas Fischer, Marc Henry, and Vadim G. Kessler.

note that residual alcohol facilitates the transformation and strongly enhances its rate. The unusually low solubility and volatility of $M^{IV}(thd)_4$ has been shown to be due to close packing and strong van der waals interactions in the crystal structures of these compounds.

4.1 Introduction

Zirconia has several interesting properties that make it an important material that is widely used in structural ceramics [1,2], gas sensors [3,4], catalysts [6-8] and dense dielectric and ferroelectric films in electronics [9,10]. With the trend of further miniaturization there has been an increasing interest in the controlled preparation of zirconia. It is a very attractive candidate for very large scale integrated circuits and as a gate dielectric in metal oxide-semiconductor (MOS) devices because of its high dielectric constant (~25) [11]. Moreover, zirconia also has a beneficially high bandgap (5.8-7.8 eV) [11] and thermal compatibility with contemporary CMOS processes [12].

Chemical vapor deposition is compatible with semiconductor processing which makes it an attractive technique for the preparation of microelectronics. The advantages of this process include the control of composition and the ability to scale it up to large areas [12]. If metal organic precursors are used, as in the present study, the deposition technique is referred to as MOCVD (metal organic chemical vapor deposition). The selection of a precursor is a fundamental aspect of the MOCVD process. The chemical compatibility of the precursor in solution and in vapor phase is necessary for their maximum usefulness [12]. In addition, solution stability and thermal stability during vapor phase transport are extremely critical towards process reproducibility. It may be considered obvious that the precursor composition does not change during storage after its preparation and before it is used, *e.g.,* the precursor is shelf stable.

The application of commercial zirconium alkoxide precursors is complicated and thus an unattractive option. The zirconium has an unsaturated coordination which makes the precursors extremely sensitive to hydrolysis and pyrolysis. Another drawback of unmodified precursors (*e.g.*, zirconium isopropoxide) is their relatively low volatility, requiring high deposition and substrate temperatures and leading to the formation of carbon contamination.

A general method used to moderate reactivity and improve the volatility is by replacing (part) of the alkoxide ligands by chelating organic ligands [12-14]. The first generation CVD precursors of oxides were zirconium and hafnium alkoxides

modified by β-diketones [13]. Modification with 2,2,6,6,-tetramethyl-3,5-heptanedione (Hthd) provides higher volatility due to the improved shielding of the metal atom by the larger terminal organic groups.

The replacement of part of the alkoxide ligands of zirconium and hafnium isopropoxide precursors has been reported. Introduction of 1 thd ligand per zirconium or hafnium atom provided dimeric $[M(O^iPr)_3(thd)]_2$ [15]. The behavior of these precursors in solution is not understood [15], and there is only a limited knowledge dealing with the preparation of films by MOCVD [16-18] starting from this precursor.

An MOCVD-precursor which is applied more often is "$Zr(O^iPr)_2(thd)_2$" [19-25]. This, nowadays, commercially available product was initially claimed to be a single compound [17]. However, in later publications it was said to be a stoichiometric mixture of mono- and dimeric structures and even suspected to be prone to some decomposition reactions [15,23]. Thus, despite being commercially available this product has not been fully characterized and even its existence has not been unequivocally proved.

The complete replacement of alkoxide ligands by Hthd leads to the formation of the complex $Zr(thd)_4$. Several studies have been devoted to the synthesis of this compound [26], however, no structural determination has been published for it. The behavior of the compound in solution and gas phase is remarkable. The compound is, in spite of very good shielding of the metal atom by the bulky organic ligands, very poorly soluble in hydrocarbon solvents and not nearly as volatile as one would expect. Nevertheless, it is frequently applied as a precursor in MOCVD applications [21,24,25,27-29].

It can be concluded that the chemistry involved in the modification of zirconium and hafnium isopropoxide precursors by Hthd is not clear. The understanding of this chemistry can be of great importance for the development of future generation CVD oxide precursors and for the preparation of materials from the precursors modified by Hthd.

In the present study, the Hthd modification of zirconium and hafnium isopropoxide has been investigated. In addition, other zirconium propoxide precursors, including zirconium *n*-propoxide and a mixed ligand precursor [30,31],

$[Zr(O^nPr)(O^iPr)_3(^iPrOH)]_2$, were modified in an attempt to reach better understanding of the chemistry involved in this process. The isolation and structural characterization of the modified species was complemented by the investigation of their solution and solid state stability in time by NMR and by monitoring their evaporation behavior by mass spectrometry.

4.2 Experimental

All manipulations were carried out in a dry nitrogen atmosphere using the Schlenk technique or a glove box. Hexane and toluene (Merck, *p.a.*) were dried by distillation after refluxing with $LiAlH_4$. 2,2,6,6,-tetramethyl-3,5-heptanedionate (Hthd) was purchased from Aldrich and used without further purification. The commercially available "$Zr(thd)_2(O^iPr)_2$" was purchased from Aldrich.

IR spectra were recorded with a Jasco-40 FT-IR spectrometer. ^1H NMR spectra were recorded in $CDCl_3$ for all compounds on a Bruker 400 MHz spectrometer at 243 K. The results of microanalysis (C, N, H) were obtained by the Chemical Analysis Group at the University of Twente, The Netherlands, using the combustion technique.

Synthesis: The zirconium propoxide precursors used as starting materials in this work are zirconium isopropoxide, ($[Zr(O^iPr)_4(^iPrOH)]_2$ 99.9%), 70 wt% solution of "$Zr(O^nPr)_4$" in *n*-propanol (both purchased from Aldrich) and $[Zr(O^nPr)(O^iPr)_3(^iPrOH)]_2$ which was prepared according to a recently developed technique [30,31]. The zirconium isopropoxide was dissolved and recrystallized from toluene prior to use in order to remove impurities. The hafnium isopropoxide was prepared by anodic oxidation of hafnium metal in isopropanol [32] and recrystallized from toluene. Hafnium *n*-propoxide was by anodic oxidation of hafnium metal in *n*-propanol [31]. All the different precursors were modified with various equivalent amounts of Hthd according to the techniques described below. The exact composition of the single crystals **1 - 8** was established with single X-ray crystallography.

$[Zr(O^nPr)_3(thd)]_2$ (1): Commercial 70% zirconium *n*-propoxide in *n*-propanol was dried (weight: 0.754 g (1.95 mmol)) under vacuum (0.1 mm Hg) and redissolved in 2 ml hexane. Upon addition of 0.36 g (1.95 mmol) of Hthd, the

yellowish sample was placed overnight in the freezer at –30 °C. The next day a significant amount of product had been formed and the solution was decanted and the obtained colorless crystals identified as **1**. (0.60 g, yield 54%). Found (%): C 53.2; H 8.2. Calculated for $Zr_2C_{40}H_{80}O_{10}$ (%): C 55.13; H 8.94. IR, cm^{-1}: 1575 s, 1538 m, 1506 s, 1469 sh, 1359 m, 1294 m, 1247 w, 1226 m, 1176 w, 1147 s, 1079 w, 1026 w, 995 w, 1079 m, 871 s, 794 sh, 761 br.

$[Zr(O^nPr)(O^iPr)_2(thd)]_2$ (**2**): The prepared $[Zr(O^nPr)(O^iPr)_3(^iPrOH)]_2$ (1.84 g, 4.76 mmol) was dissolved in 2 ml hexane and 0.88 g (4.77 mmol) Hthd was added. The sample was placed over night at –30 °C for crystallization. The obtained crystals turned out to be too small for XRD analysis. After addition of 2 ml hexane the clear solution was again placed overnight at -30 °C for crystallization. The solution was decanted and the obtained crystals (1.62 g, yield 60%) identified as **2**. Found (%): C 51.59; H 8.53. Calculated for $Zr_2C_{40}H_{80}O_{10}$ (%): C 55.13; H 8.94. IR, cm^{-1}: 1589 sh, 1579 s, 1559 w, 1539 w, 1507 s, 1293 w, 1241 w, 1227 w, 1149 s, 1020 m, 966 w, 872 s, 800 sh, 765 sh, 722 m.

$[Zr(O^iPr)(thd)_3]$ (**3**): was obtained from two different syntheses. **a)** To a solution of $[Zr(O^nPr)(O^iPr)_3(^iPrOH)]_2$ (1.32 g, 3.41 mmol) in 2 ml hexane 1.25 g (6.78 mmol) Hthd was added. The solution was stored over night at –30 °C and subsequently dried under vacuum (0.1 mm Hg). The resulting white solid was redissolved in 1.5 ml hexane and again stored at –30 °C for crystallization. The next day the solution was decanted and the obtained colorless crystals (1.0 g, yield 39%) identified as **3** and IR and element analysis were performed.

b) The analogous modification with 2 mol equivalents of Hthd was performed, however, now zirconium isopropoxide was used as the precursor. The zirconium isopropoxide (0.59 g, 1.53 mmol) was dissolved in 3 ml mixture of hexane/toluene (volume ratio 2:1) and 0.58 g (3.15 mmol) of Hthd was added. The solution was placed overnight at –30 °C, subsequently the solvents were decanted from the obtained crystals. The crystals (0.27 g; yield 23%) were identified on the basis of their unit cell parameters obtained by XRD, as $[Zr(O^iPr)_3(thd)]_2$ [15]. The decanted solution was dried under vacuum (0.1 mm Hg) and the obtained white solids were redissolved in 2 ml hexane. After storing overnight at –30 °C an amount of crystals, that again were identified as $[Zr(O^iPr)_3(thd)]_2$, were obtained. The solution

that was decanted from the crystals was stored on the lab bench in a flask with a serum cap stopper. After ~4 weeks the hexane had diffused through the stopper and big platelet crystals, identified as **3,** had formed in the flask.

Found (%): C 60.29; H 9.01. Calculated for $ZrC_{36}H_{64}O_7$ (%): C 61.80; H 9.15. IR, cm^{-1}: 2726 w, 1573 w, 1537 w, 1506 s, 1403 w, 1359 m, 1294 m, 1247 sh, 1226 s, 1172 w, 1147 s, 1080 w, 1022 m, 968 m, 935 w, 873 s, 847 w, 794 s, 761 w, 738 m.

An attempt was also made to prepare a trisubstituted compound from zirconium *n*-propoxide. Commercial 70% zirconium *n*-propoxide in *n*-propanol was dried (weight: 0.61 g (1.58 mmol)) under vacuum (0.1 mm Hg) and redissolved in 2 ml hexane. Upon addition of 0.86 g (4.67 mmol) of Hthd, the yellowish sample was dried under vacuum (0.1 mm Hg) and the remaining product dissolved in 1 ml hexane. The sample was stored on the lab bench in a flask with a serum cap. After ~4 weeks the hexane had diffused through the stopper and two types of crystals had formed in the flask. One type of crystals was not of X-ray quality, the obtained NMR spectra on this compound indicated that it was the product aimed for, *i.e.*, trisubstituted zirconium *n*-propoxide. The other type of crystals that were of X-ray quality was identified as **7a**.

$[Hf(O^nPr)_3(thd)]_2$ (4): Hafnium *n*-propoxide (1.11 g, 2.34 mmol) was dissolved in 2 ml hexane. Upon addition of 0.43 g (2.34 mmol) of Hthd, the yellowish sample was dried under vacuum (0.1 mm Hg) and the remaining product dissolved in 1 ml hexane. The sample was stored on the lab bench in a flask with a serum cap. After ~4 weeks the hexane had diffused through the stopper and single crystals had formed in the flask. The obtained crystals were identified as **4**.

$[Hf(O^iPr)(thd)_3]$ (5): Hafnium isopropoxide (weight: 0.85 g (1.79 mmol)) was dissolved in 6 ml mixture of hexane and toluene (volume ratio 1:2). After addition of 0.80 g (4.34 mmol) of Hthd, *i.e.*, 2,5 mol equivalent, the solution was removed from the mixture under vacuum (0.1 mm Hg). The obtained solid product was subsequently redissolved in 2 ml hexane. The obtained solution was left to crystallize at room temperature by diffusion of the solvent through the serum cap. After ~1 week some crystals had formed. The remaining solution was decanted from the obtained crystals and transferred to another flask that was left at room

temperature for further crystallization. The obtained crystals were identified as $[Hf(O^iPr)_3(thd)]_2$ [15]. After ~2 weeks a new product was obtained which turned out to consist of a mixture of crystals. Both types of crystals were of X-ray quality and they were identified as **5** and $[Hf(O^iPr)(OH)(thd)_2]_2$ (**6**), respectively.

$Zr(thd)_4$ (7a and **7b):** Commercial 70% zirconium *n*-propoxide in *n*-propanol was dried (weight: 1.59 g (4.10 mmol)) under vacuum (0.1 mm Hg) and redissolved in 1 ml hexane. Instantly upon addition of 3.0 g (16.3 mmol) of Hthd a white solid was formed. Additional hexane was added (2.5 ml) and the mixture was refluxed for half an hour, resulting in a clear yellowish solution. The solution was placed in the freezer at –30 °C for crystallization and an almost quantitative yield of the product was obtained. However, no X-ray quality crystals could be isolated. The obtained product was dried and redissolved upon heating in 14 ml of isopropanol. The solution was left to crystallize at room temperature and produced X-ray quality crystals. The initially crystallized batch of platelets was characterized as **7a**, while the needles formed later from the diluted solution turned out to possess the structure of **7b**. Found (%): C 64.14; H 9.42. Calculated for $ZrC_{44}H_{76}O_8$ (%): C 63.98; H 9.37. IR, cm^{-1}: 2854 s, 1593 sh, 1574 s, 1545 w, 1534 m, 1504 m, 1403 w, 1298 w, 1250 w, 1226 m, 1179 sh, 1148 m, 1620 w, 967 w, 935 w, 873 s, 792 m, 760 sh, 722 s.

$Hf(thd)_4$ (8): Hafnium isopropoxide (weight: 1.03 g (2.17 mmol)) was dissolved in 9 ml mixture of hexane and toluene (volume ratio 1:2). After addition of 1.61 g (8.74 mmol) of Hthd, the mixture was refluxed for half an hour. Subsequently the solvent was removed from the solution under vacuum (0.1 mm Hg). The obtained solid product was redissolved upon heating in 30 ml of isopropanol. The solution was left for crystallization at room temperature and X-ray quality crystals were obtained. Their structure was determined as **8**. Found (%): C 57.41; H 8.41. Calculated for $HfC_{44}H_{76}O_8$ (%): C 60.09; H 8.29, the lower values observed for C and H are possible due to the formation of hydrolyzed species during the synthesis. IR, cm^{-1}:1593 m, 1568 s, 1534 s, 1297 w, 1247 w, 1227 w, 1172 sh, 1152 m, 1077 w, 1031 w, 971 w, 866 m, 790 w, 723 s.

Crystallography: Data collection for single crystals of all compounds except (**7b**) was carried out at 22 °C on a SMART CCD 1k diffractometer with graphite

monochromated MoKα radiation. All structures were solved by standard direct methods. The coordinates of the metal atoms as well as the majority of other non-hydrogen atoms were obtained from the initial solutions and for all other non-hydrogen atoms found in subsequent difference Fourier syntheses. The structural parameters were refined by least squares using first isotropic and then, where possible (*i.e.*, not for carbon atoms in case of disordered thd-ligands such as in **6**, **7a** and **8**) also anisotropic approximations. The coordinates of the hydrogen atoms were calculated geometrically and were included into the final refinement in isotropic approximation for all the compounds except **7a** and **8**, where there location is impossible. Full refinement of the structure of $Zr(O^nPr)(thd)_3$ was not accomplished because of rather complex unresolved disorder in the *n*-propyl radical. All calculations were performed using the SHELXTL-NT program package [32] on an IBM PC. The structure of (**7b**) was determined at KTH Stockholm using a Kappa CCD diffractometer.

Computation of internal and lattice energies: In order to get more insight into the van der waals interactions at work in $M(thd)_4$ compounds, the PACHA software [34] running on an IBM PC has been used. The ability of this software to quantify the relative contributions of any kind of weak molecular interactions (hydrogen bonding, coordination links, π-π stacking, van der waals) responsible for the formation of a crystalline network has been previously demonstrated [35,36]. The basis of the method is to compare internal energies (named EB hereafter) of a crystal to the internal energies of isolated building blocks extracted from the lattice, the observed difference being the lattice energy released when those building blocks come from infinity at their right place in the crystal. For structures **7a**, **7b** and **8** the raw data coming from X-ray diffraction has been used and the corresponding lattice energies should then be considered as very rough approximations of true crystalline energies. For structure **7b**, it was noticed that methine protons on thd groups were absent from the X-ray data file. A new structure (named **7h**) has thus been generated by adding them in the O-C-C-C-O plane assuming bisection of the C-C-C bond angle and d(C-H) = 108 pm. For **7a** and **8**, it was not possible to add missing hydrogen atoms owing to the strong disorder. From **8**, it was also possible to derive two structures (named **8A** and **8B** hereafter) showing no disorder and differing only by the kind of isomer involved in

building the 3D-lattice. Corresponding internal and lattice energies have thus been estimated for these complexes without further addition of missing H-atoms.

4.3 Results and discussion

The modification of zirconium *n*-propoxide and mixed ligand precursors with 1 mol equivalent of Hthd, has provided **1** and **2**. The structures of these compounds[1,2] were determined by X-ray single crystal studies as $[Zr(O^nPr)_3(thd)]_2$ and $[Zr(O^iPr)_2(O^nPr)(thd)]_2$. These compounds display structures analogous to that obtained from zirconium isopropoxide with a corresponding amount of Hthd [15]. This latter compound was also obtained by us using the same technique as for **1** and **2** and avoiding the refluxing applied earlier by Fleeting *et al*. [15].

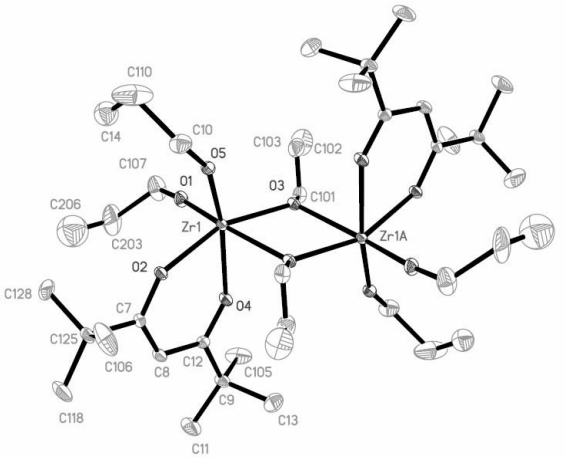

*Figure 4.1: Molecular structure of $[Zr(O^nPr)_3(thd)]_2$ (**1**).*

The largest difference between the monosubstituted complexes prepared in the present study and $[Zr(O^iPr)_3(thd)]_2$ is the presence of a *n*-propoxide ligand in the

[1] Crystal data: $C_{40}H_{80}O_{10}Zr_2$, M = 903.48, Triclinic, a = 9.407(4) Å, b = 10.086(5) Å, c = 13.957(6) Å, α = 71.288(17)°, β = 79.596(19)°, γ = 83.765(11)°, V = 1231.7(10) Å^3, T = 295(2) K, space group P-1, Z = 1, μ = 0.469 mm^{-1}, 3768 reflections measured, 3087 unique (R_{int}= 0.0267 which were used for refinement. The final discrepancy factors were R1 = 0.0614; wR2 = 0.1417 for 1787 observed reflections (I > 2sigma(I)).

[2] Crystal data: $C_{40}H_{80}O_{10}Zr_2$, M = 903.48, Monoclinic, a = 20.191(16) Å, b = 9.753(8) Å, c = 26.796(19) Å, α = 90°, β = 110.21(4)°, γ = 90°, V = 4952(6) Å^3, T = 295(2) K, space group P2(1)/c, Z = 4, μ = 0.467 mm^{-1}, 11463 reflections measured, 3408 unique (R_{int}= 0.0803 which were used for refinement. The final discrepancy factors were R1 = 0.0843; wR2 = 0.2329 for 1942 observed reflections (I > 2sigma(I)).

bridging positions. This, less bulky ligand compared to isopropoxide causes a smaller metal-metal distance, *i.e.*, 3.459(2) Å and 3.494(3) Å for **1** and **2** compared to 3.508 Å for $[Zr(O^iPr)_3(thd)]_2$. Also the angle between the oxygens in bridging positions and metal atom decreases slightly, 70.1(2)° and 69.4(5)° for **1** and **2** compared to 72.0° for $[Zr(O^iPr)_3(thd)]_2$. Consequently, the metal-oxygen bond lengths for the bridging groups will also be shorter for **1** and **2**.The metal-oxygen bond lengths of the alkoxide ligands in terminal positions are shorter in complexes **1** and **2**, *i.e.*, 1.891(6)-1.896(7) Å, 1.834(13)-1.876(12) Å and 1.931-1.944 Å for **1**, **2** and $[Zr(O^iPr)_3(thd)]_2$, respectively.

$$\tfrac{1}{2}\,[Zr(O^iPr)_4(^iPrOH)]_2 + Hthd \rightarrow \tfrac{1}{2}\,[Zr(O^iPr)_3(thd)]_2 + {}^iPrOH$$

$$\tfrac{1}{4}\,[Zr(O^nPr)_4]_4 + Hthd \rightarrow \tfrac{1}{2}\,[Zr(O^nPr)_3(thd)]_2\ (1) + {}^nPrOH$$

$$\tfrac{1}{2}\,[Zr(O^nPr)(O^iPr)_3(^iPrOH)]_2 + Hthd \rightarrow \tfrac{1}{2}\,[Zr(O^nPr)(O^iPr)_2(thd)]_2\ (\mathbf{2}) + {}^iPrOH$$

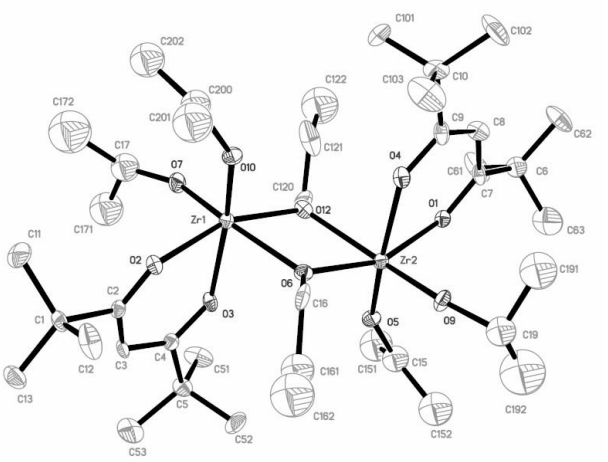

*Figure 4.2: Molecular structure of $[Zr(O^iPr)_2(O^nPr)(thd)]_2$ (**2**).*

The synthesized compounds were further characterized by ^1H NMR. The spectrum obtained by us for $[Zr(O^iPr)_3(thd)]_2$ (depicted in Figure 4.3b) differs significantly from the one published by Fleeting *et al*. [15]. In this latter work two signals were observed in the region 5.6-6.0 ppm. In contrast, only one signal (at 5.80 ppm) is present in the spectra observed by us for $[Zr(O^iPr)_3(thd)]_2$ and **1** (Figure 4.3a). The signals at these chemical shifts are characteristic of the <u>*CH*</u> of the thd-ligand and, if the centrosymmetric structures of the compounds are preserved in solution, these

ligands should be equivalent producing only one such signal as it has been observed in our work. The signal due to $\underline{CH_3}$ of the thd is present at 1.13 ppm and in both spectra with the expected ratio 1:18 to the $\underline{CH}$ signal in the integration.

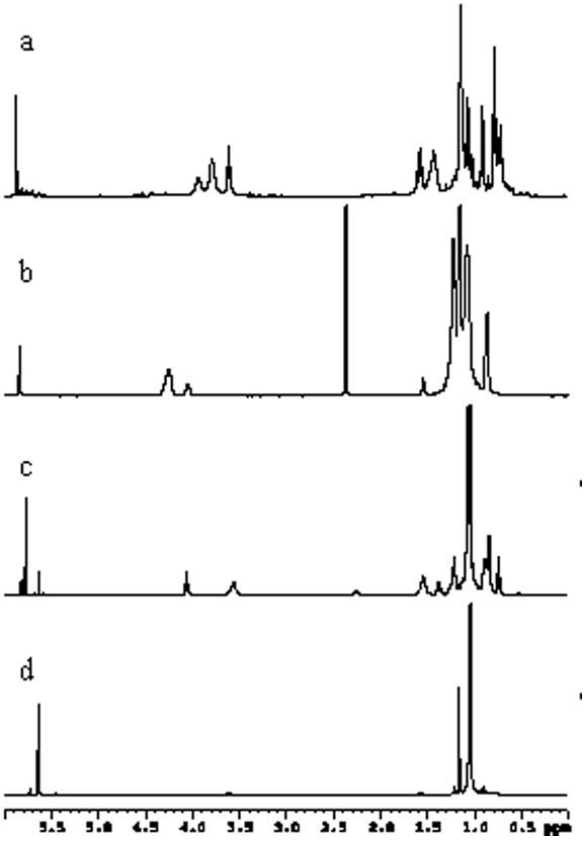

*Figure 4.3: NMR spectra of(**1** (**a**), $[Zr(O^iPr)_3(thd)]_2$ (**b**), **3** (**c**) and $Zr(thd)_4$ (**d**). The signals labeled with (*) in the spectra of $[Zr(O^iPr)_3(thd)]_2$ are assigned to toluene and hexane.*

Further interpretation of the spectra is complicated by the presence of residual solvent and the parent alcohol present. The signals labeled with (*) in the spectra of $[Zr(O^iPr)_3(thd)]_2$ (Figure 4.3b), belong to toluene and hexane, while those at 1.55 ppm and 4.05 ppm are assigned to isopropanol. This implies that the remaining signal at 4.25 ppm is due to the $\underline{CH}$ of the propoxide ligands, suggesting that the alkoxide ligands in bridging and terminal groups are in fast interchange. The spectra obtained after storing the dried crystals for 2 months, support this interpretation. During storage the remaining solvents have diffused through the

septum and consequently the spectrum showed mainly the expected signals for $[Zr(O^iPr)_3(thd)]_2$.

The assumption that the alkoxide ligands in both terminal and bridging positions result in one signal in the NMR spectra could also apply for the spectra of compound **1**. The signal at 3.94 ppm has the required ratio 3:1 compared to the *OCH* signal of thd, however it is accompanied by two unassigned signals at 3.60 and 3.78 ppm, respectively. The signal at 3.60 and the other signals marked with (●) match the positions and ratios of *n*-propanol. The signal at 3.78 ppm is probably due to unmodified precursor, since they are expected around this chemical shift [31] The presence of these signals in the spectra suggests the existence of the unmodified precursor in the sample. Consequently, the unresolved signal around 1.4 ppm is a combination of the signals due to the *CCH_2C* of the alkoxide ligands and the alcohol.

The previously discussed compounds, *e.g.*, $[Zr(O^iPr)_3(thd)]_2$ and **1** have the same type of alkoxide ligands in both the bridging and terminal positions. Compound **2**, in contrast, has *n*-propoxide ligands in the bridging positions and isopropoxide ligands in the terminal positions. This difference was clearly observed in the NMR spectra. The expected ratio of 3:4 (normalized on *CH* of the thd) for the terminal versus bridging was acquired.

The stability of the modified precursors is a requirement to make it applicable for use in MOCVD. Both the solution and shelf, *i.e.*, solid state stability of **1**, **2** and $[Zr(O^iPr)_3(thd)]_2$ have been examined. It was already mentioned above that $[Zr(O^iPr)_3(thd)]_2$, is relatively shelf stable. Upon storage for 2 months the sample contained only minor amount of a different phase. In the NMR spectra an additional small signal could be seen in the region between 5.6 and 6.0 ppm. In contrast, the solution stability in $CDCl_3$ is rather limited, after 10 days only ~40% of the signals in the region between 5.6 and 6.0 ppm were due to $[Zr(O^iPr)_3(thd)]_2$. The obtained spectrum was similar in appearance to that presented by Fleeting *et al*. [15]. The second signal present in both their spectra and ours, at slightly lower chemical shift (~5.65 ppm) than that of *CH* of the thd in the initial complex, is most likely that of $Zr(thd)_4$. The refluxing during the synthesis of this compound evidently already leads to a mixture of several compounds. These data clearly show

that the refluxing should be avoided in the modification of zirconium alkoxides in contradiction to earlier recommendations by Mehrotra [37].

$$[Zr(OR)_3(thd)]_2 \xrightarrow{t^\circ} \text{“}Zr(OR)_4\text{”} + Zr(thd)_4 + (Zr(OR)(thd)_3)$$

The stability of **1** and **2** was compared to that of $[Zr(O^iPr)_3(thd)]_2$. In $CDCl_3$ about 30% of **1** was still present after 10 days and the spectra displayed 3 signals in the region between 5.6 and 6.0 ppm, while for **2** only 20% of the total signals corresponded to the monosubstituted compound. In the latter sample, the formation of unmodified mixed ligand precursor could clearly be observed. The presence of three signals suggests that there is, in addition to mono- and tetrasubstituted, at least one more type of species. The solution stability of **1** is thus of the order of magnitude of that of $[Zr(O^iPr)_3(thd)]_2$, while that of **2** is significantly smaller. It should be noted that the data on the composition can only be used in a semi-quantitative way. Effects due to concentration differences and different dryness of the compounds, *i.e.*, parent alcohol can enhance transformation processes [38], are not taken in to account in this study. For each sample, approximately the same amount of compound was dissolved and the compounds were dried as good as possible, however the presence of residue alcohol in the samples can be seen in the NMR spectra in Figure 4.3.

The solid state stability was significantly lower for **1** and **2** compared to the isopropoxide complex. After two months the signal at 5.88 ppm was only ~10% of the total in that region for **1** and even less for **2**. Again, the transformation involved the formation of two other compounds for **1** and even three different species for **2**, *i.e.*, there were 4 signals between 5.6 and 6.0 ppm. The lack of solid state stability for **1** and **2** provides a plausible explanation for the slightly deviating values obtained by the element analysis.

On the basis of their solid state stability it can be seen that **1** and **2** have more in common with each other than with $[Zr(O^iPr)_3(thd)]_2$. A similar trend can be seen in the mass spectrometry data (Table 4.1). Compounds **1** and **2** show a clear dimeric behavior in the gas phase, the major component in the gas phase being $Zr(OPr)(thd)_2$ m/z = 515 (100%). For $[Zr(O^iPr)_3(thd)]_2$ the major fraction in the gas phase is found at m/z = 391 (100%) corresponding to $Zr(O^iPr)_2(thd)^+$.

Despite the stability, especially in solid state, and the gas phase behavior of $[Zr(O^iPr)_3(thd)]_2$, it has only resulted in a few publications dealing with the preparation of materials [16-18]. What might have had influence on the applicability of $[Zr(O^iPr)_3(thd)]_2$ is that its synthesis involved refluxing, which certainly led to the disproportionation with formation of complexes containing more thd ligands. The formation of another compound, supposedly $Zr(thd)_4$ can clearly be seen from the NMR spectra presented by Fleeting *et al*. [15]. The monosubstituted compounds presented, **1** and **2**, containing *n*-propoxide ligands in the bridging position are significantly less stable in both solid state and solution. Another difference with $[Zr(O^iPr)_3(thd)]_2$ is that **1** and **2** tend to remain dimeric in the gas phase where $[Zr(O^iPr)_3thd)]_2$ is predominantly monomeric. It can thus be concluded that the physico-chemical properties of **1** and **2** do not make them suitable for application in CVD.

*Table 4.1: Interpretation of M/z(I) spectrum of **1**, **2**, $[Zr(O^iPr)_3(thd)]_2$, $[Hf(O^iPr)_3(thd)]_2$ and **3**.*

Gas phase fragments	**1**	**2**	**$[Zr(O^iPr)_3(thd)]_2$**	**$[Hf(O^iPr)_3(thd)]_2$**	**3**
Zr((MeC)COCHC(H)O)(OCCHCO)					291 (16)
$Zr(OPr)_2$((MeC)COCHC(H)O)			311 (75)		
$Zr(OPr)_2$(OCCHCO)			347 (27)		
$M(OPr)_2(thd)$	391 (28)	391 (37)	391 (100)	481 (28)	
$M(OPr)_2$(thd)(OC) (OCCHCO)			435 (24)	515 (9)	
$M(thd)_2$	459 (73)	459 (81)	459 (100)	549 (25)	459 (14)
$M(OPr)(thd)_2$	515 (100)	515 (100)	515 (100)	605 (100)	515 (100)
$[M(thd)_2((Me_3C)COCHC(H)O]$		583 (25)		673 (56)	583 (69)
$Zr_2(OPr)_2$(thd)(OCCHCO)			615 (10)		
$M(thd)_3$		639 (21)		729 (30)	639 (75)
$Zr_2(OPr)_6(thd)$			717 (9)		
$Zr_3(OPr)_8$	739 (6)	739 (21)			
$M_2(OPr)_4(thd)_2$	785 (16)	785 (14)	785 (13)	965 (29)	
$Zr_2(OPr)_5(thd)_2$	845 (11)	843 (8)	843 (5)		

The presence of three or more signals in the NMR spectra of aged **1** and **2**, indicated the presence of more multi thd substituted compounds. According to previous studies [15,23] this should be a disubstituted species. In order to investigate the structure of this higher substituted compound, $[Zr(O^iPr)_4(^iPrOH)]_2$ and $[Zr(O^nPr)(O^iPr)_3(^iPrOH)]_2$ were modified with 2 mol equivalents of Hthd. In both samples crystals were formed upon storage at -30 °C. The ones obtained from the sample with zirconium isopropoxide were identified as $[Zr(O^iPr)_3(thd)]_2$, while,

somewhat surprisingly, a trisubstituted $Zr(O^iPr)(thd)_3$ (**3**)[3] (see Figure 4.4) compound was obtained from the mixed ligand precursor. The structure of this mononuclear compound will be discussed in more detail below.

$$\tfrac{1}{2}\,[Zr(O^iPr)_4(^iPrOH)]_2 + 2\,Hthd \rightarrow \tfrac{1}{4}\,[Zr(O^iPr)_3(thd)]_2 + \tfrac{1}{2}\,Zr(O^iPr)(thd)_3\ (\mathbf{3}) + 2\,{}^iPrOH$$

$$\tfrac{1}{2}\,[Zr(O^nPr)(O^iPr)_3(^iPrOH)]_2 + 2\,Hthd \rightarrow \tfrac{1}{4}\,[Zr(O^nPr)(O^iPr)_2(thd)]_2\ (\mathbf{2}) + \tfrac{1}{2}\,Zr(O^iPr)(thd)_3\ (3) + 2\,{}^iPrOH$$

$$\tfrac{1}{4}\,[Zr(O^nPr)_4]_4 + 2\,Hthd \rightarrow \ldots \rightarrow {}^1\!/_8\,[Zr(O^nPr)_4]_4 + \tfrac{1}{2}\,Zr(thd)_4\ (\mathbf{7}) + 2\,{}^nPrOH$$

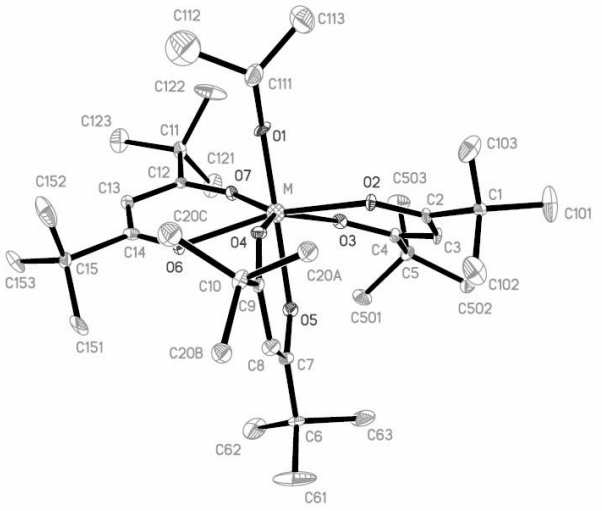

*Figure 4.4: Molecular structure of $M(O^iPr)(thd)_3$ with M = Zr (**3**) or Hf (**5**).*

An attempt was also made to obtain and isolate this mononuclear compound from zirconium isopropoxide. Compound **3** could successfully be isolated from a synthesis with zirconium isopropoxide after removal of $[Zr(O^iPr)_3(thd)]_2$ through crystallization, as described in the experimental section. The synthesis that was

[3] Crystal data: $C_{36}H_{64}O_7Zr$, M = 700.09, Monoclinic, a = 10.153(3) Å, b = 20.995(5) Å, c = 18.928(5) Å, $\alpha = 90°$, $\beta = 99.878(5)°$, $\gamma = 90°$, V = 3975.0(18) Å^3, T = 295(2) K, space group P2(1)/c, Z = 4, μ = 0.317 mm^{-1}, 12110 reflections measured, 3711 unique (R_{int}= 0.0782 which were used for refinement. The final discrepancy factors were R1 = 0.0844; wR2 = 0.2166 for 2242 observed reflections (I > 2sigma(I)).

presented for the preparation of "$Zr(O^iPr)_2(thd)_2$", *e.g.*, interaction of the isopropoxide with 2 mol equivalent Hthd and refluxing was also carried out. The obtained crystals were, again, identified as $[Zr(O^iPr)_3(thd)]_2$. It is likely, based on the amount of added modifier, that for both precursors, *i.e.*, $Zr(O^iPr)_4(^iPrOH)$ and $[Zr(O^nPr)(O^iPr)_3(^iPrOH)]_2$, a mixture of mono- and trisubstituted compounds is formed upon modification. Upon cooling the compound that crystallizes easiest will be formed initially. In case of zirconium isopropoxide, the crystals of the monosubstituted compound are formed first, while for the sample prepared from the mixed ligand alkoxide it is **3** that crystallizes more easily.

The trisubstituted compounds obtained from the two different zirconium alkoxides were characterized by NMR. A spectrum obtained from the system with zirconium isopropoxide as the precursor is depicted in Figure 4.3c. There are three signals present in the region between 5.5-6.0 ppm. The major signal at 5.75 ppm is assigned to **3**. The two minor signals are assigned to $[Zr(O^iPr)_3(thd)]_2$ (5.81 ppm) and $Zr(thd)_4$ (5.65 ppm), while there are no indications for the existence of a disubstituted compound.

The NMR spectra obtained for **3** which was prepared from the mixed ligand precursor are more complicated. There are at least five signals present in the region between 5.5-6.0 ppm. However, the presence of these five signals is not unexpected, because the unmodified precursor has both isopropoxide and *n*-propoxide ligands, thereby allowing the formation of an analogous compound of **3** with an *n*-propoxide ligand. This compound was synthesized from zirconium *n*-propoxide modified with 3 mol equivalents of Hthd, as described in the experimental section. However, the obtained crystals were not of X-ray quality. Single crystals that were identified as $Zr(O^nPr)(thd)_3$[4] were obtained as a side product in the synthesis (see ref. [30] for more details) with zirconium *n*-propoxide, strontium *n*-propoxide and 2 mol equivalents of Hthd in a mixture of *n*-propanol and toluene. The full refinement of the XRD-structure was not accomplished

[4] Crystal data: $C_{36}H_{64}O_7Zr$, M = 801.39, monoclinic, a = 10.338(4), b = 21.184(9), c = 19.202(8) Å, α = 90°, β = 99.67(5)°, γ = 90°, V = 4146(3) Å^3, T = 295 K, space group P2(1)/n, Z = 4, μ = 0.304 mm^{-1}, 4706 reflections measured, 2832 unique (R_{int} = 0.0800) which were used in all calculations. The final discrepancy factors were R1 = 0.1040; wR2 = 0.2768 for 1520 observed reflections (I > 2sigma(I)).

because of rather complex unresolved disorder in the *n*-propel radical, yet the existence of trisubstituted zirconium *n*-propoxide was clearly demonstrated. The metal-oxygen bond of the alkoxide ligands is longer in $Zr(O^nPr)(thd)_3$ compared to **3**, *i.e.*, 1.847(8) Å and 1.924(11) Å, respectively. The increase of the bond length of $Zr(O^nPr)(thd)_3$ is in good agreement with the decreased inductive effect of *n*-propoxide compared to isopropoxide ligands.

The solution and solid state stability of these compounds was also investigated. Two phenomena should be taken into account. The stability of **3** obtained from zirconium isopropoxide was investigated in both solid state and solution. In both situations it could clearly be seen that the compound was not stable in time, but after two months in solid state and two weeks in solution there was still a fair amount of **3** present. However, it was not possible to quantify the stability due to the occurrence of two phenomena. The position of different signals is strongly dependent on the temperature, and in order to distinguish the different species, the experiments were performed at low temperature, *i.e.*, 243 K. However, the solubility of $Zr(thd)_4$ is very low and it can not be excluded that at the low temperature of the experiment, the crystallization of $Zr(thd)_4$ occurs. It could be seen from the obtained complex NMR spectra that the stability is significantly less, if **3** is prepared from the mixed ligand precursor. The faster transformation towards $Zr(thd)_4$ is probably due to the facilitating effect of the residual alcohol [38].

Mass spectrometry experiments were performed on **3** obtained from zirconium isopropoxide. The main compounds in the gas phase, as can be seen in Table 4.1, were found at 515 (100%), 583 (69%) and 639 (75%) m/z, they are assigned to $Zr(O^iPr)(thd)_2$, $Zr(thd)_2((CMe_3C)COCHC(H)O)$ and $Zr(thd)_3$, respectively. The fragments in the gas phase are mainly trisubstituted, as can be expected for **3**. Similar mass spectrometry results were published by Jones *et al*. [17], but the authors assigned the fragments to origins from "$Zr(O^iPr)_2(thd)_2$".

An NMR spectrum was taken of the purchased commercial product claimed to be "$Zr(O^iPr)_2(thd)_2$". In the obtained spectrum, the ratio between the thd- and alkoxide-ligands was 3:1 based on the signals in the regions between 5.5-6.0 ppm and 3.5-4.5 ppm. There is one major signal present around 5.65 ppm corresponding to the position of $Zr(thd)_4$ and a minor one (~10% of the major signal) at 5.75 ppm

indicating the presence of **3**. This composition suggests that the presence of the unmodified precursor and that the solid modified product only contains ~2.5% of alkoxide ligands (where it should contain 50%).

Therefore, it can be concluded that the modification of zirconium propoxide precursors with more than one mol equivalent of Hthd involves the formation of a trisubstituted compound. This, in contrast to the generally assumed formation of a disubstituted compound. The isolation of a purely trisubstituted compound is complicated since the mono- and tetrasubstituted compounds tend to crystallize more easily in most cases, resulting in the obtaining of these compounds or a mixture of these compounds. The trisubstituted compounds have the tendency to rearrange to be thermodynamically stable $Zr(thd)_4$ and residual alcohol enhances this transformation.

Having the understanding of the chemistry involved in the Hthd modification of zirconium propoxide precursors it was interesting to examine if hafnium isopropoxide is modified in an analogous manner. The structure of the monosubstituted intermediate, $[Hf(O^iPr)_3(thd)]_2$, was published by Fleeting *et al.* [15]. The stability of this compound was evaluated by NMR and it was seen that its behavior upon aging in solid state and solution was analogous to that of $[Zr(O^iPr)_3(thd)]_2$. In solid state the compound is fairly stable, while in solution rearrangement to $Hf(thd)_4$ occurs.

The modification of hafnium *n*-propoxide with 1 mol equivalent of Hthd resulted in the formation of $[Hf(O^nPr)_3(thd)]_2$ (**4**)[5], which is to the best of our knowledge the first structural determination of a hafnium *n*-propoxide derivative. The compound is isomorphous with **1** of which the molecular structure is depicted in Figure 4.1. The presence of *n*-propoxide ligands causes the metal-metal distance in the structure to be smaller in **4** compared to that of $[Hf(O^iPr)_3(thd)]_2$, *i.e.*, 3.4641(16) and 3.476, respectively. This trend was also observed in the analogous zirconium compounds, however the difference is not as significant as was observed for

[5] Crystal data: $C_{40}H_{80}O_{10}Hf_2$, M = 1078.02, triclinic, a = 10.338(4), b = 21.184(9), c = 19.202(8) Å, α = 70.643(4)°, β = 79.138(5)°, γ = 83.636(4)°, V = 1280.7(4) Å^3, T = 295 K, space group p-1, Z = 4, μ = 4.094 mm^{-1}, 4404 reflections measured, 2732 unique (R_{int} = 0.0664) which were used in all calculations. The final discrepancy factors were R1 = 0.0683; wR2 = 0.1606 for 1751 observed reflections (I > 2sigma(I)).

zirconium. The metal-oxygen bond length of the alkoxide ligands in **4** are shorter than those in $[Hf(O^iPr)_3(thd)]_2$, *i.e.*, 1.891(17) and 1.909(12) for **4** and 1.927 and 1.953 Å for $[Hf(O^iPr)_3(thd)]_2$. The observed decrease of metal-oxygen bond-length is in agreement with observation, discussed above, for zirconium. The solution stability of this compound is rather poor, after 55 hours in solution ($CDCl_3$) already 30% of **4** had disappeared.

More interesting is the modification behavior of hafnium isopropoxide with more than one mol equivalents of Hthd. A sample of the precursor with 2.5 mol equivalents of Hthd was prepared. The first crystals obtained were identified as $[Hf(O^iPr)_3(thd)]_2$ and after removal of these initial crystals, two other types of crystals were obtained. The first type was identified as $Hf(O^iPr)(thd)_3$ (**5**)[6] (see Figure 4.4), and this compound is analogous to **3**.

Structures **3** and **5** contain one alkoxide and three thd ligands. The metal-oxygen bond length of the alkoxide ligand is slightly shorter in **5**, *i.e.*, 1.810(12) Å and 1.847(8) Å for **5** and **3**, respectively. However, the metal-oxygen bond length of the thd oxygen opposite the alkoxide ligand is slightly longer in **5**, *i.e.*, 2.050(13) Å and 2.017(10) Å for **5** and **3**. The other metal oxygen bond lengths in **5** are between 2.116(12) Å and 2.165(12) Å, while the difference in lengths in **3** is significantly larger 2.091(8) - 2.185(8) Å.

The other, needle-shaped crystals that were obtained upon the modification of hafnium isopropoxide with 2.5 mol equivalent of Hthd were identified as $[Hf(O^iPr)(thd)_2(OH)]_2$, (**6**)[7], and is depicted in Figure 4.5.

The difference between **6** and $[Hf(O^iPr)_3(thd)]_2$ [15] is the OH-group in bridging position, what allows the formation of a complex with one more alkoxide ligand

[6] Crystal data: $C_{36}H_{64}O_7$ Hf, M = 787.36, Monoclinic, a = 10.27(3) Å, b = 20.85(6) Å, c = 18.94(5) Å, $\alpha = 90°$, $\beta = 99.19(9)°$, $\gamma = 90°$, V = 4003(19) Å^3, T = 295(2) K, space group P2(1)/c, Z = 4, μ = 2.646 mm^{-1}, 13389 reflections measured, 4290 unique (R_{int}= 0.0963 which were used for refinement. The final discrepancy factors were R1 = 0.0790; wR2 = 0.1928 for 2670 observed reflections (I > 2sigma(I)).

[7] Crystal data: C_{50} $H_{92}O_{12}$ Hf_2, M = 1242.22, Monoclinic, a = 10.714(4) Å, b =20.285(8) Å, c = 14.321(6) Å, $\alpha = 90°$, $\beta = 102.553(9)°$, $\gamma = 90°$, V = 3038(2) Å^3, T = 295(2) K, space group P2(1)/n, Z = 2, μ = 3.464 mm^{-1}, 10029 reflections measured, 3241 unique (R_{int}= 0.0536 which were used for refinement. The final discrepancy factors were R1 = 0.0590; wR2 = 0.1300 for 2243 observed reflections (I > 2sigma(I)).

replaced by a thd-ligand. The less bulky ligand in the bridging position leads to a decrease of the angle between O(1)-Hf(1)-O(1A) in **6** compared to this angle in $[Hf(O^iPr)_3(thd)]_2$, 65.4(4)° and 72.0°, respectively. Since the metal-oxygen bond lengths of the bridging ligands are of the same order (2.129(8) Å and 2.105(8) Å for **5** and 2.192 Å and 2.102 Å for $[Hf(O^iPr)_3(thd)]_2$), resulting in slight increase of the metal-metal distance (3.5621(15) Å versus 3.476 Å). The metal-oxygen bond length of the alkoxide ligand is slightly shorter in **6** than for those in $[Hf(O^iPr)_3(thd)]_2$ (1.886(10) Å versus 1.927(6)-1.953(6) Å).

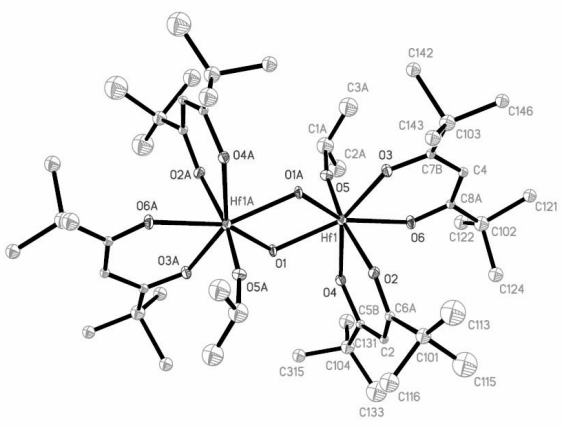

*Figure 4.5: Molecular structure of $[Hf(O^iPr)(thd)_2(OH)]_2$ (**6**).*

Compound **6** is a micro-hydrolysis product. The required water for this reaction is probably provided upon transferring the solution, which was decanted from the first crystals to a new flask. The compound **6** can be quantitatively formed from **5** and $[Hf(O^iPr)_3(thd)]_2$ upon introduction of stoichiometric amount of water. The NMR study of the freshly dried reaction mixture does not show any other signals than those corresponding to **5** and $[Hf(O^iPr)_3(thd)]_2$.

$$½\ [Hf(O^iPr)_4(^iPrOH)]_2 + 2\ Hthd \rightarrow ¼\ [Hf(O^iPr)_3(thd)]_2 + ½\ Hf(O^iPr)(thd)_3\ (5) + 2\ ^iPrOH$$

$$¼\ [Hf(O^iPr)_3(thd)]_2 + ½\ Hf(O^iPr)(thd)_3 + H_2O \longrightarrow ½\ [Hf(OH)(O^iPr)(thd)_2]_2\ (6)$$

After the isolation of **6** there was an attempt to see whether or not an analogous zirconium compound existed. However, no indication for the presence of such a compound was found in any of the obtained NMR spectra. This observation is in

good agreement with the generally observed trend to higher stability for dimeric aggregates derived from 5*d*-transition metal atoms compared to 4*d* ones [38].

NMR spectra were taken on samples containing mainly **5** and a mixture of **5** and **6**. The spectrum of **5** showed great similarity with that which was obtained for **3** as depicted in Figure 4.3c. The two major signals in the spectrum are at 5.75 and 5.63 ppm. In the mixture of **5** and **6** these same signals are still present; however, two other signals are also clearly present. These signals at 5.65 and 5.67 ppm are assigned to $Hf(thd)_4$ and to **6**. For **6** there are two signals, in a 1:1 ratio, which is expected in this region due to the presence of two types of thd ligands. The second signal of **6** is at the same chemical shift as the signal of **5** at 5.63 ppm, providing the signals to be in the expected ratio. It can be concluded that the modification of hafnium isopropoxide with Hthd proceeds in an analogous manner just as for zirconium isopropoxide. For both precursors, mono- and trisubstituted intermediates are formed. The major difference observed between the two systems is the formation of a stable micro-hydrolyzed hafnium compound, *i.e.*, **6**.

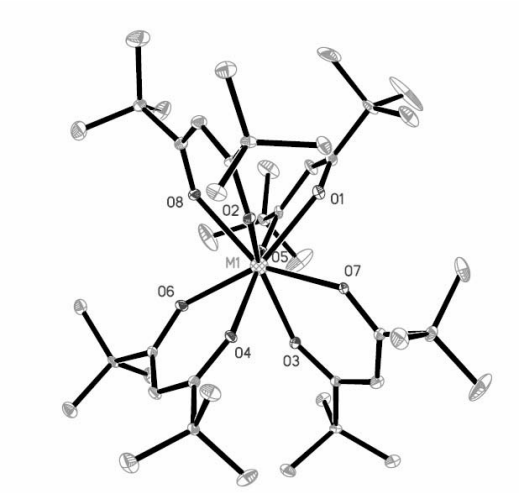

*Figure 4.6: Molecular structure of $M(thd)_4$ with M = Zr (**7a&b**) or Hf (**8**).*

The main interest in the structural characterization of the tetra-thd-substituted complexes of zirconium and hafnium was to reveal the reasons for their unusual physico-chemical properties. $M(thd)_4$, M= Zr, Hf, are known to be very poorly soluble in the hydrocarbon solvents and have quite poor volatility in comparison to other mononuclear thd-derivatives of transition metals. We succeeded in the

preparation of X-ray quality single crystals of $Zr(thd)_4$ ((**7a**)[8] & (**7b**)[9] *i.e.*, two different polymorphs were obtained) and $Hf(thd)_4$ (**8**)[10]. The ^1H NMR spectra of these compounds were as expected for these compounds. The mass-spectra of $M(thd)_4$ are also in good agreement with their molecular structures and contain the $M(thd)_3^+$-ions as the most intensive fragments (see Table 4.2), which corresponds to the dissociation of one ligand commonly observed through the electron impact. It should be noted, with respect to the observation of zirconium compounds in the MS spectra of **8**, that hafnium-samples always contain up to 2% of zirconium. The gas phase content of the latter can be higher because of relatively higher volatility of its compounds.

*Table 4.2: Interpretation of M/z(I) spectrum of **7** and **8**.*

Gas phase fragments	**7**	**8**
Zr((MeC)COCHC(H)O)(OCCHCO)	291 (14)	
[Hf(thd)-C_2H_4]		336 (12)
Zr((MeC)COCHC(CMe_3)O)(OCCHCO)	393 (18)	393 (8)
$Zr(thd)_3$	639 (100)	639 (12)
$Hf(thd)_3$		729 (100)

The molecular structures of compounds **7a**, **7b** and **8** are identical: 8 oxygen atoms, forming an Archimedes antiprism, surround the metal atoms. The coordination of each thd-ligand is slightly asymmetric with one shorter M-O distance of about 2.13 Å and one longer distance about 2.15-2.20 Å. The molecules in total have spheroid topology (Figure 4.6).

---

[8] Crystal data: C_{44} H_{76} Zr O_8, M = 824.27, Monoclinic, *a* = 22.545(6) Å, *b* = 11.275(3) Å, *c* =19.763(5) Å, $\alpha = 90°$, $\beta = 106.550(7)°$, $\gamma = 90°$, *V* = 4816(2) $Å^3$, T = 295(2) K, space group P2/c, Z = 4, $\mu = 0.273$ mm^{-1}, 10785 reflections measured, 3275 unique (R_{int}= 0.0493 which were used for refinement. The final discrepancy factors were R1 = 0.0826; wR2 = 0.2063 for 2282 observed reflections (I > 2sigma(I)).

[9] Crystal data: C_{44} H_{76} Zr O_8, M = 824.27, Triclinic, a = 12.086(7) Å, b = 19.33(4) Å, c = 21.135(8) Å, $\alpha = 97.71(10)°$, $\beta = 90.38(4)°$, $\gamma = 105.79(18)°$, V = 4703(10) $Å^3$, T = 295(2) K, space group P-1, Z = 4, $\mu = 0.279$ mm^{-1}, 54310 reflections measured, 11321 unique (R_{int}= 0.1489 which were used for refinement. The final discrepancy factors were R1 = 0.0825; wR2 = 0.1546 for 8393 observed reflections (I > 2sigma(I)).

[10] Crystal data: C_{44} H_{76} Hf O_8, M = 911.54, Monoclinic, *a* = 22.545(6) Å, *b* = 11.275(3) Å, *c* =19.763(5) Å, $\alpha = 90°$, $\beta = 106.550(7)°$, $\gamma = 90°$, *V* =4816(2) $Å^3$, T = 295(2) K, space group P2/c, Z = 4, $\mu = 2.211$ mm^{-1}, 13887 reflections measured, 4447 unique (R_{int}= 0.0729 which were used for refinement. The final discrepancy factors were R1 = 0.0763; wR2 = 0.1830 for 2945 observed reflections (I > 2sigma(I)).

Figure 4.7 shows that the structure of **7b** consists of a stacking of almost hexagonal 2D layers. Similar hexagonal layers are found in the structure of **7a**. The projections shown in Figure 4.8 make it apparent that in both structures the molecules in adjacent layers are not positioned behind each other (implying closer packing) but also not perfectly close packed. The difference between the polymorphs **7a** and **7b** can be understood comparing the equivalent projections of the two structures (view along b-axis for **7a** is equivalent to the view along a-axis for **7b**, see Figures 4.8a&b): the crystal structure of **7a** consists of a more symmetric ABAB… stacking of hexagonal 2D layers, while that of **7b** can be idealized as a slightly less symmetric ABCABC… stacking. Not quite surprisingly, the triclinic structure 7**b** formed from more dilute solutions stays even for denser packing with the unit cell volume of 4703(10) $Å^3$ compared to 4816(2) $Å^3$ for the monoclinic cell **7a**. Calculation of the distances between nearest methyl carbon atoms of the neighboring molecules gives an average of 4.4 Å, which is a relatively short distance indicating strong van der waals interactions. The latter are supposedly responsible in combination with the dense packing effect for the low solubility and volatility of these compounds.

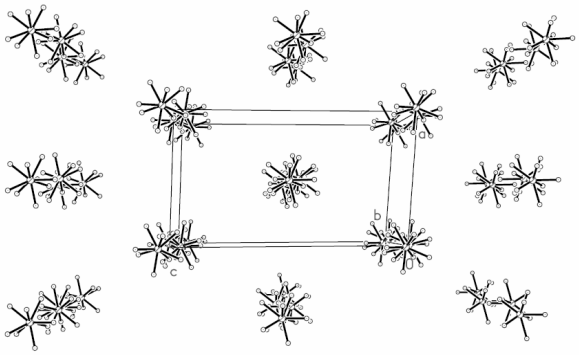

*Figure 4.7: Projection of the structure of $Zr(thd)_4$ (**7b**) along the b-axis. For clarity the C and H atoms are not displayed.*

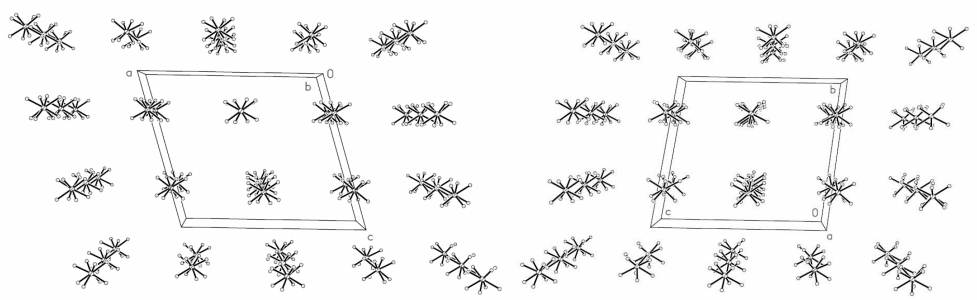

*Figure 4.8: Projections of the structure of 7**a** along the b-axis (left) and 7**b** along the a-axis (right). For clarity the C and H atoms are not displayed.*

In order to be more quantitative, the internal energy of **7b** has been evaluated as EB(**7b**) = –24061 kJ.mol^{-1} corresponding to 4 complexes per unit-cell. This has to be compared with the internal energy EB of the two crystallographically non-equivalent complexes characterized by EB(Zr1) = -5991 kJ.mol^{-1} and EB(Zr81) = -6042 kJ.mol^{-1}. The lattice energy is then E_{net}(**7b**) = 2[EB(Zr1) + EB(Zr81)] – EB(**7b**) = +5 kJ.mol^{-1}. This almost zero value is well in line with the high steric hindrance occurring in such complexes and would even mean that almost nothing is gained by packing them in a 3D-network. As methine protons on thd groups were missing in this structure, the effect of adding them was investigated leading to EB(**7h**) = –24073 kJ.mol^{-1}, EB(Zr1) = -5994 kJ.mol^{-1} and EB(Zr81) = -6045 kJ.mol^{-1}. As can easily be checked, this does not change the lattice energy which still remains slightly positive. Knowing that the enthalpy of association in the crystal should be endothermic, it follows that crystal formation should be entirely driven by entropy effects. In other words, there is no doubt that in solution a large number of solvent molecules should be immobilized around these complexes, leading to a large and positive ΔS after crystallization. For the same reasons, it follows that solubility should be rather low, owing to the large change in solvent structure that is needed for putting complexes in solution. In order to see if such considerations also apply to **7a** we have also investigated this compound leading to EB(7a) = –23792 kJ.mol^{-1}, EB(Zr1) = -5950 kJ.mol^{-1} and EB(Zr2) = -5944 kJ.mol^{-1}. The corresponding lattice energy is then found to be slightly negative E_{net}(**7a**) = -4 kJ.mol^{-1}. This very small value demonstrates again that as in the case of **7b** crystallization and solubility are also entropy controlled. Quite similar conclusions apply for **8**, despite higher internal energies:

EB(**8**) = –20042 kJ.mol^{-1}, EB(Hf1) = -4988 kJ.mol^{-1} and EB(Hf2) = -5032 kJ.mol^{-1}, that leads to E_{net}(**8**) = -2 kJ.mol^{-1}.

It is also worth noting that in the case of the $Zr(thd)_4$, the observed kinetic effect (quick formation of **7a** followed by slow recrystallization of **7b**) is due to the existence of two different isomers crystallizing within the same network (Figure 4.9). **7a** or **8** should then be viewed as a random mixture of two isomers displaying D_2 and D_4 point group symmetry. From the observation that **7b** is the thermodynamic end product, it follows that the D_4 isomer should be less solvated in solution than the D_2 isomer. In order to see if some enthalpy effect should be associated to the intergrowth of two networks based on isomers displaying D_2 and D_4 symmetry respectively, two crystalline models derived from the available X-ray data of **8** have been generated. For **8A**, a net based on the stacking of D_2 isomers, we found: EB(**8A**) = –19584 kJ.mol^{-1}, EB(Hf1) = -4934 kJ.mol^{-1} and EB(Hf2) = -4857 kJ.mol^{-1}, leading to E_{net}(**8A**) = -2 kJ.mol^{-1}, whereas for **8B**, a net based on the stacking of D_4 isomers, it comes: EB(**8B**) = –19708 kJ.mol^{-1}, EB(Hf1) = -4872 kJ.mol^{-1} and EB(Zr2) = -4982 kJ.mol^{-1}, that leads to E_{net}(**8B**) = 0 kJ.mol^{-1}. It follows that enthalpy effects associated to the mixing of both isomers should be quite low and that again crystallization should be driven by entropy effects.

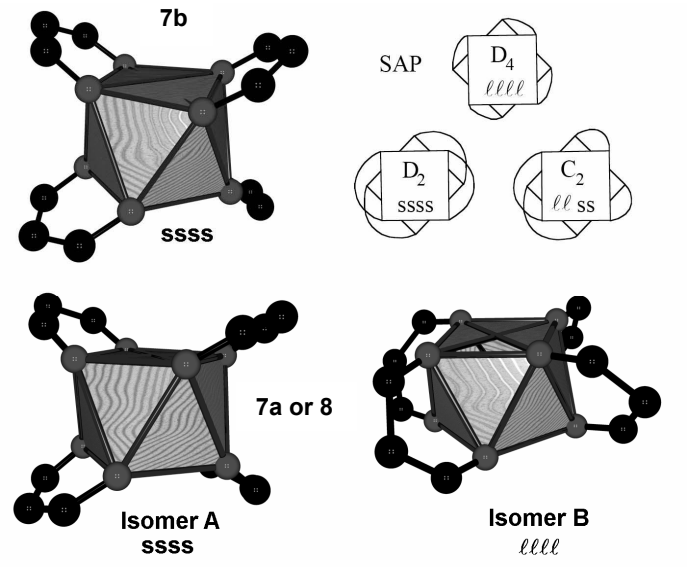

*Figure 4.9: Structural and topologic description of the isomers in the structure **7b**.*

4.4 Conclusions

The modification of zirconium and hafnium propoxide precursors with Hthd involves mono- and trisubstituted intermediate compounds. The modification does not involve a disubstituted compound, and thus, the commercial product claimed to be "$Zr(O^iPr)_2(thd)_2$" most commonly "used" for the MOCVD preparation of ZrO_2 does not exist. No evidence was found for the presence of such a compound in either zirconium or the hafnium based systems. Formation of the dimeric hydroxo-di-thd-substituted complex could be observed only for hafnium based system and occurs on micro-hydrolysis.

All heteroleptic intermediates are eventually transformed to the thermodynamically stable $Zr(thd)_4$ or $Hf(thd)_4$. The compounds obtained from isopropoxide precursors showed a higher stability than those with *n*-propoxide ligands or a combination of both types. Moreover, it is important to note that residual alcohol facilitates the transformation and strongly enhances its rate.

The unusually low solubility and volatility of $M^{IV}(thd)_4$ has been shown to be due to close packing and strong van der waals interactions in the crystal structures of these compounds.

4.5 References

1 R.J. Vacassy, C. Guizard, J. Palmeri and L. Cot, *Nanostruct. Mater*., **10**, 77 (1998).

2 C.R. Xia, H.Q. Cao, H. Wang, P.H. Yang, G.Y. Meng and D.K. Peng, *J. Membr. Sci*., **162**, 181 (1999).

3 H. Kurosawa, Y.T. Yan, N. Miura and N. Yamazoe, *Solid State Ionics*, **79**, 338 (1995).

4 C.M.S. Rodrigues, J.A. Labrincha and F.M.B. Marques, *Solid State Ionics*, **136-137**, 671 (2000).

5 N. Miura, M. Nakatou and S. Zhuiykov, *Sensor Actuat. B-Chem.,* **93**, 221 (2003).

6 Y.W Li, D.H. He, Z.X. Cheng, C.L. Su, J.R. Li and Q.M. Zhu, *J. Mol. Catal. A: Chem*., **175**, 267 (2001).

7 M.Haruta, T. Kobayashi, H. Sano and N. Yamada, *Chem. Lett.***, 829**, 405 (1985).

8 A. Knell, P. Barnickel, A. Baiker and A. Wokaun, *J. Catal*., **137**, 306 (1992).

9 S. Hoffmann, M. Klee and R. Waser, *Integr. Ferroelectr.*, **10**, 155 (1995).

10 M. Klee, U. Mackens, W. Hermann and E. Bathelt, *Integr. Ferroelectr.*, **11**, 247 (1995).

11 G.D. Wilk, R.M. Wallace and J.M. Anthony, *J. Appl. Phys*., **89**, 5243 (2001).

12 A.C. Jones, H.C. Aspinall. P.R. Chalker, R.J. Potter, K. Kukli, A. Rahtu, M. Ritala, M. Leskelä, *J. Mater. Chem.*, **14**, 3101 (2004).

13 L.G. Hubert-Pfalzgraf, *J. Mater. Chem.*, **14**, 3113 (2004).

14 T.J. Leedham, A.C. Jones, P.J. Wright, M.J. Crosbie, D.J. Williams, H.O. Davies and P. O'Brien, *Integr. ferroelectr.*, **26**, 767 (1999).

15 K.A. Fleeting, P. O'Brien, D.J. Otway, A.J.P. White, D.J. Williams and A.C. Jones, *Inorg. Chem.,* **38**, 1432 (1999).

16 A.C. Jones, T.J. Leedham, P.J. Wright, D.J. Williams, M.J. Crosbie, H.O. Davies, K.A. Fleeting and P. O'Brien, *J. Eur. Ceram. Soc*., **19**, 1431 (1999).

17 A.C. Jones, T.J. Leedham, P.J. Wright, M.J. Crosbie, P.A. Lane, D.J. Williams, K.A. Fleeting, D.J. Otway and P. O'Brien, *Chem. Vapor. Depos.*, **4**, 46 (1998).

18 D.H. Kim, J.S. Na and S.W. Rhee, *J. Electrochem. Soc.*, **148**, C668 (2001).

19 H.-W. Chen, T.-Y. Huang, D. Landheer, X. Wu, S. Moisa, G.I. Sproule and T.-S. Chao, *J. Electrochem. Soc.*, **149**, F49 (2002).

20 H.-W. Chen, D. Landheer, X. Wu, S. Moisa, G.I. Sproule, T.-S. Chao and T.Y. Huang, *J. Vac. Sci. Technol. A*, **20**, 1145 (2002).

21 H. Ahn, H.W. Chen, D. Landheer, X. Wu, L.J. Chou and T.-S. Chao, *Thin Solid Films*, **318**, 455 (2004).

22 H.W. Chen, T.Y. Huang, D. Landheer, X. Wu, S. Moisa, G.I. Sproule, J.K. Kim, W.N. Lennard and T.S. Chao, *J. Electrochem. Soc.*, **150**, C465 (2003).

23 A.C. Jones, T.J. Leedham, P.J. Wright, M.J. Crosbie, D.J. Williams, K.A. Fleeting, H.O. Davies, D.J. Otway and P O'Brien, *Chem. Vapor. Depos.*, **4**, 197 (1998).

24 J.F. Roeder, T.H. Baum, S.M. Bilodeau, G.T. Stauf, C. Ragaglia, M.W. Russell and P.C. Van Buskirk *Adv. Mater. Opt. Electr.*, **10**, 145 (2000).

25 I.-S. Chen, B.C. Hendrix, S.M. Bilobeau, Z. Wang, C. Xu, S. Johnston, P.C. Van Buskirk, T.H. Baum and J.F. Roeder, *Jpn. J. Appl. Phys.*, **41**, 6695 (2002).

26 J. Si, S.B. Desu and C.Y. Tsai, *J. Mater. Res.*, **9**, 1721 (1994).

27 C. Dubourdieu, S.B.Kang, Y.Q. Li, G. Kulesha and B. Gallois, *Thin Solid Films*, **339**, 165 (1999).

28 S. Chevalier, M. Kilo, G. Borchardt and J.P. Larpin, *Appl. Surf. Sci.*, **205**, 188 (2003).

29 M. Putkonen and L. Niinistö, *J. Mater. Chem*., **11**, 3141 (2001).

30 G.A. Seisenbaeva, S. Gohil and V.G. Kessler, *J. Mater. Chem.*, **14**, 3177 (2004).

31 Chapter 2 of this thesis.

32 E.P. Turevskaya, N.I. Kozlova, N.Y. Turova, A.I. Belokon, D.V Berdyev, V.G. Kessler and Y.K. Grishin, *Russ. Chem. Bull.*, **44**, 734 (1995).

33 SHELXTL-NT program manual, Bruker AXS, (1998).

34 M. Henry, *CHEMPHYSCHEM*, **3**, 561 (2002).

35 M. Henry and M.W. Hosseini, *New J. Chem.*, **28**, 897 (2004).

36 D.R. Turner, M. Henry, C. Wilkinson, G.J. McIntyre, S.A. Mason, A.E. Goeta and J.W. Steed, *J. Am. Chem. Soc.*, **127**, 11063 (2005).

37 M. Pathak, R. Bohra, R.C. Mehrotra, I.P. Lorenz and H. Piotrowski, *Z. Anorg. Allg. Chem.*, **629**, 2493 (2003).

38 V.G. Kessler, "*Chemistry and solution stability of alkoxide precursors,*" in Handbook of Sol–Gel Science and Technology, ed. H. Kozuka, Kluwer Academic Publishers, Boston, Chap. 1 (2004).

Chapter 5

Modification of zirconium and hafnium *t*-butoxides with β-diketones and β-diketoesters

Abstract

The modification of zirconium and hafnium *t*-butoxides with 2,2,6,6,-tetramethyl-3,5-heptanedione (Hthd) and *t*-butylacetoacetate (tbaoac) was investigated. For the modification with Hthd the formation of di- and trisubstituted compounds is observed. The molecular structures of $Zr(O^tBu)(thd)_3$ (**1**) and $Hf(O^tBu)(thd)_3$ (**2**) were determined and the existence of $Zr(O^tBu)_2(thd)_2$ (**3**) and $Hf(O^tBu)_2(thd)_2$ (**4**) was clearly seen. However, refinement of the structure of the latter two compounds was not possible. ^{1}H NMR and mass spectrometric characterization of **1**-**4** was in agreement with their molecular structure. The NMR studies of these compounds revealed that they are not stable in solution in time. The rearrangement to a tetrasubstituted compound could clearly be seen. The modification of zirconium and hafnium isopropoxide with tbaoac resulted in mono- and disubstituted compounds and the structure of $[Hf(O^iPr)_3(tbaoac)]_2$ (**5**) was determined. The NMR studies in time on solution of the tbaoac modified alkoxide demonstrated that the disubstituted compounds are stable in time. The only changes in the NMR spectra in time are due to transesterfication of the alkyl and alkoxide ligands. The NMR studies showed that the modification with ethylacetoacetate involves also the formation of mono- and disubstituted compounds and the transesterfication of the alkyl and alkoxide ligands also takes place in these systems. The thermodynamically stable disubstituted compound could be of great interest in sol-gel application and the transesterfication of the alkyl and alkoxide ligands can easily be avoided by proper choice of ligands and modifier, *i.e.*, they should be the same. NMR studies on zirconium and hafnium *t*-butoxides that were modified by

tbaoac showed that the modification involves the formation of mono-, di- and trisubstituted compounds. These compounds turned out not to be stable in solution. The size of the *t*-butoxide ligands causes steric hindrance which disables the trans-stabilization of the alkoxide ligands.

5.1 Introduction

Zirconia and hafnia have several interesting properties that make them important materials. They are widely used in structural ceramics [1,2], gas sensors [3,4], catalysts [6-8] and dense dielectric and ferroelectric films in electronics [9,10]. With the trend of further miniaturization there has been an increasing interest in the controlled preparation of zirconia. It is an extremely attractive candidate for very large scale integrated circuits and as a gate dielectric in metal oxide-semiconductors (MOS) devices because of its high dielectric constant (~25) [11]. In addition, zirconia also has a beneficial high bandgap (5.8-7.8 eV) [11] and thermal compatibility with contemporary CMOS processes.

Chemical vapor deposition is compatible with semiconductor processing, what makes it an attractive technique for the preparation of microelectronics. The advantages of this process include the control of composition and the ability to scale it up to large areas [12]. If metal organic precursors are used, as in the present study, the deposition technique is referred to as MOCVD (metal-organic chemical vapor deposition). The selection of a precursor is a fundamental aspect of the MOCVD process. The chemical compatibility of the precursor in solution and in vapor phase is necessary for their maximum usefulness [12]. In addition, solution stability and thermal stability during vapor phase transport are extremely critical for process reproducibility. It may seem obvious that the precursor composition does not change during storage after its preparation and before it is used, *e.g.,* the precursor is shelf stable.

The application of commercial zirconium and hafnium alkoxide precursors is an unattractive option. The zirconium has an unsaturated coordination what makes the precursors extremely sensitive to hydrolysis and pyrolysis. Another drawback of unmodified precursors (*e.g.*, zirconium isopropoxide) is their relatively low volatility, requiring high deposition and substrate temperatures and leading to the formation of carbon contamination.

A general method used to moderate reactivity and improve volatility is by replacing (part) of the alkoxide ligands by chelating organic ligands [12-14]. In previous work [15-17] the modification of zirconium and hafnium propoxide

precursors with acetylacetone (Hacac) and 2,2,6,6,-tetramethyl-3,5-heptanedionate (Hthd) has been discussed and it can be seen that the modification proceeds in an analogous manner. The modification involves mono- and trisubstituted intermediate compounds but it does not involve a disubstituted compound, and thus, the commercial products claimed to be "$Zr(O^iPr)_2(thd)_2$" most commonly "used" for the MOCVD preparation of ZrO_2 does not exist. No evidence was found for the presence of such a compound in either the zirconium- or the hafnium-based systems. Formation of a dimeric hydroxo-di-thd-substituted complex, $[Hf(OH)(O^iPr)(thd)_2]_2$ and related Hacac compounds, could only be observed for the hafnium-based systems and occurs on micro-hydrolysis. All heteroleptic intermediates are eventually transformed to the thermodynamically stable $M(thd)_4$ or $M(acac)_4$ compounds (M= Zr or Hf).

The Hthd and Hacac modification of precursors with larger alkoxide ligands (*i.e.*, zirconium and hafnium *t*-butoxides) has received little attention and only a few articles deal with these systems [19]. The modification is claimed to involve a disubstituted compound, but no structural data has been reported. These systems are attractive for MOCVD since one would expect high volatility for the compounds to be formed. From a scientific point of view it is interesting to evaluate the effect of larger alkoxide ligands on the formed modified compounds. In the work on the modification of propoxide precursors with Hthd [18] we observed that the metal-oxygen bond length of the alkoxide ligand decreased with an increasing inductive effect of the ligands, *i.e.*, the bond length decreased going from an isopropoxide to a *n*-propoxide ligand.

Another approach that has received some attention in recent years is the modification of zirconium and hafnium propoxides with asymmetric chelating ligands. Up to date, a limited number of structures using asymmetric chelating ligands like *t*-butylacetoacetate (tbaoac) [20,21], *N*,*N*-diethylacetoacetamide (deacam) [20], 1-methoxy-2-methyl-2-propyanolate (mmp) [22,23] and 2-(4,4-dimethyloxazolinyl)-propanolate (dmop) [24] have been reported. In these systems, disubstituted compounds are formed where the modifying ligand strengthens the bonding to the alkoxide ligands by trans-interactions. The use of *β*-ketoesters, is very interesting since these ligands are cheap and (therefore) suitable for application in sol-gel [25]. The intermediates formed upon the

modification of zirconium and hafnium isopropoxides with *t*-butylacetoacetate (tbaoac) include mono- and disubstituted compounds, while upon complete removal of the alkoxide, a tetrasubstituted compound is formed [20]. Despite the fact that the structure of this compound has not been determined and the solubility of it is very low it has recently been applied for the preparation of zirconium and hafnium films by MOCVD [26]. We were curious about the stability of the formed intermediate compounds in the modification with tbaoac and if it is possible to obtain analogous compounds when ethylacetoacetate (eaoac) is used as the modifier.

The third approach is the combination of the previous two. It is interesting to see what kinds of intermediates are formed upon the modification of zirconium and hafnium *t*-butoxides with *t*-butylacetoacetate (tbaoac). To the best of our knowledge, these combinations have not been explored before

5.2 Experimental

All manipulations were carried out in a dry nitrogen atmosphere using the Schlenk technique or a glove box. Hexane and toluene (Merck, *p.a.*) were dried by distillation after refluxing with $LiAlH_4$. Acetylacetone (Hacac), 2,2,6,6,-tetramethyl-3,5-heptanedionate (Hthd) and *t*-butylacetoacetate 97% (tbaoac) were purchased from Aldrich. Ethylacetoacetate (eaoac) 99% was purchased from Alfa Aesar. Molecular sieves were added to the Hacac to assure that it remained water free. ^{1}H NMR spectra were recorded in $CDCl_3$ for all compounds on a Bruker 400 MHz spectrometer at 243 K.

Synthesis: The zirconium propoxide precursors used as starting materials in this work are zirconium isopropoxide, ($[Zr(O^iPr)_4(^iPrOH)]_2$ 99.9%), 70 wt% solution of "$Zr(O^nPr)_4$", (all purchased from Aldrich) and $[Zr(O^nPr)(O^iPr)_3(^iPrOH)]_2$ which was prepared according to a recently developed technique [16,27]. The zirconium isopropoxide was dissolved and recrystallized from toluene prior to use in order to remove impurities. The hafnium isopropoxide was prepared by anodic oxidation of hafnium metal in isopropanol [28] and recrystallized from toluene. Zirconium *t*-butoxide (99.999%) and hafnium *t*-butoxide (99.99%) were purchased from Aldrich and used as received. All the different precursors were modified with various equivalent amounts of the modifier

according to the techniques described below. The exact composition of the single crystals **1, 2 & 5** was established with single crystal X-ray crystallography.

A sample of zirconium *t*-butoxide (weight: 0.86 g (2.25 mmol)) in 2 ml hexane was modified with 0.41 g Hthd (2.25 mmol). Crystallization occurred during cooling at -30 °C over night. Under a microscope the presence of two or three different types of crystals were observed. An attempt was made to separate the different compounds by adding 1 ml of toluene to the sample and subsequently removing the liquid phase from the flask. The remaining crystals were dissolved in 2.5 ml toluene and placed in the freezer at -30 °C for crystallization. The obtained crystals in this fraction were identified as **3**. The flask with the liquid phase removed was also placed in the freezer but no successful structural determination was performed on the crystals formed.

$Zr(O^tBu)(thd)_3$ (**1**): Zirconium *t*-butoxide (weight: 0.77 g (2.0 mmol)) was dissolved in 2 ml hexane. After the addition of 1.10 g (6.0 mmol) of Hthd, *i.e.*, 3 mol equivalents, the sample was placed over night at –30 °C for crystallization. The obtained crystals were not of X-ray quality. The sample was dried under vacuum (0.1 mm Hg) and the dried product was redissolved in 1.5 ml toluene. Crystallization occurred during cooling at -30 °C over night and the crystals were identified as **1** (yield: 0.66 g, 35%).

$Hf(O^tBu)(thd)_3$ (**2**): Hafnium *t*-butoxide (weight: 1.30 g (2.76 mmol)) was dissolved in a mixture of 2 ml hexane and 5 ml toluene. After addition of 1.53 g (8.3 mmol) of Hthd, *i.e.*, 3 mol equivalents, the sample was placed over night at -30 °C for crystallization. The solution was decanted from the obtained crystals and the crystals were identified as **2** (yield: 1.65 g, 58%).

$Zr(O^tBu)_2(thd)_2$ (**3**): Zirconium *t*-butoxide (weight: 0.90 g (2.35 mmol)) was dissolved in 2 ml hexane. After addition of 0.87 g (4.7 mmol) of Hthd, *i.e.*, 2 mol equivalents the sample was placed over night at –30 °C for crystallization. The solution was decanted from the obtained X-ray quality colorless crystals (1.62 g, yield 91%) that were identified as **3**.

$Hf(O^tBu)_2(thd)_2$ (4): Hafnium *t*-butoxide (weight: 1.56 g (3.31 mmol)) was dissolved in 2 ml toluene. After addition of 1.22 g (6.62 mmol) of Hthd, *i.e.*, 2 mol equivalents a white precipitate was formed. After addition of 6 ml hexane a clear

solution was obtained and the sample was placed over night at –30 °C for crystallization. The solution was decanted from the obtained colorless crystals and the crystals were identified as **4**.

$[Hf(O^iPr)_3(tbaoac)]_2$ (**5**): Hafnium isopropoxide (weight: 1.01 g (2.12 mmol)) was dissolved in a mixture of hexane (2 ml) and toluene (3 ml). After the addition of 0.34 g (2.12 mmol) of tbaoac the sample was placed over night at -30 °C, resulting in the formation of a white precipitate. The sample was dried under vacuum (0.1 mm Hg) and redissolved in 1.5 ml hexane. After storing overnight at –30 °C an amount of crystals, that again were identified as $[Hf(O^iPr)_3(tbaoac)]_2$ (**5**) were obtained (yield: 0.55 g, 41%).

$[Zr(O^iPr)_3(tbaoac)]_2$ and $Zr(O^iPr)_2(tbaoac)_2$ were prepared in an analogous manner as described for the preparation of **5**.

Samples of commercial 70% zirconium *n*-propoxide in *n*-propanol were dried under vacuum (0.1 mm Hg) (resulting in a typical weight around 1.5 g) and redissolved in 3 ml hexane. An equivalent amount (1-4 mol) of ethylacetoacetate (eaoac) was added and the sample was placed over night at –30 °C. The next day the samples were dried under vacuum (0.1 mm Hg) and a sample was taken for NMR analysis. The remaining viscous product was redissolved in 1 ml hexane and again placed at –30 °C.

Samples of zirconium and hafnium *t*-butoxides (typically ~1 g) were dissolved in 6 ml mixture of hexane and toluene (volume ratio 1:2). After the addition of 1, 2 or 3 mol equivalent of tbaoac the samples were stored over night at –30 °C. They were dried under vacuum (0.1 mm Hg) and samples were taken for NMR analysis. The remaining viscous product was redissolved in 2 ml toluene and again placed at –30 °C.

Crystallography: Data collection for single crystals of all compounds was carried out at 22 °C on a SMART CCD 1k diffractometer with graphite monochromated MoKα radiation. All structures were solved by standard direct methods. The coordinates of the metal atoms as well as the majority of other non-hydrogen atoms were obtained from the initial solutions and for all other non-hydrogen atoms found in subsequent difference Fourier syntheses. The

structural parameters were refined by least squares using first isotropic and then, also anisotropic approximations. The coordinates of the hydrogen atoms were calculated geometrically and were included into the final refinement in isotropic approximation for all the compounds. All calculations were performed using the SHELXTL-NT program package [29] on an IBM PC.

5.3 Results and discussion

Samples of zirconium *t*-butoxide were modified with 1, 2 and 3 mol equivalent of Hthd. All batches provided crystals. In the samples with 1 and 2 mol equivalents various types of crystals were observed, while in the sample with 3 mol equivalents of Hthd there was only one type of crystal. These crystals were characterized as $Zr(O^tBu)(thd)_3$ (**1**)[1] and its molecular structure is depicted in Figure 5.1. The hafnium analog of this compound, $Hf(O^tBu)(thd)_3$ (**2**)[2], was prepared according to the procedure described in the experimental section.

Structures **1** and **2** contain one alkoxide and three thd ligands and a selection of the bond lengths of these compounds are listed in Table 5.1. The metal-oxygen bond length of the alkoxide ligand may be slightly shorter in **1**, *i.e.*, 1.874(7) Å and 1.888(9) Å for **1** and **2**, respectively. The metal-oxygen bond lengths of the thd oxygen opposite the alkoxide ligand have the same length in both compounds, *i.e.*, 2.030(9) Å. The other metal oxygen bond lengths also have comparable values. When these compounds are compared with their isopropoxide analogs [32], *i.e.*, $Zr(O^iPr)(thd)_3$ and $Hf(O^iPr)(thd)_3$, a remarkable trend is observed. The metal-oxygen bond length of the alkoxide ligand are shorter in the propoxide compounds, *i.e.*, 1.847 Å and 1.820 Å for $Zr(O^iPr)(thd)_3$ and $Hf(O^iPr)(thd)_3$, respectively. One would expect that the metal-oxygen bond length of the alkoxide would decrease

[1] Crystal data: $C_{36}H_{66}O_7Zr$, M = 714.12, monoclinic, a = 10.417(4), b = 21.099(8), c = 19.256(7) Å, α = 90°, β = 99.988(13)°, γ = 90°, V = 4168(3) Å^3, T = 295 K, space group P2(1)/c, Z = 4, μ = 0.304 mm^{-1}, 7950 reflections measured, 3777 unique (R_{int} = 0.548 which were used in all calculations. The final discrepancy factors were R1 = 0.0740; wR2 = 0.1868 for 2366 observed reflections (I > 2sigma(I)).

[2] Crystal data: $C_{36}H_{66}O_7Hf$, M = 801.39, monoclinic, a = 10.429(2), b = 21.137(4), c = 19.345(4) Å, α = 90°, β = 99.70(4)°, γ = 90°, V = 4203.5(14) Å^3, T = 295 K, space group P2(1)/c, Z = 4, μ = 2.521 mm^{-1}, 13931 reflections measured, 4506 unique (R_{int} = 0.0413) which were used in all calculations. The final discrepancy factors were R1 = 0.0631; wR2 = 1585 for 3306 observed reflections (I > 2sigma(I)).

with the increasing size and thus inductive effect of the alkoxide ligands. In the work on the modification of zirconium propoxides [18] this trend was clearly present; the metal-oxygen bond length of a *n*-propoxide ligand is 1.924 Å, while that of an isopropoxide ligand is 1.847 Å. The deviation of the metal-oxygen bond lengths of the alkoxide ligands in **1** and **2** is due the steric hindrance in these compounds. From Table 5.1 it can be seen that most of the other metal-oxygen bond lengths are also shorter for the propoxide compounds, which also supports the steric hindrance in **1** and **2**.

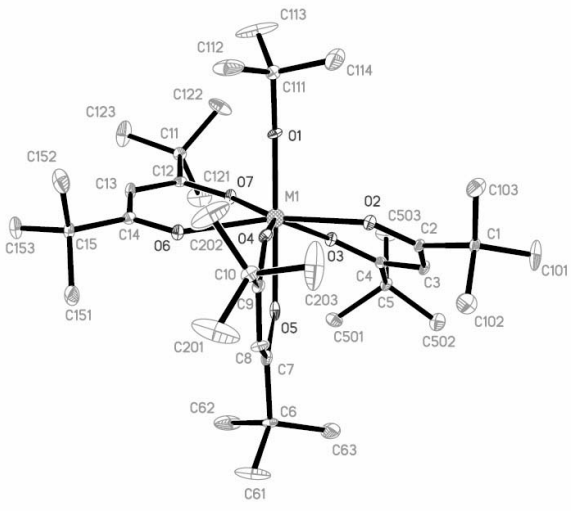

*Figure 5.1: Molecular structure of M(O^{t}Bu)(thd)$_3$ with M=Zr (**1**) and Hf (**2**).*

The sample with zirconium *t*-butoxide and 2 mol equivalents of Hthd was separated and the obtained crystals were characterized by single crystal diffractometry. The crystals turned out to be poorly reflecting and long exposure times were required to obtain a maximum number of reflections. The experiments permitted the determination of the unit cell parameters of the compounds but the quality of the data was not sufficient to refine the structure. The data clearly indicated that the metal atom was surrounded by 6 oxygen atoms, but refinement of the structure was not possible because of strong disorder between the *t*-butoxide ligands and the thd-ligands. But it was clear that this compound was the disubstituted derivative Zr(O^{t}Bu)$_2$(thd)$_2$ (**3**). The hafnium analog of this compound, Hf(O^{t}Bu)$_2$(thd)$_2$ (**4**), was prepared according to the procedure described in the experimental section. Single crystal X-ray diffraction experiments were also

performed on this compound. The reflectivity of the compound was better than that of **3**, but the data did not allow refining the structure. The structure of the titanium isomorph of **3** and **4** could also not be determined [30]. The monosubstituted $[Ti(O^tBu)_3(thd)]_2$ displays metal-oxygen bond lengths of the alkoxide ligand of 1.8017 and 1.8160 Å [30]. The disubstituted compound with benzoylacetonate, $(Ti(Bzac)_2(O^tBu)_2$ shows bond lengths of the alkoxide ligand of 1.773 and 1.796 Å [31]. The disubstituted Ti-derivatives demonstrate some additional strengthening of M-O bonding via trans-effect. The latter is supposedly also facilitated by the packing of the molecules with asymmetric ligands in the structure.

*Table 5.1: Metal-oxygen bond lengths of **1**, **2**, $Zr(O^iPr)(thd)_3$ [18] and $Hf(O^iPr)(thd)_3$ [18].*

Bond lengths [Å]	**1**	**2**	**$Zr(O^iPr)(thd)_3$**	**$Hf(O^iPr)(thd)_3$**
M-O1	1.874(7)	1.888(9)	1.847	1.810
M-O2	2.030(9)	2.030(9)	2.017	2.050
M-O3	2.140(7)	2.137(9)	2.092	2.116
M-O4	2.147(7)	2.143(9)	2.108	2.123
M-O5	2.175(7)	2.180(8)	2.123	2.154
M-O6	2.176(7)	2.183(9)	2.165	2.165
M-O7	2.211(6)	2.198(9)	2.185	2.161

It was not possible to isolate crystals of any other compounds from the sample of zirconium *t*-butoxide with 1 mol equivalent of Hthd. The crystals present in this sample were the disubstituted compounds, *i.e.*, **3**, and most likely also the unmodified precursor. All obtained compounds, *i.e.*, **1-4,** were studied by ^{1}H NMR to evaluate their stability and to confirm that no monosubstituted compound exists. The obtained spectra only display signals in the region 1-1.3 ppm and 5.5-5.8 ppm. The first chemical shift is typical for $\underline{CH_3}$ while the latter region represents the $\underline{CH}$ of the thd-ligand. A selection of the obtained spectra is displayed in Figure 5.2. It should be noted that no difference is observed in the chemical shift of the same hafnium and zirconium compounds. The spectrum of freshly prepared **2** is depicted in Figure 5.2a and the same sample is recorded again ~5 hours later. Between the experiments, which were performed at 243 K, the sample was stored at room temperature. The signals due to **2** are marked with (*****) and they are in the expected ratio of 1: 18: 3 for respectively $\underline{CH}$ and $\underline{CH_3}$ of thd and $\underline{CH_3}$ of the *t*-butoxide ligand. The position of the signals for the unmodified precursor and $Zr(thd)_4$ were obtained by measuring a reference sample and from ref [18], respectively. The

signals due to these compounds are respectively marked with (□) and (o). It can clearly be seen that upon aging in solution, compound **2** rearranges. The remaining signals that appear upon aging, depicted in Figure 5.2b, are due to the formation of **4** and will be discussed below. The rearrangement of **2** seems to mainly involve the formation of tetrasubstituted species and unmodified precursors and is represented by Eq. 5.1.

$$4\ Hf(O^tBu)_1(thd)_3 \Rightarrow 3\ Hf(thd)_4 + Hf(O^tBu)_4 \qquad (5.1)$$

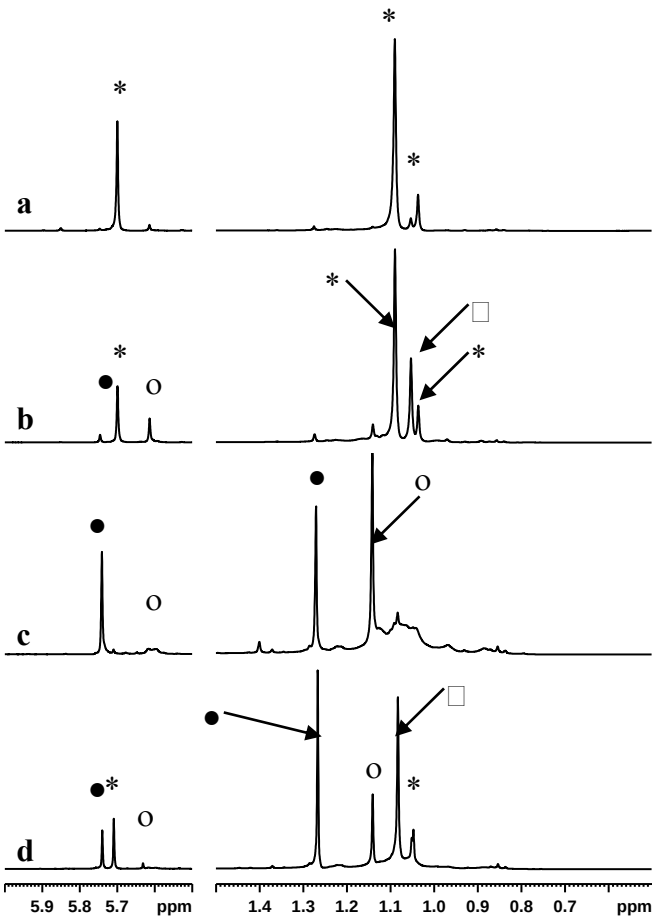

*Figure 5.2: NMR spectra fresh **2** (**a**) and aged **1** (**b**) and fresh (**c**) and aged (**d**) **3**.The signals due to **1** and **2** are marked with (*), those due to **3** and **4** with (●), $Zr(thd)_4$ with (o), unmodified t-butoxide precursor with (□). For reasons of clarity the intensities of the signals between 6 and 5.5 ppm are increased four times compared to those between 1.5 and 0.5 ppm.*

All the signals in the obtained spectra correspond to the isolated and characterized compounds and thus there is no evidence for the existence of a monosubstituted compound. The solid state stability of the compounds is quite high, after storage of the samples for about half a year in the freezer the composition remained unchanged. This is in contrast to the observed poor solution stability.

The ^{1}H NMR spectrum of freshly prepared **3** is depicted in Figure 5.2c and of the spectrum of the aged for ~3 days in solution is displayed in Figure 5.2d. The signals in the spectrum of the fresh sample can be assigned to **3** and the unmodified precursor, marked with (•) and (□), respectively. The ratio of the signals due to $\underline{CH}$ and $\underline{CH_3}$ of the thd and $\underline{CH_3}$ of the *t*-butoxide ligand are about the expected order of magnitude but cannot be determined very accurately, since the signals in the $\underline{CH_3}$ region are not resolved. This could be due to the presence of some traces of parent alcohol. Upon aging, the disubstituted compound rearranges by forming mainly compound **1** and unmodified precursor. The equation of this reaction is as follows:

$$3\ Hf(O^tBu)_2(thd)_2 \Rightarrow 2\ Hf(O^tBu)_1(thd)_3 + Hf(O^tBu)_4 \qquad (5.2)$$

A sample of which the NMR spectra is not displayed here, showed a transformation of **1** into the tetrasubstituted $Hf(thd)_4$ in the about the same time (just under 3 days) as displayed in Figure 5.2d for **3**. The solution stability of disubstituted compounds seems to be of the same order of magnitude as that of the trisubstituted compounds. The solid state stability of the disubstituted compounds is again, high, after storage of the samples for about half a year in the freezer the composition remained unchanged.

Mass spectrometry experiments were performed on compound **1**-**4** and the obtained data is summarized in Table 5.2. It should be noted that for **1**-**3** dried crystals were used while sample **4** was prepared by removing the solvents of a solution with Hthd and hafnium *t*-butoxide in the appropriate ratios. The obtained data for all samples is in good agreement with their molecular structure. The major fragment in the gas phase is in all cases the initial compound minus an alkoxide ligand. All four compounds are tremendously volatile; this is illustrated by the unusual detection of the whole molecule in the spectra of **1** and **2**. The spectrum obtained from **4** displays a signal at 727 (26.5%) M/z(I), that is assigned to $Hf(thd)_3$. This indicates the presence of compound **2** in the sample. This is probably due to the different

way in which this sample was prepared, as mentioned above, and it clearly demonstrates the easy transformation of these compounds in solution (which has also been observed by the NMR experiments). The preparation and characterization of **3** was described earlier [19]. The mass spectrometry data presented [19] displayed two large signals, at 639 (25%) and 587 (35%) that are clearly due to the presence of **1**. The formation of **1** is enhanced by the reflux step that was included in its synthesis [19].

*Table 5.2: Interpretation of M/z(I) spectrum of **1-4**.*

Gas phase fragments	**1**	**3**	**2**	**4**
M(thd) $-CH_4$	257 (0.5)	257 (7.1)		
$M(OH)(thd)^+$	291 (17.8)			
$M(OH)_2(thd)$	307 (7.5)	307 (5.9)		
$M(thd)_2$	456 (6.3)			544 (5.7)
$M(OH)(thd)_2$	473 (31.5)	473 (13.9)	561 (15.5)	561 (22)
$M(O^tBu)(thd)_2$	529 (100)	529 (100)	617 (100)	617 (100)
$M(thd)_3$	639 (100)	639 (3.41)	727 (100)	727 (26.5)
$M(OH)(thd)_3$	656 (4.6)		744 (5.9)	
$M(O^tBu)(thd)_3$	712 (0.5)		799 (2.3)	

The modification of zirconium and hafnium *t*-butoxides with Hthd involves di- and trisubstituted compounds. The presence of a trisubstituted compound is in agreement with the intermediate structures formed upon Hacac and Hthd modification of zirconium and hafnium propoxides [15,17,18]. The main difference between the structures of **1** and **2** and the propoxide analogs is the metal-oxygen bond length of the alkoxide ligand. Steric hindrance causes that the metal-oxygen bonds of the *t*-butoxide ligands in **1** and **2** to be longer than that of a propoxide ligands in for instance $Zr(O^iPr)(thd)_3$, $Zr(O^nPr)(thd)_3$ and $Hf(O^iPr)(thd)_3$ [18]. The larger *t*-butoxide ligands and the resulting steric hindrance causes that the mononuclear disubstituted compounds **3** and **4** are formed rather than dinuclear monosubstituted compounds as observed in the modification of zirconium and hafnium propoxides. The solid state stability of the formed compounds is tremendously high, upon storage for half a year no change in composition was observed. In contrast, the solution stability displayed behavior analogous to that of Hthd and Hacac modified zirconium and hafnium propoxides, *i.e.*, concentration of the modifying ligands leading to the formation of tetrasubstituted and unmodified compounds.

Another approach that is known to lead to disubstituted compounds is the use of asymmetric chelating ligands like *t*-butylacetoacetate (tbaoac). The synthesis and characterization of the mono- and disubstituted zirconium isopropoxide compounds have been reported by Devi *et al*. [20]. In another publication [21] the preparation and characterization of $Hf(O^iPr)_2(tbaoac)_2$ was reported. A sample of hafnium isopropoxide was modified with 1 mol equivalent of tbaoac according to the procedure in the experimental section. The obtained single crystals were identified as $[Hf(O^iPr)_3(tbaoac)]_2$ (**5**)[3], the molecular structure of this compounds is depicted in Figure 5.3.

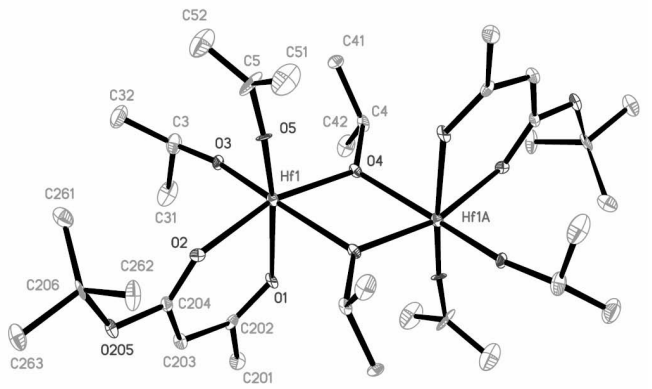

*Figure 5.3: Molecular structure of $[Hf(O^iPr)_3(tbaoac)]_2$ (**5**).*

The structure of **5** is isomorphous with $[Zr(O^iPr)_3(tbaoac)]_2$ [20] and one would expect that it has bond lengths comparable with those in $[Hf(O^iPr)_3(thd)]_2$ [23]. The metal-oxygen bond length, metal-metal non-bonding distance and the angle between the M1-O-M1A are displayed for the three compounds in Table 5.3. From these data it can be seen that the metal-oxygen bond length of the alkoxide ligands are shorter in **5** compared to those in $[Zr(O^iPr)_3(tbaoac)]_2$ and $[Hf(O^iPr)_3(thd)]_2$. More striking is the difference in metal–oxygen bond lengths of the tbaoac ligands (compare M-O1 and M-O5) and of the alkoxide in bridging position (compare M-O4 and M-O4A). In both of the other compounds the deviation between these bond lengths is significantly smaller when compared to that of **5**. The difference in bond

[3] Crystal data: $C_{30}H_{66}O_{10}Hf_2$, M = 943.81, triclinic, a = 10.962(2), b = 13.197(3), c = 16.189(3) Å, α = 74.82(3)°, β = 89.79(3)°, γ = 89.72(3)°, V = 2260.3(8) Å^3, T = 293 K, space group P-1, Z = 2, μ = 4.629 mm^{-1}, 7612 reflections measured, 4803 unique (R_{int} = 0.0941 which were used in all calculations. The final discrepancy factors were R1 = 0.0856; wR2 = 0.1947 for 2025 observed reflections (I > 2sigma(I)).

length is caused by a stronger trans-effect of the *t*-butyl containing part of the tbaoac ligand on the alkoxide ligand in bridging position. As a result of these trans-effects the geometry of the compound is strongly influenced. The effect on the metal-oxygen bond lengths has already been discussed, but the effect can also be seen in the distance between the metal atoms and the angle between the metals and the oxygen of an alkoxide in bridging position. In **5** the distance between the metal atoms is shorter compared to those in $[Zr(O^iPr)_3(tbaoac)]_2$ and $[Hf(O^iPr)_3(thd)]_2$ and also the angle between the metals and the oxygen of an alkoxide in bridging position is smaller. Thus the trans-stabilization of the alkoxide in the bridging position by the tbaoac ligand, results in the structure of **5** differing noticeably from its zirconium analog and $[Hf(O^iPr)_3(thd)]_2$.

Table 5.3: Selected bond lengths (Å) and angles (°) of ***5****, $[Zr(O^iPr)_3(tbaoac)]_2$ [20] and $[Hf(O^iPr)_3(thd)]_2$ [23] .*

Bond lengths [Å]	**5**	**$[Zr(O^iPr)_3(tbaoac)]_2$ [20]**	**$[Hf(O^iPr)_3(thd)]_2$ [23]**
M-O1	2.088(17)	2.180	2.153
M-O2	2.149(15)	2.187	2.169
M-O3	1.888(13)	1.922	1.927
M-O5	1.815(14)	1.942	1.953
M-O4	2.078(12)	2.098	2.102
M-O4A	2.213(17)	2.231	2.192
M1-M1A	3.456(19)	3.4891	3.476
M1-O-M1A	107.3(6)	107.38	108.0

It is very interesting to evaluate the stability of tbaoac modified compounds. ^{1}H NMR studies were performed on samples of **5**, $[Zr(O^iPr)_3(tbaoac)]_2$ and $Zr(O^iPr)_2(tbaoac)_2$. The syntheses of the latter two compounds are described in the experimental section. The procedures used differ from those published in the literature [20] with respect to the refluxing, *i.e.*, the samples in this study were not refluxed. Earlier studies on the modification of zirconium and hafnium alkoxides show that refluxing enhances the rearrangement of ligands [18,30] and can have a tremendous influence on the obtained product. The solution stability of the samples was monitored by recording spectra at various times. The hafnium and zirconium samples displayed the same trends. Typical spectra for a mono- and disubstituted compound are displayed in Figure 5.4a and 5.4c, respectively. The signals marked with (∗) in Figure 5.4a are due to the tbaoac ligands of the monosubstituted

compound, *i.e.*, the signals of $\underline{CH}$, $\underline{OCH_3}$ and $\underline{CCH_3}$ are found at 4.9, 1.83 and 1.53 ppm respectively. The remaining signals are due to the isopropoxide ligands (*i.e.*, the unresolved signals at 4.33 and 4.05 to $\underline{CH}$ in terminal and bridging position and 1.23 and 1.08 ppm to $\underline{CH_3}$) and some traces of hydrocarbon solvents and isopropanol. The signals marked with (•) in Figure 5.4c are assigned to the tbaoac-ligands of the disubstituted compound, *i.e.*, the signals of $\underline{CH}$, $\underline{OCH_3}$ and $\underline{CCH_3}$ are found at 4.9, 1.90 and 1.48 ppm, respectively. The remaining signals in Figure 5.4c are again, due to the isopropoxide ligands and some traces of hydrocarbon solvents and isopropanol and possibly also some traces of the unsubstituted precursor. The assignment of the different modifications is not possible on the basis of the $\underline{CH}$ proton of the tbaoac, since the chemical shift is almost identical for mono- and disubstituted species. This is in contrast to compounds modified with Hacac or Hthd [15,17,18]. Typical spectra of aged samples of mono- and disubstituted compounds are displayed in Figure 5.4b and 5.4d, respectively. The influence of aging the monosubstituted compound (Figure 5.4b) can clearly be seen at a chemical shift of 1.4-1.9 ppm. The signals assigned to the tbaoac ligand of mono- and disubstituted compounds are again marked with (∗) and (•), respectively. The rearrangement of monosubstituted to disubstituted can clearly be seen. This was also observed by Devi *et al.* [20], however, the rearrangement is not an equilibrium as they proposed. After approximately two weeks, all monosubstituted compounds had rearranged to disubstituted. It is somewhat surprising that in the preparation of $[Zr(O^iPr)_3(tbaoac)]_2$ in ref. [20] a reflux step is introduced. This will only enhance the transformation from monosubstituted to disubstituted and decrease the yield of the desired complex. This phenomena was actually observed by the authors, when they studied the products formed upon distillation of $[Zr(O^iPr)_3(tbaoac)]_2$. They report, to their surprise, the presence of disubstituted compound in the distilled product. It seems thus that the monosubstituted compounds are less stable than the disubstituted ones when zirconium and hafnium isopropoxides are modified with tbaoac. This is in contrast to all studied intermediate zirconium and hafnium propoxide compounds with symmetric chelating ligands like Hacac and Hthd [15,17,18]. For all such modified hafnium and zirconium propoxide compounds the monosubstituted intermediates were most stable.

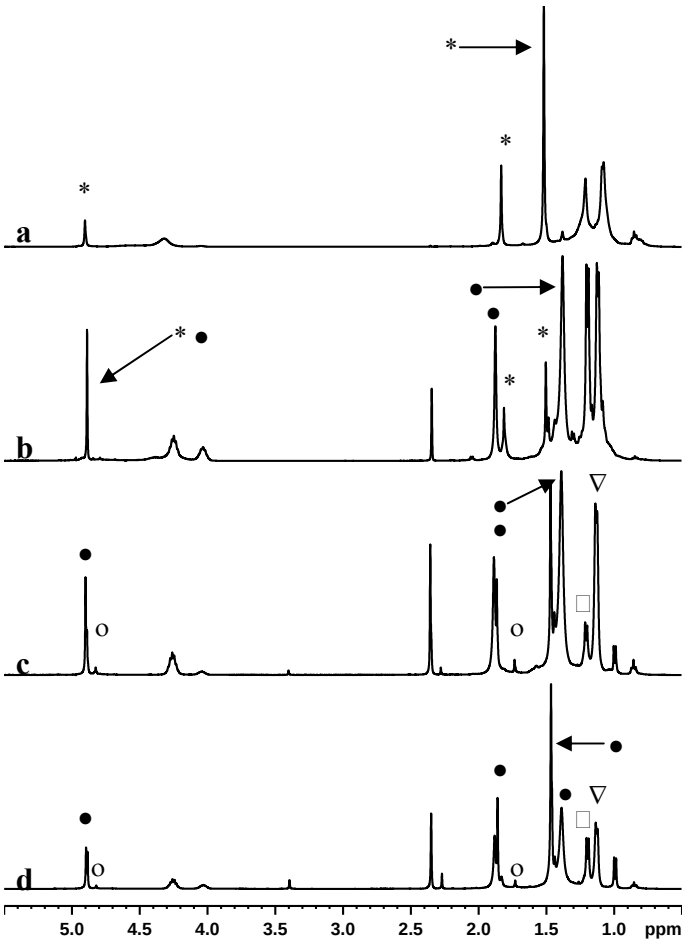

*Figure 5.4: The NMR spectra of **(a)** freshly prepared **5**, **(b)** aged $[Zr(O^iPr)_3(tbaoac)]_2$, **(c)** freshly prepared $Zr(O^iPr)_2(tbaoac)_2$ and **(d)** aged $Zr(O^iPr)_2(tbaoac)_2$. The different signals are assigned to the ligands of mono- and disubstituted compounds marked with (∗) and (•) respectively, $M(tbaoac)_4$ (M = Zr or Hf) (o), isopropoxide ligands (▽) and t-butoxide ligands (□).*

It is now interesting to evaluate how stable the disubstituted compound is in solution. If the positions of the signals due to the tbaoac ligand of the aged sample (Figure 5.4d) are compared with that of the fresh sample (Figure 5.4c), no change in position is observed. However, a closer look at the signals due to the tbaoac ligand shows that all of them consist of multiple signals, *i.e.*, two or three. The formation of $M(tbaoac)_4$ (M = Zr or Hf) is considered, but the recorded reference spectrum of these compounds shows a clear difference in the chemical shifts of the $\underline{CH}$ and $\underline{OCH_3}$. These signals are marked with (o) in the spectra of the disubstituted

compound since it is not observed in any of the spectra obtained from the monosubstituted compounds. The ratio of the signals assigned to $Zr(O^iPr)_2(tbaoac)_2$ and $Zr(tbaoac)_4$ in the spectrum of Figure 5.4c has hardly changed compared to that displayed in Figure 5.4d, which was recorded after aging the sample for two weeks at room temperature. This clearly shows that the transformation of disubstituted compounds is very slow, suggesting that these compounds are (fairly) solution stable.

It still remains unexplained what the nature of the different signals observed of the tbaoac ligand of the disubstituted compound is. A possible explanation could be the occurrence of alkyl group exchange in the tbaoac, *i.e.*, the *t*-butyl is replaced for isopropyl. Evidence for the occurrence of such a reaction can be extracted from the signals marked with (∇) and (□) in Figure 5.4c and 5.4d. The chemical shift of the signal at 1.08 ppm, marked with (∇), is the same as that of one of the signals assigned to isopropoxide in Figure 5.4a, while the chemical shift of the signal at 1.23 ppm, marked with (□), is the same as that of the *t*-butoxide ligands in $Zr(O^tBu)_4$. Upon aging, the change in the ratio of these signals, *i.e.*, an increase of the signal assigned to *t*-butoxide is observed; clearly indicating the occurrence of transesterfication. A change of the modifying ligand due to the replacement of *t*-butyl by isopropyl is also observed in the signal of $\underline{CCH_3}$ in the NMR spectra. However, the obtained spectra do not permit detailed analysis, *i.e.,* the signals are partly unresolved and overlapping.

Despite the occurrence of the alcohol exchange, $Zr(O^iPr)_2(tbaoac)_2$ is a very attractive compound. Its solution stability is superior to all the Hthd and Hacac heteroleptic homometallic zirconium and hafnium compounds studied by us [15,17,18]. It was attempted to prepare analogs of $Zr(O^iPr)_2(tbaoac)_2$ starting from zirconium *n*-propoxide and zirconium mixed ligand propoxide, $[Zr(O^nPr)(O^iPr)_3(^iPrOH)]_2$, precursors. The preparation was performed according to the procedure in the experimental section for the preparation of **5**, however the amount of added tbaoac was 2 mol equivalents. Despite several attempts and several solvent removal steps, *i.e.*, the samples were dried under vacuum (0.1 mm Hg) and redissolved in hexane, no crystallization could be observed. This is, on the one hand, due to the higher solubility of *n*-propoxide compounds and, on the other

hand, the exchange of the butyl and propyl ligands is assumed to play a role. This exchange leads to the formation of a mixture of different species in the sample, providing a multi-component system unable to crystallize.

The modification of zirconium *n*-propoxide with various amounts of ethylacetoacetate (eaoac) was also examined. This combination of precursor and modifier is occasionally applied in the preparation of sol-gel derived materials [25]. The procedures for the preparation of these compounds are described in detail in the experimental section. Initially, it was attempted to obtain single crystals from these systems for characterization, but for reasons discussed above, this was not successful. ^{1}H NMR of the samples showed that upon the modification with 1 mol equivalent a monosubstituted compound is formed, which transforms in solution in time into disubstituted and unmodified precursor. The positions of the signals assigned to the formation of the disubstituted compound were at the same position as the signals in the spectrum obtained from a sample with 2 mol equivalents eaoac. The signals in the spectra of the samples modified with 3 and 4 mol equivalents of eaoac were assigned to a mixture of di- and tetrasubstituted compounds and tetrasubstituted compounds, respectively. In all the samples, splitting of the signals of the eaoac-ligand was observed upon aging of the sample. The extent of the alcohol exchange and the rate at which it occurred seems to be less and lower than observed for the modification of isopropoxide precursors with tbaoac.

The modification of precursors with 2 mol equivalents of β-ketoesters leads to the formation of a stable compound. The stability of these disubstituted compounds opens the door for application of these systems in sol-gel and MOCVD. Up to date, no such stable compounds have been reported using chelating ligands as modifiers. The only requirement for the modification with β-ketoesters is that transesterfication of the ligands and the modifier is avoided. The transesterfication in the systems described above made them not stable in time, this can easily be avoided by the proper choice of precursor and modifier. Below we will discuss the modification of zirconium and hafnium *t*-butoxides with tbaoac. The intermediates formed in this modification are expected to be very volatile and therefore interesting for application in MOCVD. For sol-gel applications it would be

interesting to use a combination of isopropyl-acetoacetate and zirconium or hafnium isopropoxides or *n*-propyl-acetoacetate with *n*-propoxide precursors.

Samples of hafnium and zirconium t-butoxide were modified with 2 and 3 mol equivalents of tbaoac and an additional sample of zirconium *t*-butoxide was modified with 1 mol equivalent of tbaoac. In the samples with hafnium *t*-butoxide single crystals were formed, however they were not of X-ray quality. All the samples were dried and ^{1}H NMR was performed on the dried product. The spectra of zirconium *t*-butoxide with 3 and 2 mol equivalents are displayed in Figure 5.5a and 5.5b, respectively. At a chemical shift between 4.8-4.9 ppm two different signals are present, which are due to the CH of the tbaoac ligand. In the spectrum of the sample modified with 3 mol equivalents, the predominant signal is found at a slightly higher chemical shift compared to the largest signal in the sample with 2 mol equivalents. The presence of two different signals suggests the existence of two modified species. Since the minor signal (marked with (o)) which is present in both spectra at a chemical shift of 4.80 ppm, is due to the tetrasubstituted compound, it seems then that the modification of *t*-butoxides involves di- and trisubstituted intermediates. The signals in spectrum 5.5a marked with (∗), at chemical shifts of 4.9, 1.88, 1.5 and 1.06 ppm, are in a ratio of 1: 3 : 9 : 3, thus supporting the suggestion of a trisubstituted compound. The signals in spectrum 5.5b that are marked with (•) are in the expected ratio of 1 : 3 : 9 : 9 (at 4.85, 1.86, 1.40, 1.18 ppm, respectively) corresponding to a disubstituted compound. It should be noted that the signals around 1.87 ppm, corresponding to the $\underline{CH_3}$ of the tbaoac ligand, are not perfectly resolved. This is probably due to the small difference in chemical shift of this signal in the di- and trisubstituted compounds.

The NMR spectrum of the sample in which zirconium *t*-butoxide was modified with 1 mol equivalent of tbaoac is displayed in Figure 5.5c. There is a great resemblance with the spectrum of the disubstituted compound depicted in Figure 5.5b. The main difference lies in the signals marked with (∇). These signals were not present in the samples of zirconium *t*-butoxide, which were modified with more than 1 mol equivalent of tbaoac, but they were observed upon aging of the modified hafnium *t*-butoxide samples. The integration of these signals from the spectrum displayed in Figure 5.5c is difficult since the signals are not perfectly

resolved. From the hafnium spectra the ratio between the signals is determined to be 1 : 3 : 9 : 27 (4.93, 1.93, 1.58 and 1.32 ppm, respectively) corresponding to a monosubstituted compound.

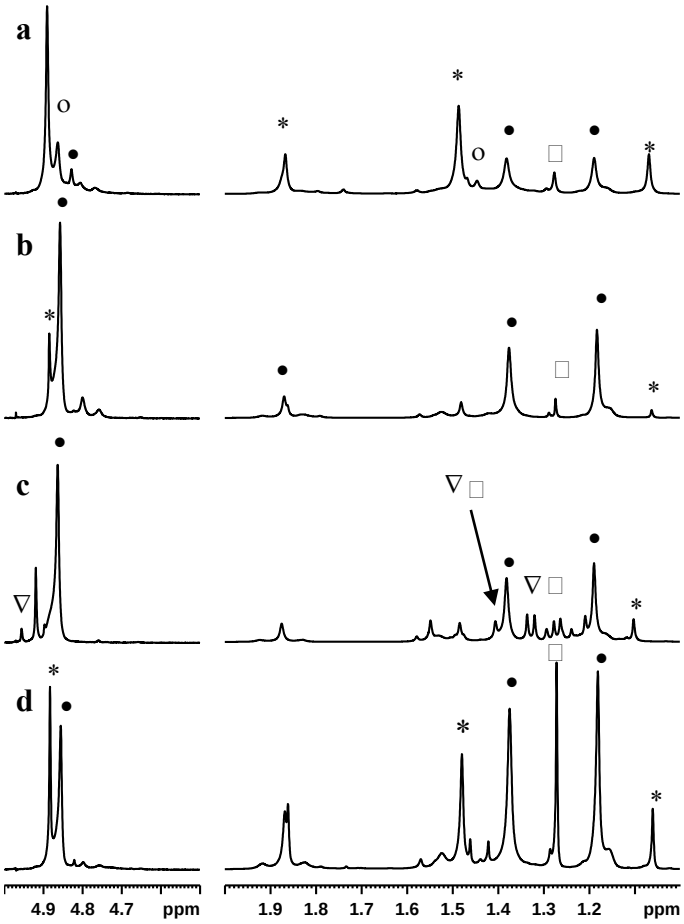

*Figure 5.5: The ^{1}H NMR spectra of (**a**) freshly prepared Zr(O^{t}Bu)(tbaoac)$_3$, (**b**) freshly prepared Zr(O^{t}Bu)$_2$(tbaoac)$_2$, (**c**) freshly prepared Zr(O^{t}Bu)$_3$(tbaoac) and (**d**) aged Zr(O^{t}Bu)$_2$(tbaoac)$_2$. The different signals are assigned to the ligands of tri-, di-, monosubstituted compounds marked with (∗), (•) and (▽) respectively, M(tbaoac)$_4$ (M = Zr or Hf) (o) and t-butoxides (□).For reasons of clarity the intensities of the signals between 5.5 and 4 ppm are increased compared to those between 2 and 1 ppm.*

The solution stability of the compounds was monitored by recording ^{1}H NMR spectra at various times after the sample preparation. The spectrum of the aged (55 hours) sample of zirconium *t*-butoxide with 2 mol equivalents of tbaoac is depicted

in Figure 5.5d. A clear increase of the signals assigned to the trisubstituted and the unmodified precursor is observed, marked with (∗) and (□), respectively. In the aged sample of zirconium modified with three equivalents of tbaoac, formation of a precipitate occurred after 55 hours. In the recorded spectrum, a slight increase in the signals due to $Zr(tbaoac)_4$ was observed and a strong increase of the signals due to unsubstituted precursor, while the ratio of tri- and disubstituted remained as it was in the fresh sample (Figure 5.5a). This indicates a rearrangement of the trisubstituted compound to a tetrasubstituted compound (its low solubility causes the formation of the precipitate). The transformation of di- and trisubstituted compounds to tetrasubstituted shows great similarities with the transformation in the Hthd system, which has been discussed above. In the sample that was modified with 1 mol equivalent the transformation of mono- to disubstituted was observed. After 55 hours about half of the monosubstituted had transformed into disubstituted and the unmodified precursor. The samples of hafnium *t*-butoxide modified with 2 and 3 mol equivalents display an analogous behavior such as the one described for the zirconium analogs. The only difference that was observed was the presence of mono- and tetrasubstituted in the sample with 2 mol equivalents of tbaoac. The monosubstituted was the first to disappear upon aging of the sample.

On basis of the NMR data, the modification of zirconium and hafnium *t*-butoxides involves mono-, di- and trisubstituted compounds. The presence of all three modified intermediate compounds has not been observed before for the modification of zirconium and hafnium alkoxides with chelating ligands. The modification of zirconium and hafnium *t*-butoxides with Hthd involves the formation of di- and trisubstituted species, as we have discussed above. For that system, we have seen that in both the di- and trisubstituted compounds the metal-oxygen bond lengths are larger due to the steric hindrance of the bulky ligands. The size of the tbaoac ligand apparently allows the formation of a monosubstituted compound. The ability for (to some extent) trans-stabilization of an alkoxide ligand by tbaoac may be another factor that enables the formation of a monosubstituted compound. The observed relative low solution stability of all tbaoac intermediate *t*-butoxide compounds implies that no thermodynamic stable compound like $M(O^iPr)_2(tbaoac)_2$ (with M=Zr or Hf) is formed. The stability of these $M(O^iPr)_2(tbaoac)_2$ is due to the trans-stabilization and results in short metal-

oxygen bonds lengths of the alkoxide ligands. The *t*-butoxide ligands are probably too large to allow such short metal-oxygen bond lengths, *i.e.*, too much steric hindrance.

5.4 Conclusions

The modification of zirconium and hafnium *t*-butoxides involves di- and trisubstituted compounds. The size of the *t*-butoxide ligands results in a disubstituted compound being formed instead of the monosubstituted propoxide compounds. The metal-oxygen bond length of the *t*-butoxide ligands is significantly longer compared to that of propoxide in analogous compounds. This clearly underlines the presence of steric hindrance in these systems.

The modification of zirconium and hafnium propoxide precursors with asymmetric chelating ligands like tbaoac and eaoac involve the formation of a mono- and a disubstituted compound. The monosubstituted compounds are not stable in solution in time, while the solution composition of the disubstituted compound does not change in time. The only effect that is observed is transesterfication of the alkyl-group of the modifying ligand and the alkoxide ligands. This can be avoided by using the same alkyl and alkoxide groups. The stability of the disubstituted zirconium and hafnium propoxide with β-ketoesters is tremendously interesting for application in sol-gel. The disubstituted compounds are one of the first stable mononuclear heteroleptic zirconium and hafnium alkoxides.

The modification of zirconium and hafnium *t*-butoxides with tbaoac leads to the formation of mono-, di- and trisubstituted compounds. None of these compounds are stable in solution. The large size of the *t*-butoxide ligands causes steric hindrance that disables the trans-stabilization which could lead to stable disubstituted compounds.

5.5 References

1 R.J. Vacassy, C. Guizard, J. Palmeri and L. Cot, *Nanostruct. Mater.*, **10**, 77 (1998).

2 C.R. Xia, H.Q. Cao, H. Wang, P.H. Yang, G.Y. Meng and D.K. Peng, *J. Membr. Sci.*, **162**, 181 (1999).

3 H. Kurosawa, Y.T. Yan, N. Miura and N. Yamazoe, *Solid State Ionics*, **79**, 338 (1995).

4 C.M.S. Rodrigues, J.A. Labrincha and F.M.B. Marques, *Solid State Ionics*, **136-137**, 671 (2000).

5 N. Miura, M. Nakatou and S. Zhuiykov, *Sensor Actuat. B-Chem.*, **93**, 221 (2003).

6 Y.W. Li, D.H. He, Z.X. Cheng, C.L. Su, J.R. Li and Q.M. Zhu, *J. Mol. Catal. A: Chem.,* **175**, 267 (2001).

7 M.Haruta, T. Kobayashi, H. Sano and N. Yamada, *Chem. Lett.***, 829**, 405 (1985).

8 A. Knell, P. Barnickel, A. Baiker and A. Wokaun, *J. Catal*., **137**, 306 (1992).

9 S. Hoffmann, M. Klee and R. Waser, *Integr. Ferroelectr.*, **10**, 155 (1995).

10 M. Klee, U. Mackens, W. Hermann and E. Bathelt, *Integr. Ferroelectr.*, **11**, 247 (1995).

11 G.D. Wilk, R.M. Wallace and J.M. Anthony, *J. Appl. Phys*., **89**, 5243 (2001).

12 A.C. Jones, H.C. Aspinall. P.R. Chalker, R.J. Potter, K. Kukli, A. Rahtu, M. Ritala and M. Leskelä, *J. Mater. Chem.*, **14**, 3101 (2004).

13 L.G. Hubert-Pfalzgraf, *J. Mater. Chem.*, **14**, 3113 (2004).

14 T.J. Leedham, A.C. Jones, P.J. Wright, M.J. Crosbie, D.J. Williams, H.O. Davies and P. O'Brien, *Integr. ferroelectr.*, **26**, 767 (1999).

15 G.I. Spijksma, H.J.M. Bouwmeester, D.H.A. Blank and V.G. Kessler, *Chem. Commun.*, 1874 (2004).

16 G.A. Seisenbaeva, S. Gohil and V.G. Kessler, *J. Mater. Chem.*, **14**, 3177 (2004).

17 Chapter 3 of this thesis.

18 Chapter 4 of this thesis.

19 A.C. Jones, T.J. Leedham, P.J. Wright, M.J. Crosbie, P.A. Lane, D.J. Williams, K.A. Fleeting, D.J. Otway and P. O'Brien, *Chem. Vapor. Depos.*, **4**, 46 (1998).

20 U. Patil, M. Winter, H.W. Becker and A. Devi, *J. Mater. Chem.,* **13**, 2177 (2003).

21 A. Baunemann, R. Thomas, R. Becker, M. Winter, R.A. Fischer, P. Ehrhart, R. Waser and A. Devi, *Chem. Commun*., 1610 (2004).

22 P.A. Williams, R.L. Roberts, A.C. Jones, P.R. Chalker, N.L. Tobin, J.F. Brickley, H.O. Davies, L.M. Smith and T.J. Leedham, *Chem. Vapor. Depos*., **8**, 163 (2002).

23 K.A. Fleeting, P. O'Brien, A.C. Jones, D.J. Otway, A.J.P. white and D.J. Williams., *J. Chem. Soc., Dalton Trans*., 2853 (1999).

24 Y.F. Loo, R. O'Kane, A.C. Jones, H.C. Aspinall, R.J. Potter, P.R. Chalker, J.F. Bickley, S. Taylor and L.M. Smith, *J. Mater. Chem*., **35,** 1896 (2005).

25 U. Wellbrock, W. Beier and G.H. Frischat, *J. Non-Cryst. Solids*. **147**, 150 (1992).

26 S. Pasko, L.G. Hubert-Pfalzgraf and A. Abrutis, *Mater. Lett.*, **59**, 1836 (2005).

27 Chapter 2 of this thesis.

28 E.P. Turevskaya, N.I. Kozlova, N.Y. Turova, A.I. Belokon, D.V. Berdyev, V.G. Kessler and Y.K. Grishin, *Russ. Chem. Bull*., **44**, 734 (1995).

29 SHELXTL-NT program manual, Bruker AXS, (1998).

30 R.J. Errington, J. Ridland, W. Clegg, R.A. Coxall and J.M. Sherwood, *Polyhedron*, **17**, 659 (1998).

31 U. Schubert, H. Buhler and B. Hirle, *Chem. Ber*., **125**, 999 (1992).

32 Chapter 6 of this thesis.

Chapter 6

Modification of zirconium propoxide precursors by diethanolamine

Abstract

The modification of different zirconium propoxide precursors with diethanolamine (H_2dea) was investigated by characterization of the isolated modified species. Upon modification of zirconium *n*-propoxide and $[Zr(O^nPr)(O^iPr)_3(^iPrOH)]_2$ with 0.5 mol equivalent of H_2dea the complexes $[Zr_2(O^nPr)_6(OC_2H_4)_2NH]_2$ (**1**) and $[Zr_2(O^nPr)_2(O^iPr)_4(OC_2H_4)_2NH]_2$ (**2**) were obtained. However, ^{1}H NMR studies of these tetranuclear compounds showed that these are not time- stable in both solution and solid form. The effect of this time instability on material properties is demonstrated by light scattering and TEM experiments. Modification of zirconium isopropoxide with either 0.5 or 1 mol equivalent of H_2dea results in formation of the trinuclear complex, $Zr\{\mu\text{-}\eta^3\text{-}NH(C_2H_4O)_2\}_3[Zr(O^iPr)_3]_2(^iPrOH)_2$ (**3**) containing a unique nona-coordinated central zirconium atom. This complex **3** is one of the first modified zirconium propoxide precursors shown to be stable in solution for long periods of time. The particle size and morphology of the products of sol-gel synthesis are strongly dependent on the time factor and eventual heat treatment of the precursor solution. Reproducible sol-gel synthesis requires the use of solution stable precursors.

6.1 Introduction

The alkoxides of zirconium are widely used as precursors in the preparation of oxide materials for various applications, ranging from porous membranes [1-3] and matrices for catalysts [4,5], to dense dielectric and ferroelectric thin films for electronic devices [6,7]. Despite of their common use, neither the homometallic nor the heterometallic zirconium alkoxide complexes have been sufficiently explored.

Since the application in, for instance, MOCVD (metal-organic chemical vapor deposition) or sol-gel may be complicated due to extreme sensitivity to hydrolysis and pyrolysis, zirconium precursors are often modified. A general method used to moderate reactivity is the exchange of the alkoxide ligands by chelating organic ligands [8]. In sol-gel studies, acetic acid and acetylacetone are most often applied for this purpose [9]. Acetic acid has the undesired ability to react with alcohol upon release of water and in recent work we showed [10] that the stabilizing effect with acetylacetone is time dependent and disappears completely beyond addition of 1 mol equivalent. It was also shown that the destabilization occurs rapidly and that there can be a tremendous effect on the prepared materials [10]. The stability of the modified precursor formed should be considered. For MOCVD, shelf stability is an obvious requirement, but even for sol-gel applications where the modification is performed *in situ* its influence might not be unimportant.

In our search for a stable modified zirconium precursor we have applied diethanolamine, H_2dea, as a stabilizing agent. To the best of our knowledge, no reports have been published on zirconium precursor structures formed upon modification with H_2dea; however, the structure of zirconium *n*-propoxide modified with 0.5 mol equivalent of N-methyl-diethanolamine has been reported [11].

In the present study we attempted to prepare an analogous compound through the modification of zirconium *n*-propoxide with the more common H_2dea. In addition, other zirconium propoxide precursors, including zirconium isopropoxide and a mixed ligand precursor $[Zr(O^nPr)(O^iPr)_3(^iPrOH)]_2$ were modified in an attempt to reach a better understanding of the chemistry involved upon modification with H_2dea. In addition to isolation and structural characterization of the modified

precursors, their stability in time and the possible influence on material properties were evaluated.

6.2 Experimental

All manipulations were carried out in a dry nitrogen atmosphere using the Schlenk technique or a glove box. Hexane and toluene (Merck, *p.a.*) were dried by distillation after refluxing with $LiAlH_4$ and metallic sodium, respectively. Diethanolamine, H_2dea, was purchased from Aldrich and used without further purification.

IR spectra of nujol mulls were registered with a Perkin Elmer FT-IR spectrometer 1720 X or Bio-Rad FT-IR spectrometer FTS 375 C with a DTGS detector. ^{1}H NMR spectra were recorded in $CDCl_3$ for compound **1-3** and in toluene for compound **3** solutions on a Bruker 400 MHz spectrometer at 243 K. The results of microanalysis (C, N, H) were obtained by Mikrokemi AB, Uppsala, Sweden, using the combustion technique, and the results of the analysis were in agreement with the expected for the obtained complexes. The particle size distribution was measured by dynamic light scattering (ZetaSizer 3000HSa, Malvern, UK). The transmission electron microscopy (TEM) experiments were performed on a PHILIPS CM30 Twin/STEM.

Synthesis: The zirconium propoxide precursors used as starting materials in this work are zirconium isopropoxide, ($[Zr(O^iPr)_4(^iPrOH)]_2$ 99.9 %), 70 wt% solution of "$Zr(O^nPr)_4$" in *n*-propanol (both purchased from Aldrich) and $[Zr(O^nPr)(O^iPr)_3(^iPrOH)]_2$ which was prepared according to a recently developed technique [12,13]. All three different precursors were modified with both 0.5 and 1 mol equivalent of H_2dea, however only three cases crystals could be isolated. The exact composition of the synthesized samples **1**, **2** and **3** was established with single X-ray crystallography.

$[Zr_2(O^nPr)_6(OC_2H_4)_2NH]_2$ (**1**): Commercial 70% zirconium *n*-propoxide in *n*-propanol was dried (weight: 1.87 g (4.8 mmol)) under vacuum and redissolved in 2 ml hexane. Upon addition of 0.25 g (0.24 mmol) of H_2dea, the colorless sample was placed overnight in the freezer at –30 °C. Subsequently, the sample was dried in vacuum (0.1 mm Hg). The formed solid product was redissolved in 1 ml hexane

and placed in the freezer for crystallization. The next day a significant amount of product had been formed and after several days the solution was decanted and the obtained crystals (1.58 g, yield 75%) identified as **1**. IR, cm^{-1}: 1300 w, 1280 m, 1252 m, 1136 w, 1085 br, 1021 vw, 997 w, 973 w, 953 vw, 917 m, 886 m, 862 m, 842 m, 826 sh, 782 s, 758 w, 718 m, 627 sh, 599 sh, 551 br, 478 sh.

$[Zr_2(O^nPr)_2(O^iPr)_4(OC_2H_4)_2NH]_2$ (2): The prepared $[Zr(O^nPr)(O^iPr)_3(^iPrOH)]_2$ (1.07 g, (2.8 mmol)) was dissolved in 2 ml hexane and 0.14 ml (0.13 mmol) H_2dea was added drop wise. The sample was stored overnight in the freezer, before removal of the solvents. After redissolving the formed solids in 1 ml hexane the sample was placed back into the freezer; it took several days before the first crystals were formed. After 23 days the solution was decanted and the obtained crystals (0.62 g, yield 0.51%) identified as **2**. IR, cm^{-1}: 1337 m, 1302 w, 1272 w, 1247 w, 1143 w, 1096 w, 1068 br, 1015 w, 1000 w, 971 w, 953 w, 920 m, 888 w, 858 vw, 840 w, 820 w, 721 s, 667w, 657 w.

$Zr\{\mu\text{-}\eta^3\text{-}NH(C_2H_4O)_2\}_3[Zr(O^iPr)_3]_2(^iPrOH)_2$ (3): The modification of zirconium isopropoxide with 0.5 equivalent mol of H_2dea was performed by dissolving 0.89 g (2.3 mmol) precursor in a 3 ml mixture of hydrocarbons (hexane/toluene in a volume ratio of 2:1). After addition of the equivalent amount of H_2dea the colorless sample was placed overnight in the freezer at -30 °C. Subsequently, the solvents and released isopropanol were removed in vacuum (0.1 mm Hg), and the dried compound was redissolved in 1 ml hexane and placed in the freezer for crystallization. A product was obtained after several weeks of crystallization. The white product was analyzed and found to consist of two crystal types. Single crystal XRD identified these as $Zr\{\mu\text{-}\eta^3\text{-}NH(C_2H_4O)_2\}_3[Zr(O^iPr)_3]_2(^iPrOH)_2$ and unreacted zirconium isopropoxide [12].

An analogous experiment with the addition of 1 mol equivalent H_2dea was performed in order to obtain pure **3**. The yield was 79% (1.09 g zirconium isopropoxide, 0.30 ml H_2dea, 1.1 g of compound **3**).

IR, cm^{-1}: 3383 br, 1358 sh, 1338 s, 1323 s, 1299 s, 1272 w, 1253 s, 1233 s, 1218 w, 1163 s, 1128 s, 1109 w, 1077 br, 1042 w, 992 s, 961 sh, 926 sh, 898 s, 867 sh,

844 s, 774 w, 750 w, 723 s, 669 s, 625 sh, 594 sh, 564 br, 544 sh, 505 br, 486 w, 474 w, 458 sh, 447 w, 423 w.

Preparation of the sols for TEM analysis was carried out using zirconium *n*-propoxide. The solvent of commercial zirconium *n*-propoxide was removed under vacuum (yielding ~2.5 g). The residue was redisolved in *n*-propanol (mol ratio 1:10) with the addition of ½ mol equivalent of H_2dea. The sample was optionally refluxed for half an hour. Subsequently, the obtained modified precursor was hydrolyzed by a mixture of water and *n*-propanol (volume ratio 1:20, ratio zirconium *n*-propoxide and H_2O 1:2), resulting in a colorless (without refluxing) or slightly yellowish sol (with refluxing).

The samples for light scattering and TEM experiments were prepared from the gelled sols by dissolving ~0.05 g in 20 ml *n*-propanol and subsequent peptization with 0.3 ml 0.05 M nitric acid solutions. The samples were ultrasonically treated for 15 minutes. The particle size of the clear solution was determined by light scattering. For TEM analysis a drop of the solution was deposited on a copper supported carbon grid.

Crystallography: Data collection for all single crystals was carried out at 22 °C on a SMART CCD 1k diffractometer with graphite monochromated MoKα. Structures were solved by direct methods. The coordinates of the metal atoms were obtained from the initial solutions and for all other non-hydrogen atoms found in subsequent difference Fourier syntheses. The structural parameters were refined by least squares fitting using both isotropic and anisotropic approximations. The coordinates of the hydrogen atoms were calculated geometrically and were included into the final refinement in isotropic approximation for all the compounds. All calculations were performed using the SHELXTL-NT program package [14] on an IBM PC.

6.3 Results and discussion

The structures of the obtained complexes, **1** and **2**, formed upon the modification of zirconium *n*-propoxide and the mixed ligand derivative closely resemble the structure Grainsford *et al.* [11] obtained upon modification of zirconium *n*-propoxide with N-methyl-diethanolamine.

Both complexes **1** and **2** are tetranuclear and centrosymmetric, and thus possess two different types of positions for the zirconium atoms. The terminal zirconium atoms are hexa-coordinated with three alkoxide ligands in terminal position and therein bridging position, two from *n*-propoxide groups and one from dea. The other position is filled with a hepta-coordinated zirconium that is surrounded with one terminal and five alkoxide ligands in bridging position, two from *n*-propoxide groups and three from dea, and a nitrogen from the H_2dea ligand.

Complexes **1**[1] and **2**[2] (Figure 6.1 and 6.2) do not differ greatly from the analogous complex found by Grainsford *et al*. [11]. The different surrounding of the nitrogen atom is likely to cause some difference in bonding lengths, though they are marginal (Zr-N 2.363(7), 2.35(2), 2.411 Å for **1**, **2** and the complex in ref. [11]), respectively. There is no noticeable influence of nitrogen on the distances to the bridging alkoxide ligands connected to the modifying agent ((Zr-O 2.211(6), 2.153(14), 2.202 Å for **1**, **2** and the complex in ref. [11]), respectively.

The most significant difference between **1** and **2** lies in the presence of the more bulky isopropoxide ligands in **2**. They are placed exclusively in the terminal positions. The *n*-propoxide ligands remain bridging. The presence of smaller (*n*-chain structure) bridging ligands appears to be a critical condition for the isolation of this type of molecular structure.

The yield of compound **2** is significantly lower than that of **1**. This can either be due to higher solubility in the hydrocarbon solvent or to lower stability in solution. The latter will be discussed below.

---

[1] Crystal data: $C_{44}H_{102}N_2O_{16}Zr_4$, M = 1280.16, Monoclinic, a = 10.708(3) b = 17.749(4), c = 16.968(5) Å, α = 90°, β = 99.960(7)°, γ = 90°, V = 3176.3(15) Å^3, T = 295(2) K, space group P2(1)/c, Z = 2, μ = 0.693 mm^{-1}, 10369 reflections measured, 3392 unique (R_{int} = 0.0766 which were used in all calculations. The final discrepancy factors were R1 = 0.0543; wR2 = 0.1239 for 1909 observed reflections (I > 2sigma(I)).

[2] Crystal data: $C_{44}H_{102}N_2O_{16}Zr_4$, M = 1280.16, Monoclinic, a = 17.384(4), b = 20.675(4), c = 18.166(4) Å, α = 90°, β = 90.316(5)°, γ = 90°, V = 6529(2) Å^3, T = 295(2) K, space group P2(1)/c, Z = 4, μ = 0.674 mm^{-1}, 7226 reflections measured, 4205 unique (R_{int} = 0.0982 which were used in all calculations. The final discrepancy factors were R1 = 0.0841; wR2 = 0.2022 for 1915 observed reflections (I > 2sigma(I)).

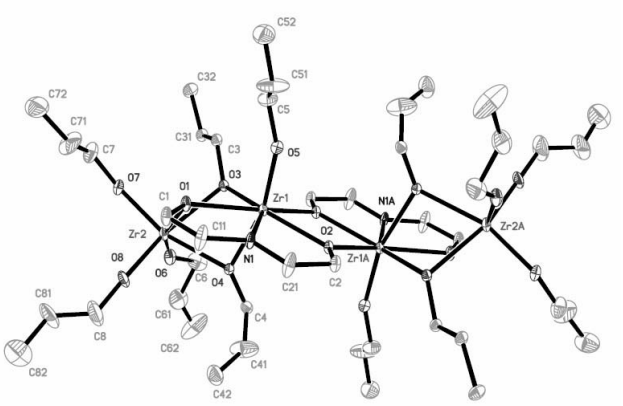

*Figure 6.1: Molecular structure of $[Zr_2(O^nPr)_6(OC_2H_4)_2NH]_2$ (**1**).*

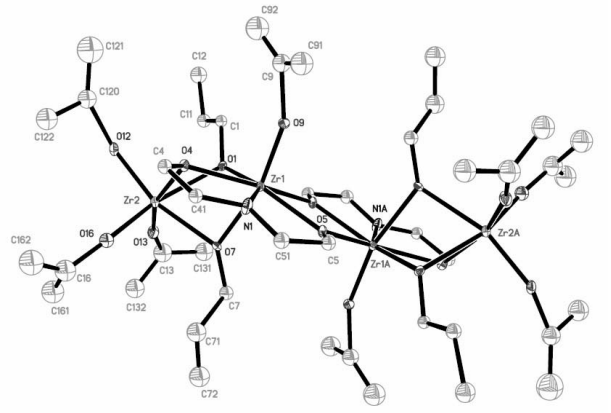

*Figure 6.2: Molecular structure of $[Zr_2(O^nPr)_2(O^iPr)_4(OC_2H_4)_2NH]_2$ (**2**).*

The molecular structure of complex **3**[3], obtained upon modification of zirconium isopropoxide with either 0.5 or 1 mol equivalent of H_2dea, $Zr\{\mu\text{-}\eta^3\text{-}NH(C_2H_4O)_2\}_3[Zr(O^iPr)_3]_2(^iPrOH)_2$, Figure 6.3 is completely different from **1** and **2** and rather unique. It is a trinuclear complex with isopropoxide ligands only present at the terminal metal positions. Zirconium atoms in this complex are situated in two different types of position, a nona-coordinated central and two hexa-coordinated terminal. The existence of a nona-coordinated zirconium

[3] Crystal data: $C_{36}H_{85}N_3O_{14}Zr_3$, M = 1057.74, Triclinic, a = 12.086(6), b = 15.180(7), c = 16.576(9) Å, α = 73.136(13)°, β = 85.788(17)°, γ = 68.52(2)°, V = 2706(2) Å^3, T = 295(2) K, space group P-1, Z = 4, μ = 0.620 mm^{-1}, 9128 reflections measured, 5702 unique (R_{int} = 0.0556 which were used in all calculations. The final discrepancy factors were R1 = 0.0777; wR2 = 0.1883 for 2439 observed reflections (I > 2sigma(I)).

has only been reported under aqueous conditions [15-17], and in a heterometallic zirconium-titanium analogue of **3**, recently reported by us [18] (discussed in detail in reference [19]).

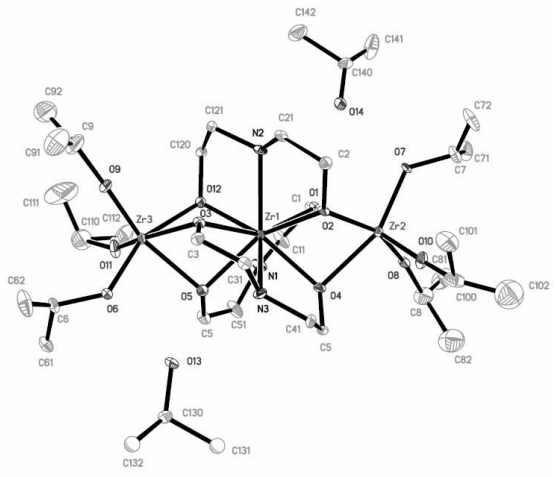

Figure 6.3 Molecular structure of $Zr\{\mu\text{-}\eta^3\text{-}NH(C_2H_4O)_2\}_3[Zr(O^iPr)_3]_2(^iPrOH)_2$ (**3**).

The compound described by Harben *et al.* [16] has rather uniform bond lengths (*i.e.*, Zr – N 2.225, 2.228 Å; Zr – OH_2 2.261 Å; Zr – O – C 2.244, 2.248, 2.242, 2.240 Å; Zr – O – N 2.126, 2.123 Å), indicating a high degree of ionic bonding. Complex **3** on the contrary is more covalently bonded, indicated by predominantly shorter Zr-O bond lengths (*i.e.*, 2.193(9), 2.202(9), 2.207(8), 2.206(8), 2.231(9), 2.250(9) Å), while the Zr-N bond lengths are longer (*i.e.*, 2.375(10), 2.447(11), 2.485(11) Å) involving much weaker, supposedly predominantly electrostatic, interactions. There is no direct analogy between the complex by Harben *et al.* [15] and **3**, thus **3** should be considered as a new class of nona-coordinated zirconium compounds.

The structure of **3** gave us an idea for the preparation of new heterometallic precursors. The presence of two types of positions, a nona-coordinated and a hexa-coordinated, provides the possibility to construct new species *via* self-assembly according to Molecular Structure Design Concepts [20]. For example, the hexa-coordinated position appears to be able to host other, smaller, atoms than zirconium. In a preliminary communication [18], we have recently reported the application of this model to the preparation of a new Zr-Ti complex. The molecular

structure of the complex obtained was studied by X-ray crystallography and characterized as $Zr\{\mu\text{-}\eta^3\text{-}NH(C_2H_4O)_2\}_3[Ti(O^iPr)_3]_2$.

This heterometallic complex, derived from **3** [18], has a central Zr atom, with coordination in a very regular tricapped trigonal prism (see Figure 6.4) with the oxygen atoms composing the vertices of the prism (Zr(1)-O(2) 2.196(3), Zr(1)-O(3) 2.199(3) and Zr(1)-O(4) 2.210 (3) Å) and the nitrogen atoms as capping vertices (Zr(1)-N(1) 2.440(6), Zr(1)-N(2) 2.439(5) Å). The coordination of the outer Ti atoms is a trigonally distorted octahedra with, in principle, only two types of Ti-O distances: bridging (Ti-O 2.137(3)-2.147(3) Å) and terminal (Ti-O 1.836(5)-1.853(4) Å).

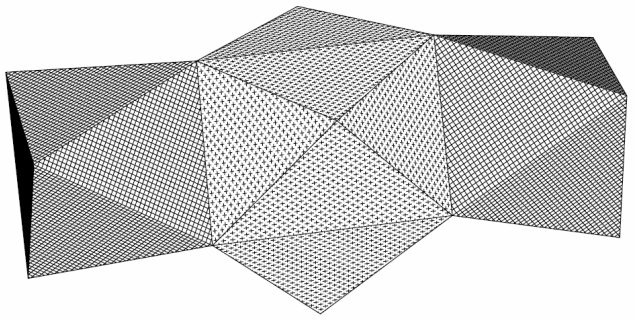

*Figure 6.4: Polyhedral presentation of the molecular structure of **3** and $Zr\{\mu\text{-}\eta^3\text{-}NH(C_2H_4O)_2\}_3[Ti(O^iPr)_3]_2$.*

The tricapped trigonal prismatic coordination of the central zirconium in complex **3** is slightly less regular. This is due to the smaller polarising effect of the outer zirconium atoms compared to titanium, different placement of the molecules in relation to the crystallographic elements of symmetry (triclinic for **3**, the molecule occupying a general position, and tetragonal in the heterometallic complex with the Zr atom placed on a 2(1) axis) and the presence of hydrogen-bonded isopropanol. The hydrogen bonding clearly leads to elongation of one of the Zr-O bonds at each side of the molecule; Zr(1)-O(4) 2.250(9) Å and Zr(1)-O(5) 2.231(9) Å compared to shorter Zr(1)-O(1) 2.207(8), Zr(1)-O(12) 2.193(9), Zr(1)-O(3) 2.202(9) and Zr(1)-O(2) 2.206(8) Å. The influence of the hydrogen-bonded alcohol also effects the outer zirconium atoms. The trigonally distorted octahedron has one longer bridging Zr-O bonding due to each hydrogen-bonded alcohol (2.252(9) Å and 2.287(9) Å against 2.170(9) - 2.201(8) Å). The presence of solvating isopropanol

molecules is confirmed by the presence of a broad δ-OH band at 3383 cm^{-1} in the IR spectra.

We have carried out an investigation of the time stability in solution as well as in the solid of three isolated compounds. The ^{1}H NMR spectra of the freshly prepared samples of **1** and **2** in deuterochloroform (Figure 6.5a and b for **1** and **2**, respectively) can be rationalized as corresponding to the molecular structures observed in the solid state.

The spectrum of **1** (Figure 6.5a) clearly shows the presence of *n*-propoxide ligands (marked with *), the signals at 0.9, 1.52 and 3.93 ppm are respectively assigned to $\underline{CH_3}$, $\underline{CH_2}$ and $\underline{OCH_2}$. The intensities are in accordance to what is expected, except for the $\underline{CH_3}$ signal which overlaps with that of some remaining hexane. The signal of $\underline{CH_2N}$ of the diethanolamine is at 2.6, 2.88 and 3.94 ppm, the presence of other peaks is in agreement with the XRD data where different N-C bond lengths were also found. The signals of $\underline{CH_2O}$ of the diethanolamine are poorly resolved between 3.7 and 4.4 ppm. However, the intensity of the signals is comparable with that of the $\underline{CH_2N}$ signals and close to the expected ratio of 1:3 with the signal of $\underline{OCH_2}$ at 3.93 ppm.

The spectrum of **2** (Figure 6.5b) is less well resolved, albeit that the differences and concurrences with **1** can clearly be seen. The *n*-propoxide (marked with *) and isopropoxide ligands are approximately in the ratio 1:2, as in complex **2**. Precise determination of this ratio is inaccurate due to overlap with the hexane signal. The intensity of $\underline{CH_2}$, around 1.6 ppm, is the same as that of the unresolved signals of $\underline{NCH_2}$ between 2.5 and 3.5 ppm. The unresolved peaks between 4.05 and 4.5 have an area three times larger than that of the $\underline{NCH_2}$, and may then be assigned to the presence of the $\underline{OCH_2}$ of the *n*-propoxide and diethanolamine and the $\underline{CH}$ of the isopropoxide.

The spectra recorded after 16 days displayed dramatic changes for both complexes, indicating that rearrangement had occurred. Initially such rearrangements were thought to be caused by the solvent. Halide-containing solvents such as $CDCl_3$ can alkylate amines *via* the Hoffman reaction. However, the spectra of a fresh sample of crystals aged for three weeks at room temperature showed an analogous spectrum as displayed in Figure 6.5c. The most striking difference between this

spectrum and the initial (Figure 6.5c) one is the significant increase of the peak at 3.6 ppm and the broadening of the *n*-propoxide peaks (marked with *). The former is, as could be seen from two-dimensional ^{1}H-^{13}C HMQC spectroscopy, according to the appearance of OCH_2 of *n*-propoxide in a bridging position; supporting a possible rearrangement of **1** towards an *n*-propoxide analogue of **3** upon the formation of zirconium *n*-propoxide with a M_4O_{16} [21,22] type of structure (as shown in Eq. 6.1). It can be concluded that complexes **1** and **2** are not stable in time.

$$6\ [Zr_2(O^nPr)_6(OC_2H_4)_2NH]_2 \Rightarrow 4\ Zr\{\eta^3\mu_2\text{-}NH(C_2H_4O)_2\}_3[Zr(O^nPr)_3]_2 + 3\ Zr_4(O^nPr)_{16} \quad (6.1)$$

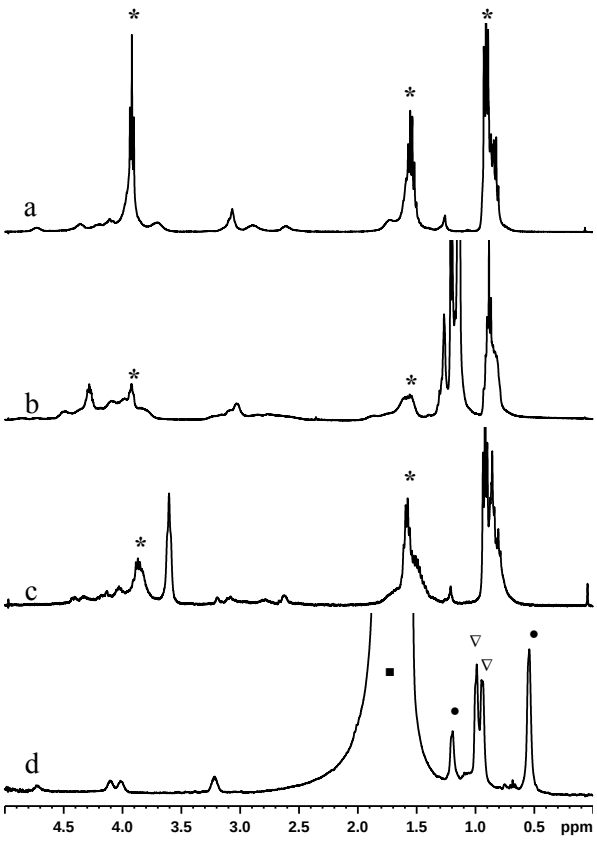

*Figure 6.5; NMR spectra of freshly prepared **1** (**a**) and **2** (**b**); crystals of **1** aged for 3 weeks at room temperature (**c**), and **3** fresh (in toluene) (**d**). The signals assigned to the n-propoxide are marked with (*). The signals corresponding to toluene and hexane are marked with (■) and (●), and those assigned to **3** with (▽), respectively.*

For complex **3** a rapid change in structure occurs in $CDCl_3$, resulting in precipitation of an insoluble polymer. No precipitations occurred when **3** was dissolved in toluene; the corresponding spectra did not change for several days (Figure 6.5d). Since the spectra were recorded in non-deuterated toluene, some peaks of the complex may overlap with those of the solvent.

The signals corresponding to toluene and hexane are marked with (■) and (●), respectively, and those assigned to **3** with (*). The signals at 3.22, 4.02 and 4.12 ppm are assigned to the $\underline{CH_2}$ of the diethanolamine ligands, the one at 3.22 ppm to $\underline{NCH_2}$ and the later two to $\underline{OCH_2}$. The splitting of the signal assigned to $\underline{OCH_2}$ may be a result of the longer bond lengths due to hydrogen-bonded isopropanol (see above). However, in the solid state the ratio between longer and normal bond lengths is 2:4, while dissolved in solution it seems to be more like 3:3. The signal at 4.72 ppm that is assigned to the $\underline{CH}$ of the isopropoxide ligands and the solvating isopropanol is in a ratio of 8:12 to that of $\underline{NCH_2}$, which is in accordance with the molecular structure. An analogous spectrum was obtained after storing the sample for several days at room temperature, demonstrating the time stability of complex **3**.

However, can this time stability of complex **3** really be considered a beneficial property, with respect to the preparation of materials? In the case of application in MOCVD and related techniques the absence of shelf stability will clearly influence the formed materials. The influence on sol-gel processed materials is not obvious, since the modification is *in situ*. The influence is evaluated by comparing the properties of gels by light scattering and TEM. The gels were obtained from the sols prepared from zirconium *n*-propoxide modified with 0.5 mol equivalent H_2dea. The only difference between the two samples was the refluxing after the addition of the modifier. Refluxing is often applied in sol-gel syntheses and accelerates possible transformations. The first indication that the refluxing had some sort of influence was observed after the addition of the nitric acid/propanol mixture. The sample that had not been refluxed almost instantly turned into a colorless gel, while the refluxed sample was a clear yellowish sol. The latter sol became a yellowish gel 24 hours later.

The light scattering experiments on the gelled sols also showed a difference. The sample that had not been refluxed consisted of particles with an average size of ~300 nm. In contrast to this mono-dispersed sample the refluxed sample consisted of particles in the order of 40 nm (between 10 and 30% of the sample) and with larger particles ranging from 130 – 150 nm. The TEM analysis is consistent with this observation based on light scattering. Figure 6.6 represents the typical appearance of the two samples.

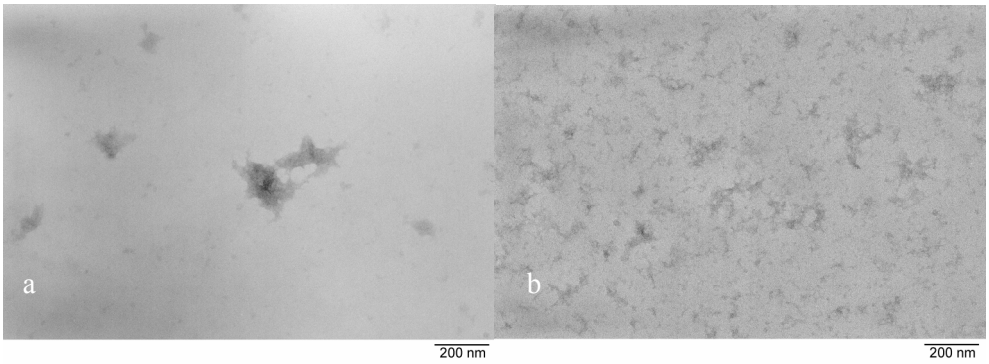

*Figure 6.6: TEM pictures of gelified sols of zirconium n-propoxide modified with 0.5 mol equivalent of H_2dea without (**a**) and with (**b**) refluxing before hydrolysis.*

It can clearly be seen that the presence or absence of refluxing has a great influence on the sol and gel properties. Thus even a short time storage, *e.g.*, during synthesis, may cause considerable effects for the synthesis of materials for high-tech applications. Since complex **3** is stable in time, it can be considered as an interesting precursor for the preparation of materials.

Another advantage of **3**, over **2** and other mixed alkoxide precursors, might be the presence of only one type of alkoxide ligand attached to a unique zirconium atom. Different alkoxide groups or alkoxides attached to differently coordinated metal atoms will differ in reactivity, which can have a significant influence on the structure of the materials formed.

6.4 Conclusions

Complexes **1** and **2** were obtained upon modification of zirconium *n*-propoxide and mixed ligand precursor with 0.5 mol equivalent of H_2dea. However, these tetranuclear compounds were not stable in solution and solid form, and the effect of

the absence of this stability on materials has been demonstrated to relevant. The trinuclear complex, $Zr\{\mu\text{-}\eta^3\text{-}NH(C_2H_4O)_2\}_3[Zr(O^iPr)_3]_2(^iPrOH)_2$, obtained upon modification of zirconium isopropoxide with either 0.5 and 1 mol equivalent of H_2dea, has a unique nona-coordinated central zirconium atom. This attractive nona-coordination of the central zirconium atom in **3** already led to the development of an analogous titanium-zirconium complex and will lead to a whole new series of interesting heterometallic complexes. Another unique feature of **3** is its solution stability, which is lacking in the modification of zirconium isopropoxide with for instance Hacac, and its time stability both dissolved in solution and in solid state.

6.5 References

1 S. Benfer, U. Popp, H. Richter, C. Siewert and G. Tomandl, *Sep. Purif. Technol*., **22-23**, 231 (2001).

2 R.J. Vacassy, C. Guizard, J. Palmeri and L. Cot, *Nanostruct. Mater*., **10**, 77 (1998).

3 C.R. Xia, H.Q. Cao, H. Wang, P.H. Yang, G.Y. Meng and D.K. Peng, *J. Membr. Sci*., **162**, 181 (1999).

4 M.Haruta, T. Kobayashi, H. Sano and N. Yamada, *Chem. Lett.***, 829**, 405 (1985).

5 A. Knell, P. Barnickel, A. Baiker and A. Wokaun, *J. Catal*., **137**, 306 (1992).

6 S. Hoffmann, M. Klee and R. Waser, *Integr. Ferroelectr.,* **10**, 155 (1995).

7 M. Klee, U. Mackens, W. Hermann and E. Bathelt, *Integr. Ferroelectr.,* **11**, 247 (1995).

8 J. Livage, M. Henry and C. Sanchez, *Prog. Solid St. Chem*., **18**, 259 (1988).

9 U. Schubert, *J. Sol-Gel Sci. Technol.*, **26**, 47 (2003).

10 G.I. Spijksma, H.J.M. Bouwmeester, D.H.A. Blank and V.G. Kessler, *Chem Commun*, 1874 (2004).

11 G.J. Gainsford, N. Al-Salima and T. Kemmitt, *Acta Crystallogr., Sect. E.: Struct. Rep. Online*, **58**, m619 (2002).

12 G.A. Seisenbaeva, S. Gohil and V.G. Kessler, *J. Mater. Chem.*, **14**, 3177 (2004).

13 Chapter 2 of this thesis.

14 SHELXTL-NT program manual, Bruker AXS, (1998).

15 S.M. Harben, P.D. Smith, R.L. Beddoes, D. Collision and C.D. Garner, *Angew. Chem. Int.. Ed*., **36**, 1897 (1997).

16 G.R. Willey, T.J. Woodman, W. Ficher and M.G.B. Drew, *Transition Met. Chem*., **23**, 467 (1998).

17 W. Ma, H. van Koningsveld, J.A. Peters and T. Maschmeyer, *Chem. Eur. J*., **7**, 657 (2001).

18 G.I. Spijksma, H.J.M Bouwmeester, D.H.A. Blank and V.G. Kessler, *Inorg. Chem. Comm*., **7**, 953 (2004).

19 Chapter 7 of this thesis.

20 V.G. Kessler, *Chem. Commun*., 1213 (2003).

21 V.W. Day, W.G. Klemperer and M.M. Pafford, *Inorg. Chem.*, **40**, 5738 (2001).

22 Chapter 2 of this thesis.

Chapter 7

Synthesis and characterization of diethanolamine modified heterometallic alkoxide precursors*

Abstract

The preparation and characterization of heterometallic alkoxide compounds, which are formed upon the modification of mixtures of homometallic alkoxides with diethanolamine (H_2dea) is discussed in this chapter. The structures of these products are $Zr\{\mu\text{-}\eta^3\text{-}NH(C_2H_4O)_2\}_3[Ti(O^iPr)_3]_2$ (**1**) and $Hf\{\mu\text{-}\eta^3\text{-}NH(C_2H_4O)_2\}_3[Ti(O^iPr)_3]_2$ (**2**). These trinuclear complexes have a unique nona-coordinated central zirconium or hafnium atom and a hexa-coordinated titanium atom. These compounds are also among the first thermodynamically stable zirconium-titanium and hafnium-titanium precursors. Mass spectrometric characterizations of these compounds demonstrate that they are volatile. This property and the stability of the compounds make them attractive single source precursors for MOCVD and ALD applications. The precursors are also interesting candidates for application in sol-gel. The preparation of **1** from zirconium *n*-propoxide involves the formation of an *n*-propoxide analogue of **1**, but does not yield any crystalline material. It is demonstrated that **1** can be prepared from $[Zr(O^nPr)(O^iPr)_3(^iPrOH)]_2$, however, it is in a lower yield compared to when zirconium isopropoxide is used.

---

* Part of this chapter has been published in:
"Molecular design approach to a stable heterometallic zirconium-titanium alkoxide-potential precursor of mixed-oxide ceramics", Gerald I. Spijksma, Henny J.M. Bouwmeester, Dave H.A. Blank, Vadim G. Kessler, *Inorg. Chem. Comm.,* **7,** 953-55 (2004).

Finally, it was evaluated whether or not zirconium-titanium heterometallic compounds could be obtained using triethanolamine as modifier. The single crystals obtained from a systems containing zirconium isopropoxide, titanium isopropoxide and H_3tea turned out to be $Ti_2(O^iPr)_2(\{\mu\text{-}\eta^4\text{-}NH(C_2H_4O)_2\}_3)_2$ (**4**) and it seems that the formation of a homometallic compound is favored over a heterometallic one in this system. Quantum chemical calculations indicate that the anticipated compound will have tremendously long metal-nitrogen bond lengths. This is an explanation as to why the formation of **4** is thermodynamically favored.

7.1 Introduction

Sol-gel materials are used in a broad spectrum of applications, ranging from mesoporous materials for catalyst supports and membranes [1,2] to high-tech applications as thin films, fibers [3,4], aerogels [5] and (nano-) particles [6-8]. Application of thin films can be as a micro-membrane layer [9-11], high-temperature thermal barrier coatings or ferroelectrics [12]. Despite being commonly used, both the homometallic and heterometallic alkoxide complexes remain insufficiently explored. Because the application of unmodified precursors like zirconium and hafnium in for instance MOCVD or sol-gel is difficult due to their extreme sensitivity to hydrolysis and pyrolysis, the precursor is often modified. A general method used to moderate reactivity and improve the volatility is by replacing (part) of the alkoxide ligands by chelating organic ligands [13-15]. In sol-gel studies, acetic acid and acetylacetone are most often applied for this purpose [15]. Acetic acid has the undesired side effect of reacting with alcohol upon the release of water, and in recent work we showed [16,17] that the stabilizing effect with acetylacetone disappears completely beyond addition of 1 mol equivalent. In our search for a stable modified zirconium precursor we applied diethanolamine, H_2dea, as the stabilizing agent. To the best of our knowledge, no reports have been published on zirconium precursor structures formed upon modification with H_2dea. Yet, the structure for the modified product of zirconium *n*-propoxide with 0.5 mol equivalent of N-methyl-diethanolamine has been published [18]. In our study [19], an analogous compound was prepared from zirconium *n*-propoxide with 0.5 mol equivalent H_2dea. The modification of $[Zr(O^iPr)_4(^iPrOH)]_2$ with ≤ 1 mol equivalent of H_2dea, gave an interesting trinuclear $Zr\{\mu\text{-}\eta^3\text{-}NH(C_2H_4O)_2\}_3[Zr(O^iPr)_3]_2(^iPrOH)_2$ complex with a nona-coordinated central zirconium atom. This very unusual coordination of zirconium has been observed a few times in aqueous environments [20-22] but now it has been observed for the first time under non-aqueous conditions. This uncommon geometry inspired us to prepare a new family of heterometallic precursors.

The presence of two types of positions on $Zr\{\mu\text{-}\eta^3\text{-}NH(C_2H_4O)_2\}_3[Zr(O^iPr)_3]_2(^iPrOH)_2$, a nona-coordinated and a hexa-coordinated, provides us with the possibility of constructing new species *via* self-

assembly according to the Molecular Structure Design Concept [23]. For example, the hexa-coordinated position appears to be able to host smaller atoms like titanium, while hafnium should be able to be located in the nona-coordinated position. Moreover, the compounds can be prepared with several alkoxide ligands. Here we report the application of this model for the preparation of a new family of heterometallic complexes.

7.2 Experimental

All manipulations were carried out in a dry nitrogen atmosphere using the Schlenk technique or a glove box. Hexane and toluene (Merck, *p.a.*) were dried by distillation after refluxing with $LiAlH_4$ and isopropanol (Merck, *p.a.*) was purified by distillation over $Al(O^iPr)_3$. Diethanolamine (H_2dea) and triethanolamine (H_3tea) (98%) were purchased from Aldrich. Molecular sieves were added to the H_2dea to assure that it remained water free. ^{1}H NMR spectra were recorded in d_8-toluene (99.6 %, Aldrich), which was stored with molecular sieves, for all compounds on a Bruker 400 MHz spectrometer at 243 K.

Synthesis: The zirconium propoxide precursors used as starting materials in this work are zirconium isopropoxide, $([Zr(O^iPr)_4(^iPrOH)]_2$ 99.9%) and 70 wt% solution of "$Zr(O^nPr)_4$ in *n*-propanol (both purchased from Aldrich) and $[Zr(O^nPr)(O^iPr)_3(^iPrOH)]_2$ which was prepared according to a recently developed technique [24,25]. The zirconium isopropoxide was dissolved and recrystallized from toluene prior to use in order to remove impurities. The hafnium isopropoxide was prepared by anodic oxidation of hafnium metal in isopropanol [26] and recrystallized from toluene. The titanium isopropoxide (99.999% pure) and titanium *n*-propoxide (98% pure) were both obtained from Aldrich. Combinations of the different precursors were modified with H_2dea according to the techniques described below. The exact composition of the single crystals **1**, **2** and **4** was established with single crystal X-ray crystallography.

$[Zr\{\mu\text{-}\eta^3\text{-}NH(C_2H_4O)_2\}_3[Ti(O^iPr)_3]]$ (1): Several synthetic pathways were explored for the preparation of this compound. In the first one, 0.57 g (1.5 mmol) of zirconium isopropoxide was dissolved in a 3 ml mixture of hexane/toluene (volume ratio 2:1), subsequently 0.84 g (~3.0 mmol) titanium isopropoxide and

0.46 g (~4.4 mmol) H_2dea was added. The sample was dried under vacuum (0.1 mm Hg) and redissolved in 2 ml hexane. After cooling overnight in a freezer at -30 °C, the obtained colorless octahedral crystals were separated from the solvent by decantation. The yield was ~1.1 g (~59%) of compound **1**. The yield can be increased significantly when **1** is crystallized from a more concentrated solution. With additional crystallization steps the compound can be obtained in a quantitative yield.

The synthesis was also performed starting with $[Zr(O^nPr)(O^iPr)_3(^iPrOH)]_2$ as the precursor. The precursor (0.94 g, ~2.4 mmol mol) was dissolved in 2 ml hexane and subsequently 1.39 g (~4.8 mmol) titanium isopropoxide and finally 0.78 g (~ 7.2 mmol) diethanolamine was added. The sample was dried under vacuum (0.1 mm Hg) and redissolved in 2 ml hexane. After cooling overnight in a freezer at -30 °C, the obtained colorless octahedral crystals were separated from the solvent by decantation. The yield was ~0.8 g (~26%) of compound **1**.

It was also attempted to prepare **1** by exchanging the *n*-propoxide ligands of **3** (preparation described below) for isopropoxide ligands. About 4.5 g of **3** was dissolved in 2 ml hexane and 5 ml isopropanol. After 3 sequences of solvent removal and redissolving in a 5 ml isopropanol and 2 ml hexane solution, the sample was dried once more and redissolved in hexane. The solution was stored in a freezer at -30 °C, but no single crystals were formed after ~1 month. The sample was subsequently placed on the lab bench and the hexane was allowed to diffuse through the rubber stopper. This yielded a minor amount of crystals and a yellow-brownish viscous liquid. The formed crystals turned out not to be of X-ray quality.

In another attempt to prepare **1**, zirconium *n*-propoxide (2.0 g, ~5.2 mmol) was dried and redissolved in 2 ml hexane. Subsequently 2.96 g titanium *n*-propoxide (~10.4 mmol), 1.68 g H_2dea (~15.6 mmol) and 6 ml isopropanol were added. The next day, the sample was dried again and redissolved in 2 ml hexane and 6 ml isopropanol, this sequence was repeated once more. After removal of the solvent under vacuum, the dried product, a yellow viscous liquid, was dissolved in 2 ml hexane and placed in the freezer to crystallize. No single crystals were obtained from this solution.

An analogous synthesis was performed using zirconium *n*-propoxide (1.24 g, 3.2 mmol), titanium isopropoxide (1.81 g, ~6.4 mmol), diethanolamine (1.02 g, ~9.6 mmol) and 2 ml hexane as solvent (*i.e.*, no additional isopropanol was added in this synthesis). This procedure did not result in the formation of single crystals of **1**.

Analytical samples of crystals of **1** were dried in vacuum (0.1 mm Hg) prior to spectral analysis. Found (%): C 38.8; N 5.0; H 7.5. Calculated for $C_{30}H_{69}N_3O_{12}Ti_2Zr$ (%): C 42.3; N 4.9; H 8.1. The IR spectra were recorded of the compound in nujol mulls, cm^{-1}: 1358 sh, 1327 w, 1280 w, 1241 w, 1167 sh, 1160 m, 1124 s, 1085 m, 1060s, 1007 w, 988 s, 941 m, 914 s, 879 m, 844 s, 673 sh, 602 s, 571 sh, 447 s.

$[Hf\{\mu\text{-}\eta^3\text{-}NH(C_2H_4O)_2\}_3[Ti(O^iPr)_3]]$ (**2**): Hafnium isopropoxide solvate (0.78 g, ~1.65 mmol) was dissolved in a mixture of hexane and toluene (5 ml and volume ratio 1:1). Subsequently, the appropriate amounts of titanium isopropoxide and H_2dea (0.94 g (~3.3 mmol) and 0.53 g (~4.9 mmol), respectively) were added. The sequence of solvent removal under vacuum (0.1 mm Hg) and redissolving in 1.5 ml hexane was performed twice. After cooling overnight in a freezer at -30 °C, the obtained colorless octahedral crystals were separated from the solvent by decantation. The yield was ~1.8 g (~80%) of compound **2**.

Analytical samples were dried in vacuum (0.1 mm Hg) prior to spectral analysis. Found (%): C 36.38; N 4.5; H 6.7. Calculated for $C_{30}H_{69}N_3O_{12}Ti_2Zr$ (%): C 38.4; N 4.5; H 7.3. The IR spectra were recorded of the compound in nujol mulls, cm^{-1}: 1160 m, 1124 s, 1084 m, 1063s, 988 s, 914 s, 842 s

$[Zr\{\mu\text{-}\eta^3\text{-}NH(C_2H_4O)_2\}_3[Ti(O^nPr)_3]]$ (**3**): Zirconium *n*-propoxide (1.4 g, ~3.6 mmol mol) was dried and redissolved in 2 ml hexane and subsequently 2.06 g (~7.2 mmol) titanium isopropoxide and 1.17 g (~ 10.8 mmol) diethanolamine were added. The sample was dried under vacuum (0.1 mm Hg) and redissolved in 2 ml hexane and subsequently placed at -30 °C several days for crystallization. The sequence of drying, redissolving and cooling for crystallization was repeated two more times. The composition of the yellowish product is assumed to be that of **3**.

$Ti_2(O^iPr)_2(\{\mu\text{-}\eta^4\text{-}NH(C_2H_4O)_2\}_3)_2$ (**4**): 0.73 g (1.86 mmol) of zirconium isopropoxide was dissolved in a 3 ml mixture of hexane/toluene (volume ratio 2:1), subsequently 1.08 g (~3.8 mmol) titanium isopropoxide and 0.56 g (~3.8 mmol) H_3tea were added. The milk like sample was refluxed for 30 minutes and subsequently dried under vacuum (0.1 mm Hg) and redissolved in 2 ml hexane (were it remained a yellow, milk like solution). After cooling overnight in a freezer at -30 °C, the obtained colorless octahedral crystals were separated from the solvent by decantation. The crystals were characterized as $Ti_2(O^iPr)_2(\{\mu\text{-}\eta^4\text{-}NH(C_2H_4O)_2\}_3)_2$ by X-ray diffraction. The synthesis was performed in an analogous manner with zirconium isopropoxide, titanium isopropoxide and triethanolamine in a ratio of 1 : 1 : 2. Again the obtained single crystals consisted only of $Ti_2(O^iPr)_2(\{\mu\text{-}\eta^4\text{-}NH(C_2H_4O)_2\}_3)_2$.

$Ti_2(O^iPr)_2(\{\mu\text{-}\eta^4\text{-}NH(C_2H_4O)_2\}_3)_2$ was also prepared by dissolving titanium isopropoxide (1.84 g, 6.5 mmol) in 4 ml of hexane. Upon the addition of H_3tea (0.97 g, 6.5 mmol) the color of the solution changed from colorless to yellow and an increase in temperature of the solution was observed. The solvents were removed under vacuum (0.1 mm Hg). It was attempted to redissolve the obtained solid product in a 4 ml mixture of solvent (toluene and isopropanol in a volume ratio of 1:1). The sample was subsequently refluxed and toluene was added until a clear solution had formed. The sample was cooled overnight in a freezer at -30 °C, and the obtained crystals (almost quantitative yield) were separated from the solvent by decantation. The crystals were characterized and determined to be that of **4**.

Crystallography: Data collection for single crystals of all compounds was carried out at 22 °C on a SMART CCD 1k diffractometer with graphite monochromated MoKα radiation. All structures were solved by standard direct methods. The coordinates of the metal atoms as well as the majority of other non-hydrogen atoms were obtained from the initial solutions and for all other non-hydrogen atoms found in subsequent difference Fourier syntheses. The structural parameters were refined by least squares using first isotropic and then also anisotropic approximations. The coordinates of the hydrogen atoms were calculated geometrically and were included into the final refinement in isotropic

approximation for all the compounds. All calculations were performed using the SHELXTL-NT program package [27] on an IBM PC.

Calculations: All quantum chemical calculations were made using the program package *Gaussian 03* (Rev. C.02) [28], employing the hybrid density function B3PW91. The basis sets used for H, C, N and O were of 6-311G quality including additional diffusion and polarization functions. The basis sets used for Zr and Hf employed quasi-relativistic (MWB) effective-core potentials, thus taking scalar relativistic effects into account, replacing 28 and 60 electrons, respectively, with adapted basis sets of (8s7p6d)/[6s5p3d] quality [29]. All metal complexes and ligands were geometrically optimized to a maximum of symmetry (Figure 7.1).

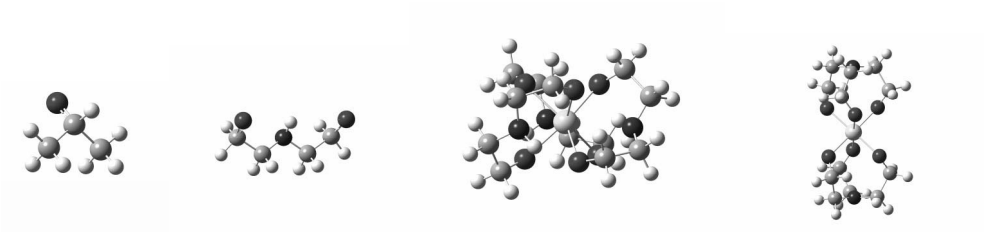

Figure 7.1: Optimized geometries dea^{2-} (C_s), tea^{2-} (C_3), (C_i), $Zr/Hf(dea)_3^{2-}$ (C_1, however close to C_3) and $Zr/Hf(tea)_2^{2-}$ (D_3).

7.3 Results and discussion

The first heterometallic compound aimed for in this study has a nona-coordinated zirconium central atom and two hexa-coordinated titanium atoms in the terminal position. Mixing of the components, zirconium and titanium isopropoxide and H_2dea, in a ratio of Zr : Ti : L = 1 : 2 : 3 in hydrocarbon solvent as described in the experimental section provided the anticipated complex in a very high yield.

The molecular structure of the obtained complex was studied by X-ray crystallography, it was characterized as $Zr\{\mu\text{-}\eta^3\text{-}NH(C_2H_4O)_2\}_3[Ti(O^iPr)_3]_2$ (**1**)[1] depicted in Figure 7.2. The coordination of the central zirconium atom is a very regular tricapped trigonal prism (see Figure 6.4) with the oxygen atoms composing

[1] Crystal data: $C_{30}H_{69}N_3O_{12}Ti_2Zr$, M = 850.90, tetragonal, a = 11.6171(12) Å, b = 11.6171(12) Å, c = 32.053(5) Å, α = 90°, β = 90°, γ = 90°, V = 4325.7(9) Å^3, T = 295 K, space group P4(3)2(1)2, Z = 1, μ = 0.650 mm^{-1}, 25389 reflections measured, 5091 unique (R_{int}= 0.0412 which were used for refinement. The final discrepancy factors were R1 = 0.0521; wR2 = 0.1411 for 3126 observed reflections (I > 2sigma(I)).

the vertices of the prism (Zr(1)-O(2) 2.196(3), Zr(1)-O(3) 2.199(3) and Zr(1)-O(4) 2.210 (3) Å) and the nitrogen ones –the capping vertices (Zr(1)-N(1) 2.440(6), Zr(1)-N(2) 2.439(5) Å). This high-symmetry coordination indicates high stability of the chelated core with uniform charge distribution and highly covalent bonding.

The titanium atoms reside in a trigonally distorted octahedron with, in principle, only two types of Ti-O distances: one bridging (Ti-O 2.137(3)-2.147(3) Å) and one terminal (Ti-O 1.836(5)-1.853(4) Å). This coordination is much more symmetric than that of octahedral titanium homo- and heterometallic β-diketonate complexes [30,31], where 3 different bond lengths occur (very short terminal 1.77-1.80 Å, intermediate alkoxide bridging, 1.95-2.05 Å, and slightly longer ones to the oxygen atoms of β-diketonate ligands, 2.02-2.08 Å), which may be the reason for the high solution stability of complex **1,** as will be discussed below, in comparison with these species.

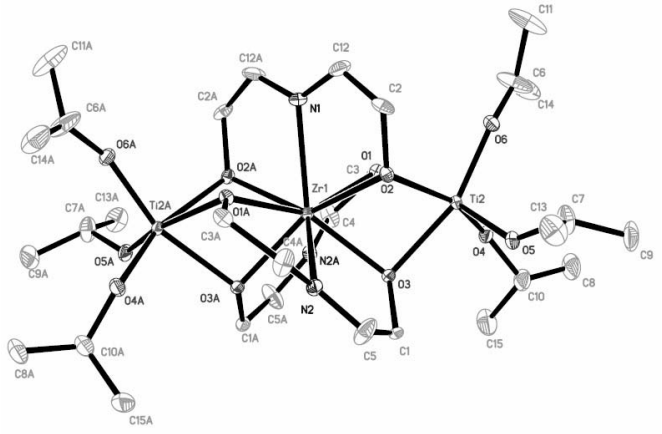

*Figure 7.2: Molecular structure of Zr{μ-η^3-NH($C_2H_4O)_2$}$_3$[Ti($O^iPr)_3$]$_2$ (**1**)*

A typical ^{1}H NMR spectrum of **1** is depicted in Figure 7.3a. The spectrum of **1** is significantly more complex than one would expect. Compound **1** has 4 different proton containing groups, *i.e.*, $\underline{CH_3}$, and $\underline{CH}$ of the alkoxide ligands and $\underline{NCH_2}$ and $\underline{OCH_2}$ of the diethanolamine ligand, and a corresponding number of signals are expected. Some of the signals in the spectrum are due to traces of the hydrocarbon solvents used during the synthesis or to the toluene in the d_8-toluene used as the solvent for the NMR samples. These signals are present between 0 and 2.15 ppm and marked with (*) in Figure 7.3a. Two dimensional NMR was performed to get

more insight into the NMR spectra. The proton-proton and proton-carbon coupling experiments (typical spectra are displayed in Figure 7.4a and 7.4b, respectively) indicated that the signals at 1.45 and 5.0 are due to the protons of $\underline{CH_3}$, and $\underline{CH}$ of the alkoxide ligands, respectively. It was also found that some traces of propanol were present in the sample.

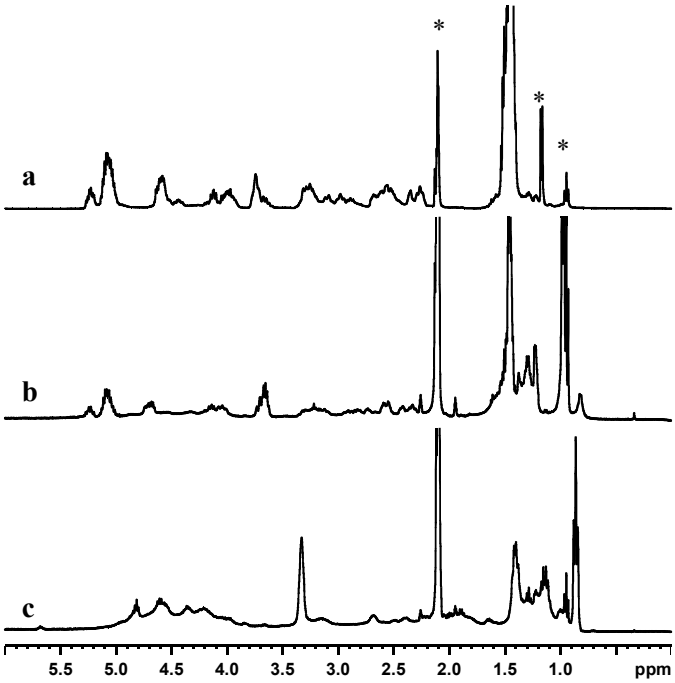

*Figure 7.3: The proton NMR spectra (a) **1**. (b) **2** and (c) **3**. The signals corresponding to hydrocarbon solvents are marked with (*).*

The assignment of signals to the diethanolamine ligands was not possible, since multiple signals were observed. A different carbon chemical shift, *i.e.*, ~50 and 70 ppm, is observed in the proton-carbon coupling spectra for the signals between 2.2 -3.4 and 3.7- 5.3 ppm (see Figure 7.4b). The signals in the respective areas are assigned to the protons of $\underline{OCH_2}$ and $\underline{NCH_2}$ of the diethanolamine ligands. The integration of the area of all signals assigned to $\underline{OCH_2}$ and $\underline{NCH_2}$ is in the expected ratio with that of the alkoxide ligands.

We assumed that the presence of various signals due to $\underline{OCH_2}$ and $\underline{NCH_2}$ of the diethanolamine ligands is caused by alcohol exchange and solvation. In the work on the preparation of homometallic H_2dea modified zirconium precursors, the

bonding of alcohol is actually observed in the solid compound $Zr\{\mu\text{-}\eta^3\text{-}NH(C_2H_4O)_2\}_3[Zr(O^iPr)_3]_2(^iPrOH)_2$. The proton-proton NMR coupling (Figure 7.4a) experiments also support the idea of alcohol exchange and solvation. It seems that the protons in $\underline{OCH_2}$ and $\underline{NCH_2}$ are in all cases coupled to the same species, but at different chemical shifts. ^{1}H NMR spectra of two samples from the same batch of crystals from compound **1** were recorded. A drop of isopropanol was added to one of the samples. The spectra displayed a large difference in the position of the signals due to $\underline{OCH_2}$ and $\underline{NCH_2}$ which confirms the alcohol exchange and solvation of **1** and **2** in the solution.

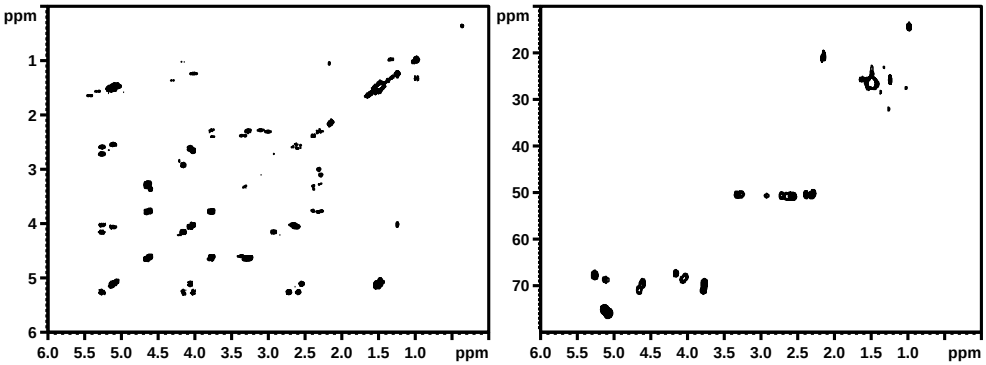

*Figure 7.4: The proton-proton and proton-carbon coupling NMR spectra of **1**.*

The obtained compound **1** is stable in both solid state and solution. Identical ^{1}H NMR spectra were obtained for fresh and aged samples of **1**. The aged samples were either stored for 2 months as a solid or for up to one month in toluene. In both cases, the samples were stored at room temperature.

We showed that it is possible to prepare a compound that has a nona-coordinated central zirconium atom and two hexa-coordinated titanium atoms in the terminal position. It was also of interest to see if the same approach would be valid for hosting a hafnium atom. The main difference between zirconium and hafnium is the smaller atomic radius of the hafnium, resulting from lanthanide contraction. A sample of the aimed compound was prepared according to the procedure described above and the obtained crystals were identified as

$Hf\{\mu\text{-}\eta^3\text{-}NH(C_2H_4O)_2\}_3[Ti(O^iPr)_3]_2$ (**2**). The molecular structure of **2**[2] is analogous to that of $Zr\{\mu\text{-}\eta^3\text{-}NH(C_2H_4O)_2\}_3[Ti(O^iPr)_3]_2$, which is depicted in Figure 7.2.

The bond lengths, listed in Table 7.1, indicate a larger deviation and larger average length in the metal-oxygen bond lengths of the central atom for **2**, *i.e.*, 2.196(3) - 2.210(3) Å for compound **1** compared to 2.190(11) - 2.237(13) Å for **2**. The distance between the central metal atom and the titanium is, however, shorter for **2**. This is due to the shorter titanium-oxygen bonds, *i.e.*, 2.112(15), 2.119(15), 2.127(14) and 2.145(4), 2.147(3), 2.137(3) for **2** and **1**, respectively. The alkoxide ligands are more strongly bonded to the titanium atom in **2** compared to **1**, as can be seen from the shorter titanium-oxygen bond lengths. The bond length distribution indicates that the bonds around hafnium have a more pronounced electrostatic character compared to that of zirconium, which results in a higher covalent input for Ti-O bonds.

*Table 7.1: selected bond lengths of **1** and **2** where M is either Zr or Hf.*

Bond lengths [Å]	**1**	**2**
M-O1	2.210(3)	2.190(11)
M-O2	2.196(3)	2.215(12)
M-O3	2.199(3)	2.237(13)
M-N1	2.440(6)	2.43(2)
M-N2	2.439(5)	2.448(17)
M-Ti	3.2035(8)	3.166(4)
Ti-O1	2.145(4)	2.112(15)
Ti-O2	2.147(3)	2.119(15)
Ti-O3	2.137(3)	2.127(14)
Ti-O4	1.836(5)	1.833(17)
Ti-O5	1.849(4)	1.808(15)
Ti-O6	1.853(4)	1.794(17)

The ^1H NMR spectra of **2** is depicted in Figure 7.3b and is quite similar to that obtained from **1**. At a chemical shift of 0-2.15 ppm the presence of hydrocarbon solvents and some residual alcohol is observed. The effect of alcohol exchange and solvation due to the presence of residual alcohol on the chemical shift of the

[2] Crystal data: $C_{30}H_{69}N_3O_{12}Ti_2Hf$, M = 938.17, tetragonal, a = 11.620(3), b = 11.620(3), c = 31.987(7) Å, α = 90°, β = 90°, γ = 90°, V = 4318.9(18) Å^3, T = 295 K, space group Pna2(1), Z = 4, μ = 2.812 mm^{-1}, 13246 reflections measured, 2639 unique (R_{int} = 0.1350) which were used in all calculations. The final discrepancy factors were R1 = 0.0808; wR2 =0.1514 for 1776 observed reflections (I > 2sigma(I)).

protons of $\underline{OCH_2}$ and $\underline{NCH_2}$ of the diethanolamine ligands has already been discussed above. For this reason a quantitative interpretation of the NMR spectra of these compounds is not possible.

With the quantum chemical calculations it was evaluated if there exists any electronic reason for a difference in the stability of **1** and **2**. The difference in total energy of the geometrically optimized structures was taken as an estimate of the binding energy. Any difference in electronic stability would become apparent from the calculations on the different systems. However, considering that the Group 4 cations formally have a +4 charge and that the ligands are multidentate and negatively charged, one should expect a dominance of electrostatic interaction and minimal effects of electronic factors.

For the reaction of interest in the parent study, we observed

$$M^{4+} + 3\ dea^{2-} \rightarrow M(dea)_3^{2-} \qquad (7.1)$$

that reaction (7.1) is associated with a binding energy of about 9400 kJ/mol in both cases. The difference between zirconium and hafnium is less than 0.5% (49 kJ/mol). This system bears some additional interest; since non-equivalence between the ligands can be observed resulting in a real symmetry that is lower than the ideal C_3 one. The reason is not fully clear, since the difference in energy is quite small. In the low-symmetry configuration Zr-O distances fall into two groups; one side with three distances around 2.19 Å and one side with the remaining three distances around 2.26 Å. The Hf-O distances also fall into two groups with average values of 2.18 and 2.25 Å, respectively. The Zr-N distances divide into two short distances at 2.58 and one longer at 2.68 Å for, with the corresponding values for M = Hf being 2.58 and 2.72 Å.

In conclusion it must be noted that a survey like this based on quantum chemical calculations will be very narrow-sighted. It will only address the states more or less arbitrarily chosen from a very complex potential energy surface. With this limited view, it is clear that there is no significant difference in stability between zirconium and hafnium in the complex compounds studied here. This does not mean that they will have to exhibit the same kinetic or thermodynamic stability. In an experimental system, several competing reaction products and reaction paths may

co-exist, not included in this computational study, and manifest themselves in a dramatic difference in real stability of one class of compounds with respect to the other. Nevertheless, there is no inherent electronic difference in stability for the zirconium and hafnium compounds included in this study. The experimental stability has not displayed any differences either.

We also evaluated whether or not compounds **1** and **2** can be prepared through different synthesis pathways. For zirconium, various propoxide precursors are available, *i.e.*, zirconium isopropoxide, 70 wt% solution of "$Zr(O^nPr)_4$" and the mixed ligand propoxide precursor $[Zr(O^nPr)(O^iPr)_3(^iPrOH)]_2$, while for hafnium only hafnium isopropoxide is commercially available. Our objective was to see if compound **1** can be obtained using another and cheaper zirconium propoxide precursor. The possible pathways are depicted in Figure 7.5 and the route marked with '6' has been used above to prepare **1**.

The route starting from cheap zirconium and titanium *n*-propoxides (reaction 1) involves the formation of an *n*-propoxide analogue of **1** and subsequent exposure to an excess of isopropanol. Upon addition of the H_2dea to the solution with the precursors, a temperature increase of the mixture was observed. A temperature increase was also observed earlier in the preparation of **1** and **2**. Details of the synthesis are provided in the experimental section. Despite several drying steps and subsequent addition of hexane, no single crystals were obtained. The latter is probably due to the extreme high solubility of *n*-propoxide compounds and to the difficulty of removing all of the *n*-propanol from the system. In the NMR spectra obtained from this sample, Figure 7.3c, a large signal at 3.3 ppm is assigned to the parent alcohol, and also a large number of unresolved signals are observed. This latter effect is again due to alcohol exchange and salvation. The existence of **3** is confirmed in ref. [32] where is shown that the derived unique materials of **1** and **3** are identical.

The sample was subsequently dissolved in an excess amount of isopropanol. The ligand exchange that was aimed for, in reaction 2, is the same as that in reaction 4. In the latter reaction, zirconium *n*-propoxide is transformed into $Zr(O^nPr)(O^iPr)_3(^iPrOH)]_2$ where the alkoxides in the terminal position are isopropoxide ligands. The synthesis of $Zr(O^nPr)(O^iPr)_3(^iPrOH)]_2$ is described

elsewhere [24,25]. After 3 sequences of solvent removal and redissolving in an isopropanol/hexane mixture, the sample was dried once more and redissolved in hexane. We attempted to crystallize the yellowish solution by storing it at a low temperature and when that did not have the desired result, it was subsequently stored at room temperature and the solvent was allowed to diffuse through the rubber stopper. This yielded a minor amount of crystals and a viscous liquid, however the formed crystals were not of X-ray quality. The ^{1}H NMR of the crystals was analogous to that obtained for **1**. The spectrum of the viscous liquid was also very similar to that of **1**, but in the spectrum the presence of *n*-propanol and isopropanol could clearly be seen.

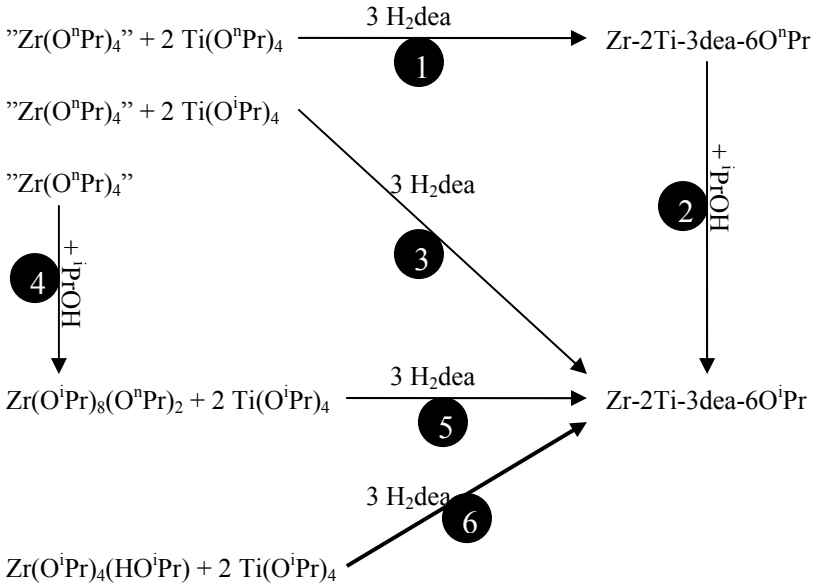

*Figure 7.5: Scheme of the possible synthetic pathways for the formation of **1**.*

We also attempted to prepare **1** in one step from zirconium *n*-propoxide. This was done either by using titanium isopropoxide or by using titanium *n*-propoxide with an excess amount of isopropanol. The product of these syntheses was a yellowish viscous liquid, and despite all attempts, no single crystals were obtained. The ^{1}H NMR spectrum of these viscous liquids was similar to that obtained from the synthesis through reaction 1 and 2. Obviously, the presence of *n*-propoxide has been of great influence on the crystallization behavior.

A way to avoid the presence of an excessive amount of *n*-propoxide and *n*-propanol in the synthesis, is through the preparation and crystallization of $Zr(O^nPr)(O^iPr)_3(^iPrOH)]_2$ from zirconium *n*-propoxide. The preparation of $Zr(O^nPr)(O^iPr)_3(^iPrOH)]_2$ (reaction 4) was mentioned above and is described in detail in ref [24] and [25]. The preparation of **1** from $Zr(O^nPr)(O^iPr)_3(^iPrOH)]_2$ is described in the experimental section. The obtained single crystals were characterized as **1** on the basis of the determined unit cell parameters. The yield is the main difference between the synthesis of **1** from $Zr(O^nPr)(O^iPr)_3(^iPrOH)]_2$ and zirconium isopropoxide. The yields are 26% and 59%, respectively and it should be noted that the yield from the synthesis with zirconium isopropoxide was obtained from a solution with a significantly lower concentration. The lower yield for the synthesis using $Zr(O^nPr)(O^iPr)_3(^iPrOH)]_2$ as the precursor is probably due to the remaining *n*-propanol in the system. The yield for both syntheses can probably be increased through drying of the liquid phase which is removed from the crystals and redissolving the dried product in hexane and subsequent crystallization at low temperature. The pathway using $[Zr(O^nPr)(O^iPr)_3(^iPrOH)]_2$ as a precursor is thus an alternative to the more expensive zirconium isopropoxide. However, this method is significantly more labor intensive and the synthesis consumes more chemicals, *e.g.*, the precursor needs to be prepared since it is not commercially available. We can conclude that with two types of alkoxide ligands, a multi component system is obtained, which results in a lower yield upon crystallization.

The compounds **1-3** were also characterized by mass spectrometry. The fragments that are observed in the gas phase will provide information on the composition of the sample and will also indicate if the compounds are suitable for application in MOCVD and/or ALD. The observed fragments in the spectrum of **1** are perfectly in agreement with its molecular structure, though some fragments indicate the presence of a minor amount of a Zr_2-Ti compound. The large signal at 639 M/z(I) (97.1%) is assigned to M-Ti(dea)(OPr) with $M = Zr\{\mu\text{-}\eta^3\text{-}NH(C_2H_4O)_2\}_3[Ti(O^iPr)_3]_2$ the interpretation of the MS-spectrum for **1** is given in Table 7.2. In the spectrum of **2,** the same fragment is observed at 727 M/z(I) (81.3%). This fragment and low mass species (*i.e.*, < 269 and < 290 for compound **1** and **2** respectively) are the main species present in the spectra of **1** and **2**. The intensity of these low mass fragments is significantly higher in the spectrum

of **2** which indicates that more decomposition occurs for **2**. The spectrum of **3** displayed only low mass fragments, which indicates decomposition of the compound due the electron impact and implies that this compound is not volatile. The presence of a relatively larger amount of high-mass fragments of **1** indicates that the gas phase stability is higher for this compound. However, both compounds seem to be volatile and can therefore be considered attractive single source precursors for MOCVD and ALD applications.

*Table 7.2: Interpretation of M/z(I) spectrum of **1**.*

Gas phase fragments	z(I)		
$TiO(OH)(OC_3H_6)^+$	139 (59.6)	$Zr_2(dea)_2(OPr)_3(C_2H_4)^+$	548 (4.4)
$Ti(OPr)_2H^+$, $ZrO(OPr)(OH)^+$	167 (50.5)	M-$Ti(OPr)_3$ -(OPr) -CH_3	550 (3.7)
$TiO(OPr)(OC_3H_6)^+$, $ZrO(OPr)(OH)^+$	181 (62.7)	M -dea -3OPr	569 (3.4)
$Ti(dea)(OPr)^+$	210 (88.9)	M -$Ti(OPr)_3$	624 (0.7)
$TiO(dea)(OC_3H_6)^+$	225 (100)	M-Ti(dea)(OPr)	639 (97.1)
$Zr(dea)O(OCH_2)^+$	239 (27.8)	M -3(OPr)	672 (0.9)
$Zr(dea)O(OPr)^+$	252 (6.3)	M -2(OPr)	731 (1.6)
$Zr(dea)(OC_2H_4)(OH)^+$	254 (48.6)	$Zr_2Ti(dea)_3(OPr)_5^+$	774 (2.0)
$Zr(dea)(OPr)(OH)^+$	269 (100)	M –Opr	790 (1.8)
M-$Ti(OPr)_2$ -3(OPr)	447 (2.2)	M -CH_3	834 (1.6)
M-Ti(dea)(OPr) -3(OPr) –H	461 (4.3)	M –H	848 (0.3)
M-Ti(dea)(OPr) -2(OPr) -CH_3	506 (3.2)	$Zr_2Ti(dea)_3(OPr)_5(C_2H_4)^+$	876 (0.1)
M-Ti(dea)(OPr) -2(OPr)	521 (6.6)		

The possibility to prepare heterometallic compounds, using triethanolamine as the modifier, was also briefly examined. The anticipated compounds were expected to be structural analogs of $[La(tea)_2\{Nb(O^iPr)_4\}_3]$ [33]. The initial sample consisted of zirconium isopropoxide, titanium isopropoxide and H_3tea in a ratio of 1:2:2. The crystals, which were obtained according to the procedure described in the experimental section, were identified by X-ray diffraction as $Ti(O^iPr)_2(\{\mu\text{-}\eta^4\text{-}NH(C_2H_4O)_2\}_3)_2$ (**4**)[3] (Figure 7.6). The formation of this homometallic compound, earlier reported by Harlow [34], with a high yield, suggests that this compound is thermodynamically favored over the anticipated compound.

[3] Crystal data: $C_{36}H_{76}N_4O_{16}Ti_4$, M = 1012.61, triclinic, a = 12.3569(17) Å, b = 13.3690(18) Å, c = 14.448(2) Å, α = 90°, β = 92.176°, γ = 90°, V = 2385.0(6) Å^3, T = 295 K, space group P-1, Z = 2, μ = 1.410 mm^{-1}, 4059 reflections measured, 1864 unique (R_{int}= 0.0644 which were used for refinement. The final discrepancy factors were R1 = 0.0431; wR2 = 0.0791 for 1197 observed reflections (I > 2sigma(I)).

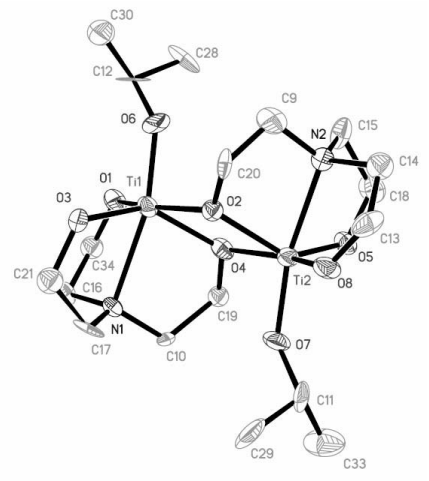

*Figure 7.6: Molecular structure of $Ti(O^iPr)_2(\{\mu\text{-}\eta^4\text{-}NH(C_2H_4O)_2\}_3)_2$ (**4**).*

Quantum chemical calculations were performed to evaluate if there exist any electronic reason why the anticipated compound was not obtained. The binding energy in reaction (7.2) is about 10100 kJ/mol with a difference of about 0.3% (36 kJ/mol).

$$M^{4+} + 2\ tea^{2-} \rightarrow M(tea)_2^{2-} \qquad (7.2)$$

Because of the high symmetry we only identified one M-O distance of 2.121 Å for zirconium and 2.113 Å for hafnium. The M-N distances are quite long emerging to 3.796 and 3.779 Å, respectively for M = Zr and Hf. These long M-N distances, the corresponding distances in **4** are 2.417(17) and 2.243(17) and for both **1** and **2** around 2.4 Å, respectively, are a probable reason why the formation of **4** is thermodynamically favored.

In this paper, we have demonstrated the formation of thermodynamically stable heterometallic compounds. The stability of **1** and **2** makes these compounds attractive for the preparation of materials and the presence of only one type of reactive alkoxide ligands attached only to Ti atoms can be a great advantage. Composite materials can possess unique or improved material properties. For preparation of composite zirconium and titanium materials the interested reader is referred to ref. [35] and references herein. The preparation of these composites is typically performed by, for example, adding zirconium-oxy-nitrate hydrate to titanium alkoxide sols [36]. Utilizing heterometallic precursors will supposedly

lead to a more homogeneous distribution of the different metal atoms, since they are incorporated in the particle structure, and thus mixed at an atomic level. The sol-gel application of these precursors will be discussed elsewhere [32].

There is thus a great potential for heterometallic precursors in the preparation of titanium-zirconium and titanium-hafnium composite materials. The heterometallic titanium-zirconium precursors available in the literature [37,38], are considered less suitable compared to the one presented in this paper. The precursors reported in the literature [37,38] have (different) alkoxide ligands attached to both the zirconium and titanium atoms. Alkoxide ligands attached to titanium have a different reactivity than those attached to zirconium, which can effect the homogeneity of the doping in the derived composite materials. Moreover, we have observed decomposition in time [19] for analogous homometallic species, supposedly into the trimeric complex with a nona-coordinated central zirconium atoms. It is possible to conclude, that the bimetallic trinuclear $Zr\{\mu\text{-}\eta^3\text{-}NH(C_2H_4O)_2\}_3[Ti(O^iPr)_3]_2$ and $Hf\{\mu\text{-}\eta^3\text{-}NH(C_2H_4O)_2\}_3[Ti(O^iPr)_3]_2$ with a nona-coordinated central zirconium or hafnium atom presented in this work are attractive potential precursors for mixed metal oxide materials due to their solution stability and the one type of reactive alkoxide group. In addition, the observed volatility of these compounds makes them attractive single source precursors for the preparation of thin films by MOCVD or ALD.

7.4 Conclusions

We have demonstrated the preparation and characterization of heterometallic alkoxide compounds formed upon modification with diethanolamine (H_2dea). The structures of $Zr\{\mu\text{-}\eta^3\text{-}NH(C_2H_4O)_2\}_3[Ti(O^iPr)_3]_2$ (**1**) and $Hf\{\mu\text{-}\eta^3\text{-}NH(C_2H_4O)_2\}_3[Ti(O^iPr)_3]_2$ (**2**) were determined by single crystal X-ray diffraction. These trinuclear complexes have a unique nona-coordinated central zirconium or hafnium atom and a hexa-coordinated titanium atom. These compounds are some of the first thermodynamically stable zirconium-titanium and hafnium-titanium precursors. The mass spectrometry characterizations of these compounds demonstrate that these compounds are volatile, and that the stability of the compounds makes them attractive single source precursors for MOCVD and ALD applications. The precursors are also interesting candidates for application in

sol-gel. The preparation of **1** from zirconium *n*-propoxide did not yield single crystals of the anticipated compound and it involved the formation of a *n*-propoxide analogue of **1**. It has been demonstrated that **1** can be prepared from $[Zr(O^nPr)(O^iPr)_3(^iPrOH)]_2$, however, in a lower yield compared to when zirconium isopropoxide is used. We evaluated whether or not zirconium-titanium heterometallic compounds can be obtained using triethanolamine as a modifier. Single crystals obtained showed the composition $Ti_2(O^iPr)_2(\{\mu\text{-}\eta^4\text{-}NH(C_2H_4O)_2\}_3)_2$. Thus, it seems that in this system the formation of a homometallic compound is more favored than a heterometallic one. Quantum chemical calculations indicate that the anticipated compound will have tremendously long metal-nitrogen bond lengths. This is an explanation as to why the formation of **4** is thermodynamically favored.

7.5 References

1 V.I. Parvulescu, H. Bonnemann, V. Parvulescu, U. Endruschat, A. Rufinska, Ch.W. Lehmann, B. Tesche and G. Poncelet, *Appl. Catal. A*, **214**, 273 (2001).

2 H.C. Zeng, J. Lin, W.K. Teo, F.C. Loh and J.L. Tan, *J. Non-Cryst. Solids*, **181**, 49 (1995).

3 G. De, A. Chatterjee, D. Ganguli, *J. Mater. Sci. Lett*., **9**, 845 (1990).

4 G. Emig, E. Fitzer and R. Zimmermann-Chopin, *Mat. Sci. Eng. A*, **189**, 311 (1994).

5 A. Lecomte, F. Blanchard, A. Dauger, M.C. Silva and R. Guinebretiere, *J. Non-Cryst. Solids*, **225**, 120 (1998).

6 P. Lobmann, U. Lange, W. Glaubitt, F. Hutter and D. Sporn, *High Preformance Ceramics 2001, Proceedings Key Engineering Materials*, **224**, 613 (2002).

7 J. Livage, F. Babonneau, M. Chatry and L. Coury, *Ceram. Int.*, **23**, 13 (1997).

8 M. Chatry, M. Henry, C. Sanchez and J. Livage, *J. Sol-gel Sci Technol.,* **1**, 233 (1994).

9 R.J. Vacassy, C. Guizard, J. Palmeri and L. Cot, *Nanostruct. Mater*., **10**, 77 (1998).

10 C.R. Xia, H.Q. Cao, H. Wang, P.H. Yang, G.Y. Meng and D.K. Peng, *J. Membr. Sci*., **162**, 181 (1999).

11 S. Benfer, U. Popp, H. Richter, C. Siewert and G. Tomandl, *Separ. Purif. Technol*., **22-23**, 231 (2001).

12 I. Arcon, B. Malic, M. Kosec and A. Kodre, *Mater. Res. Bull*., **38**, 1901 (2003).

13 J. Livage, M. Henry and C. Sanchez, *Prog. Solid St. Chem*., **18**, 259 (1988).

14 J. Livage and C. Sanchez, *J. Non-Cryst. Solids,* **145**, 11 (1992).

15 U. Schubert, *J. Sol-Gel Sci. Techol*., **26**, 47 (2003).

16 G.I. Spijksma, H.J.M. Bouwmeester, D.H.A. Blank and V.G. Kessler, *Chem. Commun.*, 1874 (2004).

17 Chapter 3 of this thesis.

18 G.J. Gainsford, N. Al-Salima and T. Kemmitt, *Acta Crystallogr., Sect. E.: Struct. Rep. Online*, **58**, m619 (2002).

19 Chapter 6 of this thesis.

20 S.M. Harben, P.D. Smith, R.L. Beddoes, D. Collision and C.D. Garner, *Angew. Chem.Int. Ed*., **36**, 1897 (1997).

21 G.R. Willey, T.J. Woodman, W. Ficher and M.G.B. Drew, *Transition Met. Chem*., **23**, 467 (1998).

22 W. Ma, H. van Koningsveld, J.A Peters and T. Maschmeyer, *Chem. Eur. J*., **7**, 657 (2001).

23 V.G. Kessler, *Chem. Commun*., 1213 (2003).

24 G.A. Seisenbaeva, S. Gohil and V.G. Kessler, *J. Mater. Chem.*, **14**, 3177 (2004).

25 Chapter 2 of this thesis.

26 E.P. Turevskaya, N.I. Kozlova, N.Y. Turova, A.I. Belokon, D.V Berdyev, V.G. Kessler and Y.K. Grishin, *Russ Chem. Bull*., **44**, 734 (1995).

27 SHELXTL-NT program manual, Bruker AXS, (1998).

28 M.J. Frisch, G.W. Trucks, H.B. Schlegel, G.E. Scuseria, M.A. Robb, J.R. Cheeseman, J.A. Montgomery, Jr., T. Vreven, K.N. Kudin, J.C. Burant, J.M. Millam, S.S. Iyengar, J. Tomasi, V. Barone, B. Mennucci, M. Cossi, G. Scalmani, N. Rega, G.A. Petersson, H. Nakatsuji, M. Hada, M. Ehara, K. Toyota, R. Fukuda, J. Hasegawa, M. Ishida, T. Nakajima, Y. Honda, O. Kitao, H. Nakai, M. Klene, X. Li, J.E. Knox, H.P. Hratchian, J.B. Cross, C. Adamo, J. Jaramillo, R. Gomperts, R.E. Stratman, O. Yazyev, A.J. Austin, R. Cammi, C. Pomelli, J.W. Ochterski, P.Y. Ayala, K. Morokuma, G.A. Voth, P. Salvador, J.J. Dannenberg, V.G. Zakrzewski, S. Dapprich, A.D. Daniels, M.C. Strain, O. Farkas, D.K. Malick, A.D. Rabuck, K. Raghavachari, J.B. Foresman, J.V. Ortiz, Q. Cui, A.G. Baboul, S. Clifford, J. Cioslowski, B.B. Stefanov, G. Liu, A. Liashenko, P. Piskorz, I. Komaromi, R.L. Martin, D.J. Fox, T. Keith, M.A. Al-Laham, C.Y. Peng, A. Nanayakkara, M. Challacombe, P.M.W. Gill, B. Johnson, W. Chen, M.W. Wong, C. Gonzalez, J. A. Pople, *Gaussian 03, Revision C.02 Gaussian*, Inc., Wallingford CT, (2004).

29 D. Andrae, U. Häussermann, M. Dolg, H. Stoll and H. Preuss, *Theor. Chim. Acta*, **77**, 123 (1990).

30 R.J. Errington, J. Ridland, W. Clegg, R.A. Coxall and J.M. Sherwood, *Polyhedron*, **17**, 659 (1998).

31 V.G. Kessler, S. Gohil and S. Pavola, *Dalton Trans*., 544 (2003).

32 Chapter 10 of this thesis.

33 V.G. Kessler, L.G. Hubert-Pfalzgraf, S. Halut and J.-C. Daran, *J. Chem. Soc., Chem. Commun*., 705 (1994).

34 R.L. Harlow, Acta Crystallogr. Sect. C., Cryst. Struct. Commun., **39**, 1344 (1983).

35 J. Sekulic, A. Magraso, J. E. ten Elshof and D. H. A. Blank, *Micropor. Mesopor. Mater.,* **72**, 49 (2004).

36 D.-S. Bae, K.-S. Han, S.-H. Choi and E.J.A. Pope, "*Synthesis and characterization of TiO_2–ZrO_2 composite membranes*." In: Sol–Gel Processing of Advanced Materials, Ceramic Transactions vol. 81, American Ceramic Society, USA, p. 349 (1998).

37 G.J. Gainsford, N. Al-Salim and T. Kemmitt, *Acta Crystallogr., Sect. E.: Struct. Rep. Online*, **58**, m636 (2002).

38 G.J. Gainsford, N. Al-Salim and T. Kemmitt, *Acta Crystallogr., Sect. C: Cryst. Struct. Commun*., **28**, m509 (2002).

Chapter 8

The effect of modifying ligands on the sol-gel processing of metal alkoxide precursors*

Abstract

The influence of modifying ligands on the sol-gel chemistry of metal alkoxides and the effect of these ligands on the morphology of the derived materials is considered in this paper. A comparison of the bond lengths and of the effective charges of metal atoms in modified and unmodified compounds combined with data from simple calorimetric experiments indicate that the reactivity of modified metal alkoxides increases rather than decreases upon modification. A new concept is presented concerning the reaction mechanism involved in the sol-gel processing of metal-alkoxides. These compounds are generally known as strong Lewis bases and rather weak Lewis acids in contrast to silicon esters, derivatives of a non-metal, which have extremely low both acidity and basicity by Lewis. Ligand exchange and hydrolysis proceeds then for metal alkoxides through a proton-assisted S_N1 mechanism analogous to that for acid-catalyzed hydrolysis of silicon alkoxides, and not an S_N2 mechanism, which is operative for the base-catalyzed hydrolysis of alkoxysilanes. The exchange of ligands, hydrolysis and also the condensation reaction proceed for metal alkoxides almost instantaneously. The products of the fast hydrolysis and condensation sequence consist of micelles templated by self-assembly of ligands (mainly oxo-spiecies). Another striking difference compared with traditional silica sol-gel is the mobility of the modifying ligands. The concept

---

* Part of this chapter has been submitted to: *J. Sol-Gel Sci. Technol.*:
"The effect of modifying ligands on the sol-gel processing of metal-alkoxides", Gerald I. Spijksma, Gulaim A. Seisenbaeva, Henny J.M. Bouwmeester, Dave H.A. Blank, Vadim G. Kessler.

presented here provides explanations for commonly observed material properties and allows for the development of new strategies for the preparation of materials.

The formation of dense nanoparticles from acetylacetone modified or acid 'catalyzed' system and the formation of dense films from acetylacetone modified precursors are discussed in this work. The sol particles for these systems are direct micelles containing oxo-species and a surface covered with acetylacetone or positively charged centers as a result of the acid addition. The formation of inverted micelles, which can be obtained by the appropriate choice of solvents, allows for the formation of hollow spheres. The modifying acetylacetone ligands act as the surfactant and form the interface between the hollow sphere and the solvent. Another example, formed from a direct micellar system, is the formation of zirconia nano-rods from a highly anisotropic diethanolamine (H_2dea) modified precursor. The alkoxide ligands of the precursor in bridging positions play a decisive role in the formation of the nano-rods. In the absence of these growth-directing ligands a micro porous material can be obtained for H_2dea modified precursors. The results obtained in this work have been exploited by groups at SLU to develop a method for gel encapsulation in aqueous media. The proper choice of a modified titanium alkoxide allows for the preparation of a sol *via* direct micelles in alcohol, whereas subsequent transfer of the sol to aqueous conditions leads to the possibility of encapsulation in biocompatible conditions.

8.1 Introduction

Sol-gel is a very common method used to prepare metal-oxide materials applied in a wide variety of fields including structural ceramics [1,2], sensors [3-5], catalysts [6,7], optics [8,9] and electronics [10,11]. Despite being widely applied, the chemistry of the sol-gel synthesis utilizing metal alkoxide precursors is poorly understood. The generally assumed concepts for the sol-gel chemistry of transition metals are derived from abundant studies on silica. It is known from the work on silica that the formation of a sol particle is initiated upon the addition or release of water. The water initiates the hydrolysis and subsequent condensation reactions [*e.g.*, 12,13]. Common silicon alkoxides, the alkoxysilanes, are, however, essentially stable to hydrolysis by water in the absence of catalysts. Catalysts applied in hydrolysis of alkoxysilanes are protolytes, acids or bases.

The hydrolysis of a silicon alkoxide leads to the formation of a reactive Si-OH group. The following three-step S_N2 mechanism is generally proposed for the base-catalyzed reaction: The first step is the nucleophilic addition of a water molecule (hydroxide anion) to the positively charged Si atom. This leads to a transition state, where the coordination number of Si has been increased by one. The second step involves a proton transfer within the intermediate state leading to the next transition state. A proton from the entering water molecule is transferred to the negatively charged oxygen of an adjacent OR group. The third step is the departure of the better leaving group, which should be the most positively charged species within the second transition state. This S_N2 mechanism is summarized in Scheme 8.1.

Scheme 8.1

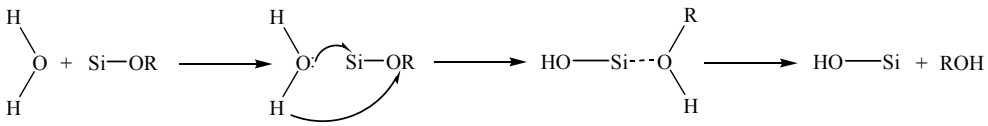

After the initial hydrolysis, the product can react further either *via* another hydrolysis reaction or a condensation reaction. In order to get non-branched or limitedly branched oligomers, the hydrolysis should be followed by a condensation

reaction. Condensation is a complex process and, depending on the experimental conditions, three competitive mechanisms have to be considered: alcoxolation, oxolation and olation [*e.g.*, 12,13].

Alcoxolation is a reaction by which a bridging oxo-group is formed through elimination of an alcohol molecule. The mechanism is basically the same as for hydrolysis with Si replacing H in the entering group. Oxolation follows the same mechanism as alcoxolation, but a proton is the leaving group. Olation can occur when full coordination of Si is not achieved. In this case, bridging hydroxo groups can be formed through elimination of a solvent molecule. The latter can be either H_2O or ROH depending on the water concentration in the medium. All these reactions are catalyzed by protons (acidic medium).

The kinetics of nucleophilic substitution is governed by the charge distribution. The reaction is strongly favored when the nucleophilic character of the entering group and the electrophilic strength of the central atom are high. The basic catalysis for silicon alkoxides, following this mechanism, is a relatively slow reaction. For the derivatives of silicon, the speed of hydrolysis is strongly increased by the introduction of chelating ligands such as diol residues [14], probably due to enhanced charge distribution through chelation.

Up to now, the principal difference between silica and transition metals has not been underlined in sol-gel literature. However, it is well known that TEOS, a typical precursor for the preparation of silica sols, and "$Zr(O^nPr)_4$", a commonly used precursor for zirconia sols, show remarkably different reactivity. "$Zr(O^nPr)_4$" hydrolyzes several orders of magnitude faster than TEOS. This difference in reactivity is commonly explained only by the difference in charge density on the metal atoms (δ(M) in $M(OET)_4$ 0.32 and 0.65 for Si and Zr, respectively) [12,15,16] and the access to higher coordination numbers for the transition metal.

The difference between complexes of silicon and those of the majority of metals has been well documented in coordination chemistry and reactivity studies. It has long been known that the ligand exchange in metal alkoxides is essentially an immediate reaction [17], the major part of the alkoxide ligands being removed upon hydrolysis of titanium and zirconium derivatives in the course of **milliseconds** [18]. Metal alkoxides (in contrast to silicon, which is a ***non-metal***)

are known to be rather strong Lewis bases, and are as such broadly used in organic catalysis. The substitution reaction mechanism for metal alkoxides was shown to be the proton-assisted S_N1-transformation (see Scheme 8.2).

Scheme 8.2:

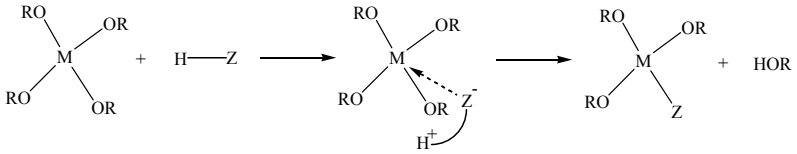

This reaction starts with protonation of the most negatively charged oxygen atom in the coordination sphere of the metal atom with subsequent simultaneous entrance of the nucleophile Z and release of an alcohol molecule [19]. The major factor influencing the speed of this reaction is the acidity of HZ, while the nucleophilic properties of the entering ligand Z play only a marginal role [20]. In contrast to the derivatives of silicon, the ratio in reaction rates of hydrolysis and polycondensation is essentially a constant value in organic solvents, not influenced essentially in the chemically unmodified alkoxides by the pH of the water solution used for hydrolysis [18]. According to ^{17}O NMR studies, the ratio between different types of bridging and terminal oxygen atoms turned out to be essentially constant for the same type of alkoxide ligand and solvent [21]. It has been proposed that for non-modified metal alkoxides the morphology of the particles results not from the kinetics of hydrolysis-polycondensation [22], but from surface phenomena [18] and does not provide dendritic (fractal) polymer structures as for silicon [12, 23], but rather dense particles. The core of these particles, if obtained at room temperature, is rather rarely a perfectly crystalline oxide probably because of the highly negative reaction entropy for the dehydration reaction. It has been well documented that the non-hydrolytic room temperature sol-gel synthesis of oxides and sulfides results always in highly crystalline nanoparticles [24,25].

The hydrolysis of metal alkoxides occurs much faster than that of silicon and was therefore considered to be more difficult to control. Stable colloid solutions, useful for further applications, can only be obtained using modification by chelating ligands [26,27], *e.g.*, β-diketonates [28-31], alkanolamines [32-33], or using acid as a "catalyst" [34-36]. They are supposed to slow down the rate of hydrolysis and

inhibit polycondensation [21] *via* shielding of the metal atom by the attached chelating ligand [37].

The effect of the modifiers on structure, stability and reactivity of a precursor has rarely been considered, despite its great impact on sols for the preparation of thin films, membranes and nanoparticles. How does the incorporation of modifiers influence the structure of the formed sol particles? Can the sol-gel chemistry of modified metal alkoxides be kinetically controlled in analogy to that of silica, as is generally assumed? Do the formed dendrites still have the non-hydrolysable ligand attached to the same modified metal atom? In the present chapter, it is attempted to provide answers to these questions.

8.2 Evidence for the role of modifying ligands

8.2.1 Bond lengths

The first indication that the role of the modifying ligands is different from what is generally assumed can be seen when the structure of the modified precursor is compared with that of the corresponding unmodified ones. One would expect that if the modifier would shorten the metal-oxygen bond length of an alkoxide ligand, it would reduce the reactivity of the alkoxide ligands towards hydrolysis.

From data in literature, presented in Table 8.1, it is apparent that introduction of 1 mol equivalent of acetylacetone (Hacac) to zirconium isopropoxide leads to a pronounced elongation of all zirconium-oxygen bonds [38-40] in the modified complexes. This effect is, as expected, less evident when the modification is performed with an analogous ratio of more bulky 2,2,6,6,-tetramethyl-3,5-heptanedione (Hthd) [41,42]. The modification with 1 mol equivalent of the asymmetric *t*-butylacetoacetate results in a complex that has a strong deviation in bond lengths [43], with some of them being elongated compared to the bond lengths in the unmodified precursor. The terminal alkoxide ligands in $Zr\{\mu\text{-}\eta^3\text{-}NH(C_2H_4O)_2\}_3[Zr(O^iPr)_3]_2(^iPrOH)_2$, obtained upon the modification of zirconium isopropoxide with 1 mol equivalent of H_2dea [44], seem to form an exception; the bond lengths are slightly shortened.

Table 8.1: Metal-oxide bond lengths of zirconium isopropoxide and Hacac, H_2dea, Hthd and tbaoac modified zirconium isopropoxide.

Position alkoxide	$[Zr(O^iPr)_4(HO^iPr)]_2$ [38]	$[Zr(O^iPr)_3(acac)]_2$ [38-40]	$Zr(O^iPr)(acac)_3$ [39,40]	$[Zr(O^iPr)_3(thd)]_2$ [41]
Bridging	2.171	2.258		2.219
Bridging	2.156	2.134		2.119
Terminal	1.936	1.955	1.922	1.944
Terminal	1.935	1.947		1.931
Terminal	2.079			

Position alkoxide	$Zr(O^iPr)(thd)_3$ [40]	$Zr(dea)_3(Zr(O^iPr)_3)_2$ (^{i}PrOH)$_2$ [44]	$[Zr(O^iPr)_3(tbaoac)]_2$ [43]	$Zr(O^iPr)_2(tbaoac)_2$ [43]
Bridging			2.098	
Bridging			2.231	
Terminal	1.847	1.988	1.942	1.908
Terminal		1.927	1.922	1.908
Terminal		1.901		

For titanium precursors, a comparison of bond lengths in modified and unmodified compounds is shown in Table 8.2. The only structure of an unmodified precursor, $Ti(O^iPr)_4$, has recently been reported by Schubert [45] and it was obtained as a fragment in the modification of titanium isopropoxide with dimethyl-ethanolamine [46]. It should be noted that the unmodified precursor is penta-coordinated while the Hthd, Hacac [47] and tbaoac [48,49] modified structures are hexa-coordinated. The metal-oxygen bond lengths of the alkoxide ligands in these modifications are (slightly) elongated compared to those in the unmodified precursor. The increase in bond length is most dominant for the modification of titanium with Hthd, which is a stronger chelating ligand compared to Hacac.

Table 8.2: Metal-oxide bond lengths of titanium isopropoxide and Hacac, Hthd and tbaoac modified titanium isopropoxide.

Position alkoxide	$Ti(O^iPr)_4$ [46]	$[Ti(O^iPr)_3(acac)]_2$ [47]	$[Ti(O^iPr)_3(thd)]_2$ [47]	$Ti(O^iPr)_2(tbaoac)_2$ [48,49]
Terminal	1.766(11)	1.784	1.8017	1.784
Terminal	1.799(7)	1.782	1.8160	1.784
Terminal	1.804(14)			
Bridging	1.893(12)	1.969	1.9677	
Bridging	2.066(9)	2.101	2.0941	

The elongated bond lengths, which are observed for modified titanium and zirconium compounds, indicate an increase in effective charges on the metal atoms and a decreased shielding of the metal atoms compared to the alkoxide solvates

otherwise present in solution [38-40]. This higher effective charge will definitely not moderate the reactivity and probably even promotes hydrolysis.

8.2.2 Charge distribution model

The charge distribution model provides a simple approximation of the partial charge on metal atoms and ligands [12,15,16]. Accordingly, calculations show an increase in charge and, hence, in reactivity, on going from silicon, titanium and zirconium precursors: δ(M) in $M(OET)_4$ is 0.32, 0.93and 0.65 for Si, Ti and Zr, respectively [15,16]. The trend observed when changing the size of the alkoxide ligands is in good agreement with experimental observations: δ(M) in $Ti(OR)_4$ is 0.66, 0.63, 0.61, 0.60 for R = CH_3, C_2H_5, *n*-C_4H_9, *n*-C_6H_{13}, respectively [15]. If the reactivity would be moderated upon introduction of modifying ligands one would expect a decrease in the partial charge on the metal atom. The charge distribution model, which has been applied on modified and unmodified zirconium and titanium precursors (Table 8.3), shows in each case an increase in partial charge on the metal atom (represented by δ). Again, the introduction of modifying ligands seems to increase the reactivity of the modified precursors rather than moderating it as is generally assumed in literature.

Table 8.3: Partial charge on zirconium and titanium atoms. Calculated for unmodified and for Hacac, Hthd, H_2dea and tbaoac modified compounds. The molecular structures are taken from the references, the structure of $Ti(O^iPr)_2(thd)_2$ is assumed to be monomeric based on observation in [47], however no structure has been determined up to date.

Compound	δ Zr
$Zr_4(O^nPr)_{16}$ [50]	0.639
$[Zr(O^iPr)_4(HO^iPr)]_2$ [38]	0.641
$[Zr(O^iPr)_3(acac)]_2$ [38-40]	0.658
$Zr(O^iPr)(acac)_3$ [39,40]	0.691
$[Zr(O^iPr)_3(thd)]_2$ [41]	0.644
$Zr(O^iPr)(thd)_3$ [42]	0.648
$[Zr_2(O^nPr)_6(OC_2H_4)_2NH]_2$ [44]	0.658
$Zr(dea)_3(Zr(O^iPr)_3)_2(^iPrOH)_2$ [44]	0.657
$[Zr(O^iPr)_3(tbaoac)]_2$ [43]	0.661
$Zr(O^iPr)_2(tbaoac)_2$ [43]	0.675

Compound	δ Ti
$Ti(O_iPr)_4$ [46]	0.614
$[Ti(O^iPr)_3(acac)]_2$ [47]	0.632
$Ti(O^iPr)_2(acac)_2$ [51]	0.638
$[Ti(O^iPr)_3(thd)]_2$ [47]	0.618
$Ti(O^iPr)_2(thd)_2$ [47]	0.620
$Ti(O^iPr)_2(tbaoac)_2$ [48,49]	0.621

8.2.3 Calorimetric experiments†

Simple calorimetric measurements were performed to evaluate the temperature effect of the introduction of the modifying ligands and water addition to modified and unmodified precursor solutions. Zirconium *n*-propoxide was modified with 1 mol equivalent of Hacac, diethanolamine, triethanolamine or acetic acid. Immediately after addition of the stabilizer an apparent increase in temperature is recorded. This change in temperature can be attributed to the heat evolved from exothermic ligand exchange [29], mixing and other chemical reactions. The latter effects were studied by conducting experiments using solutions without the precursor. The temperature change for mixing the modifier with *n*-propanol was found to be endothermic for acetylacetone ($\Delta T \approx -5$ ºC) and for acetic acid, diethanolamine and triethanolamine the effect was within the error of the measurement. In all cases where the modifier is added to a precursor solution, an exothermic effect is observed (see Figure 8.1). After the initial increase, an exponential decrease in temperature is observed due to equilibration with the surroundings. This suggests that ligand exchange is completed within the period in which the initial temperature increase is observed (*i.e.*, modification is thus instantaneous upon addition of the modifier).

After the addition of the modifier, the precursor solutions were cooled to room temperature. Subsequently, 2 mol equivalents of water were added and the observed heat effects are depicted in Figure 8.2. A precipitate immediately formed upon addition of the water/propanol mixture to the unmodified and acetic acid modified precursors. A clear yellowish sol formed from the solution containing the Hacac modified precursor; however, a small amount of crystals were formed about one hour after the addition of the water. These crystals are most likely $Zr(acac)_4$,

† The precursor, Zirconium *n*-propoxide (70% (wt) in *n*-propanol, Aldrich) was mixed with *n*-propanol (99.7% anhydrous, Aldrich) in a 1/10 molar ratio. Stabilizers acetylacetone (pro analyze, Merck), diethanolamine (Aldrich), triethanolamine (pro analyze, Merck), or glacial acetic acid (100%, Merck)) was added with a precursor/stabilizer molar ratio of 1:2 or 1:1. Finally, 2 equivalent mol of water was added to 30 grams of stabilized precursor using a syringe. During the addition of the stabilizers and water the temperature was monitored (using the temperature probe of a Brookfield DV-2 Digital Viscometer). All experiments were conducted in dry nitrogen atmosphere in a glove box, to avoid hydrolysis of the moisture sensitive precursor.

present in the solution before hydrolysis takes place [39,40]. For both the acetic acid modified and unmodified precursor an increase in temperature is observed upon the addition of water, followed by a modest heat release due to the hydrolysis and condensation sequence. The temperature remains unchanged after the initial increase and subsequent decrease at a rate which is lower than the expected exponential decrease in temperature due to equilibration with the surroundings. In contrast, the addition of water to precursors modified with Hacac, diethanolamine and triethanolamine (not shown in Figure 8.2) leads to an instant temperature increase. This temperature increase suggests that the reactivity of the precursor molecule has increased upon modification and that hydrolysis occurs almost instantaneously.

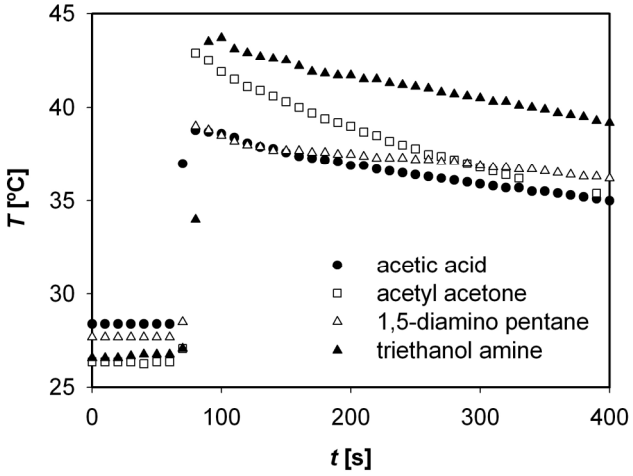

Figure 8.1: Temperature versus time when a stabilizer is added to the solution with precursor.

In an earlier calorimetric study on the hydrolysis and condensation reactions of transition metal alkoxides by Blanchard *et al.* [52], the exothermic behavior of the hydrolysis and condensation sequence was attributed to an increase in the coordination number. The authors noted that the hydrolysis, oxolation and alkoxolation are substitution reactions and do not involve coordination expansion. The increase of the coordination number was proposed to take place in the early stages of hydrolysis, *i.e.*, the authors assumed that the hydrolysis proceeds according to a nucleophilic addition reaction (S_N2 mechanism) as observed for

silicon alkoxides (in basic media). It is necessary to underline that the increase in a coordination number itself is in literature **not** associated with exothermal effects if not leading to increased charge distribution (facilitated reactivity) [53].

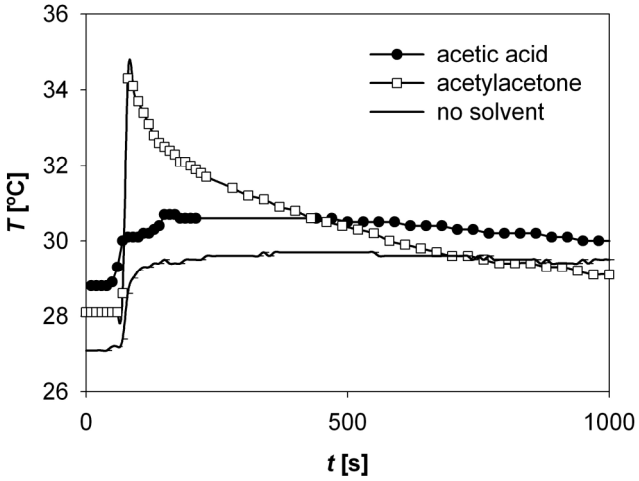

Figure 8.2: Temperature versus time when water is added to the (modified) zirconium n-propoxide precursor solutions.

Blanchard *et al.* [52] based their conclusions on observations made for the hydrolysis of titanium alkoxides. The authors observed a decrease of the enthalpy of hydrolysis and condensation upon increasing the amount of Hacac. The enthalpy of the unsubstituted precursor was about twice that of a monosubstituted, while almost no enthalpy effect was observed for the disubstituted precursor. This seems to be in contrast to our observations of the heat release for the Hacac modified zirconium precursors. The modification of titanium alkoxides with Hacac involves unsubstituted and mono- and disubstituted compounds [47]. The hydrolysis of the monosubstituted titanium species enhances their disproportionation into unsubstituted and disubstituted compounds [51]. Since the enthalpy effects of the hydrolysis of the disubstituted compounds are marginal, the enthalpy effect for the monosubstituted compound is expected to be about half of that observed for the unsubstituted precursor. The explanation for the enthalpy effect of the disubstituted titanium species can be found in its molecular structure. The partial charge of the titanium atom increases in correlation to the increasing the amount of modifying ligand, as can be seen from Table 8.3. The observed decrease in enthalpy for the

disubstituted compounds, while the partial charge on the metal atom increases is a clear indication that the hydrolysis reaction does not proceed via an S_N2 mechanism (as depicted in Scheme 8.1). The charge of the metal atom does not appear to be decisive for the observed enthalpy effect. In contrast, the negative charge on the oxygen atom of the alkoxide ligand provides an indication of a proton-assisted S_N1 mechanism as will be discussed in detail below. A difference in the total thermal effect for disubstituted precursor can also be caused by different nature of its hydrolysis product with those of the non-substituted titanium alkoxide.

8.3 Proposed mechanism for modified metal alkoxides

The observed metal-alkoxide bond lengths, the change in the partial charge on metal atoms upon modification and the heat developed upon addition of water all indicate that the introduction of modifying additives results in more reactive species. As a matter of fact, an analogous effect is observed when silicon alkoxides are modified with diols and polyols. The formed compounds are extremely moisture sensitive in utmost contrast with the unmodified precursors [14]. It is likely that the hydrolysis and ligand exchange processes in modified alkoxide precursors follow the same proton-assisted S_N1 mechanism as for non-modified metal alkoxides, which starts with protonation or the hydrogen bonding of the incoming ligand to the most negatively charged oxygen atom in the coordination sphere followed by the release of the protonated ligand and an almost simultaneous entrance of the next one. The activation energies for the ligand exchange processes are typically 30-40 kJ/mol, which are of the same order of magnitude as thermal motion of atoms in the molecule [19]. The impossibility of kinetic control and the S_N2 reaction mechanism for titanium alkoxides has recently been demonstrated on the basis of theoretical calculations by Henry *et al.* [54]. The results show that the S_N2 type transformation requires an activation energy of about 600 kJ/mol, which is 15-20 times higher than those observed experimentally.

The question remains: what role do the modifying ligands play in the hydrolysis and condensation sequence? Why are protons or chelating ligands required for the controlled preparation of sols with small particles? Moreover, the formation of a

precipitate is avoided in the presence of protons or chelating ligands, while it is formed instantly upon addition of water to metal alkoxides in the absence of protons or chelating ligands.

It does not seem realistic that the stability of resulting colloids is due to the moderating influence of either the protons or chelating ligands on the polycondensation process. The condensation reaction has largely the same speed and the same kind of dependence on the presence of protons except when concentrated acid solutions are used. Protons are well known to be catalysts in both hydrolysis and polycondensation at low acidity, while β-diketonate ligands are commonly appreciated as charge-stabilizing fragments, and are more likely to facilitate both reactions [53].

The role of modifying ligands is thus unlikely to be due to the homogeneous reactivity of metal alkoxides. Metal alkoxides, in contrast to silicon alkoxides, are characterized by the kinetically unhindered reactivity and thermodynamic control of their reactions in homogeneous solutions [22,56]. The role of heteroligands has to be sought in influencing the microheterogeneity arising through the hydrolysis and polycondensation sequence.

This led us to the conclusion that the hydrolysis of modified metal alkoxides leads not to polymeric sols but to colloidal solutions containing Micelles Templated by Self-Assembly of Ligands (MTSAL), *i.e.*, the ligands act as surfactants during their formation. The mechanism and the products of the hydrolysis and condensation sequence are completely different, *i.e.*, dense objects versus. fractals [12, 23] for metal alkoxides and silicon alkoxide, respectively. The reactivity of modified metal alkoxides follows the same pattern as for non-modified ones, the modifying ligands influencing the extent of surface interactions [18], which on their turn play a major role in determining the size, morphology and stability of the particles.

Hydrolysis of metal alkoxides leads to formation of dense metal oxide-hydroxide cores (normally not ideally ordered because of high reaction entropy involved by hydrogen bonding). Upon further growth the outer surface is covered with the modifying ligands, while the core looses partly the absorbed water becomes constituted mainly by metal-oxo bonds (as depicted in Figure 8.3). Sanchez *et al.* [21] have in fact observed the formation of MTSALs in their study of hydrolysis of

titanium alkoxides by ^{17}O NMR. However, these authors called them "polymeric building blocks" and did not recognize them as colloidal particles, *i.e.*, micelles. In publications by Bartlett *et al.* [57,58] such a mechanism has been proposed but not developed any further.

It is obvious that various parameters like the choice of precursor, modifier and solvent etc. have a great influence on the obtained materials, as discussed in more detail below. However, the by Ranjit and Klabunde [59] proposed direct relation between the choice of solvent, gelation time and the hydrolysis and condensation sequence does not exist. The gelation is not a cross-linking of inorganic polymers but a heterogeneous diffusion-controlled process and the growth of the oxide or oxide-hydroxide particles is simply facilitated by polar solvents and hindered by non-polar ones.

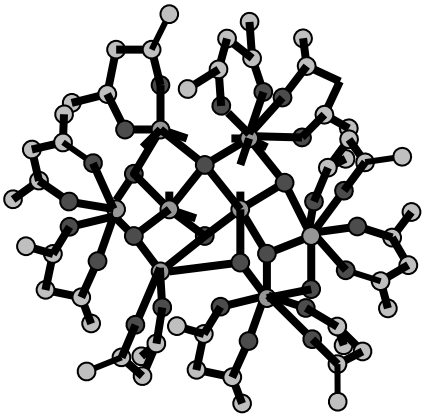

Figure 8.3: Schematic representation of oxo-species formed upon hydrolysis and condensation of modified alkoxide precursors.

8.4 Properties of sols and derived materials

The proposed mechanism of Micelles Templated by Self-Assembly of Ligands provides an opportunity to develop new strategies for materials preparation. It also provides insight into the formation mechanisms of materials. Various known and new concepts for the preparation of sol-gel derived materials will be discussed below.

8.4.1 Direct micelles applying chelating ligands

The solvent used for the preparation of sols is generally (the parent) alcohol and acetylacetone is a commonly used modifying ligand of precursors for sol-gel applications [24-31]. Sol-particles obtained from these systems are described above and depicted in Figure 8.3. An analogous concept is expected for the systems where an acid is used as an additive, for example, the sol preparation from titania precursors [60-62].

About a decade ago Sanchez *et al*. [30] reported that the size of sol particles, which we now believe are micelles formed upon the hydrolysis of Hacac modified zirconium *n*-propoxide, depends on the amount of water added and that of the modifier. This observation is not surprising since these two quantities determine the available species for the core and the shell, respectively. Nowadays the preparation of nanoparticles from these types of systems is a well established technology, but the film formation from these systems is not understood. Both products from direct micelles will be discussed below.

Nanoparticles

As mentioned above, there is abundant literature on the formation of nanoparticles from metal alkoxide precursors and the interested reader is referred to a recent review on liquid phase synthesis by Cushing *et al*. [60]. The general method for the preparation of titania nanoparticles proceeds through the hydrolysis and condensation of the precursor in the presence of an acid. Hsu *et al*. [63] performed a study on the effect of various parameters on the size and morphology of the particles. They concluded that the ratio of alkoxide/water and the amount of acid are the most influential. The formation of zirconia nanoparticles using acetylacetone as the modifying ligand is described in, for instance, ref. [31].

It is interesting to mention the preparation of TiO_2, V_2O_3, Nb_2O_5, Ta_2O_5, In_2O_3 and $BaTiO_3$ nanoparticles by a non-hydrolytic sol-gel approach [64-66]. In this method, the transformation into oxide materials occurs through an ether elimination or alkyl halide elimination involving alcohols, for example, *t*-butanol and $C_6H_5CH_2OH$, that are able to provide relatively stable alkyl cations. The formation of oxides from such reactions was first observed in 1840's [67]. The mechanism of this reaction

was established in 1950-es by Bradley *et al.* [68]. Its first application as a tool for preparation of ultra fine powders of oxide (molybdate) materials was reported by Kessler *et al.* [25]. Vioux *et al*. [69] reported then the synthesis of Al_2O_3, TiO_2 and ZrO_2 and related mixed oxides with silica by co-condensation between chlorides and alkoxides. TiO_2, V_2O_3, Nb_2O_5, Ta_2O_5, In_2O_3 and $BaTiO_3$ were recently synthesized by solution thermolysis of alkoxides by Niederberger *et al.* [64-66]. The ether elimination reaction is exploiting the property of alkoxide ligand as a Lewis base and leads to the formation of oxo-species [70] showing thus, great analogy with the mechanism proposed here. Oxo-species have also been observed for a great number of other metal alkoxide systems, including molybdenum [25], zirconium [71-73], hafnium [74], aluminum [75] and tantalum [76].

Dense films

The formation of dense films from sols obtained *via* direct micelles from Hacac modified zirconium *n*-propoxide was reported by Chatry *et al.* [30]. The non-porous character was assigned to the very dense packing of the Hacac containing oligomers. It is not very realistic that the mobile modifying ligands are incorporated into the material. During drying, the hydrophilic cores of the micelles will start to interconnect, forcing the hydrophobic ligands to concentrate on the outer surface of the formed layer (as depicted in Figure 8.4). The growth of the layer is terminated as soon as the outer surface is saturated with ligands. During heat treatment the organics on the surface are removed and densification of the thin metal oxide network occurs, yielding a thin, dense film. The surface of these films is very smooth, as is shown in, for instance, ref [76,77]. Repetitive deposition and heat treatment leads to a linear increase in thickness of the film [78,79], where a slight deviation may be found in the thickness of the first layer. It should be noted that in the study on hafnia films [79] the precursor solution, containing Hacac modified hafnium ethoxide precursors, was refluxed prior to deposition. The refluxing will undoubtedly lead to the formation of $Hf(acac)_4$. This will presumably lead to the incorporation of modifying ligands into the formed film, *i.e.*, the mobility of the ligands in $Hf(acac)_4$ can be too low to allow a high concentration on the surface, which may cause some deviation in layer thickness and porosity of the calcined films. Both sides of the interface of subsequential layers consist solely of

the metal oxide material and therefore they are not seen in SEM images of a cross-section of the film (as reported by ref. [76,77]).

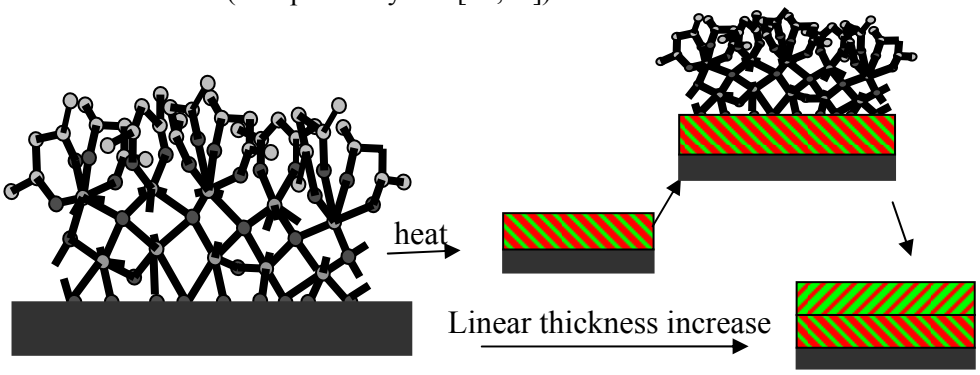

Figure 8.4: Schematic representation of film formation from Hacac modified precursors.

It should be noted that sols from direct micelles are commonly used for the preparation of micro-porous membranes [1,2,80-84]. For the preparation of titania membranes an acid is added as the modifier, while acetylacetone is often added for zirconia ones. The observed porosity in these systems is probably due to the porosity of the support and the required controlled drying of the film.

8.4.2 Inverted micelles with chelating ligands

Materials with interesting morphology can be obtained by using a precursor modified with (hydrophobic) chelating ligands, but now generating inverted micelles instead of direct micelles. Inverted micelles are typically obtained when a small amount of polar solvent is introduced into a non-polar one and the droplets of the former are stabilized by a surfactant (Figure 8.5a). When, subsequently, the water and propanol solution is quickly added by a syringe to a 0.3-1.0 molar hexane solution of zirconium isopropoxide modified with 1 mol equivalent of acetylacetone, a clear sol is obtained. This procedure is regardless of the employed metal alkoxide precursor, *i.e.*, similar results are obtained using titanium and zirconium *n*-propoxide precursors. Transmission electron microscopy (TEM) of the powder formed after evaporation of the solvents shows the occurrence of hollow nanospheres with 200-250 nm in diameter [85]. Drying by evaporation of the solvent results in the cracking and opening of (a considerable part of) these spheres (depicted schematically in Figure 8.5c). The most exciting feature is that their walls

are extremely thin, typically about 5 nm [85]. The wall thickness of the spheres can be determined from the TEM image of a crack in the sphere as indicated in Figure 8.5d. These extremely thin walls are in contrast to those reported earlier for silica spheres prepared by colloid templation, where wall thicknesses of 50-200 nm were observed for spheres having a total diameter of about 500 nm [86].

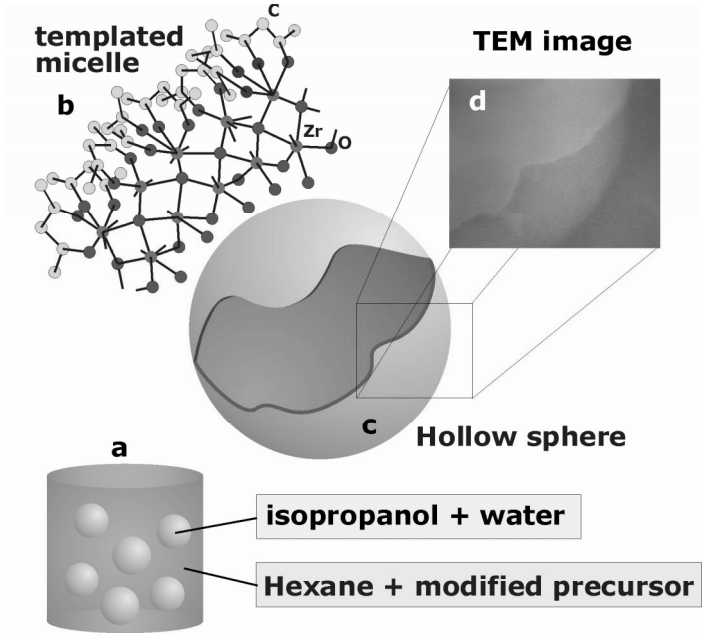

*Figure 8.5: Schematic representation of micelles formed in a hexane and isopropanol/water solution. Formation of the micelles (**a**), cross section of hollow spheres obtained from the templated micelle (**b**), the cracks formed upon drying of the hollow spheres (**c**), and TEM image of an enlargement of a crack.*

The unusual morphology obtained supports the idea that the spheres consist of shells that originate from the templated micelles by self-assembly of ligands. They are made amphiphilic by concentration of the hydrophobic acac-ligands on the outer surface and hydrophilic OH-ligands on the inner surface (Figure 8.5b). Hydrophilic compounds, such as the dyes Eriochrome Black T or Methylene Blue, are selectively encapsulated within these spheres, when they are soluted in a water/propanol medium, used for the hydrolysis of modified zirconium alkoxide in hexane. The encapsulation could easily be followed by visual observations as the color of the dye disappears when it is encapsulated, as it remains practically unchanged if the solution of the modified alkoxide in the parent alcohol is

hydrolyzed, *i.e.*, no inverted micelles can be formed in this system. An analogous effect is observed for solutions of titanium *n*-propoxide modified with 1 mol equivalent of Hacac. These systems open the way for encapsulation of extremely strong biomedical agents, for example, protein-based ones, even as single molecules in the thin-walled shells. In Chapter 9, the preparation and encapsulation will be discussed in detail.

It has also been shown that during the formation of films from sols, derived from inverted micelles, part of the spherical morphology is conserved. The present results provide clear evidence for the existence of these films. During the process of deposition and drying the morphology (partly) changes due to the redistribution of ligands and it is expected that with optimization of the deposition and drying conditions better and more reproducible results can be obtained.

8.4.3 Direct micelles with chelating and bridging ligands

One of the major differences between β-diketones and alkanolamines is the ability of the latter to act as both chelating and bridging ligand. The mobility of alkanolamine ligands is thus strongly reduced. The morphology of the formed direct micelles was evaluated by using a highly anisotropic precursor. We reported elsewhere [44] that the commercially available zirconium *n*-propoxide with 0.5 mol equivalent of diethanolamine (H_2dea) leads to formation of a tetranuclear precursor complex with the formula $[Zr_2(O^nPr)_6(OC_2H_4)_2NH]_2$. Transmission electron microscope (TEM) observations show that the zirconia sol prepared[‡] from this precursor contains both amorphous and structured material (Figure 8.6). Light

[‡] A sol was prepared from the modified precursor, $[Zr_2(O^nPr)_6(OC_2H_4)_2NH]_2$, in *n*-propanol (final solvent to precursor ratio 50:1), followed by rapid addition of 2 mol equivalent of water in a 20 times larger volume of *n*-propanol. The gelation occurred shortly after addition of the water. The initial chemical modification and preparation of sols was carried out in dry nitrogen atmosphere using a Schlenk line or a glove box. The solvents were purified according to conventional techniques (see *e.g.*, ref. 39 for details). Approximately 0.05 g of the gelled sols was transferred in 20 ml n-propanol and subsequently peptized with 0.3 ml 0.05 M nitric acid. For TEM analysis, a drop of this solution was deposited on a copper grid supported by an amorphous carbon film. Particle size in the obtained sols was determined using light scattering technique with a Zetasizer 3000HS instrument. Transmission Electron Microscopy (TEM) images were obtained with PHILIPS CM30 Twin/STEM instrument. High resolution electron microscopy experiments were performed on a JEOL JEM-3010 microscope.

scattering experiments confirm an average particle size for the sol of ~300 nm. High-resolution transmission electron microscopy (HRTEM) shows that the formed nanorods have a length of up to 400 nm with an apparent diameter of 6-8 nm. We believe that the nanorods could be longer if the growth time were increased. Energy dispersive X-Ray spectroscopy (EDX) on a group of nanorods indicates that these are solely made up of zirconium and oxygen.

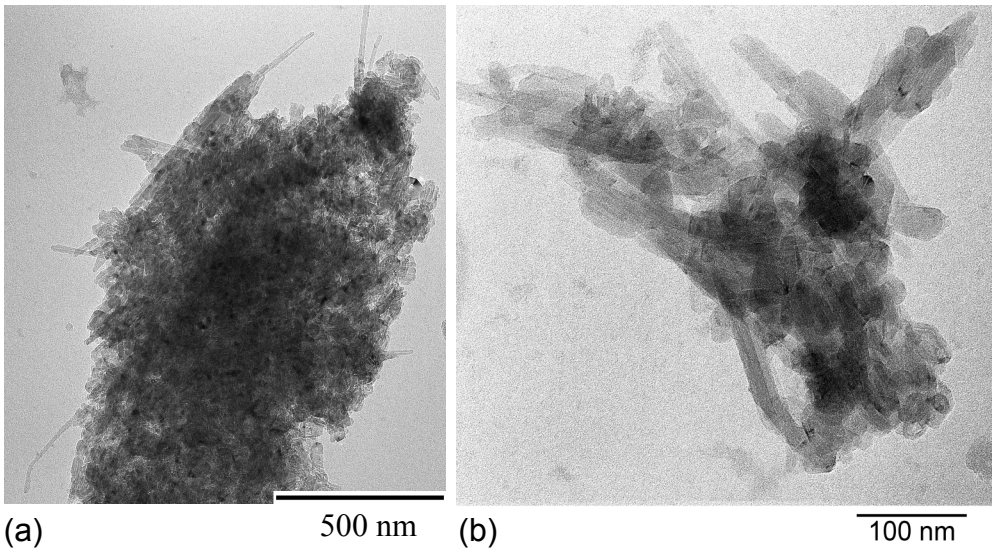

*Figure 8.6: Transmission electron micrographs (TEM) of zirconia sol samples with **a**. Sample containing both amorphous and structured material, showing zirconia nanorods up to a length of 400 nm. **b**. Sample containing mainly structured material.*

The structure of the tetranuclear zirconia precursor complex is analogous to that of $[Zr_2(O^nPr)_6(OC_2H_4)_2NCH_3]_2$ as reported by Gainsford *et al*. [87]. Four alkoxide groups are in terminal positions and two are in bridging positions as shown in Figure 8.7a. The reactivity of the bridging alkoxide groups is considered to be higher than that of the terminal ones. Therefore the bridging alkoxide groups will hydrolyze first upon the addition of water, initiating growth by condensation of the linear precursor molecules in a side-to-side manner (Figure 8.7b). The chelating and bridging dea ligands are forced outwards. The saturation of the outer surface of the coupled molecules with these ligands will prevent further growth. It is here that the acidity of the solution plays an important role. Protonation of the nitrogen atoms in the precursor complex avoids precipitation of material, but also facilitates the release of modifier ligands during the process of polycondensation and

subsequent densification. The modifier molecule is thus self-sacrificing in the process of ordering. As polymerization and gelation proceeds, the pH increases. At a high pH the tendency to release the modifier ligands has diminished, preventing further growth of the precursor molecules in a side-to-side manner. The sole possibility for growth at this point would then be the oriented attachment of the nanorod fragments into nanorods, *i.e.*, along the linear axis of the linear precursor complex, via hydrolysis and condensation of the terminal alkoxide groups (Figure 8.7c). The pH sensitivity of the amine groups in the precursor complex thus would allow control over the size of the nanorod fragments and, hence, over the diameter of the resulting nanorods. Note further that the role of the acid conditions is in contrast to that in the sol-gel chemistry of silica where the acid acts purely as a catalyst. Clear evidence for the proposed role of the acid in this study is the pH value of 9.3 found for the water used to wash the gel. Remaining modifier molecules at the nanorod surface could be removed by peptization while leaving the remaining zirconia central core intact, thus leading to a nitrogen-free material. Electron energy loss spectroscopy (EELS) spectra and EDX confirmed the presence of zirconium and oxygen. No nitrogen was detected in either the amorphous or the ordered material.

HRTEM provides clear evidence that the linear tetranuclear precursor molecules, which act as building blocks for growth, show directed growth along the linear axis of the precursor molecule. Figure 8.8 shows an electron micrograph of a zirconia nanorod embedded in amorphous zirconia. The insets show either a fast Fourier transform (FFT) image (Figure 8.8b) or an enlarged view (Figure 8.8c) of the different areas indicated. The FFT image (Figure 8.8b) taken from the fairly ordered region confirms ordering of the precursor molecules in layers. The dark lines in Figure 8.8c seem to correspond to rows of zirconium atoms. The average diameter of the nanorod is estimated to ~20 layers of 2.96 Å, *i.e.*, ~6.0 nm, which is one order of magnitude smaller than those obtained with template-assisted techniques.

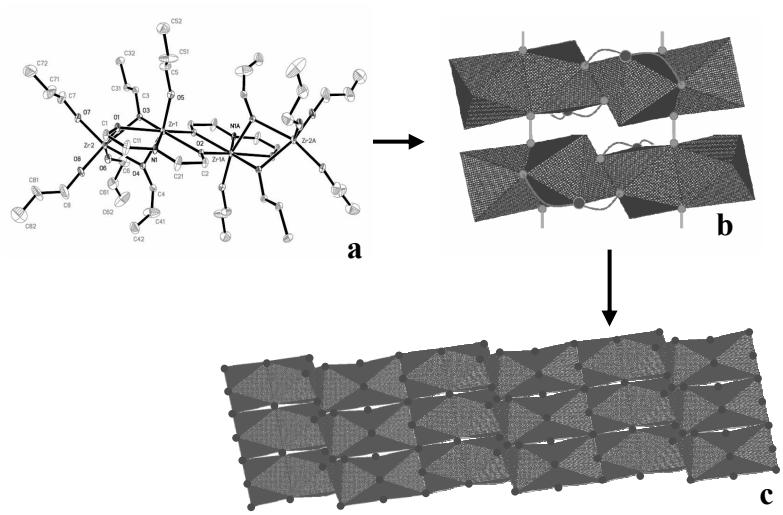

Figure 8.7: Schematic diagram showing growth of a zirconia nanorod. ***a****) Molecular structure of* $[Zr_2(O^nPr)_6(OC_2H_4)_2NH]_2$ *obtained after modification of zirconium n-propoxide with 0.5 equivalent mol* H_2*dea.* ***b****) Upon hydrolysis of the bridging alkoxide groups and subsequent condensation, the linear precursor molecules are aligned in a side-to-side manner.* ***c****) Subsequent growth of nanorod fragments into a nanorod.*

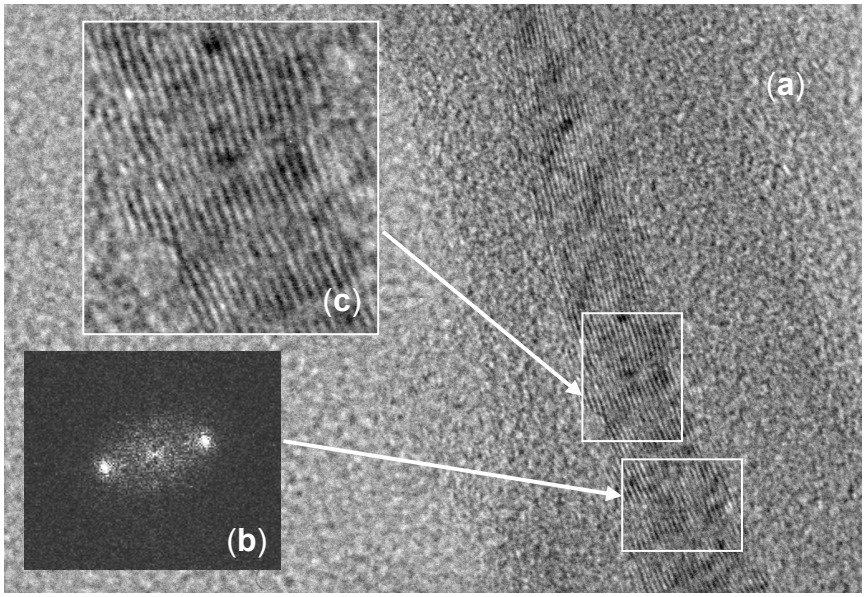

*Figure 8.8: HRTEM image showing a zirconia nanorod embedded in amorphous zirconia (****a****). The insets show either a Fourier transform image (****b****) or an enlarged view (****c****) of the areas indicated.rconia (****a****). The insets show either a Fourier transform image (****b****) or an enlarged view (****c****) of the areas indicated.*

The simultaneous presence of ordered and amorphous material suggests different regimes in the hydrolysis-polycondensation sequence. In the initial stage of the reaction, when the concentration of water is still high, the rates of hydrolysis and polycondensation are similar, resulting in the formation of an ordered material. As the reaction proceeds, the water concentration lowers. The unequal rates of hydrolysis and polycondensation will lead to a lack of suitable building blocks for ordering. At the same time the diffusion of water becomes important. Both these factors favor formation of the amorphous phase.

Using zirconium *n*-propoxide and H_2dea in a 1:1 ratio a thermodynamically stable trinuclear complex is formed, with the formula $Zr\{\mu\text{-}\eta^3\text{-}NH(C_2H_4O)_2\}_3[Zr(O^nPr)_3]_2(^nPrOH)_2$ which adopts a structure similar to that reported for $Zr\{\mu\text{-}\eta^3\text{-}NH(C_2H_4O)_2\}_3[Zr(O^iPr)_3]_2(_iPrOH)_2$ [44] . This trinuclear complex lacking alkoxide groups in bridging positions is also obtained after aging (for several days) or refluxing of tetranuclear $[Zr_2(O^nPr)_6(OC_2H_4)_2NH]_2$. TEM images of the sol prepared from the trinuclear zirconia precursor complex showed, in majority, amorphous material. A minor fraction of ordered zirconia was found due to the presence of the tetranuclear complex as an impurity. No ordered structures were found if the sol was prepared introducing a reflux step at 92 °C for 30 min prior to the addition of water. Completely amorphous material was also obtained for the sol prepared from the tetranuclear precursor complex, the preparation of which included a similar reflux step. These observations emphasize the role of the bridging alkoxide groups to induce and guide the ordering of the precursor molecules and subsequent growth into a nanoscaled architecture.

Current approaches for the preparation of inorganic nanowires or nanorods are based on sophisticated physical methods, such as arc discharge, or template-directed chemical synthesis routes [88-90]. In the latter, the template controls the dimensions of the produced nanostructures, restricting minimum dimensions to ~80 nm [91-93]. Application of template-directed techniques usually requires removal of the template after the formation of the nanostructure. Here we have shown the spontaneous formation of nanoscale rods, consisting of ordered zirconia, from a highly anisotropic molecular precursor during sol preparation.

It can thus be seen that from a highly anisotropic molecular precursor, a nanostructured material can be obtained during sol preparation. The presence of alkoxide ligands in bridging positions seems to play a decisive role in the formation of such a material. In the absence of these growth directing ligands, precursors modified with a bridging and chelating agent will lead to MTSAL, which does not display a pronounced anisotropy.

(Micro-) porous material

The formation of non-linear material from a $Zr\{\mu\text{-}\eta^3\text{-}NH(C_2H_4O)_2\}_3[Zr(O^iPr)_3]_2$ precursor has already been mentioned above. The morphology of material derived from $Zr\{\mu\text{-}\eta^3\text{-}NH(C_2H_4O)_2\}_3[Ti(O^iPr)_3]_2$ [94] and the *n*-propoxide analogue [95] is discussed in detail elsewhere [96]. The materials obtained from these two precursors surprisingly turned out to be srilankite, where a mixture of titania and zirconia phases were expected. The morphology of the materials seems to be rather independent from the type of MTSAL, *i.e.*, for direct and inverted micellar systems microporous materials are obtained. It is not possible to assign the observed minor differences in porosity to the sol formation mechanism. The alkoxide ligands were different for the precursors used to prepare sols by direct and inverted micelles. Moreover, the precursor concentrations were different. This turned out to have a significant influence on the pH, *i.e.*, more modifying ligands need to be removed to reach the same pH in more diluted systems. Further, we demonstrated that both the pH of the sol and the sintering temperatures of the derived sol both have a great influence on the pore-morphology of the derived materials [96].

8.4.4 Transfer of direct micelles into aqueous conditions

For a number of applications, it is important that the MTSAL concept is performed under aqueous conditions. Micelles present in water solutions are normally stabilized by an electric charge on their surface, positive in acidic and negative in basic media [97]. Therefore, in order to create biocompatible conditions, application of templated micelles for encapsulation of single-cell organisms has to occur in predominantly aqueous pH-neutral media with low content of alcohols. As a proof-of-principle we have chosen to work with the derivatives of longer chain titanium alkoxides (*n*-propoxide and *n*-butoxide) and modify them with basic

chelating ligands, *i.e.*, triethanolamine. The sols were prepared by hydrolysis in parent alcohols with diluted solutions of nitric acid (0.1 M HNO_3 up to H_2O:Ti = 1-1.5:1). The sols are thus formed by direct micelles. Determination of the particle size in the prepared sols by light scattering technique yielded a sharp distribution with a maximum diameter of 3.4 nm, which is a value typical for sol particles obtained through hydrolysis of modified metal alkoxides [30,37].

Mixing the sols with a nine times larger volume of isotonic solution of NaCl leads to a slightly opaque water-based sol that transforms within several minutes into a compact, semi-transparent gel. Charging of the basic ligands on the surface of the micelles provides a possibility to transfer these microheterogeneous particles into aqueous solution without phase separation. The charge is relatively low, which results in a quick gelation. The obtained gel is practically pH-neutral and biocompatible, which opens the prospects of application of modified metal alkoxides in biotechnology.

This concept has been exploited successfully by the groups at SLU for the gel encapsulation in aqueous media. Proper choice of the modified titanium alkoxide allows for the preparation of a sol via direct micelles in alcohol and subsequent transferring of the sol to aqueous condition leads to the possibility of encapsulation in biocompatible conditions.

8.5 Conclusions

The sol-gel chemistry for metal alkoxides is clearly different from that generally assumed for silicon alkoxides. Ligand exchange and hydrolysis of modified metal-alkoxides proceeds through a S_N1 mechanism, where the hydrolysis mechanism for silicon alkoxides proceeds through a S_N2 mechanism. The reactivity of the metal alkoxide precursors is increased rather than decreased upon addition of modifying ligands (in contrast to earlier suppositions [97]), as concluded from the comparison of the bond lengths in modified and unmodified compounds, calculation of charge on the metal atoms using the charge regulation model and data from calorimetric experiments. The high reactivity of the modified precursors causes the ligand exchange, hydrolysis and also the condensation reactions to proceed almost instantaneously upon the addition of water. Another striking difference with traditional silica sol-gel is the large mobility of the modifying ligands.

Moreover, the modifying ligands have a large influence on the material that is eventually formed. We proposed a concept for the formation of products of the fast hydrolysis and condensation sequence; they are formed through templated micelles by self-assembly of ligands and they consist of oxo-spiecies. The following approaches are covered in the present work and all of them are schematically depicted in Figure 8.9. The formation of dense nanoparticles from acetylacetone modified or acid 'catalyzed' system and the formation of dense films from an acetylacetone modified precursors. The sol particles for these systems are direct micelles containing oxo-species and the surface covered with acetylacetone or protons. The formation of inverted micelles, which can be achieved by an appropriate choice of solvents, allows for the formation of hollow spheres. The modifying acetylacetone ligands act as a surfactant in these systems and will form the interface between the hollow sphere and the solvent. Another example, which is formed from a direct micellar system, is the formation of zirconia nano-rods from a highly anisotropic diethanolamine (H_2dea) modified precursor. The alkoxide ligands of the precursor in bridging positions play a decisive role in the formation of the nano-rods. In the absence of these growth-directing ligands, a microporous material can be obtained from H_2dea modified precursors. The last example in this work on the templated micelles by self-assembly of ligands concept deals with the gel encapsulation of glass beads or bacteria. Proper choice of modified titanium alkoxide allows for the preparation of sol *via* direct micelles in alcohol and subsequent transferring of the sol to aqueous condition allows for encapsulation under biocompatible conditions. All these different morphologies of materials derived from modified metal alkoxides are schematically summarized in Figure 8.9.

Finally, it was demonstrated that the modifying agent has a pronounced influence on the morphology of sol-gel materials. A new and interesting area within the field of materials chemistry and science has been discovered and has yet to be explored.

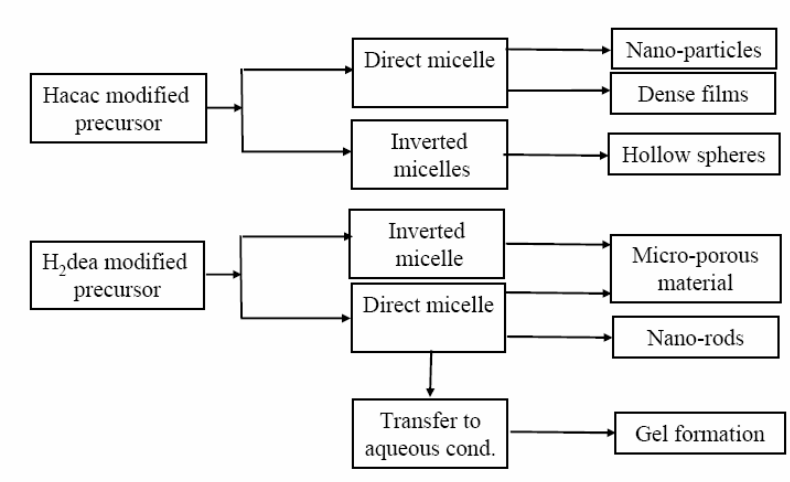

Figure 8.9: Schematic representation of the possible different material morphologies from different modified precursor systems.

8.6 References

1 R.J. Vacassy, C. Guizard, J. Palmeri and L. Cot, *Nanostruct. Mater*., **10**, 77 (1998).

2 C.R. Xia, H.Q. Cao, H. Wang, P.H. Yang, G.Y. Meng and D.K. Peng, *J. Membr. Sci*., **162**, 181 (1999).

3 H. Kurosawa, Y.T. Yan, N. Miura and N. Yamazoe, *Solid State Ionics*, **79,** 338 (1995).

4 J. Riegel, H. Neumann and H.–M. Wiedemann, *Solid State Ionics*, **152**, 783 (2002).

5 N. Miura, M. Nakatou and S. Zhuiykov, *Sensor Actuat. B-Chem*., **93**, 221 (2003).

6 Y.W.Li, D.H. He, Z.X. Cheng, C.L. Su, J.R. Li and Q.M. Zhu, *J. Mol. Catal. A: Chem.*, **175**, 267 (2001).

7 A. Knell, P. Barnickel, A. Baiker and A. Wokaun, *J. Catal*., **137**, 306 (1992).

8 J. Gottmann and E.W. Kreutz, *Surf. Coat. Tech.*, **119**, 1189 (1999).

9 R. Reisfeld, *J. Alloy Compd*., **341**, 56 (2002).

10 X.Y. Zhao and D. Vanderbilt, *Phys. Rev. B*, Art., **65**, No. 07510 (2002).

11 V. Fiorentini and G. Gulleri, *Phys. Rev. Lett*., Art., **89**, No. 266101 (2002).

12 J. Livage and C. Sanchez, *J. Non-Cryst. Solids,* **145**, 11 (1992).

13 C.J. Brinker and G.W. Sherer, "*Sol-gel science: The physics and chemistry of sol-gel processing*," Academic Press, San Diego, (1990).

14 D. Brandhuber, V. Torma, C. Raab, H. Peterlik, A. Kulak and N. Husing, *J. Mater. Chem*., **17**, 4246 (2005).

15 J. Livage, M. Henry and C. Sanchez, *Prog. Solid St. Chem*., **18,** 259 (1988).

16 J. Livage and M. Henry, "*A predictive model for inorganic polymerization reactions*," in ultrastructure processing of advanced ceramics, Eds J.D. Makenzie and D.R. Ulrich, Wiley, New York, (1988).

17 J.H. Wengrovius, M.F. Garbauskas, E.A. Williams, R.C. Going, P.E. Donahue and J.F. Smith, *J. Amer. Chem. Soc.*, **108**, 982 (1986).

18 M.T. Harris, A. Singhal, J.L. Look, J.R. Smith-Kristensen, J.S. Lin and L.M. Toth, *J. Sol-Gel Sci. Technol.*, **8**, 41 (1997).

19 K.C. Fortner, J.P. Bigi and S.N. Brown, *Inorg. Chem.,* **44**, 2803 (2005).

20 G. Fornasieri, L. Rozes, S. Le Calve, B. Alonso, D. Massiot, M.N. Rager, M. Evain, K. Boubekeur and C. Sanchez, *J. Amer. Chem. Soc.*, **127**, 4869 (2005).

21 J. Blanchard, F. Ribot, C. Sanchez, P.V. Bellot and A. Trokiner, *J. Non-Cryst. Solids*, **265**, 83 (2000).

22 V.G. Kessler, *J. Sol-Gel Sci. Technol.*, **32**, 11 (2004).

23 C.J. Brinker, K.D. Keefer, D.W. Schaefer, R.A. Assink, B.D. Kay and C.S. Ashley, *J. Non-Cryst. Solids,* **63**, 45 (1984).

24 N.Ya. Turova, V.G. Kessler and S.I. Kucheiko, *Polyhedron*, **10**, 2617 (1991).

25 G.A. Seisenbaeva, S. Gohil, K. Jansson, K. Herbst, M. Brorson and V.G. Kessler, *New J. Chem*., **27**, 1059 (2003).

26 U. Schubert, *J. Sol-Gel Sci. Technol*., **26**, 47 (2003).

27 U. Schubert, *J. Mater. Chem.*, **15**, 3701 (2005).

28 R. Brenier and A. Gagnaire, *Thin Solid Films*, **392**, 142 (2001).

29 C. Sanchez and J. Livage, *New. J. Chem.*, **14**, 513 (1990).

30 M. Chatry, M. Henry, C. Sanchez and J. Livage, *J. Sol-gel Sci. Technol*., **1**, 233 (1994).

31 J. Livage, F. Babonneau, M. Chatry and L. Coury, *Ceram. Int.*, **23**, 13 (1997).

32 T. Okubo, T. Takahashi, M. Sadakata and H. Nagamoto, *J. Membr. Sci.*, **118**, 151 (1996).

33 Y. Takahashi and Y. Matsuoka, *J. Mater. Sci.*, **23**, 2259 (1988).

34 M.A. Anderson, M.J. Gieselmann and Q. Xu, *J. Membr. Sci.*, **39**, 243 (1988).

35 B.E. Yoldas, *J. Mater. Sci.*, **21**, 1087 (1986).

36 A. Julbe, C. Guizard, A. Larbot, L. Cot and A. Giroir-Fendler, *J. Membr. Sci.*, **77,** 137 (1993).

37 C. Sanchez, F. Ribot and P. Toledano, *Chem. Mater.*, **3**, 762 (1991).

38 G.A. Seisenbaeva, S. Gohil and V.G. Kessler, *J. Mater. Chem.*, **14**, 3177 (2004).

39 G.I. Spijksma, H.J.M. Bouwmeester, D.H.A. Blank and V.G. Kessler, *Chem. Commun.*, 1874 (2004).

40 Chapter 3 of this thesis.

41 K.A. Fleeting, P. O'Brien, D.J. Otway, A.J.P. White, D.J. Williams and A.C. Jones, *Inorg. Chem.,* **38**, 1432 (1999).

42 Chapter 4 of this thesis.

43 U. Patil, M. Winter, H.W. Becker and A. Devi, *J. Mater. Chem.*, **13**, 2177 (2003).

44 Chapter 6 of this thesis.

45 U. Schubert , private communication, (2005).

46 Cambridge Crystallographic Data Centre, Structure 269602.

47 R.J. Errington, J. Ridland, W. Clegg, R.A. Coxall and J.M. Sherwood, *Polyhedron*, **17**, 659 (1998).

48 R. Bhakta, R. Thomas, F. Hipler, H.F. Bettinger, J. Muller, P. Ehrhart and A. Devi, *J. Mater. Chem*., **14**, 3231 (2004).

49 R. Bhakta, F. Hipler, A. Devi, S. Regnery, P. Ehrhart and R. Waser, *Chem. Vap. Depos*., **9**, 295 (2003).

50 W. Day, W.G. Klemperer and M.M. Pafford, *Inorg. Chem.*, **40**, 5738 (2001).

51 J. Ridland, PhD Thesis, University of Newcastle upon Tyne, UK, (1998).

52 J. Blanchard, M. In, B. Schaudel, and C. Sanchez, *Eur. J. Inorg. Chem*., 1115 (1998).

53 F. Basolo and R. Pearson, "*Mechanisms of Inorganic Reactions*," Wiley Eastern Private Ltd; 2nd edition, (1973).

54 A. Senouci, M. Yaakoub, C. Huguenard and M. Henry, *J. Mater. Chem.*, **14**, 3215 (2004).

56 V.G. Kessler, *Chem. Commun*., 1213 (2003).

57 M.J. Percy, J.R. Bartlett, L. Spiccia, B.O. West and J.L. Woolfrey, *J. Sol-gel Sci. Technol.*, **19**, 315 (2000)

58 M.J. Percy, J.R. Bartlett, J.L. Woolfrey, L. Spiccia and B.O. West, *J. Mater. Chem*., **9**, 499 (1999).

59 K.T. Ranjit and K.J. Klabunde, *Chem. Mater.*, **17**, 65 (2005).

60 B.L. Cushing, V.L. Kolesnichenko and J. O'Connor, *Chem. Rev*., **104**, 3893 (2004).

61 A. Mills, G. Hill, M. Crow and S. Hodgen, *J. Appl. Electrochem*., **35**, 641 (2005).

62 J. Sekulic, J.E. ten Elshof and D.H.A. Blank, *Adv. Mater*., **16**, 1546 (2004).

63 J.-P. Hsu and A. Nacu, *Langmuir*, **19**, 4448 (2003).

64 N. Pinna, M. Antonietti and M. Niederberger, *Colloid Surfaces A,* **250**, 211 (2004).

65 N. Pinna, G. Neri, M. Antonietti and M. Niederberger, *Angew. Chem. Int. Ed*., **43**, 4345 (2004).

66 J. Polleux, N. Pinna, M. Antonietti, C. Hess, U. Wild, R. Schlögl and M. Niederberger, *Chem. Eur. J*., **11**, 3541 (2005).

67 D.C. Bradley, R.C. Mehrotra and C.P. Gaur, "*Metal alkoxides*," Academic Press, Londen, (1978).

68 D.C. Bradley, B.N. Chakravarti, A.K. Chatterjee, W. Wardlaw and A. Whitley, *J. Chem. Soc*., 2381, (1956).

69 R. Corriu, D. Leclercq, P. Lefevre, P.H. Mutin and A. Vioux, *Chem. Mater*., **4**, 961 (1992).

70 N.Ya. Turova, E.P. Turevskaya, V.G. Kessler and M.I. Yanovskaya, "*The chemistry of metal alkoxides*," Kluwer Academic Press, Boston, (2002).

71 Chapter 2 of this thesis.

72 E.P. Turevskaya, N.I. Kozlova, N.Y. Turova, A.I. Belokon, D.V Berdyev, V.G. Kessler and Y.K. Grishin, *Russ Chem. Bull*., **44**, 734 (1995).

73 V.W. Day, W.G. Klemperer and M. Pafford, *Inorg. Chem*., **44**, 5397 (2005).

74 Z.A. Starikova, V.G. Kessler, N.Y. Turova, D.E. Tcheboukov, E.V. Suslova, G.A. Seisenbaeva and A.I. Yanovsky, *Polyhedron*, **23**, 109 (2004).

75 N.Ya. Turova, A.V. Korolev, D.E. Tchebukov and A.I. Belokon, *Polyhedron*, **15**, 3869 (1996).

76 Pia Werndrup, PhD Thesis, SLU, Sweden, (2005).

77 P. Werndrup, M. Verdenelli, F. Chassagneux, S. Parola and V.G. Kessler, *J. Mater. Chem.,* **14**, 344 (2004).

78 G.A. Seisenbaeva, E.V. Suslova, M. Kritikos, V.G. Kessler, L. Rapenne, M. Andrieux, F. Chassagneuz, S. Parola, *J. Mater. Chem*., **14**, 3150 (2004).

79 A. Barau, M. Anastasescu, V. Teodorescu, M.G. Blanchin and M. Zaharescu, Abstracts of the 13th International Workshop on Sol-Gel Science and Technology, August 21-26 2005, Los Angeles, USA, P. 90 (2005).

80 P. Puhlfürß, A. Voigt, R. Weber and M. Morbe, *J. Membr. Sci.*, **174**, 123 (2000).

81 T. Van Gestel, C. Vandecasteele, A. Beukenhoudt, C. Dotremont, J. Luyten, R. Leysen, B. Van der Bruggen and G. Maes, *J. Membr. Sci.,* **209,** 379 (2002).

82 J. Sekulic, J.E. ten Elshof and D.H.A. Blank, *Adv. Mater*., **16**, 1546 (2004).

83 T. Tsuru, D. Hironaka, T. Yoshioka and M. Asaeda, *Desalination*, **147**, 213 (2002).

84 T. Van Gestel, H. Kruidhof and H. J. M. Bouwmeester, In Preparation (2005).

85 Chapter 9 of this thesis.

86 F. Caruso, R.A. Caruso and H. Möhwald, *Science*, **282**, 1111 (1998).

87 G.J. Gainsford, N. Al-Salim and T. Kemmitt, *Acta Crystallogr., Sect. E.: Struct. Rep. Online*, **58**, m636 (2002).

88 H.Q. Cao, Y. Xu, J.M. Hong, H.B. Liu, G. Yin, B.L. Li, C.Y. Tie and Z. Xu, *Adv. Mater*., **13**, 1393 (2001).

89 B.B. Lakshmi, P.K. Dorhout and C.R. Martin, *Chem. Mater*., **9**, 857 (1997).

90 H. Cao, X. Qui, Y. Liang and Q. Zu, *Appl. Phys. Lett*., **83**, 761 (2003).

91 X. Hui, D.-H. Qin, Z. Yang and H.-L. Li, *Mater. Chem. Phys*., **80**, 524 (2003).

92 H.Q. Cao, X.Q. Qiu, B. Luo, Y. Liang, Y.H. Zhang, R.Q. Tan, M.J. Zhao and Q.M. Zhu, *Adv. Funct. Mater*., **14**, 243 (2004).

93 S.J. Limmer, S. Seraji, M.J. Forbess, Y. Wu, T.P. Chou, C. Nguyen and G.Z. Cao, *Adv. Mater*., **13**, 1269 (2001).

94 G.I. Spijksma, H.J.M Bouwmeester, D.H.A. Blank and V.G. Kessler, *Inorg. Chem. Comm*., **7**, 953 (2004).

95 Chapter 7 of this thesis.

96 Chapter 10 of this thesis.
97 C. Sanchez, J. Livage and M. Henry, *J. Non-Cryst. Solids*, **100**, 65 (1988).

Chapter 9

Hollow nanospheres by hydrolysis of modified metal alkoxides and their encapsulating properties

Abstract

Heteroligands like acetylacetone are shown to play the role of surfactants in the formation of micelles resulting from the hydrolysis of modified metal alkoxides. The resulting solutions are not, as previously expected, polymeric colloids, but Micelles Templated by Self-Assembly of Ligands (MTSAL). MTSAL's formed in inverted micellar systems, such as water/alcohol – hydrocarbon, are hollow nanospheres able to selectively encapsulate hydrophilic compounds. The presence of very reactive hydroxide groups inside the spheres implies that they have the ability to transformation, and that during the process of this transformation, the templating ligands are eliminated. This transformation was observed in the zirconium system where it is possible to form the poorly soluble $Zr(acac)_4$, however, the results for this transformation were not noticeable in the titanium system after several months.

9.1 Introduction

The encapsulation of organic compounds, particles or solids is of great interest in research areas ranging from material science and chemical engineering to medicine and pharmaceutics. The applications of encapsulated compounds range from pigment stabilization [1], protection of active ingredients in cosmetic industries [2], magnetic particles [3] and controlled drug delivery [4]. The latter application led to the development of drug encapsulation by self-assembly of organic polymers [5-8]. The application of nano capsules as reactors for specific chemical or biochemical processes [9] is a related area, which is new and growing intensely. It applies templation by organic surfactants.

Encapsulation using inorganic empty shells has recently been addressed and the synthesis of hollow silica nanospheres has been reported by inorganic polymerization on the surface of spherical organic colloid particles [10] as well as through colloid templating with surfactants [11,12]. The application of these approaches is hampered by the need to remove the colloid templates, which is a complicated task. A thermal treatment permits the burn out of the templates [10], but this procedure is incompatible with the possible applications. An additional disadvantage of these approaches lies in the comparably large size of the shells – about 0.5 μm in average diameter with a wall thickness of up to 200 nm [11,12].

Application of metal alkoxides has not previously been considered for the preparation of hollow nanospheres, however, in the present paper, we will demonstrate the possibility of preparing metal oxide hollow nanospheres by self-assembly on hydrolysis of these precursors. It is assumed that the hydrolysis of metal alkoxides results in the very quick formation of polymeric oxo-hydroxide species in a manner analogous to that of silicon alkoxides, but characterized by a much higher speed and, therefore, the reactivity is much harder to control [13]. Preparation of dense oxide particles from metal alkoxides is, in contrast to the preparation of the hollow nanospheres, a well-developed technology. The preparation of dense oxide particles requires introduction of, either, protons (an acid) or chelating ligands (most commonly β-diketonates or β-ketoesterates) into the solution of an alkoxide precursor prior to hydrolysis. It has been considered by

some authors that modifications decrease the speed of the hydrolysis of metal alkoxides and even "inhibits" polycondensation of the hydrolysis products [14].

In our recent study of the molecular structures of zirconium alkoxides modified by acetylacetone [15-17], we could clearly observe that the introduction of this commonly applied β-diketonate ligand leads to pronounced elongation of all metal-oxygen bonds. This indicates an increase in efficient charges on the metal atoms and even decreased shielding of the metal atoms compared to the alkoxide solvates otherwise present in solution [15-17]. These changes in the molecular structure imply the possibility of facilitating the hydrolysis reaction. Calorimetric monitoring of the heat release from hydrolysis used in a comparison of a solution modified with Hacac and an unmodified system supports the idea of an enhanced hydrolysis rate. The evolution of reaction heat was significantly faster in the chemically modified system compared to the unmodified system.

The explanation that the stability of resulting colloids is due to the inhibiting effect of the protons and chelating ligands on the polycondensation process does not appear realistic either. Protons are well known to be catalysts in both hydrolysis and polycondensation at low acidity, while β-diketonate ligands are commonly appreciated as charge-stabilizing fragments, and are more likely to facilitate both reactions [18]. The answer to the question about the role of modifying ligands is unlikely to be found in the homogeneous reactivity of metal alkoxides. These molecules, in contrast to silicon alkoxides, are characterized by the kinetically unhindered reactivity and thermodynamic control of their reactions in homogeneous solutions [19,20]. The role of heteroligands had to be sought in influencing the microheterogeneity arising through the hydrolysis and polycondensation. For a detailed discussion on the role of the heteroligands the interested reader is referred to ref. [21]. The products of the hydrolysis and condensation sequence of modified metal alkoxides are obviously not polymeric colloids but *Micelles Templated by Self-Assembly of Ligands* (MTSAL). Sanchez *et al*. [14] have in fact observed the formation of MTSALs in their study of hydrolysis of titanium alkoxides by ^{17}O NMR. However, these authors called them "polymeric building blocks" and did not recognize them as emulsion particles, *i.e.*, micelles.

The aim of the present work is the application of MTSALs for constructing hollow nanospheres of metal oxides (*e.g.*, titania, zirconia) and the investigation of their encapsulation ability and reactivity.

9.2 Experimental

All manipulations were carried out in a dry nitrogen atmosphere using the Schlenk technique or a glove box. Hexane (Merck, *p.a.*) was dried by distillation after refluxing with $LiAlH_4$, *n*-propanol and isopropanol (Merck, *p.a.*) were dried by distillation after refluxing with the corresponding $Al(OPr)_3$ (for details see ref. [16]). Acetylacetone (Hacac) and 2,2,6,6,-tetramethyl-3,5-heptanedionate (Hthd) were purchased from Aldrich. Molecular sieves were added to the Hacac to assure that it remained water free.

The zirconium propoxide precursors used as starting materials in this work are zirconium isopropoxide, ($[Zr(O^iPr)_4(^iPrOH)]_2$ 99.9%) and 70 wt% solution of "$Zr(O^nPr)_4$" in *n*-propanol (both purchased from Aldrich). The zirconium isopropoxide was dissolved and recrystallized from toluene prior to use in order to remove impurities. The titanium isopropoxide (99.999% pure) and titanium *n*-propoxide (98% pure) were both obtained from Aldrich. $[Zr(O^iPr)_3(acac)]_2$ was prepared acceding to recently developed techniques [17].

Sol preparation: The inverted micelles are typically obtained when a small amount of polar solvent is introduced into a non-polar one and the droplets of the former are stabilized by a surfactant. In this study a water solution in isopropanol (1:20 volume ratio) is inserted into a larger volume of hexane, which results in a clear emulsion. Subsequently, the water and propanol solution is quickly added by a syringe to a 0.3-1.0 molar hexane solution of the modified precursor (the metal to water ratio was maintained around 1), and a clear sol is obtained. The detailed composition of the prepared samples is summarized in Table 9.1.

The samples for light scattering and TEM experiments were prepared from the product of the dried sols which were dissolved in ~20 ml of either isopropanol or *n*-propanol. The samples were ultrasonically treated for 15 minutes. The particle size of the clear solution was determined by light scattering. For TEM analysis a drop of the solution was deposited on a copper supported carbon grid.

Table 9.1: Composition of the prepared samples.

Sample name	Precursor	Modifier	Ratio $Zr:H_2O$	Concentration Zirconium [mol/l]	Hexane : propanol
HS1	$[Zr(O^iPr)_3(acac)]_2$	-	1.04	1	2
HS2	$[Zr(O^iPr)_3(acac)]_2$	-	1.1	0.98	2
HS3	$[Zr(O^iPr)_3(acac)]_2$	-	1.01	0.29	2
HS4	$[Zr(O^iPr)_3(acac)]_2$	-	1	0.3	8.8
HS5	$[Zr(O^iPr)_3(acac)]_2$	-	0.92	0.58	4.4
HS7	$Ti(O^nPr)_4$	1 mol Hacac	1.03	0.3	2
HS8	$Zr(O^nPR)_4$	1 mol Hacac	0.99	0.3	2
HS9	$Zr(O^nPR)_4$	1 mol Hthd	1.02	0.3	2

Characterization: Particle size in the obtained sols was determined using a light scattering technique with a Zetasizer 3000HS instrument. Transmission Electron Microscopy (TEM) images have been obtained with PHILIPS CM30 Twin/STEM instrument. Samples were characterized by Scanning Electron Microscopy (LEO Gemini 1550 FEG - SEM, UK). The formed single crystals were identified by determination of their unit cell parameters. Data collection for single crystals of all compounds was carried out at 22 °C on a SMART CCD 1k diffractometer with graphite monochromated MoKα radiation. All calculations were performed using the SHELXTL-NT program package [22] on an IBM PC.

9.3 Results and discussion

The concept for the preparation is surprisingly simple and is depicted in Figure 9.1. Inverted micelles are created by the appropriate choice of solvents. The continuous phase, which also contains the modified precursor, consists of a hydrocarbon solvent, hexane in the present case. The core of the inverted micelle consists of isopropanol and the water required for hydrolysis. The presence of the two reactants for the sol-gel process in two different phases leads to a reaction at the interface, *i.e.*, on the surface of the formed inverted micelle. If the rate of hydrolysis, condensation and redistribution of ligands is of the right order of magnitude a beautiful core is formed by self-assembly. The boundary of the core that stays in contact with the hexane solvent will accumulate a high concentration of hydrophobic acac-ligands. The mobility of acac-ligands, required for the

redistribution of ligands in the proposed mechanism, has been observed in other studies using Hacac modified alkoxide species [15-17].

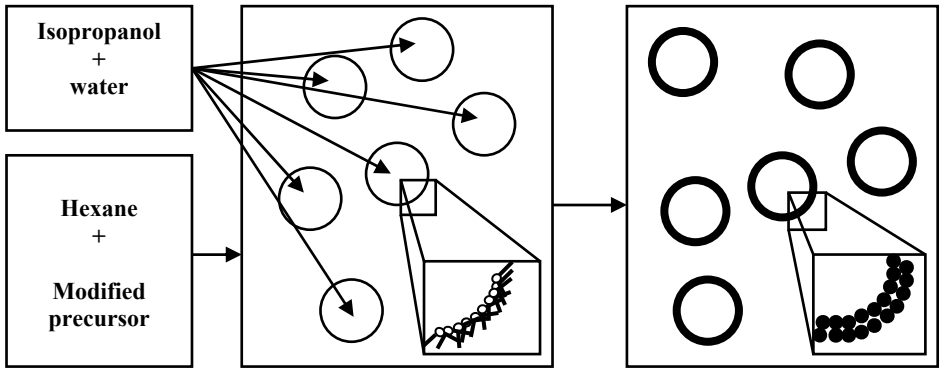

Figure 9.1: The strategy in the creation of inverted micelles via micellar templation by self-assembly of ligands (MTSAL concept).

The proposed mechanism was initially evaluated using zirconium isopropoxide monosubstituted with acac-ligands and with a ratio of hexane and isopropanol of 2:1, and water and zirconium of 1:1. After the rapid addition of the hydrolysis + propanol solution to the precursor solution, a clear, yellowish sol was obtained. The characterization of the obtained sols turned out to be complicated. In general, the available techniques for the characterization of sols are limited to light scattering and SAXS.

SAXS experiments were performed using the capillaries filled with the sol. However, quantitative interpretation of the obtained scattering curves is not possible. The experimental SAXS data is normally fitted with a specific function that describes the scattering curve of certain morphology, *e.g.*, the Teixeira function describes the scattering curve of a fractal object [23]. Since particles in the sol phase are expected to be hollow spheres and to the best of our knowledge there are no functions describing the morphology of these systems. SAXS characterization of these systems can thus only be used for comparison of differences between sols.

Light scattering on these samples did not provide reliable data either. The mixture of hexane and isopropanol, each of which has its own scattering behavior, in combination with the presence of metal-oxide particles, probably causes the inability to measure light scattering on these systems. It was attempted to dilute the

sample by increasing the amount of hexane, in the hope that lower concentrations of propanol and metal oxides in the samples would permit light scattering experiments. The addition of hexane and also the addition of propanol to these sols instantly leads to the formation of a precipitate. The formation of a precipitate upon dilution of a sol is very unusual and does not occur in systems with direct micelles, a dilution step is generally included in the materials preparation from sols. The formation of the precipitate in the inverted micelle systems is actually a clear indication for the proposed concept. A change in the solvent composition changes the energies of surface interactions responsible for the stability of obtained particles and thus is able to destabilize them.

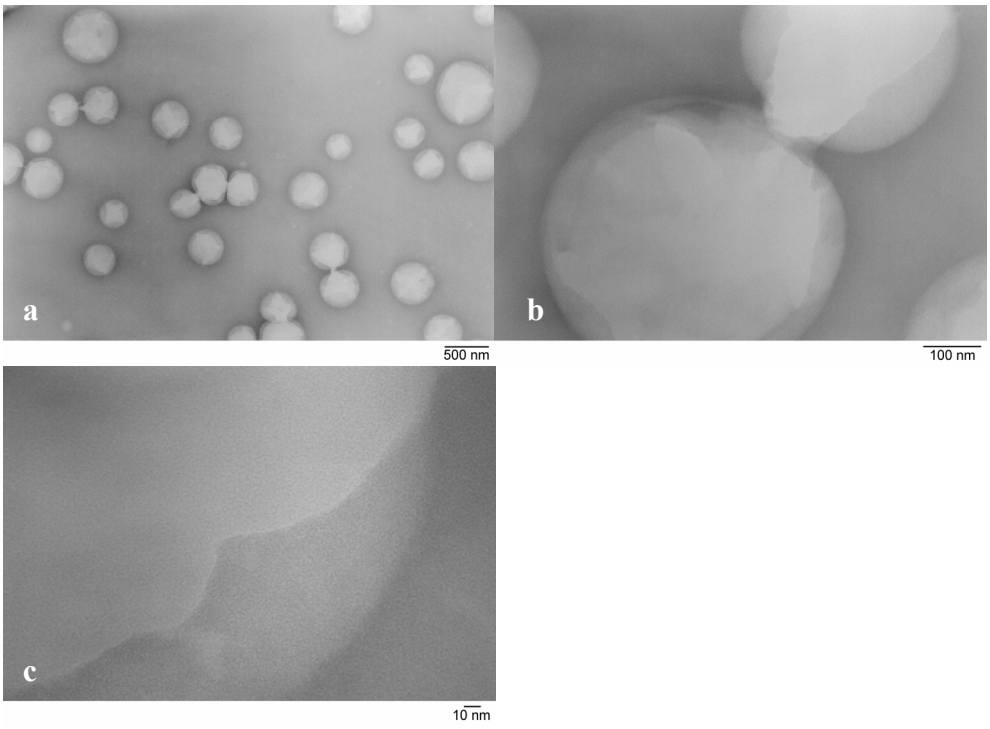

*Figure 9.2: TEM images of the hollow metal oxide nanospheres: (**a**) an overview, (**b**) coalescing spheres with connected hollow rooms, (**c**) a crack in a sphere (Sample HS1).*

The apparent stagnant structure of the formed materials, supposedly the anticipated hollow spheres, provided the possibility that (part of) its morphology is conserved upon the slow evaporation of the solvents. The sols were dried by evaporation of the solvents to the air and a slightly yellowish powder was obtained. The powder was redissolved in alcohol and deposited on a carbon grid, which was characterized

by transmission electron microscopy (TEM). Spherical entities with a diameter around 200-250 nm were observed, as depicted in Figure 9.2a. Some coalescence was observed (Figure 9.2b) as has also been reported for the preparation of much bigger oxide spheres by spray-drying [24]. The light color of the spheres in the TEM picture is a clear indication that they are hollow, since filled metal-oxide nanoparticles are dark(er) in appearance due to higher absorption of electrons. The most exciting feature is that their walls are extremely thin, typically about 5 nm (Figure 9.2c). The wall thickness of the spheres can be determined from the TEM image of a crack in the sphere in Figure 9.2c.

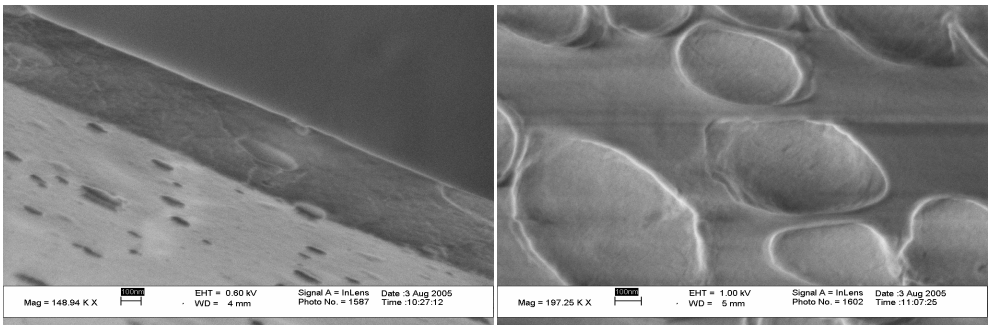

Figure 9.3: SEM images of material deposited on a carbon grid. A film containing the hollow entities is formed. The pictures displayed here were taken on sample HS5.

The samples on the grids were also characterized by SEM and typical images are depicted in Figure 9.3. The material on the grids turned out to consist of films in which cavities are present. The presence of these cavities originates and supports the idea of the formation of the hollow spheres during the sol synthesis. The mechanism for film formation from sols, using Hacac modified metal alkoxide that are obtained *via* direct micelles, is described elsewhere [21]. These films are dense and their preparation and SEM and TEM characterization have been reported by various research groups [25,26]. In our samples, part of the material has formed a dense film, but a fraction has conserved its original morphology. The shape of the spheres has become ellipsoidal, as can be seen from the cross section of the film (Figure 9.3a). For obvious reasons this is due to the one-dimensional shrinkage of and gravity effect on the films. The top view, as depicted in Figure 9.3b, which is taken in same direction as the TEM images, displays circles which are not perfect. With the SEM it was possible to take images of the missing parts of the hollow spheres depicted in Figure 9.3. These parts remained on the grid when the film

curled up. The thickness of these frangments was between 5 and 10 nm, confirming that the wall thickness of the hollow spheres is in the order of up to a few metal atom layers.

Several parameters are expected to influence the size and size distribution of the prepared hollow spheres. A change of the ratio isopropanol/hexane will lead to a change in micelles and subsequently smaller metal oxide spheres, a matter which will be evaluated below. A tremendous effect was observed due to molecular composition variations of the precursor solution, as is described in more detail elsewhere [17]. The utilized monosubstituted zirconium precursor has a tendency to concentrate its modifying ligands on a metal atom, upon the formation of the thermodynamically stable $Zr(acac)_4$. Aging the precursor or its solution leads to the formation of a mixture containing unmodified, mono-, tri- and unreactive tetrasubstituted compounds in the precursor solution [17]. The presence of this mixture of compounds was found to significantly influence the size distribution of the obtained spheres. For a solution of a freshly prepared precursor the yielded spheres predominately had a diameter around 250-300 nm, while those formed from an aged precursor or precursor solution varied in size from 20-500 nm. Light scattering experiments were performed on the solutions in which the powder is dissolved and subsequently used for deposition of the material on the grids. The results of these experiments and the particle size distribution on basis of TEM observations are depicted in Figure 9.4c. The narrow size distribution of the fresh sample was observed by both techniques. The only difference, which is also observed for the experiments discussed below, is a shift in the size measured. The values measured by light scattering are larger. This is probably due to shrinkage of the material during drying. The difference between samples prepared from fresh and aged precursors was also observed in the SAXS experiments (which are described in more detail in ref. [17]); however, as explained above, quantitative interpretation of this data was not possible.

Changes in the ratio of hexane and propanol and the amount of water will lead to different sizes of the emulsion droplet and subsequently to different sizes for the inverted micelle. The influence of these parameters on the size of the hollow spheres was evaluated. Samples with various ratios of solvents were prepared; the composition of these samples (HS1, HS3-5) corresponds with that listed in

Table 9.1. The TEM images of these samples are depicted in Figure 9.5 (sample HS1) and Figure 9.6 (samples HS3-5), and the size distributions (on basis of the TEM image and light scattering experiments) are also depicted in Figure 9.6

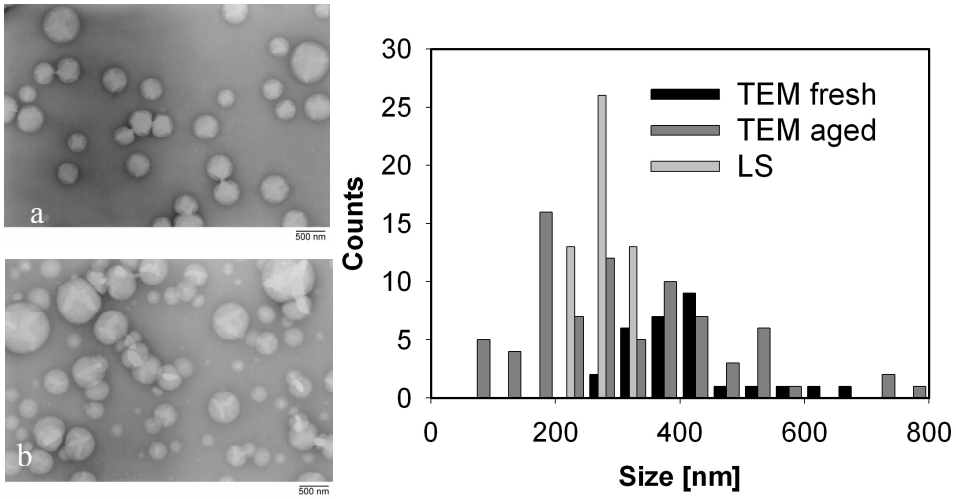

*Figure 9.5: TEM images of sample HS1 & HS2 (**a** and **b**, respectively) and particle size distributions.*

The size distributions determined by light scattering and on the basis of the TEM match fairly well in the most cases. For sample HS3 a fairly broad distribution is observed in the TEM, but the light scattering experiments indicate a maximum just under 400 nm. The difference in synthesis between this sample and HS1, which is depicted in Figure 9.4a&c, is the amount of water in the system. In both samples the zirconium: water ratio is maintained around 1, however, a decrease in the zirconium concentration in sample HS3 (0.3 M compared to 1.0 M in sample HS1) also implies a decrease of water in the system. As a result, the formed hollow spheres increase in size from around 300 to 400 nm.

The scattering behavior and the size distribution in TEM observed entities show the same trend in sample HS4, and the large particles have a size around 200 nm. This sample was compared to HS3, which displayed a maximum in the size distribution of 400 nm, a higher hexane to isopropanol ratio, *i.e.*, the ratio in HS3 is 2 compared to 8.8 in HS4. The decrease in propanol leads to an expected decrease in sphere size.

The reproducibility of the observed trends was evaluated by sample HS5. In this sample it was also expected to decrease the size by decreasing the amount of water and at the same time increase due to a smaller hexane:propanol ratio. If the size of the resulting spheres scales according to the trends observed earlier, the effect of changing the solvent ratio appears to have a larger effect than the increase in the amount water, a slight increase in size is expected. The resulting sphere size was around 250, which is thus in agreement with our expectations.

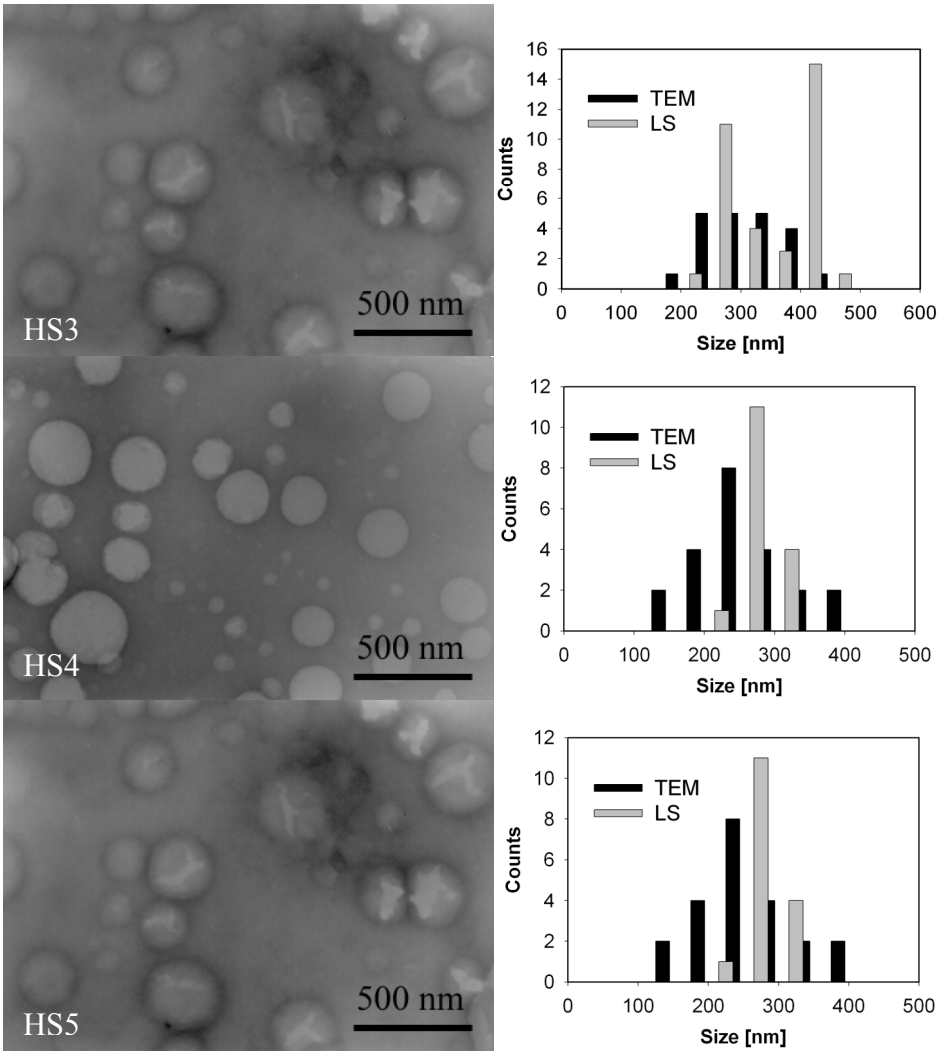

Figure 9.6: TEM images and particle size distributions of sample HS3, HS4 & HS5 (top down).

After having explored some of the parameters of the formation of hollow spheres from the acac-substituted zirconium isopropoxide precursor, it was interesting to evaluate whether it would be possible to achieve comparable results using other precursors and modifiers. A mono-acac-substituted titanium precursor was prepared according to procedures in ref. [27] and the amount of water and the solvent ratios were chosen in accordance with sample HS3. A precipitate was instantly formed upon the addition of the hydrolysis solution to the precursor solution. Apparently, the formation of hollow spheres was not possible for this system.

The reason for the system's inability to form hollow spheres from a modified titanium isopropoxide precursor probably lies in the disproportioning of the ligands. The monosubstituted titanium isopropoxide precursors have a strong tendency to rearrange to a disubstituted and a unsubstituted precursor [28]. The unsubstituted compound has a significantly higher reactivity towards water when compared to the disubstituted compound [29]. The unmodified precursors will mainly hydrolyze at hydrolysis ratios up to h = 1. A precipitate is formed since no ligand is present which can act as a surfactant and thus the formation of hollow spheres is not possible. It might be possible to enhance the reactivity of the modified titanium isopropoxide by adding a small amount of acid to the hydrolysis medium. The addition of protons is a method which has been proved to enhance the reactivity of alkoxides [18].

In contrast to the modified titanium isopropoxide precursor, it was possible to prepare hollow spheres from a Hacac modified titanium *n*-propoxide precursor. The TEM image of a sample of a titanium *n*-propoxide precursor modified with 1 mol equivalent of Hacac is depicted in Figure 9.7. The size of the spheres in this sample is around 200-250 nm, which is significantly lower compared to an analogous zirconium isopropoxide sample, *i.e.*, HS3 has the same parameters for the sol preparation and the found sphere size was ~400 nm.

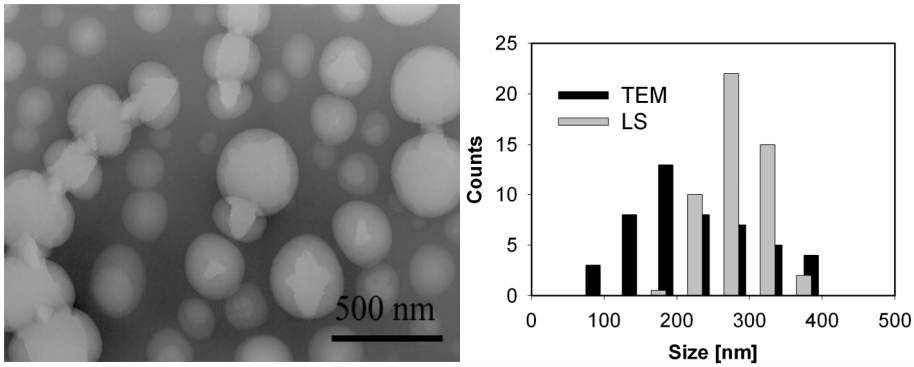

Figure 9.7: TEM image of titanium n-propoxide derived material and size distributions (sample HS7).

The possibility of using a Hacac modified zirconium *n*-propoxide precursor was also evaluated. The resulting hollow spheres (sample HS8) were more uniform and had a size distribution between 100-150 nm, which is significantly lower than when to an equal composition using modified zirconium isopropoxide. The formation of smaller sized spheres for *n*-propoxide systems, which was observed for both zirconium and titanium *n*-propoxide, is as one would expect. The ability of alcohols to form emulsions improves with the length of the chain, *i.e*., there is an increase going from isopropanol, *n*-propanol, *n*-butanol.

The possibility to use Hthd as the modifying ligand was also briefly examined. This bulkier modifier has a stronger chelating effect than Hacac and leads to less reactive modified species, *i.e*., the metal-oxygen bond length of the alkoxide ligands in the modified species is shorter [30,31]. The sol obtained from the Hthd systems (sample HS8) did not differ in appearance from the Hacac modified zirconium sols. No precipitation was formed during the hydrolysis and condensation sequence as was seen in the titanium isopropoxide system. However, the dried samples did not display the expected morphology whereas the TEM samples displayed an amorphous film. Further examination of this system is required to pin point what caused the formation of this amorphous material.

Encapsulation

The possibility of preparing hollow spheres made it very interesting to examine their ability to encapsulate organic molecules and evaluate their possible reactivity. We used two organic dyes, *i.e.*, methylene blue (3,9-bis-dimethylaminofenazotioniumchloride) and Eriochrome Black T (Erio-T) and added them to the propanol/water solution. The strongly colored solutions were used as the hydrolysis medium. The dye containing propanol/water solutions was added to solutions of the Hacac modified zirconium isopropoxide precursors in, either, hexane or isopropanol for comparison. If encapsulation occurs in the system where the precursor is dissolved in hexane it should give a distinctly different color compared to the systems that have no ability to form inverted micelles and thus encapsulation.

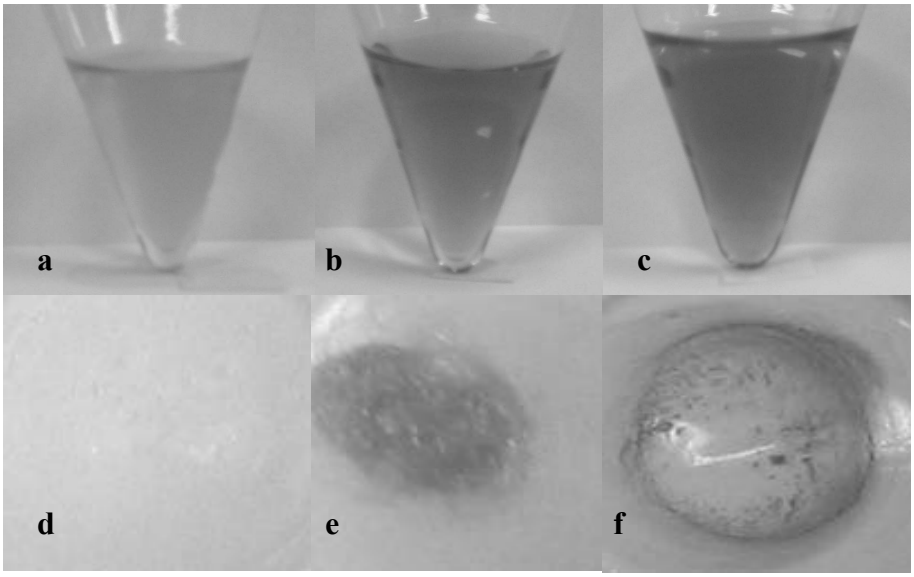

*Figure 9.8: Eriochrom Black T solutions with the same total concentration in **(a)** emulsion formed by introduction of propanol/water solution of the dye into hexane solution of the modified precursor, **(b)** emulsion formed by introduction of propanol/water solution of the dye into propanol solution of the modified precursor, **(c)** solution in hexane/propanol/water mixture as in **(a)** but in the absence of precursor. The powder obtained upon drying of solution **a-c** is depicted in **d-f**, respectively.*

For the system with the Erio-T dye, the resulting color of the prepared hexane based emulsion (Figure 9.8a) differed significantly from the system containing

only isopropanol as the solvent (Figure 9.8b) and the reference solution that contained the same concentration of the dye (Figure 9.8c). It should be noted that no noticeable color difference was observed for the dye dissolved in pure hexane or propanol. The colors of the reference solution and of the emulsion derived from the propanol-only solution are very similar. This is also in agreement with what should be expected for the propanol-only based emulsion, since there is no possibility for the formation of inverted micelles and thus, encapsulation. The only slight difference between Figure 9.8b and 0.8c is probably due to the presence of the zirconia particles. A clear difference can be seen between the color of those systems and the system where encapsulation is expected (Figure 9.8a). This solution is almost colorless, which clearly indicates a different behavior in the inverted micellar system. All solutions were dried and an almost white powder was obtained for the system with the encapsulated dye (Figure 9.8d). In contrast, the powder obtained from the propanol system (Figure 9.8e) and the reference solution (Figure 9.8f) is purple. An analogous behavior was observed when methylene blue dye was used. The observed color for the system where encapsulation occurs was yellow and for the system with only propanol, the color turned reddish.

It can thus be seen that with both dyes a distinct difference in color is observed. The change of color in the methylene blue system, where a difference between the pure indicator and both zirconium systems is observed, suggests that there is an interaction between zirconium cations and the indicator. The difference between the pure propanol and propanol/hexane systems indicates that there is a difference between the formed metal-oxide species in both systems. The particles formed from direct micelles, *i.e.*, in the system with propanol solvent, are dense metal-oxo cores of which the outer surface is covered with the modifying ligands. For a detailed discussion on the formation of this kind of species the interested reader is referred to ref. [21]. The difference between the direct and inverted micellar systems is found on the inside of inverted micelles since the boundary of the core that stays in contact with the hexane solvent will also consist of a high concentration of hydrophobic acac-ligands. The inside of the cores is expected to be covered with OH-groups. The fact that the difference between the inverted and direct micelles lies on the inside of the spheres proofs that the dyes are

encapsulated in the hollow spheres, since this is the only place where an difference in interaction with the dye can occur.

The zirconia nanoshells for the encapsulation of both dyes were prepared from a system where the solvent ratio hexane to isopropanol was 2:1. After the initial color change, as depicted in Figure 9.8a, precipitation occurred within a few minutes. Both crystalline and amorphous materials were produced. The life time of the system with Erio-T dye was significantly increased by lowering the amount of isopropanol and thus decreasing the size of the hollow spheres. After 15 hours precipitation was observed, again providing amorphous and crystalline components. The crystalline material obtained from both dyes was investigated in order to get insight into the processes occurring in the nano-spheres and to see if there is any reactivity from the hydroxide groups situated on the inner surface of the spheres (the formation mechanism for the MTSALs explaining the reasons of this unusual reactivity). The crystalline material in both cases consisted of $Zr(acac)_4$.

Encapsulation of the charged hydrophilic species, such as both of the chosen dyes, is evidently causing a partial reconstitution of the micelles. The protons of the hydroxide groups located on the inner side of the shells are apparently rather mobile. Their interaction with the organic reactants leads to proton transfer that destabilizes the micelles and causes formation of the $Zr(acac)_4$ molecules *via* ligand transfer. One of the driving forces for the destruction of the hollow spheres is the formation of the poorly soluble $Zr(acac)_4$. In the titanium system, the formation of a completely Hacac substituted compound does not occur and it can thus be expected that the stability of the encapsulated systems is significantly higher. Preliminary results on titanium systems are in agreement with this expectation, no observable change in the samples has occurred up to several months after preparation.

We have demonstrated that the templated micelles by self-assembly of ligands concept allows the preparation of hollow spheres and the ability to encapsulate hydrophilic molecules. These thin-walled shells have the potential for application in drug delivery. Moreover, these nanocapsules have the capability to include

encapsulation for pigment stabilization, protection of active ingredients in cosmetic industries, magnetic particles or ink.

9.4 Conclusions

It can thus be concluded that sol-gel processing of Hacac modified zirconium and titanium alkoxide precursors proceeds on the interface of a formed inverted micelle. The hydrolysis and condensation sequence involves the rearrangement of the acac ligands to the outer surface of the formed spheres and the formation of hydroxide groups on the inner surface. The mechanism allows encapsulation of hydrophilic compounds inside the hollow spheres. The presence of very reactive hydroxide groups inside the spheres implies their ability to transformation, and thereby eliminating the templating ligands. This transformation was observed in the zirconium system where it is possible to form the poorly soluble $Zr(acac)_4$, however, the results for this transformation were not noticeable in the titanium system after several months.

9.5 References

1 F. Tiarks, K. Landfester and M. Anonietti, *Macromol. Chem. Phys.*, **202**, 51 (2001).

2 N. Lapidot, O. Gans, F. Biagini, L. Sosonkin and C. Rottman, *J. Sol-Gel Sci. Technol.*, **26**, 67 (2003).

3 K. Landfester and L. Ramirez, *J. Phys.: Condens. Mater*., **15**, S1345 (2003).

4 T.M. Allen and P.R. Cullis, *Science*, **303**, 1818 (2004).

5 E.V. Batrakova, S. Li, Y. Li, V.Yu, Alakhov, W.F. Elmquist and A.V. Kabanov, *J. Control. Release*, **100**, 189 (2004).

6 S.-S. Feng, G. Ruan and Q.-T. Li, *Biomaterials*, **25**, 5181 (2004).

7 Z. An, G. Lu and H. Möhwald, J. Li, *Chem. Eur. J.*, **10**, 5848 (2004).

8 D.M. Vriezema, J. hoogboom, K. Velonia, K. Takazawa, P.C.M. Christianen, J.C. Maan, A.E. Rowan and R.J.M. Nolte, *Angew. Chem. Int. Ed*., **42**, 772 (2003).

9 P.Y. Bolinger, D. Stamou and H. Vogel, *J. Amer. Chem. Soc*., **126**, 8594 (2004).

10 F. Caruso, R.A. Caruso and H. Möhwald, *Science*, **282**, 1111 (1998).

11 D. Grosso, G.J.A.A. Soler-Illia, E.L. Crepaldi, B. Charleux and C. Sanchez, *Adv. Funct. Mater.*, **13**, 37 (2003).

12 C.Z. Yu, B.H. Tian, J. Fan, G.D. Stucky and D.Y. Zhao, *Chem. Lett*., 62 (2002).

13 C. Sanchez, J. Livage and M. Henry, *J. Non-Cryst. Solids*, **100**, 65 (1988).

14 J. Blanchard, F. Ribot, C. Sanchez, P.V. Bellot and A. Trokiner, *J. Non-Cryst. Solids*, **265**, 83 (2000).

15 G.I. Spijksma, H.J.M. Bouwmeester, D.H.A. Blank and V.G. Kessler, *Chem. Commun.*, 1874 (2004).

16 G.A. Seisenbaeva, S. Gohil and V.G. Kessler, *J. Mater. Chem.*, **14**, 3177 (2004).

17 Chapter 3 of this thesis.

18 F. Basolo and R. Pearson, "*Mechanisms of Inorganic Reactions*," Wiley Eastern Private Ltd; 2nd edition, (1973).

19 V.G. Kessler, *Chem. Commun*., 1213 (2003).

20 V.G. Kessler, *J. Sol-Gel Sci. Technol.*, **32**, 11 (2004).

21 Chapter 8 of this thesis.

22 SHELXTL-NT program manual, Bruker AXS, (1998).

23 J. Teixeira, *J. Appl. Cryst*., **21**, 781 (1988).

24 N. Baccile, D. Grosso and C. Sanchez, *J. Mater. Chem*., **13**, 3011 (2003).

25 P. Werndrup, M. Verdenelli, F. Chassagneux, S. Parola and V.G. Kessler, *J. Mater. Chem.,* **14**, 344 (2004).

26 M. Chatry, M. Henry, C. Sanchez and J. Livage, *J. Sol-gel Sci. Technol.*, **1**, 233 (1994).

27 R.J. Errington, J. Ridland, W. Clegg, R.A. Coxall, and J.M. Sherwood, *Polyhedron*, **17**, 659 (1998).

28 J. Ridland, PhD Thesis, University of Newcastle upon Tyne, UK, (1998).

29 J. Blanchard, M. In, B. Schaudel and C. Sanchez, *Eur. J. Inorg. Chem*., 1115 (1998).

30 Chapter 3 of this thesis.

31 Chapter 4 of this thesis.

Chapter 10

Preparation of microporous membrane materials from heterometallic titanium-zirconium precursors*

Abstract

Via sol-gel synthesis, composite titania-zirconia and titania-hafnia materials have been prepared from the precursors $Zr\{\mu\text{-}\eta^3\text{-}NH(C_2H_4O)_2\}_3[Ti(O^iPr)_3]$ (**1**), $Hf\{\mu\text{-}\eta^3\text{-}NH(C_2H_4O)_2\}_3[Ti(O^iPr)_3]$ (**2**), and $Zr\{\mu\text{-}\eta^3\text{-}NH(C_2H_4O)_2\}_3[Ti(O^nPr)_3]$ (**3**). The materials obtained after drying have been heat treated at various temperatures, in the range of 275-1200 °C. Nitrogen sorption measurements indicate the microporous nature of these materials when heat treated at temperatures around 400 °C. At lower temperatures, the materials appear to be nitrogen dense. With an increase in temperature, a significant decrease in the amount the micropores is observed and mesopores start to develop. Above 750 °C crystallization occurs and the presence of microporosity is no longer observed. Some key parameters for the sol-gel synthesis in the preparation of these materials have been evaluated. The acidity of the hydrolysis medium showed a dramatic influence on the sols. This can be explained by the removal of the basic stabilizing ligands when protons are introduced. The removal of the ligands leads to densification, and the resulting materials show only limited micropore volume. The initial results on the preparation and performance of the membranes derived from **3** are very promishing.

---

* Part of this chapter has been submitted for publication to *Adv. Mater.*:
"Zirconia titania composite microporous membrane material derived from diethanolamine modified precursors," Gerald I. Spijksma, Cindy Huiskes, Nieck E. Benes, Henk Kruidhof, Dave Blank, Vadim Kessler, and Henny J.M. Bouwmeester.

10.1 Introduction

In general, a major part of the total costs of chemical processes is associated with the molecular separation of different components, for instance the separation of products from reactants. In particular, for applications involving harsh conditions (high temperature, high pressure, aggressive chemicals, etc.) practical and economical viability is limited by the absence of robust unit operations for molecular separation. Clearly, for such processes, technological developments allowing sustained efficient separation would be of great consequence.

Membrane technology is considered a promising tool for achieving efficient separation [1]. A membrane is a semi-permeable barrier between two phases, which selectively influences the movement of one or more of the components present. For applications involving harsh conditions, inorganic membranes are considered particularly interesting. Inorganic materials generally possess superior structural stability compared to their organic counterparts, *e.g.*, no compaction and swelling [2]. Small pores present in an inorganic material, *i.e.*, pores with molecular dimensions, allow selective manipulation of the permeation of various components present. The overall transport of a particular component through the material is a complicated function of a component's mobility and its extent of sorption [3]. When small pores are present the mobility of the largest molecules is generally the lowest. The extent of sorption is generally determined by the affinity of a component for the pore surface, which in turn is influenced by, for instance, the presence of surface hydroxyl groups.

An inorganic membrane material which is commonly used is sol-gel derived silica. However, the moderate hydrothermal stability of this material means that its lasting application under harsh conditions is limited [4]. Particularly promising alternative materials for stable high performance membranes are sol-gel derived amorphous oxides of transition metals, such as TiO_2 and ZrO_2. These materials show superior stability compared to silica, however, their synthesis is complicated by the high reactivity of the required precursors [5].

Up to date, a few groups have been able to prepare amorphous TiO_2 [6-9] and ZrO_2 [10] membranes for aqueous nanofiltration. All of these membranes were prepared

from precursors that were modified either with chelating ligands or by adding acid to stabilize the colloidal sol-particles.

We recently proposed a model describing the mechanisms underlying the sol-gel synthesis of metal-oxide materials [11]. The model suggests that these materials are the product of templated micelles formed by self-assembly of ligands. It was demonstrated that choice of modifying ligands has a tremendous influence on the final materials morphology. When only chelating ligands or protons are used, the materials have the tendency to form spherical (nano-) particles and when coated, they form dense films. Nitrogen sorption measurements do not indicate a clear microporous nature of the derived materials. The selectivity of these materials observed in molecular separations could possibly be attributed to a pore structure that develops in the otherwise dense layer during burn-out of ligands, which have assembled upon drying. Therefore, these pores are a result of the coating/drying procedure and not an inherent property of the materials [11]. Previously, we have shown that this tendency to form dense materials can be avoided by using ligands which are both chelating and bridging. Therefore, we consider diethanolamine modified precursors interesting candidates for the preparation of intrinsically microporous materials, to be applied, for instance, as microporous membranes.

The recently developed $[Zr\{\mu\text{-}\eta^3\text{-}NH(C_2H_4O)_2\}_3[Ti(O^iPr)_3]]$ (**1**) precursor [12,13] seems to be an attractive starting point for the preparation of inorganic microporous composite materials. The precursor is thermodynamically stable, which avoids possible rearrangement of ligands. In contrast, Hacac modified precursors exhibit the tendency to concentrate modifying ligands on a single metal atom. This eventually yields mixtures of unreactive tetrasubstituted compounds and unmodified precursors [14,15]. Another advantage of **1** could lie in the mixing of metals at the atomic level. This can aid in avoiding phase transitions from amorphous to crystalline material, observed for pure titania and zirconia [16-19]. Commonly, zirconia is used as a dopant to avoid the phase transitions of titania [16,17], and yttria is a common dopant for zirconia [18,19]. The dopant is introduced by incorporation of nitrate salts into the sol, mixing of different sols, or by mixing of precursors prior to sol preparation. All these approaches can lead to homogenously mixed systems, however, probably not at the atomic level.

In the present study, the sol-gel synthesis of microporous materials derived from diethanolamine modified heterometallic precursors is attempted. The resulting material morphology and phase behavior are studied using nitrogen sorption, TGA/DSC, and XRD.

10.2 Experimental

All manipulations were carried out in a dry nitrogen atmosphere, using the Schlenk technique or a glove box. Hexane (Merck, *p.a.*) was dried by distillation after refluxing with $LiAlH_4$, *n*-propanol and isopropanol (Merck, *p.a.*) were dried by distillation after refluxing with the corresponding $Al(OPr)_3$ (for details see ref [20]). Diethanolamine (H_2dea) was purchased from Aldrich and was used as received.

The zirconium propoxide precursors used in this work are zirconium isopropoxide, ($[Zr(O^iPr)_4(^iPrOH)]_2$ 99.9%) and 70 wt% solution of "$Zr(O^nPr)_4$" (both purchased from Aldrich). Zirconium isopropoxide was dissolved in toluene and recrystallized prior to use. The titanium isopropoxide (99.999% pure) and titanium *n*-propoxide (98% pure) were both obtained from Aldrich. The hafnium isopropoxide was prepared by anodic oxidation of the hafnium metal in isopropanol [21] and recrystallized from toluene. $[Zr\{\mu\text{-}\eta^3\text{-}NH(C_2H_4O)_2\}_3[Ti(O^iPr)_3]]$ (**1**) and $[Hf\{\mu\text{-}\eta^3\text{-}NH(C_2H_4O)_2\}_3[Ti(O^iPr)_3]]$ (**2**) were prepared according to the procedure reported in ref. [13].

Sol preparation: Typical sols derived from **1** were prepared by dissolving 10.0 g of the precursor in a 90 ml mixture of hexane and isopropanol (volume ratio 2:1). Subsequently, a 0.10 M HNO_3 hydrolysis solution of 3 mol equivalent water and isopropanol (volume ratio 1:19), was rapidly added to the precursor mixture under vigorously stirring. Sols derived from **2** were prepared by mixing the zirconium *n*-propoxide and titanium *n*-propoxide together with diethanolamine and *n*-propanol (volume ratio 1:2:3:50). The hydrolysis solution, consisting of 10 mol equivalent water and 50 mol equivalent *n*-propanol (with respect to the zirconium precursor), was slowly added (~ 1 ml/min) to the precursor solution under vigorously stirring. The effect of pH was investigated by acidifying the hydrolysis solution, *i.e.*, 1.0 M HNO_3.

The sols from the hafnium-titanium precursor **2** were prepared in an analogous manner as described for the sols of **1**. The concentrations of the precursor solutions were in both syntheses the same and the amount of the hydrolysis solution was adjusted so that in both syntheses 3 mol equivalents of water was added to the precursor.

Powder and membrane formation: Powders were obtained by drying the sols overnight in a 10 cm Petri dish, followed by calcining in air for 3 hours in the range 250-800 °C. Membranes were prepared by dip-coating home made supported γ-alumina membranes two times with a sol derived from 2 under class 100 clean room conditions, followed by drying overnight and sintering at 400 °C for 3 hours in air.

Characterization: The particle size distributions in the sol were measured by dynamic light scattering (ZetaSizer 3000 HSa, Malvern). Thermo gravimetric analysis (TGA) and differential scanning calorimetric analysis (DSC) were performed using a combined TGA/DSC apparatus (Setsystem 16/18, Setaram). Measurements were performed in a nitrogen flow (20 ml/min) with a heating rate of 10 °C/min in the temperature interval 25-1200 °C. To analyze the burn-out of ligands, some experiments were repeated with a 50 ml/min helium sweep flow and a heating rate of 30 °C/min. A Gas Chromatograph – Mass Spectrometer (GC-MS) coupled to the TGA/DSC apparatus was used for detection of nitrogen in the sweep gas. The phase transformation behavior of dried uncalcined powder was studied by temperature programmed X-ray diffraction experiments (X'Pert-MPD, PANalytical, The Netherlands, tube: 40 kV, 50 mA, Cu$K\alpha_{1,2}$, θ compensating divergence slit: 10 mm length, 0.2 mm receiving slit, anti-scatter slit 10 mm). The X-ray diffraction pattern of calcined powders were recorded at ambient temperature (X'Pert-APD, PANalytical, The Netherlands, tube: 40 kV, 50 mA, Cu$K\alpha_{1,2}$, θ compensating divergence slit: 12 mm length, 0.1 mm receiving slit, 2° anti scattering slit). Pore size distributions were determined from volumetric nitrogen sorption experiments (Micromeretics, ASAP 2000). Prior to sorption measurements, samples were degassed at 250 °C under vacuum for 48 hours. Membranes were characterized by Scanning Electron Microscopy (LEO Gemini 1550 FEG - SEM, UK), XPS (Quantera XPS microprobe, Physical Electronics),

Membrane performance was analyzed by dead-end gas permeation (200 °C, p_{feed}=5 bar, $p_{permeate}$=1 atm).

10.3 Results and discussion

Clear sols were prepared from the heterometallic [Zr{μ-η^3-NH(C_2H_4O)$_2$}$_3$[Ti(O^{i}Pr)$_3$]] precursor. The sols were prepared in a solvent mixture of hexane/isopropanol (for details see the Experimental section) and powder was obtained by drying the sol over night.

Figure 10.1 shows TGA/DSC data for uncalcined powder derived from **1**. A sharp initial weight loss is observed with an onset at 50 °C, corresponding to the removal of adsorbed solvent molecules. Subsequently, a gradual decrease in weight is observed up to 300 °C. This is attributed to the removal of ligands from the outer surface of the material. Mass spectrometer analysis confirmed the presence of nitrogen in the sweep gas, originating from the amine groups of the ligands. In the range ~300-350 °C, a sharp decrease in weight is observed, which is accompanied by a large change in the heat flow centered at 350 °C. This can be attributed to the removal of ligands located inside the material. Mass spectrometry confirmed a high concentration of nitrogen in the sweep gas. Further increase of temperature to 450-600 °C causes removal of the remaining alkoxide ligands.

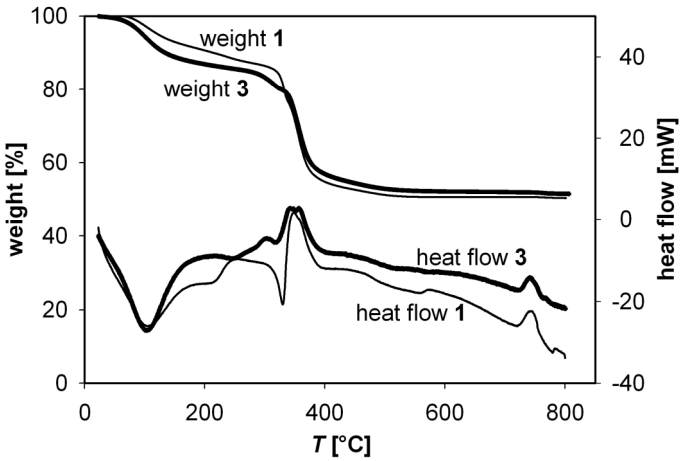

*Figure 10.1: TGA/DSC curves of titanium-zirconium material derived from **1** and **3**.*

The DSC data suggest that a phase transition occurs at ~750 °C. This temperature is considerably higher than those of phase transformations observed in pure titania and zirconia [16-19]. To confirm this, observation XRD experiments were performed on powders calcined at various temperatures and a selection of diffractograms is displayed in Figure 10.2. The formation of another phase is clearly observed at 750 °C, which is in agreement with the TGA/DSC data. The diffraction pattern obtained at 800 °C is clearly not in correspondence with the common patterns for titania or zirconia phases, *i.e.*, rutile, anatase and tetragonal or monoclinic.

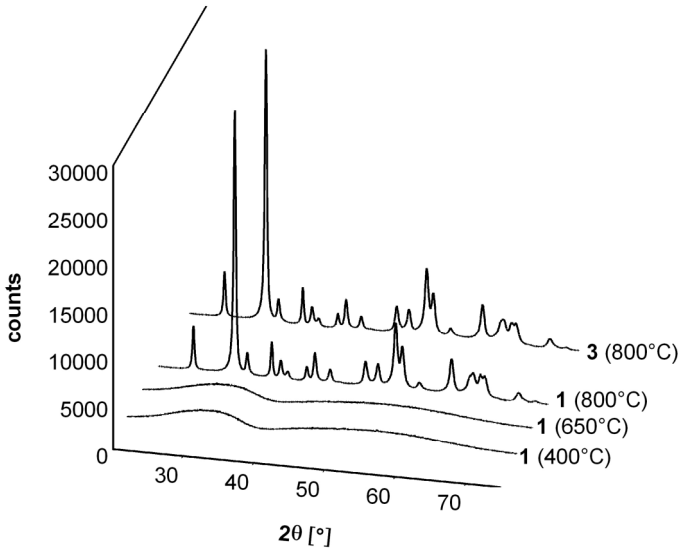

*Figure 10.2: XRD diffractograms for powders derived from **1** calcined at 400-650-800 °C and from **3** calcined at 800 °C.*

The broad peaks observed are indicative of a small particle size. For the powders calcined at 800 °C the diffractogram corresponds to orthorhombic Ti_2ZrO_6, commonly referred to as Srilankite [22]. Srilankite is found in nature as a volcanic mineral, and up to date, it could only be prepared at very high pressures and temperatures [23]. Sol-gel derived materials, prepared using mixtures of the precursor instead of a heterometallic precursor, showed XRD patterns that do not agree with that of pure srilankite [24]. The formation of pure srilankite *via* sol-gel synthesis presented in this work is thus very remarkable, and can be attributed to

the particular properties of the heterometallic precursor. Srilankite is of great interest to, for example, optics and dielectrics [25,26].

The beneficial properties observed for the heterometallic titanium zirconium precursor may also conceivably be observed for precursors based on different metal atoms. For instance, using **2** as precursor [13], the hafnium based analogue of srilankite could possibly be obtained. Powder from this precursor was prepared according to the procedure described in the experimental section and the TGA/DSC curves of the powder are depicted in Figure 10.3.

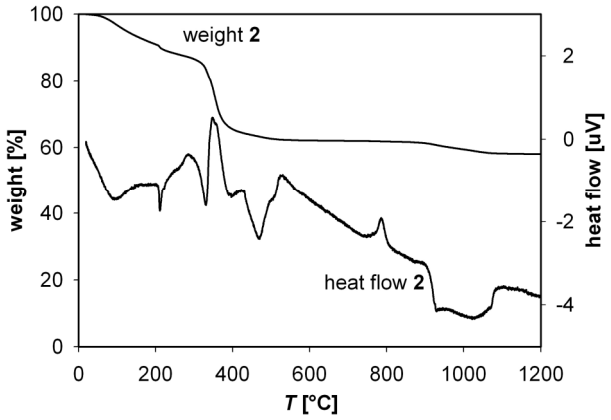

*Figure 10.3: TGA/DSC curves of titanium-hafnium material prepared from **2**.*

Between 25 and 500 °C a number of different groups are removed from the powder in an analogous manner as described above for the powder derived from **1**. At a temperature between 750 and 800 °C, a change in the trend of the heat flow is observed, while no noticeable change in the mass of the sample is seen. This indicates the occurrence of a phase transformation. From 950 °C changes in the mass of the sample and the heat flow are observed, this could be due to another phase transition or decomposition.

The phase behavior was studied using XRD and a selection of the obtained diffractograms is depicted in Figure 10.4. The material appears to be amorphous up to a temperature of 650 °C. At 750 °C (spectrum is not displayed) the formation of an orthorhombic crystalline phase is observed. The diffraction pattern at 800 °C is almost identical to that obtained for the srilankite material. The small shifts

observed in the peaks are most likely due to the different radii of hafnium and zirconium. Around 1100 °C (spectrum not displayed) a signal appears at ~26,5° 2θ, this suggests that decomposition occurs. The phases present at 1200 °C were indentified as $ZrTiO_4$ and rutile, confirming the phase transformation.

For materials obtained from the heterometallic precursors the phase transition from amorphous to orthorhombic occurs at high temperature (~750 °C). This makes them attractive for candidates for the preparation of microporous materials, for instance, to be used as membranes. The state of the art preparation of porous composites is typically performed by, for example, adding zirconium-oxy-nitrate hydrate to titanium alkoxide sols [16,17] or by mixing zirconium and titanium sols [27]. For a more elaborated discussion on the preparation of composite zirconium and titanium materials the interested reader is referred to ref. [16] and refs herein. In all of these strategies the crystallization of titanium and/or zirconium is observed at temperatures far below the temperature at which the phase transition towards the orthorhombic phase is observed in this work. The remarkable phase behavior of the materials derived from the heterometallic precursors is probably a result of the exceptionally homogeneous distribution of the different metal atoms, *i.e.*, on an atomic scale.

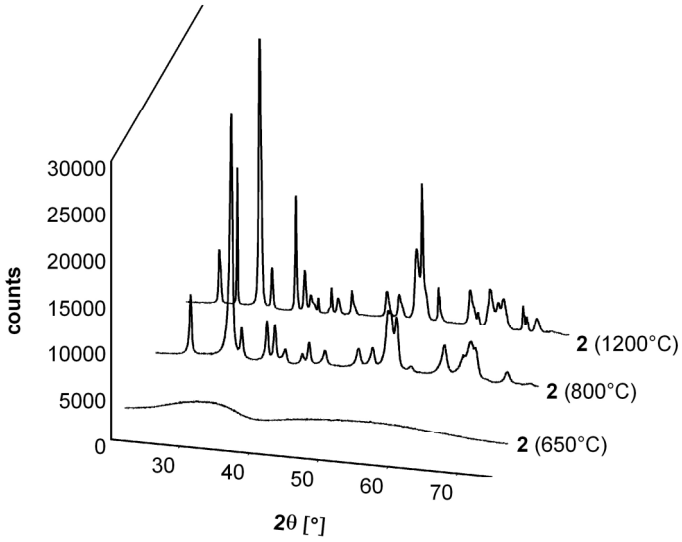

*Figure 10.4: XRD diffractograms for powders derived from **2** calcined at 650-800-1200 °C.*

Similar to silica, the materials derived from **1** and **2** are amorphous up to a certain temperature. This amorphous nature could possibly allow them to be microporous. This would make them applicable as membrane materials, for instance for nanofiltration and/or pervaporation processes. For silica, the state of the art of microporous membranes, microporosity is obtained using a 'polymeric' sol. The oligomers in the sol are polymeric structures with fractal dimensions in the range : $1 < df < 2.04$, and radii of gyration between 0.8 and 4 nm [28]. The BET surface area of these materials is between 400 and 900 m^2/g, depending on the synthesis conditions. Due to their microporous nature these materials show type I nitrogen sorption behavior [29].

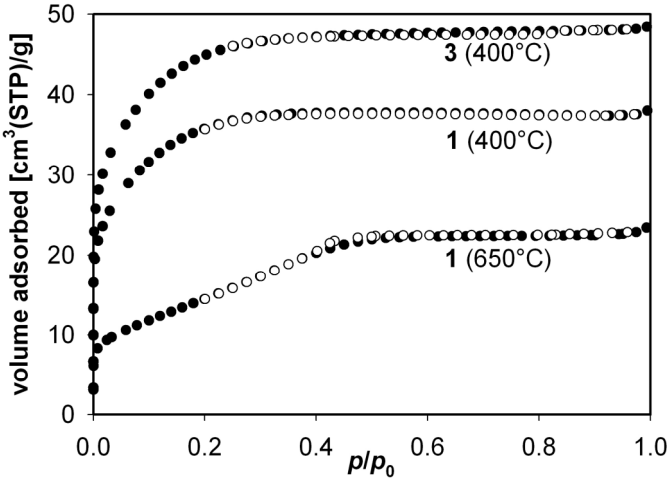

*Figure 10.5: Nitrogen sorption isotherms at 77K for the samples derived from **1** calcined at 400 and 600 °C and for a sample sderived from **3** calcined at 400 °C.*

In Figure 10.5 nitrogen sorption isotherms are presented for the powders derived from calcined at either 400 or 650 °C. The isotherm for the sample calcined at 400 °C is of Type I [29] with a high sorption capacity, which is only a factor of ~4 lower than that of state-of-the-art microporous silica [30]. The observed Type I sorption behavior is characteristic for microporous materials and, to the best of our knowledge, has not been reported before for zirconia- and titania-based materials. Commonly, sorption isotherms for these materials show a hysteresis loop, indicative for mesoporous materials possibly containing some micropores [31]. The material sintered at 650 °C no longer shows distinctive Type I sorption behavior. In

accordance with data from XRD the powder calcined at 800 °C has lost its amorphous nature and appears to be dense to nitrogen.

Figure 10.6 displays the pore size distributions for various materials calculated using the Horvath-Kawazoe method, assuming cylindrical pores (Saito-Foley model [32]). The samples calcined at 400 °C show a narrow pore size distribution, with the majority of pores being smaller than 1 nm. For the material calcined at 650 °C the average pore size is larger, but the pore volume has decreased significantly. An increase of the calcination temperature above the crystallization temperature, *i.e.*, 800 °C, leads to a complete disappearance of the micropores. For particles from powders calcined at 275 °C also no sorption of nitrogen was observed.

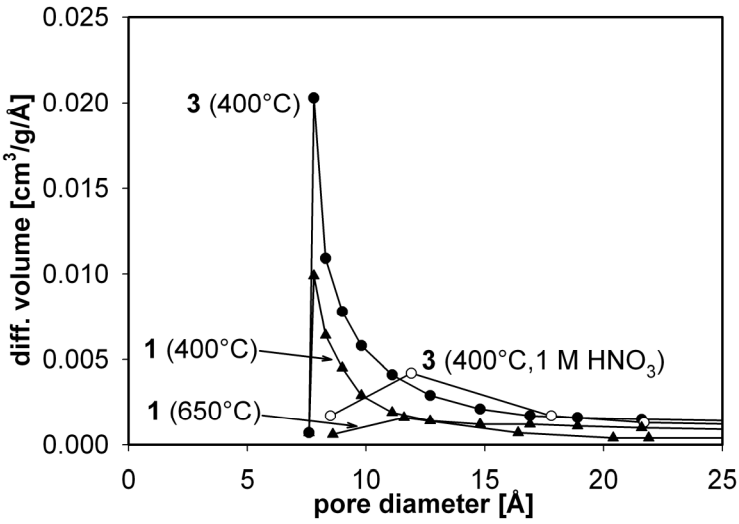

*Figure 10.6: Pore size distribution as function of the sintering temperature fpr samples of **1** and **3** calcined at various temperatures. 1 M HNO_3 refers to an acidified hydrolysis solution.*

We have seen that both the thermal properties and the morphology of the material derived from **1** displays great potential for the preparation of microporous membranes. The thermal properties of the material derived from **2** are also very promising. However, both of these precursor systems have drawbacks. For practical reasons it is often preferred to work with long chain alcohols, *e.g.*, *n*-propanol or *n*-butanol. This, on one hand, is due to the viscosity of these

alcohols, they provide a viscosity to the sol that allows deposition of films. On the other hand, the price of these precursors is significantly lower compared to that of, for instance, zirconium isopropoxide, *i.e.*, this latter precursor is about 10 times as expensive as zirconium *n*-propoxide. This price difference is obviously due to the reasons discussed elsewhere, *i.e.*, zirconium isopropoxide has a dinuclear structure where zirconium *n*-propoxide is a mixture of various compounds [33]. It would thus be interesting to see if the *n*-propoxide analog of **1**, would also lead to the formation of pure srilankite. The drawback for the preparation of this precursor is that it is not possible to crystallize it [13] and it can thus only be prepared by mixing zirconium *n*-propoxide, titanium *n*-propoxide and H_2dea in the proper ratios. The fact that it is not possible to purify the precursor by crystallization can have an influence on the purity of the precursor system and subsequently on the derived materials.

Figure 10.1 displays the TGA/DSC curves obtained powder derived from **3** according to the procedure described in the experimental section. The trend of the curves for this powder are similar to those obtained for the material obtained from **1**.

The phase purity of materials derived from **3** was evaluated by comparing its XRD difractograms for powder calcined at 800 °C with that of material derived from **1**. Both diffractograms are displayed in Figure 10.2 and it can be seen that the diffractograms are identical for both materials. The presence of oxo-species in the zirconium *n*-propoxide precursor [30] and impurities due to the mixing of the different starting materials does not seem to influence the properties of the derived materials.

The nitrogen sorption isotherm of the material derived from **3** was also determined (see Figure 10.5). The isotherm is clearly of Type I, and the saturation sorption capacity for the material derived from **3** is slightly larger, compared to the material derived from **1**, but this is likely due to experimental issues discussed in more detail below. The pore size distribution (Figure 10.6) of the material derived from **3** exhibits the largest volume of sub-nanometer pores. Apart from the larger sorption volume, the material derived from **3**, sintered at the same temperature, shows an almost similar pore-size distribution as that of the material derived from **1**.

The apparent difference in pore volume between the material derived from **3** and **1** cannot be addressed by any of the synthesis parameters at this point, since several parameters differed in the preparation of the sols. The morphology of the sol-gel derived material is determined by the choice of conditions throughout the entire synthesis pathway going from precursor to the eventual calcined material. The parameters involved in the synthesis include *e.g.*, the choice of precursor, the solvents used, concentrations, hydrolysis conditions, aging times of sols, deposition and drying conditions and heat treatment. All of these parameters can be used to optimize the synthesis of materials with specific properties, *e.g.*, for the application in microporous membranes. The influence of some of these parameters will be evaluated below.

The difference between the zirconium-titanium precursors used in this study lies in their alkoxide ligands, *i.e.*, isopropoxide vs. *n*-propoxide. In other work on the modification of zirconium and hafnium precursors we observed [34,35] that the metal-oxygen bond length of the alkoxide ligand decreased with an increasing inductive effect of the ligands, *i.e.*, the bond length decreased going from a isopropoxide to a *n*-propoxide ligand. This difference is also expected for the precursors discussed in this work. The difference in the bond lengths of the alkoxide ligands results in a different reactivity of the precursors [36], *i.e.*, the longer bond length of the *n*-propoxide ligands makes it more reactive. The difference in reactivity might lead to a difference in materials properties.

Another difference between the two different syntheses is the choice of solvent. For the isopropoxide precursor hexane and isopropanol are used, while in the other system, *n*-propanol is used. For the latter system the solvent has to be the parent alcohol, since it is not possible to separate or isolate this precursor from *n*-propanol. The choice of solvent can also have an influence on the morphology of the resulting sol-particles. In previous work [36] we have described that the formation of sol particles from pure alcohol systems proceeds through the formation of direct micelles. The sol particles for systems where acetylacetone modified zirconium and titanium alkoxides are used, it is known that sol particles are spherical oxo-species. The use of hexane and isopropanol as solvents can or will lead to an inverted micellar system. For Hacac modified precursors it results in the formation of hollow spherical sol particles [36,37]. It is not expected that the

morphology of the formed sol-particles, from either direct or inverted micellar systems, are analogous for a H_2dea modified system compared that observed for the Hacac modified systems. Since the mobility of the modifying ligands in the case of H_2dea modification is significantly lower *i.e.*, H_2dea acts both as a bridging and a chelating ligand, where Hacac is only chelating. It is interesting then to see whether the material obtained from a direct micellar system possesses the same microporous morphology as observed for the material from an inverted micellar system.

From the preparation of nanorods from zirconium *n*-propoxide modified with 0.5 mol equivalent [36] it is known that the pH plays an important role in the formation of the eventual product. The mobility of the diethanolamine ligands is influenced by the pH. Acidification of the hydrolysis solution may have a significant influence on the size and properties of the formed sol-particles, and thus on the properties of materials derived from these particles. Acidification causes protonation of amine-based ligands, such as the diethanolamine used in the present study, rendering them into better leaving groups. Consequently, more ligand molecules will be removed and, hence, densification of the colloidal sol particles will occur. This is essentially confirmed by the results from light scattering experiments. These indicate the presence of particles in the sol with a size of 50 nm when the hydrolysis solution is acidified, whereas the particle size is only 5 nm when water is used instead. Figure 10.6 shows the effect of acidification of the hydrolysis solution on pore size distribution of a powder calcined at 400 °C. Clearly, acidification of the hydrolysis solution results in a substantial decrease in the total micropore volume, combined with a shift of the average pore a larger value.

The further exploration of the effect of various synthesis parameters on the sol and material properties of these systems is still ongoing. Meanwhile these systems have been explored for the preparation of membranes[*]. Supported zirconia-titania films were prepared from a sol derived from **3** and characterized by SEM, XPS and single gas permeance. Figure 10.7a shows a SEM micrograph of the cross section

[*] This work is conducted at the University of Twente in collaboration with dr. ir. Nieck Benes (Eindhoven University) within the scope of his VIDI-grant. The experimental work is mainly performed by Cindy Huiskes.

of a resulting film. Clearly, a distinct layer with a thickness below 100 nm is present on top of the support. In agreement, XPS data indicate the presence of a ~20 nm layer of titanium zirconium oxide on top of the support, and ~60 nm infiltration of this material into the support.

Figure 10.7b shows single gas permeance data for different gases through the supported composite zirconia-titania film. The permeance for hydrogen is $3.0 \cdot 10^{-7}$ mol·m^{-2}s^{-1}Pa^{-1}, which is comparable to that of state-of-the-art silica membranes [30]. For methane the permeance is approximately a factor 2.8 lower, corresponding well with the square root of the ratio of molar masses of these molecules, *i.e.*, the Knudsen selectivity. The permselectivity of hydrogen with respect to propane is 6.7. This value is larger than the Knudsen selectivity (4.7) suggesting that mass transport does not only occur *via* Knudsen diffusion. With respect to butane the observed permselectivity is 54, which is considerably higher than expected for Knudsen diffusion. These data suggest that the pores in the composite film are larger compared to typical silica membranes, which show very high hydrogen/methane permselectivity, but are sufficiently small to inhibit the mobility of the larger butane molecules.

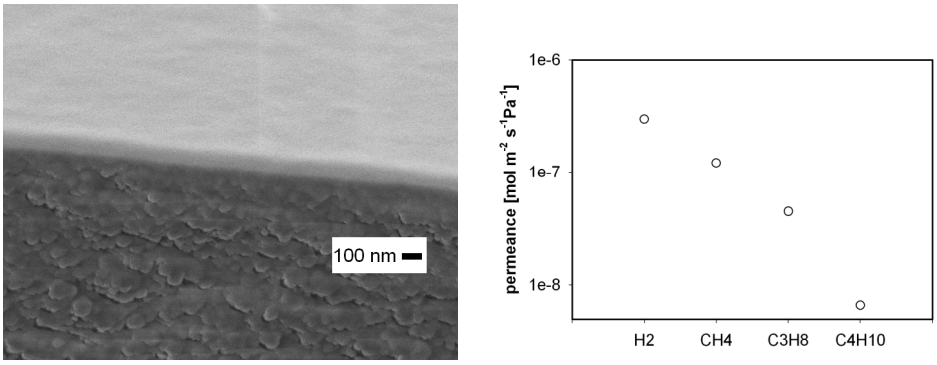

Figure 10.7: a) SEM micrograph of a membrane cross-section, and b) dead-end single gas permeance.

10.4 Conclusions

The preparation of orthorhombic phased materials from heterometallic zirconium-titanium and hafnium-titanium materials has been demonstrated. The derived material was subsequently heat treated at 800 °C. Srilankite, both the orthorhombic zirconium and titanium phase, has been prepared from **1** and **3**. The corresponding

hafnium-titanium orthorhombic phase was prepared from **3**. Srilankite is considered an interesting material for optical applications and dielectrics. The possibility of preparing it *via* sol-gel opens the door for the application of this interesting material.

One potential application, which is discussed within the scope of this work, is the use of srilankite as a material for microporous membranes. The material, derived from both zirconium-titanium precursors, displays a type 1 N_2 sorption isotherm which is typical for microporous systems when it is calcined at 400 °C. With an increase of the calcinations temperature a significant decrease of the amount the micropores is observed, *i.e*., the average pore size becomes larger, whereas the pore volume becomes dramatically smaller. An increase of calcinations temperature above the crystallization temperature, *i.e*., 800 °C, leads to a complete disappearance of the pores.

For the preparation of microporous membranes, the zirconium-titanium *n*-propoxide precursors is considered the most interesting candidate. Some of the key parameters for sol-gel synthesis of derived materials are evaluated. The influence of the solvents, *i.e.*, propanol and a mixture of propanol and hexane, does not seem to be very dominant, this is in contrast to systems where Hacac is used as a modifying ligand. The acidity of the hydrolysis medium was shown to have a dramatic influence on the derived sols and materials. The addition of acid leads to the removal of more of the basic modifying ligands and results in the densification of the derived material. The further exploration of the effect of various synthesis parameters on the sol and material properties of these systems is still ongoing. The initial results on the preparation and performance of the membranes derived from **3** are very promishing.

10.5 References

1 Innovation Roadmap Separation Technology, http://www.scheidingstechnologie.nl/RoadmapFinalReport.pdf, (2004).

2 A.J. Burggraaf and L. Cot, "*Fundamentals of Inorganic Membrane Science and Technology*,"X*VIII*, 690 (1996).

3 J.M. Van de Graaf, E. Van der Bijl, A. Stol, F. Kapteijn and J.A. Moulijn, *Ind. Eng. Chem. Res.*, **37**, 4071 (1998).

4 J. Campaniello, C.W.R. Engelen, W.G. Haije, P.P.A.C. Pex and J.F. Vente, *Chem. Commun*., 834 (2004)

5 J.C. Brinker and G.W. Scherer, "Sol-Gel Science: The Physics and Chemistry of Sol-Gel Processing," Elsevier, Florida, (1990).

6 P. Puhlfürß, A. Voigt, R. Weber and M. Morbe, *J. Membr. Sci*., **174**, 123 (2000).

7 T. Tsuru, D. Hironaka, T. Yoshioka and M. Asaeda*, Desalination*, **147**, 213 (2002).

8 T. Van Gestel, C. Vandecasteele, A. Buekenhoudt, C. Dotremont, J. Luyten, R. Leysen, B. Van der Bruggen and G. Maes, *J. Membr. Sci.*, **209**, 379 (2002).

9 J. Sekulic, J.E. ten Elshof and D.H.A. Blank, *Adv. Mater*., **16**, 1546 (2004).

10 T. Van Gestel, H. Kruidhof and H.J.M. Bouwmeester, In Preparation (2005).

11 Chapter 8 of this thesis.

12 G.I. Spijksma, H.J.M. Bouwmeester, D.H.A. Blank and V.G. Kessler, *Inorg. Chem. Comm*., **7**, 935 (2004).

13 Chapter 7 of this thesis.

14 G.I. Spijksma, H.J.M. Bouwmeester, D.H.A. Blank and V.G. Kessler, *Chem. Commun.*, 1874 (2004).

15 Chapter 3 of this thesis.

16 J. Sekulic, A. Magraso, J.E. ten Elshof and D.H.A. Blank, *Micropor. Mesopor. Mater*., **72**, 49 (2004).

17 D.-S. Bae, K.-S. Han, S.-H. Choi and E.J.A. Pope, "*Synthesis and characterization of TiO_2–ZrO_2 composite membranes*," In: Sol–Gel Processing of Advanced Materials, Ceramic Transactions vol. 81, American Ceramic Society, USA, p. 349 (1998)

18 L. Shi, K.C. Tin and N.B. Wong, *J. Mater. Sci*., **34**, 3367 (1999).

19 C.R. Foschini, O. Treu, S.A. Juiz, A.G. Souza, J.B.L. Oliveira, E. Longo, E.R. Leite, C.A. Paskocimas and J.A. Varela, *J. Mater. Sci*., **39**, 1935 (2004).

20 G.A. Seisenbaeva, S. Gohil and V.G. Kessler, *J. Mater. Chem*., **14**, 3177 (2004).

21 E.P. Turevskaya, N.I. Kozlova, N.Y. Turova, A.I. Belokon, D.V. Berdyev, V.G. Kessler and Y.K. Grishin, *Russ Chem. Bull*., **44**, 734 (1995).

22 A. Willgallis and H. Harti, *Z. Kristallogr*., **164**, 59 (1983).

23 U. Troitzsch, A.G. Christy and D. J. Ellis, *J. Am. Ceram. Soc*., **87**, 2058 (2004).

24 J.-C. Buhl and A. Willgallis, *Cryst. Res. Technol*., **24**, 263 (1989).

25 H. Köstlin, G. Frank, G. Hebbinghaus, H. Auding and K. Denissen, *J. Non-Cryst. Solids*, **218**, 347 (1997).

26 International Roadmap of Semiconductor Industry (ITRS), http://public.itrs.net/ (accessed 04-May-2005).

27 Q.Y. Xu and M.A. Anderson, *J. Am. Ceram. Soc*., **76**, 2093 (1993).

28 R.S.A. De Lange, J.H.A. Hekkink, K. Keizer and A.J. Burggraaf, *J.Membr.Sci*., **99**, 57 (1995).

29 IUPAC Recomendations, *Pure Appl. Chem*., **57**, 603 (1985).

30 R. De vos, PhD thesis, University of Twente, The Netherlands, (1998).
31 J. Sekulic, PhD thesis, University of Twente, The Netherlands, (2005).
32 A. Saito and H.C. Foley, *AIChE J.*, **37**(3), 429 (1991).
33 Chapter 2 of this thesis.
34 Chapter 4 of this thesis.
35 Chapter 5 of this thesis.
36 Chapter 8 of this thesis.
37 Chapter 9 of this thesis.

Chapter 11

Conclusions and recommendations

Abstract

The main conclusions of the conducted research and the recommendations resulting from them are discussed. The effect of modifying ligands on the sol-gel process is briefly highlighted, followed by a discussion on the precursor modification and the (up to date identified) resulting material morphologies for the different modifiers that were examined in this study. The used modifiers include *β*-diketones (acetylacetone (Hacac) and 2,2,6,6,-tetramethyl-3,5-heptanedionate (Hthd)), *β*-diketoesters (ethylacetoacetate (eaoac) and *t*-butylacetoacetate (tbaoac)) and alkanolamines (diethanolamine (H_2dea)).

11.1 Introduction

The application that was aimed for when this research project was formulated was the synthesis and characterization of a new generation of thin oxide layers with nanostructured pore morphologies. One of the key issues for the development of these materials was the understanding of the chemistry involved in the preparation. The anticipated synthesis method for the preparation of the materials is sol-gel. The lack of understanding of the role of modifying ligands was in the early stages of the research identified as the main challenge.

The general aim of the work described in this thesis became understanding of the influence of modifying ligands on precursors and sol particles. More specifically, their role in the mechanisms and transformations due to the hydrolysis and condensation sequence were requested. To be able to evaluate the role in the sol-gel process the interaction of the modifier with the alkoxide precursor needs to be understood. Therefore the structure and stability of the modified precursors is examined. The scope with respect to the modification of precursors is to find a modification that is thermodynamically stable since the use of a stable precursor will contribute to the reproducible preparation of materials. The main conclusions of the conducted research and the recommendations resulting from them are discussed below.

11.2 Role of modifying ligands in the sol-gel process

In this thesis a new concept is presented concerning the reaction mechanism involved in the sol-gel processing of metal-alkoxides. Ligand exchange and hydrolysis proceed through a proton assisted S_N1 mechanism, in contrast to a S_N2 hydrolysis mechanism, which is operative for silicon alkoxides in basic media. The exchange of ligands, hydrolysis and also the condensation reaction proceeds almost instantaneously for metal alkoxides. The products of the fast hydrolysis and condensation sequence consist of micelles templated by self-assembly of ligands (mainly oxo-spiecies). Another striking difference compared with traditional silica sol-gel is the mobility of the modifying ligands. The concept presented provides explanations for commonly observed material properties and allows for the development of new strategies for the preparation of materials. The morphology of the obtained materials is strongly influenced by the modifier that is used. The

precursor modification and the (up to date identified) resulting material morphologies will be discussed for the different modifiers that were examined in this study.

11.3 β-diketones

The β-diketones considered in this study were acetylacetone (Hacac) and 2,2,6,6,-tetramethyl-3,5-heptanedionate (Hthd). The modification of zirconium and hafnium propoxides with Hacac is frequently applied in sol-gel synthesis and Hthd is the modifier for the first generation zirconium and hafnium alkoxide MOCVD sources. The modification of propoxide precursors is generally assumed to include the formation of species modified with 0.5 (only for Hacac modification), 1 and 2 mol equivalents. It was found that the modification involves the formation of rather unstable mono- and trisubstituted zirconium compounds and no evidence was found for the existence of 0.5 and 2 mol equivalent modified species. The modification of zirconium and hafnium *t*-butoxides with 2,2,6,6,-tetramethyl-3,5-heptanedione (Hthd) involves the formation of di- and trisubstituted compounds. The difference in modification between the *t*-butoxide and propoxide precursors is due to the larger size of the alkoxide ligand. The formation of a monosubstituted compound is not possible due to steric hindrance. The steric hindrance causes also that the expected inductive effect of the larger alkoxide ligands *i.e.*, the metal-oxygen bond lengths of the alkoxide ligands of the *t*-butoxides are expected to be shorter than those of the propoxides, is not observed. The influence of steric hindrance on the length of the metal–oxygen bonds of the alkoxide ligands is also observed in the Hthd modification of hafnium propoxides. The metal–oxygen bond lengths of the alkoxide ligands are not following the trend one would expect on basis of the inductive effect of the different alkoxide ligands, *i.e.*, the *n*-propoxide compound displays shorter bond compared to the isopropoxide. This effect is not observed in the zirconium isomorphs, which reflects the smaller atomic radius for hafnium compared to zirconium, resulting from lanthanide contraction.

The NMR studies of these compounds revealed that all the obtained compounds are not stable in solution in time. The rearrangement to a tetrasubstituted compound could clearly be seen. This solution instability makes these systems unattractive for

application in preparations, where high reproducibility of prepared materials is required.

The sol particles for Hacac modified systems are direct micelles containing oxo-species and a surface covered with acetylacetone. The material preparation from these systems leads to the formation of dense nanoparticles and dense films. The Hacac modified precursor systems are thus not suitable for the preparation of microporous membranes. The reported porosity in these systems is probably due to the porosity of the support and the required controlled drying of the film.

The formation of inverted micelles, which can be obtained by the appropriate choice of solvents, allows the formation of hollow spheres. The hydrolysis and condensation sequence involves the rearrangement of the acac ligands to the outer surface of the formed spheres and the formation of hydroxide groups on the inner surface. The mechanism allows encapsulation of hydrophilic compounds inside the hollow spheres. The possible use of these interesting materials is not yet defined. The potential for application of these thin-walled shells could include encapsulation for pigment stabilization, protection of active ingredients in cosmetic industries, magnetic particles or ink.

11.4 β-diketoesters

The application of β-diketoesters for the modification of precursors is rarely considered. The modification of zirconium and hafnium propoxides with ethylacetoacetate (eaoac) and *t*-butylacetoacetate (tbaoac) resulted in mono- and disubstituted compounds. The formation of a disubstituted compound in these systems, which is in contrast with the modification with β-diketones, is attributed to trans-stabilization of the alkoxide ligand by the alkyl containing site of the chelating ligand. The NMR studies in time on solution of the tbaoac modified propoxide precursors demonstrated that the disubstituted compounds are stable in time. The only changes in the NMR spectra in time are due to transesterfication of the alkyl and alkoxide ligands.

The modification for zirconium and hafnium *t*-butoxides by *t*-butylacetoacetate (the alkyl and alkoxide ligands are similar, thus transesterfication is not possible in these systems), involved the formation of mono-, di- and trisubstituted compounds.

The steric hindrance arising from the larger alkoxide ligands makes that the trans-stabilization of the alkoxide ligands does not occur. This results in the modified species not stable in solution, *i.e.*, rearrangement to a tetrasubstituted compounds occurs also in these systems.

The stable disubstituted compounds could be of great interest in sol-gel application and the transesterfication of the alkyl and alkoxide ligands can easily be avoided by proper choice of ligands and modifier, *i.e.*, they should be the same. The effect of these modifying ligands on the sol-gel processing of and the morphology of the derived materials has not been investigated yet.

11.5 Alkanolamines

The modification of precursors by alkanolamines involved mainly the use of diethanolamine. The modification of zirconium *n*-propoxide and mixed ligand precursor with 0.5 mol equivalent of H_2dea resulted in the compounds $[Zr_2(O^nPr)_6(OC_2H_4)_2NH]_2$ and $[Zr_2(O^nPr)_2(O^iPr)_4(OC_2H_4)_2NH]_2$. These complexes were only moderately stable in both solution and solid state. A very interesting feature from these modified precursors (in our studies we used the pure *n*-propoxide modification) is the formation of zirconia nanorods. Their formation proceeds through a sol-gel synthesis involving direct micelles. The alkoxide ligands of the precursor in bridging positions play a decisive role in the formation of the nanorods. Further exploration and optimization of these very interesting systems is required.

The obtained trinuclear complex, $Zr\{\mu\text{-}\eta^3\text{-}NH(C_2H_4O)_2\}_3[Zr(O^iPr)_3]_2(^iPrOH)_2$, obtained upon modification of zirconium isopropoxide with 1 mol equivalent of H_2dea, displayed solution stability. The presence of two types of positions in the latter compound, a nona-coordinated and a hexa-coordinated one, provided the possibility to construct new species *via* self-assembly. This was demonstrated by the development of an analogous titanium-zirconium and titanium-hafnium compounds. In the absence of alkoxide ligands in bridging position, which are growth-directing ligands for the formation of nanorods, microporous materials can be obtained. The material, derived from the zirconium-titanium precursors and calcined at temperatures around 400 °C, displays a *type 1* N_2 sorption isotherm

which is typical for microporous systems. These systems show a great potential for the preparation of microporous membranes.

Another fascinating property of these heterometallic precursors is the ability to form srilankite phase materials. The formation of srilankite from sol-gel derived materials occurs around 750 °C. It would be tremendously interesting to see whether or not this phase can also be obtained by MOCVD or ALD processing of these precursors, as srilankite is a potential high-k material. The hafnium-titanium and especially the zirconium-titanium compounds are volatile, which is a requirement for the proposed processing.

The interesting properties of these materials have contributed to two initiatives for their further exploitation. The first one focuses on the preparation of microporous membranes from the zirconium-titanium precursor. The initial results evaluating the influence of several synthesis parameters are included in this thesis. It is shown that the influence of the solvents, *i.e.*, propanol and a mixture of propanol and hexane, seems not to be very dominant. The acidity of the hydrolysis medium and the speed of addition have a dramatic influence on the properties of the derived sols and materials. The addition of more acid leads to the removal of more of the basic modifying ligands and a densification of the material occurs.

The other initiative (for which a funding proposal is due to be submitted at time this is written) involves the development of new precursors that have modifying ligands in both chelating and bridging position (as is the case for the diethanolamine modified precursors). It includes the synthesis of suitable ligands, evaluation of the effect of these ligands on the sol-gel process and derived materials and should eventually lead to microporous membranes.

The in this thesis proposed mechanism for sol-formation, MTSAL, has been exploited by groups at SLU to develop a method for gel encapsulation in aqueous media. The proper choice of a modified titanium alkoxide, *i.e.*, alkanolamines modified, allows for the preparation of a sol *via* direct micelles in alcohol, whereas subsequent transfer of the sol to aqueous conditions leads to the possibility of gel-encapsulation in biocompatible conditions. Further exploration of these tremendously interesting systems will be conducted at SLU.

Summary

This thesis deals with the influence of modifying ligands on the structure and stability of zirconium and hafnium precursors. The applicability of the obtained modified alkoxides has been evaluated for MOCVD and sol-gel. Furthermore, the influence of the introduction of heteroligands on the sol-gel process and their effect on the derived materials has been addressed. A specific focus has been on the preparation of microporous materials by sol-gel for the application in membranes.

Several precursors like $[Zr(O^iPr)_4(^iHOPr)]_2$, $[Hf(O^iPr)_4(^iHOPr)]_2$ and $[Zr(O^nPr)(O^iPr)_3(^iPrOH)]_2$ have been used of which the molecular structures are known. In contrast, the composition of commercial "$Zr(O^nPr)_4$" was not known, since it is hidden by the added *n*-propanol. Its composition consists of (at least) four compounds of which $Zr_4(O^nPr)_{16}$ (65-70%) is the major one. The other compounds include $Zr_3O(O^nPr)_{10}$ and most likely another tetranuclear oxo-specie. The molecular structure of the major compound in hafnium *n*-propoxide seems to be different from that in zirconium *n*-propoxide. The presence of $Zr_3O(O^nBu)_{10}$ in zirconium *n*-butoxide was demonstrated by mass spectrometric experiments.

Precursor modification

The modification chemistry of β-diketones, β-diketoesters and alkanolamines on zirconium and hafnium alkoxide precursors was investigated. The modification of zirconium and hafnium propoxides with acetylacetone (Hacac) is frequently applied in sol-gel synthesis and it is generally assumed to include the formation of species modified with 0.5, 1 and 2 mol equivalents. On the basis of the characterization of isolated compounds, however, it was found that modification involves the formation of rather unstable mono- and trisubstituted zirconium compounds. No evidence was found for the existence of 0.5 and 2 mol equivalent modified species. The poor stability of these compounds upon modification with Hacac needs to be considered if they are used for the preparation of materials.

The mechanism of modification of zirconium and hafnium propoxide precursors with 2,2,6,6,-tetramethyl-3,5-heptanedionate (Hthd) was found to be analogous to that proposed above for the modification with Hacac. It involves mono- and trisubstituted intermediate compounds and does not involve a disubstituted

compound. Thus, the commercial product claimed to be "$Zr(O^iPr)_2(thd)_2$" and most commonly "used" for the MOCVD preparation of ZrO_2 does not exist. The isolation of purely trisubstituted compounds is complicated since the mono- and tetrasubstituted compounds tend to crystallize more easily in most cases. As a result these compounds or a mixture are obtained. In the obtained trisubstituted compounds, the expected increased inductive effect on going from *n*-propoxide to isopropoxide ligands is clearly observed. Formation of the dimeric hydroxo-di-thd-substituted complex, $[Hf(O^iPr)(OH)(thd)_2]_2$, was observed only for the hafnium-based system and results from a reaction of $Hf(O^iPr)(thd)_3$ and $[Hf(O^iPr)_3(thd)]_2$ upon micro-hydrolysis. Most of the obtained compounds have a limited stability which makes them rather unsuitable for MOCVD applications.

A structural characterization of the tetra-thd complexes of zirconium and hafnium was performed in order to reveal the reasons for their unusual physico-chemical properties. It was found that the relatively short distance between the nearest methyl carbon atoms of the neighboring molecules due to strong van der waals interactions in combination with the dense packing effect are most likely responsible for the low solubility and volatility of these compounds.

The modification of zirconium and hafnium *t*-butoxides with 2,2,6,6,-tetramethyl-3,5-heptanedione (Hthd) has been investigated. For the modification with Hthd, the formation of di- and trisubstituted compounds is observed. The difference in modification between the *t*-butoxide and propoxide precursors is due to the larger size of the alkoxide ligand. The formation of a monosubstituted compound is not possible due to steric hindrance. NMR studies of these compounds revealed that in solution they are not stable in time. The rearrangement to a tetrasubstituted compound could clearly be seen. The expected inductive effect of the larger alkoxide ligands *i.e.*, the metal–oxygen bonds of the alkoxide ligands of the *t*-butoxides are expected to be shorter than those of the propoxides, is not observed due to the steric hindrance,

The modification of zirconium and hafnium isopropoxide with ethylacetoacetate and *t*-butylacetoacetate (tbaoac) results in mono- and disubstituted compounds. NMR studies of solutions of the tbaoac modified alkoxides indicated that the disubstituted compounds are stable in time. The only changes observed in the

NMR spectra are due to transesterfication of the alkyl and alkoxide ligands. The thermodynamically stable disubstituted compounds could be of great interest in sol-gel application and the transesterfication of the alkyl and alkoxide ligands can easily be avoided by proper choice of ligands and modifier, *i.e.*, they should be the same.

NMR studies on zirconium and hafnium *t*-butoxides modified by tbaoac showed that modification involves the formation of mono-, di- and trisubstituted compounds. It turned out that these compounds are not stable in solution. In these systems the disubstituted compounds were not stable, the size of the *t*-butoxide ligands causes steric hindrance which disables the trans-stabilization of the alkoxide ligands.

The modification of zirconium *n*-propoxide and mixed ligand precursor with 0.5 mol equivalent of H_2dea results in formation of $[Zr_2(O^nPr)_6(OC_2H_4)_2NH]_2$ and $[Zr_2(O^nPr)_2(O^iPr)_4(OC_2H_4)_2NH]_2$. These complexes are only moderately stable in both solution and solid state. The trinuclear complex, $Zr\{\mu\text{-}\eta^3\text{-}NH(C_2H_4O)_2\}_3[Zr(O^iPr)_3]_2(^iPrOH)_2$, obtained upon modification of zirconium isopropoxide with either 0.5 and 1 equivalent mol of H_2dea, displays solution stability. The presence of two zirconium cations coordinated differently, a nona-coordinated and a hexa-coordinated one, provides the possibility to derive new species from this precursor *via* self-assembly. This was demonstrated by the development of an analogous titanium-zirconium and titanium-hafnium compounds, $Zr\{\mu\text{-}\eta^3\text{-}NH(C_2H_4O)_2\}_3[Ti(O^iPr)_3]_2$ and $Hf\{\mu\text{-}\eta^3\text{-}NH(C_2H_4O)_2\}_3[Ti(O^iPr)_3]_2$.

Role of modifying ligands in the sol-gel processing

The influence of modifying ligands on the sol-gel chemistry of metal alkoxides and the effect of these ligands on the morphology of the derived materials has been considered. A comparison of the bond lengths and of the effective charges of the metal atoms in modified and unmodified compounds combined with data from simple calorimetric experiments indicated that the reactivity of modified metal alkoxides increases rather than decreases upon modification. A new concept is presented concerning the reaction mechanism involved in the sol-gel processing of

metal-alkoxides. Ligand exchange and hydrolysis proceeds through a proton-assisted S_N1 mechanism, in contrast to a S_N2 hydrolysis mechanism, which is operative for silicon alkoxides in basic media. The exchange of ligands, hydrolysis and also the condensation reaction proceeds almost instantaneously for metal alkoxides. The products of the fast hydrolysis and condensation sequence consist of micelles templated by self-assembly of ligands (mainly oxo-spiecies). Another striking difference compared with traditional silica sol-gel is the high mobility of the modifying ligands. The concept presented in this thesis provides explanations for commonly observed material properties and allows for the development of new strategies for the preparation of materials.

The formation of dense nanoparticles from acetylacetone modified or acid 'catalyzed' system and the formation of dense films from acetylacetone modified precursors are discussed in this thesis. The sol particles for these systems are direct micelles containing oxo-species and a surface covered with acetylacetone or positively charged centers as a result of the acid addition. The formation of inverted micelles, which can be obtained by the appropriate choice of solvents, allows the formation of hollow spheres. The modifying acetylacetone ligands act as surfactant and form the interface between the hollow sphere and the solvent. The formation of hollow spheres was demonstrated for zirconium *n*-propoxide, zirconium isopropoxide and titanium *n*-propoxide precursors. Additionally, the possibility to encapsulate hydrophilic species in these spheres is shown. Another example, formed from a direct micellar system, is the formation of zirconia nanorods from a highly anisotropic diethanolamine (H_2dea) modified precursor. The alkoxide ligands of the precursor in bridging positions play a decisive role in the formation of the nanorods. In the absence of these growth-directing ligands a microporous material can be obtained for H_2dea modified precursors. The results presented in this thesis have been exploited by groups at SLU to develop a method for gel encapsulation in aqueous media. The proper choice of a modified titanium alkoxide allows for the preparation of a sol via direct micelles in alcohol, whereas subsequent transfer of the sol to aqueous conditions leads to the possibility of encapsulation in biocompatible conditions.

The formation of microporous materials with diethanolamine modified precursors was further explored using the developed heterometallic precursors. The

preparation of srilankite from $Zr\{\mu\text{-}\eta^3\text{-}NH(C_2H_4O)_2\}_3[Ti(O^iPr)_3]$ and $Zr\{\mu\text{-}\eta^3\text{-}NH(C_2H_4O)_2\}_3[Ti(O^nPr)_3]$ and $Hf\{\mu\text{-}\eta^3\text{-}NH(C_2H_4O)_2\}_3[Ti(O^iPr)_3]$ precursor has been demonstrated. The material is formed after drying and annealing at ~750 °C of sol-gel derived powder. The materials derived from the zirconium-titanium containing precursors display a type 1 N_2 sorption isotherm, which is typical for a microporous material, when they are calcined at temperatures around 400 °C. These materials show great potential for the preparation of microporous membranes. For the preparation of the membranes, the influence of several synthesis parameters was evaluated. The influence of the solvents, *i.e.*, propanol and a mixture of propanol and hexane, seems not to be very dominant. The acidity of the hydrolysis medium and the speed of addition have a dramatic influence on the derived sols and materials. The addition of more acid leads to the removal of most of the modifying ligands. As a result, the pH of the solution increases and densification of the sol particles occurs.

Samenvatting

Dit proefschrift behandelt de invloed van modificerende liganden op de structuur en stabiliteit van zirkonium en hafnium precursors. De toepasbaarheid van de verkregen gemodificeerde alkoxides is geëvalueerd voor MOCVD en sol-gel toepassingen. Voorts wordt aandacht besteed aan de invloed van de introductie van hetero-liganden op het sol-gel proces en hun effect op de afgeleide materialen. Een bijzonder aandachtspunt is daarbij de bereiding van micro-poreuze materialen *via* de sol-gel synthese voor toepassing als membranen.

Er is gebruik gemaakt van verschillende precursors zoals $[Zr(O^iPr)_4(^iHOPr)]_2$, $[Hf(O^iPr)_4(^iHOPr)]_2$ en $[Zr(O^nPr)(O^iPr)_3(^iPrOH)]_2$, waarvan de moleculaire structuren bekend zijn. Daarentegen was de samenstelling van commercieel "$Zr(O^nPr)_4$" onbekend, omdat deze wordt verborgen door de toegevoegde *n*-propanol. De samenstelling hiervan bestaat uit een viertal componenten, waarvan 65-70% $Zr_4(O^nPr)_{16}$ is. De andere componenten bevatten $Zr_3O(OPr)_{10}$ en andere oxo-componenten. De aanwezigheid van $Zr_3O(OBu)_{10}$ is ook aangetoond in een analoge studie uitgevoerd op het commercieel verkrijgbare zirkonium *n*-butoxide.

Precursor modificatie

De chemische modificatie van *β*-diketones, *β*-diketoesters en alkanolamines op zirkonium en hafnium alkoxide precursors is onderzocht. De modificatie van zirkonium en hafnium propoxides met acetaylacetone (Hacac) wordt veelvuldig toegepast in de sol-gel synthese en in het algemeen wordt aangenomen dat dit de vorming van de verbindingen gemodificeerd met 0.5, 1 en 2 mol equivalenten omvat. Op basis van de karakterisering van de geïsoleerde verbindingen bleek dat de modificatie leidt tot de vorming van redelijk onstabiele mono- en tri-gesubstitueerde zirkonium samenstellingen. Geen bewijs is gevonden voor het bestaan van 0.5 en 2 mol equivalent gemodificeerde verbindingen. De gebrekkige stabiliteit van deze samenstellingen na modificatie met Hacac moet in overweging worden genomen als ze gebruikt worden voor de bereiding van materialen.

Het mechanisme van modificatie van zirkonium en hafnium propoxide precursors met 2,2,6,6,-tetramethyl-3,5-heptanedionate (Hthd) bleek analoog te zijn aan dat hierboven beschreven is voor de modificatie met Hacac. Modificatie leidt wel tot

mono- en tri-gesubstitueerde samenstellingen tot gevolg, maar niet tot een di-gesubstitueerde samenstelling. Het commerciële product waarvan beweerd wordt dat het "$Zr(O^iPr)_2(thd)_2$" is en dat veelvuldig "gebruikt" wordt voor de MOCVD bereiding van Z_rO_2 bestaat dus niet.

De isolatie van pure tri-gesubstitueerde samenstellingen is gecompliceerd, omdat de mono- en tetra-gesubstitueerde samenstellingen in de meeste gevallen de neiging hebben gemakkelijker uit te kristalliseren. Het gevolg hiervan is dat deze samenstellingen of een mengsel hiervan verkregen wordt. In de verkregen tri-gesubstitueerde verbindingen wordt het verwachte toegenomen inductieve effect van *n*-propoxide naar isopropoxide ligands duidelijk waargenomen. De vorming van het dimere hydroxo-di-thd gesubstitueerde complex, $[Hf(O^iPr)(OH)(thd)_2]_2$, is enkel waargenomen voor het op hafnium gebaseerde systeem en is het resultaat van een reactie van $Hf(O^iPr)(thd)_3$ en $[Hf(O^iPr)_3(thd)]_2$ ten gevolge van micro-hydrolyse. De meeste van de verkregen samenstellingen hebben een beperkte stabiliteit waardoor ze minder geschikt zijn voor MOCVD toepassingen.

Een structurele karakterisering van de tetra-thd complexen van zirkonium is uitgevoerd om de hun ongebruikelijke eigenschappen te kunnen verklaren. Gevonden werd dat de relatief korte afstanden tussen de meest nabije methyl koolstofatomen van de naburige moleculen, ten gevolge van de sterke van der waals interacties, in combinatie met effect van dichte spakking het meest waarschijnlijk verantwoordelijk geacht worden voor de lage oplosbaarheid en vluchtigheid van deze verbindingen.

De modificatie van zirkonium en hafnium *t*-butoxiden met 2,2,6,6,-tetramethyl-3,5-heptanedione (Hthd) is onderzocht. Voor de modificatie met Hthd is de vorming van di- en tri-gesubstitueerde samenstellingen waargenomen. Het verschil in modificatie tussen de *t*-butoxide en propoxide precursors is het gevolg van de grotere omvang van het alkoxide ligand. Door sterische hindering is de vorming van een mono-gesubstitueerde samenstelling niet mogelijk. NMR studies van deze samenstellingen hebben aangetoond dat ze in oplossing niet stabiel zijn in tijd. De transformatie naar een tetra-gesubstitueerde samenstelling was duidelijk waarneembaar. Het verwachte inductieve effect van de grotere alkoxide liganden, d.w.z.. de metaal-zuurstofbindingen van de alkoxide liganden van de *t*-butoxiden

worden verwacht korter te zijn dan die van de propoxiden, is niet waargenomen door de sterische hindering.

De modificatie van zirkonium en hafnium isoproxide met ethylacetoacetate en *t*-butylacetoacetate (tbaoac) leidt tot mono- en di-gesubstitueerde samenstellingen. NMR studies van oplossingen van de tbaoac gemodificeerde alkoxiden hebben aangetoond dat de di-gesubstitueerde samenstellingen stabiel zijn in tijd. De enige veranderingen in de NMR spectra zijn het gevolg van transesterficatie van de alkyl- en alkoxideliganden. De thermodynamisch stabiele di-gesubstitueerde samenstellingen kunnen van groot belang zijn voor sol-gel toepassing en de transesterficatie van de alkyl- en alkoxideliganden kan gemakkelijk voorkomen worden door een correcte keuze van liganden en additief, d.w.z. ze moeten hetzelfde zijn.

NMR studies aan zirkonium en hafnium *t*-butoxides gemodificeerd door tbaoac hebben aangetoond dat modificatie de vorming van mono-, di- en tri-gesubstitueerde samenstellingen tot gevolg heeft. Gebleken is dat deze samenstellingen in tijd niet stabiel zijn in oplossing. In deze systemen waren de di-gesubstitueerde samenstellingen niet stabiel, de grootte van de *t*-butoxide liganden zorgt voor een sterische hindering die de trans-stabilisatie van de alkoxide liganden uitschakelt.

De modificatie van zirkonium *n*-propoxide en gemende-ligand precursor met 0.5 mol equivalent H_2dea leidt tot vorming van $[Zr_2(O^nPr)_6(OC_2H_4)_2NH]_2$ en $[Zr_2(O^nPr)_2(O^iPr)_4(OC_2H_4)_2NH]_2$. Deze complexen zijn slechts matig stabiel in zowel oplossing als vaste stof. Het tri-nucleaire complex, $Zr\{\mu\text{-}\eta^3\text{-}NH(C_2H_4O)_2\}_3[Zr(O^iPr)_3]_2(^iPrOH)_2$, verkregen door modificatie van zirkonium isoproxide met zowel 0.5 en 1 equivalent mol H_2dea, blijkt stabiel in oplossing te zijn. De aanwezigheid van twee zirkonium kationen die op verschillende wijzen worden gecoördineerd - een nona- en een hexa-coördinatie - geeft de mogelijkheid om nieuwe verbindingen af te leiden van deze precursor *via* zelf-assemblage. Dit werd gedemonstreerd door de bereiding van analoge titanium-zirconium en titanium-hafnium samenstellingen, $Zr\{\mu\text{-}\eta^3\text{-}NH(C_2H_4O)_2\}_3[Ti(O^iPr)_3]_2$ en $Hf\{\mu\text{-}\eta^3\text{-}NH(C_2H_4O)_2\}_3[Ti(O^iPr)_3]_2$.

Rol van modificerende liganden op het sol-gel proces

De invloed van modificerende liganden op de sol-gel chemie van metaal alkoxiden en het effect van deze liganden op de morfologie van afgeleide materialen werden bestudeerd. Een vergelijking van de bindinglengtes en van de effectieve lading van de metaalatomen in gemodificeerde en ongemodificeerde verbidningen heeft, in combinatie met gegevens van eenvoudige calorimetrische experimenten hebben aangetoond dat de reactiviteit van metaal alkoxiden toeneemt in plaats van afneemt als deze gemodificeerd worden. Een nieuw concept wordt beschreven voor het reactie mechanisme tijdens sol-gel processing van metaal-alkoxiden.

Ligand-uitwisseling en hydrolyse vinden plaats door een proton-ondersteund S_N1 mechanisme, in tegenstelling tot een S_N2 hydrolyse mechanisme dat aktief is voor silicium alkoxide in alkalische media. De uitwisseling van liganden, hydrolyse alsmede de condensatie-reactie vinden bijna onmiddellijk plaats voor metaal alkoxiden. De producten van dit snelle hydrolyse en condensatie proces bestaan uit micellen gevormd door zelf-assemblage van liganden. Een ander opmerkelijk verschil met traditionele silica sol-gel chemie is de hoge mobiliteit van de modificerende liganden. Het concept dat in dit proefschrift beschreven wordt voorziet in verklaringen van veelvuldig waargenomen materiaal-eigenschappen en maakt de ontwikkeling van nieuwe strategieën voor de bereiding van materialen mogelijk.

In dit proefschrift worden de vorming of dichte nano-deeltjes van acetylacetone-gemodificeerd of zuur ‘gekataliseerd’ systeem en de vorming van dichte films van acetylacetone-gemodificeerde precursors besproken. De sol deeltjes voor de systemen zijn micellen die oxo-groepen bevatten en een oppervlak dat bedekt is met acetylacetone of positief geladen centra ten gevolge van de toevoeging van zuur. De vorming van omgekeerde micellen, die verkregen kunnen worden door een geschikte keuze van oplosmiddelen, leidt tot vorming van holle bollen. De modificerende acetylacetone liganden gedragen zich als surfactanten en vormen het interface tussen bol en oplosmiddel. De vorming van bollen werd aangetoond voor zirkonium *n*-propoxide, zirkonium isopropoxide en titanium *n*-propoxide precursoren. Vervolgens is de mogelijkheid aangetoond om hydrofiele componenten in deze deze bollen te omkapselen. Een ander voorbeeld, gevormd

via een micellen systeem, is de vorming van zirconia nano-rods uit een hoge anisotropische diethanolamine (H_2dea)- gemodificeerde precursor. De alkoxide liganden van de precursor in de brugposities spelen een belangrijke rol in de vorming van de nano-rods. In de afwezigheid van deze liganden die de groei sturen kan een micro-poreus materiaal worden verkregen voor de H_2dea gemodificeerde precursoren.

De resultaten beschreven in dit proefschrift zijn door groepen van SLU gebruikt voor het ontwikkelen van een methode voor gel-inkapseling onder waterige omstandigheden. De juiste keuze van een gemodificeerde titanium alkoxide precursor leidt tot vorming van een sol in alkohol via micellen in alcolhol, welke vervolgens wordt overgebracht naar waterige condities wat de mogelijkheid geeft voor inkapseling onder bio-compatibele omstandigheden.

De vorming van microporeuze materialen van diethanolamine-gemodificeerde precursoren is verder onderzocht met ontwikkelde hetero-metallische precursoren. De bereiding van srilankite van $Zr\{\mu\text{-}\eta^3\text{-}NH(C_2H_4O)_2\}_3[Ti(O^iPr)_3]$ en $Zr\{\mu\text{-}\eta^3\text{-}NH(C_2H_4O)_2\}_3[Ti(O^nPr)_3]$ en $Hf\{\mu\text{-}\eta^3\text{-}NH(C_2H_4O)_2\}_3[Ti(O^iPr)_3]$ is aangetoond. Deze fase wordt gevormd na het drogen en annealen op ~750 °C van het via sol-gel synthese verkregen poeder. De materialen van de zirkonium-titanium precursoren vertonen een type 1 N_2 soptie isotherm, wat kenmerkend is voor micro-poreuze materialen als ze gecalcineerd worden op een temperatuur rond 400 °C. Deze materialen zijn zeer interessant voor bereiding van micro-poreuze membranen. Voor de bereiding van de membranen is de invloed van verschillende parameters geëvalueerd. De invloed van de oplosmiddelen, te weten propanol en een mengsel van propanol en hexaan, lijkt niet groot. De zuurgraad van de hydrolyse oplossing en de snelheid van toevoeging ervan hebben daarentegen een groot effect op de eigenschappen van de gevormde solen en materialen, Toevoeging van meer zuur leidt tot verwijdering van het merendeel van de modificerende liganden. Als gevolg hiervan stijgt de pH van de oplossing en treedt er een verdichting op van de sol deeltjes.

Acknoledgments

The research described in this thesis would not have been accomplished without the help of a large number of people. During my PhD collaboration was established between IMS of the University of Twente and Vadim Kessler's research group at SLU (Uppsala, Sweden). I spent a significant portion of the last two years in Uppsala.

Dave, I am very grateful that you have stimulated a stay abroad from our first meeting after you were assigned as professor at IMS. You have given me the chance to develop as an individual and you were always there when I needed support or advice.

Vadim, our contact goes back as far as August 2003 in Sydney. Your comments on my poster at the conference there resulted in me coming to Uppsala. Your supervision, dedication and numerous other contributions have resulted in the accomplishment of this thesis and will without any doubt lead to much more!

Henny and Nieck, the two of you should be thanked for convincing me to do a PhD thereby providing me with a unique opportunity. The road to accomplishing this thesis has had its share of twists and turns. Nevertheless, we got nice things started and hopefully they will last for a long time. Guys, thanks for everything.

A lot of the data presented in this thesis was obtained in the labs of the UT or SLU and a large number of people have contributed in the process of obtaining it.

The technical support within IMS has helped me a lot. Cindy and Mieke thank you for all the experiments! Herman, Gerrit, Attila, Wika, and Henk I could not have done this without your help. Marion, thanks for all the help with the administrative work!

Beatriz thank you for your help so far and I promise that the work will be rounded up in the near future.

Tijana, thanks for everything.

Rico bedankt voor de TEM metingen en je geduld als het sample weer een onverwacht resultaat gaf. Mark bedankt voor de last-minute metingen!

Rolf and Suresh, your help with the NMR and mass spectrometry experiments was irreplaceable. Tack så mycket!

Gunnar and Bernt, thank you for making teaching lab courses an enjoyable experience.

Gulaim, thank you for all your contributions and sorry for all the mess I made.

Lars thanks so much for the support with getting proper quality graphs!

Also a lot of people outside the UT and SLU were involved in the accomplishment of this thesis

Margareta, thank you for performing the HRTEM experiments.

Jaap and Wim bedankt voor de wetenschappelijke discussies. Jaap de tijd in Sydney, Uppsala, Amsterdam en Los Angeles was erg aangenaam. Waar zien we elkaar weer?

George van der Donk and Wim Pyckhout-Hintzen for the attempts to perform SAXS measurements.

Thanks to Marc Henry and Lars Kloo for their calculations used in this thesis. Andreas Fischer is kindly acknowledged for his single crystal XRD work.

All the guys that I have worked with at the University of Newcastle upon Tyne. Special thanks goes to John Errington for facilitating this opportunity (*i.e.*, your house, office, lab). Nick Wright, without your help it wouldn't have worked!. John Ridland, thanks for the great scientific discussions!

Several organizations are kindly acknowledged for the financial support received to facilitate my stays abroad.

The Netherlands Organization for Scientific Research (NWO) and EXXONMOBIL Chemical Benelux for facilitating the research at SLU with a travel grant and travel award, respectively.

The THIOX network of ESF for the travel grant for the stay in Newcastle.

After all those mentioned above, there are a large number of people that have contributed tremendously the past period.

The ‘family’ in Uppsala and in particular one of them. Joris bedankt voor alles!

To everyone who still puts up with me...

To many who became friends along the way...

To those whose help was truly appreciated.

Edwin & Linda, Johan, Aafke, jullie steun en medeleven was geweldig!

Pa en ma bedankt voor alles!

Katarina, there is no-one that has read this thesis like you have and your rewording it in terms like “the bubbles are really pretty” kept me going. The last year has been awesome. Thanks for everything!!